COST 207
Digital land mobile radio communications

Published by the
COMMISSION OF THE EUROPEAN COMMUNITIES

Directorate-General
Telecommunications, Information Industries and Innovation

L-2920 Luxembourg

LEGAL NOTICE

Neither the Commission of the European Communities nor any person acting on behalf of the Commission is responsible for the use which might be made of the following information

Cataloguing data can be found at the end of this publication

Luxembourg : Office for Official Publications of the European Communities, 1989

ISBN 92-825-9946-9 Catalogue number: CD-NA-12160-EN-C

© ECSC-EEC-EAEC, Brussels • Luxembourg, 1989

Printed in France

Commission of the European Communities

information technologies and sciences

COST 207

Digital land mobile radio communications

COST 207 Management Committee

M. Failli (Chairman)
SIP-Direzione Generale
Via Flaminia, 189
I-00196 Roma

Final report
(14 March 1984 - 13 September 1988)

Directorate-General
Telecommunications, Information Industries and Innovation

1989

EUR 12160 EN

This report summarizes the results of the activities of COST 207 "Digital Land Mobile Radio Communications".

It is organized around the three research areas into which the project has been subdivided: propagation, baseband processing and modulation.

The main activities and results carried out within the project are as follows:

- The definition of frequency-selective fading simulator characteritics and the choice of parameter setting for GSM test measurements, taking into account the results of propagation measurements carried out in different countries participating in COST 207.

- Measurements of man-made noise in the 900 MHz band and construction of a noise simulator.

- Modulation methods originally seen as possible candidates for the GSM system; GTFM, PAM/FM and GMSK.

- Adaptive baseband equalization techniques.

- Forward error-correction codes.

- Specification of the 13 Kbit/s net bit-rate codec and corresponding test sequencies.

- Specifications relating to voice-activated transmission intended to conserve battery energy in hand-held terminals, and to reduce interferences.

CONTENTS

1.	**Origins of the COST 207 and objectives**	1
2.	**Project participation and organization**	2
3.	**Activities and Results**	4
4.	**Proposal for a follow-on project**	6
5.	**Conclusive remarks**	6

Annex 1: Final Report of the WG1 on Propagation

Annex 2: Final Report of the WG2 on Baseband Processing

Annex 3: Final Report of the WG3 on Modulation Methods

Annex 4: List of participants in the Management Committee

Annex 5: Proposal for a follow-on project on the "Evolution of land mobile radio (including personal) communication"

1. COST 207 ORIGINES AND OBJECTIVES

From the beginning of the 1980's land mobile radio systems in most countries have been experiencing a very rapid expansion with an increasing degree of system sophistication. Today, public systems using the 160, 450 and 900 MHz frequency bands have been planned and operated, generally on a national basis, and only in a few cases does the same system serve more than one country.

The possibility of using standard system throughout Europe, together with the advantages to both the manufacturers and subscribers of a larger scale market, led the CEPT in 1982 to establish the "Mobile Special Group"(GSM) with the task of producing guidelines and specifications for a harmonized European public mobile communications system for the 1990's in the 900 MHz frquency band. The basic system parameters had to be defined by December 1986. However, the GSM was not prepared to perform all the necessary activities within the group. On the contrary, the group identified those Administrations and Research bodies carrying out related activities with the aim of co-ordinating with those activities in order to obtain the best utilization of European-wide resources.

In this context, it appeared that the COST framework was particularly suited to co-ordinate research activities on well-defined subjects and to produce results for direct application to the envisaged European system.

The COST 207 project was set up in March 1984 with the objective to co-ordinate research activities already underway in Europe and to stimulate new studies on well defined aspects of digital land mobile radio communications. The reason for contracting on digital techniques reflected the fact that, although it was not possible to state at that time whether the GSM system would use digital or analogue speech transmission, it was practically certain that the signalling would be digital. Furthermore, the knowledge of analogue transmission was already advanced.

The technical programme of the project was subdivided into three research areas: propagation, baseband processing and modulation according to the following content:

a) Propagation

- Collation of data, preferably from modulated transmission, related to topography.

- Development of compatible methods and procedures for predicting propagation characteristics from topographical data for both wanted and interfering signals. Full use of such results will require harmonized data bases.

- Development of narrow-band and wide-band fading simulators.

b) Baseband processes

Study and demonstration for the mobile radio environment of:

- optimum speech encoding processes taking into account that these processes may differ in the two directions of transmission;

- methods for providing communication privacy;

- signalling and data transmission techniques.

c) Modulation

- Study and demonstration of optimum modulation techniques taking into account spectrum efficiency, channel capacity, performance requirements, radio channel characteristics and cost factors.

2. PROJECT PARTICIPATION AND ORGANIZATION

The Memorandum of Understanding (MoU) was signed by ten countries (Belgium, Denmark, Federal Republic of Germany, Finland, France, Italy, Netherlands, Sweden, Switzerland and United Kingdom).

ESA sent observers during the second half of the activity. The list of participants is attached as Annex 4, while the list of the participating institutions (administrations, research institutes, industries and universities) is given below:

Direction Générale des PTT (Switzerland)

Forschungsinstitut der DBP (Federal Republic of Germany)

University of Erlangen (Federal Republic of Germany)

Telecom Denmark

Aalborg University (Denmark)

Storno (Denmark)

Telecommunications Research Laboratory (Denmark)

CNET (France)

CSELT (Italy)

SIP (Italy)

Bologna University (Italy)

Fondazione Bordoni (Italy)

Istituto Superiore PT (Italy)

Dr Neher Laboratories PTT (Netherland)

Swedish Telecom Adm. (Sweden)

Ericsson (Sweden)

Technical Research Centre of Finland (VTT)

General Directorate of P.T. (Finland)

Rutherford Appleton Laboratory (United Kingdom)

British Telecom Research Laboratories (United Kingdom)

University of Leeds (United Kingdom)

ESA-ESTEC

After the signature of the MoU, the Project Management Committee (MC) was formally established in Brussels in June 1984.

Mr. R. Failli was elected Chairman and Mr. G. de Brito Vice-Chairman. The Commission of the European Communities was in charge of the technical secretariat. The appointment of Chairman and Vice-Chairman were re-confirmed in the following years.

The Management Committee met three times a year, the last meeting took place in Stockholm on September 1988. The project, which was originally foreseen to last three years, obtained a time extension of eighteen months in order to complete its activity.

The activity of the COST 207 was allotted to three working groups dealing with: propagation aspects (WG1), under the chairmanship of Dr. Lorenz (Federal Republic of Germany), baseband processing (WG2), Chairman Mr. de Brito (France), and modulation techniques (WG3), Chairman Mr. Swain (United Kingdom).

In order to avoid overlap between the activity of COST 207 WG2 and that of a group of experts on speech coding for mobile radio applications established by the transmission group of CEPT, a "Joint COST 207 - CEPT TM3 Group of experts"(JEG) was established towards the end of 1985. Chairman of the JEG was Mr. Natvig (Norway - CEPT TM3) and Vice-Chairman Mr. de Brito (France, COST 207). In this group, the larger part of WG2 activity was concentrated.

3. ACTIVITIES AND RESULTS

The main study activities carried out within the project are as follows:

- The definition of frequency-selective fading simulator characteritics and the choice of parameter setting for GSM test measurements, taking into account the results of propagation measurements carried out in different countries participating in COST 207. A special campaign of measurement was carried out during Spring 1987 in order to characterize the propagation in hilly terrain. Testing of prototype selective fading simulators was also carried out.

- Measurements of man-made noise in the 900 MHz band and construction of a noise simulator.

- Modulation methods originally seen as possible candidates for the GSM system; GTFM, PAM/FM and GMSK.

- Adaptive baseband equalization techniques.

- Forward error-correction codes.

- Specification of the 13 Kbit/s net bit-rate codec and corresponding test sequencies. Validation of the specifications of five hardware codecs produced by different sources.

- Specifications relating to voice-activated transmission intended to conserve battery energy in hand-held terminals, and to reduce interferences.

Moreover, the COST 207 project studied other matters for which it was not possible to reach final conclusions within the framework of the project. In particular it is worth mentioning:

- Prediction of area coverage and the application of topographical data bases.

- Antenna aspects, especially diversity.

The results obtained by the three working groups are given as:

ANNEX 1: Final report of the WG1 on Propagation

ANNEX 2: Final report of WG2 on Baseband Processing

ANNEX 3: Final report of WG3 on modulation methods

4. FOLLOW-ON PROJECT

According to the requirements of the MoU, at the end of the project the M.C. examined the possibilities and advantages of a follow on project, directed towards exploring the practicality of other land mobile communication systems and expanding European expertise in the field. As a result of the examination a proposal for a new project on the evolution of land mobile radio (including personal) communication has been put forward and it is attached as Annex 5.

5. CONCLUSIVE REMARKS

The COST 207 Project has been fully coordinated with the CEPT GSM activity. No problems of co-ordination have been experienced with other international bodies.

The results of the Project have been obtained from the voluntary contributions of members and experts of the COST 207 Project. Participating countries have contributed significantly to the activity within the WG's and the M.C.

No precise calculation of the total cost of the project activities has been carried out, but the cost has been estimated to be of the order of 10-20 millions ECU.

Interim results have been already presented in a coordinated way to the International Conference on Mobile Radio Communications held in Venice July 1987 and to the third Nordic Digital Mobile Seminar held in Copenhagen in September 1988. Moreover, documents have also been transmitted to the RACE Project R1043 and to the Technical subcommittee TR 45.3 of EIA (Electrical Industry Association of the USA) on Digital cellular standards following their specific request. Requests for documents have also been received from several industrial companies.

The M.C. has decided to respond in a positive way to any further request of this kind, with the caviat that the origin of the documents be identified and mentioned when they are used.

ANNEX 1

Final Report of the Working Group 1 on Propagation

CONTENTS

0 INTRODUCTION 13

1 RADIO PATH LOSS PREDICTION TECHNIQUES 15
1.1 Introduction 15
1.2 Base station effective antenna height 17
1.3 Empirical methods 18
1.3.1 Okumura 18
1.3.2 Blomquist and Ladell 19
1.3.3 Ibrahim and Parsons (I-P) 20
1.3.4 Application and performance of empirical models 20
1.4 Methods based on topographical data bases 23
1.4.1 Longley and Rice (LRC) 23
1.4.2 Modifications to the Longley and Rice model 25
1.4.3 British Broadcasting Corporation (BBC) 26
1.4.4 Division of Radio Technology (DRT) 26
1.4.5 Deutsche Bundespost (DBP) 27
1.4.6 Finnish PTT (FIN) 28
1.5 Comparison of different models with measurements performed in London and Ipswich 30
1.5.1 Measurements in London 31
1.5.2 Measurements in Ipswich 33
1.6 Influence of land cover and correction factors 37
1.7 Influence of urban structure and street orientation 40
1.8 Methods to estimate diffraction loss 42
1.9 Conclusions 45
1.10 References 46

2 MULTIPATH PROPAGATION 49

2.1 INTRODUCTION TO THE MULTIPATH MOBILE RADIO CHANNEL 49
2.1.1 List of symbols 49
2.1.2 Introduction 49
2.1.3 Two and three ray path models 50
2.1.3.1 Two path model 50
2.1.3.2 Three path model 52
2.1.4 Multipath channels 53
2.1.5 Definitions 53

2.1.5.1 Frequency and time domain transfer functions 53
2.1.5.2 Definitions of parameters used to describe the impulse response 55
2.1.6 Statistical reduction of measurements 58
2.1.7 References 59

2.2 MEASUREMENT TECHNIQUES 65
2.2.1 Introduction 65
2.2.2 Methods of measuring multipath distortion 65
2.2.2.1 Pseudorandom sequence sounding 65
2.2.2.1.1 Correlation techniques 65
2.2.2.1.2 Matched filter techniques 67
2.2.2.1.3 Comments on correlation and matched filter sounding 67
2.2.2.1.4 Vehicle speed and averaging distance 69
2.2.2.2 Pulse measurements 70
2.2.2.2.1 General 70
2.2.2.2.2 Comments on the pulse sounders 72
2.2.3 Frequency domain techniques 73
2.2.3.1 Spaced frequency technique 73
2.2.3.2 Frequency stepping technique 73
2.2.4 Summary and conclusions 75
2.2.5 References 77

2.3 SUMMARY OF RESULTS 89
2.3.1 Introduction 89
2.3.2 Measurements in France 90
2.3.3 Measurements in the UK 92
2.3.3.1 Measurements in London 92
2.3.3.2 Measurements in Cumbria 93
2.3.3.3 Comments on the data processing 95
2.3.3.4 Measurements in Leeds 95
2.3.3.4.1 Description of the environment 95
2.3.3.4.2 Results 96
2.3.4 Measurements in the Netherlands 98
2.3.5 Measurements in Sweden 98
2.3.6 Measurements in Switzerland: first campaign 99
2.3.6.1 Locations 99
2.3.6.2 Data processing and results 100
2.3.7 Measurements in Switzerland: second campaign 101

2.3.7.1 Locations 101
2.3.7.2 Description of the processing 102
2.3.7.2.1 Cut-off-level 102
2.3.7.2.2 Correlation side-peaks 102
2.3.7.3 Results 103
2.3.8 Measurements in Italy 106
2.3.8.1 Description of the environment 106
2.3.8.2 Results 107
2.3.9 Measurements in Japan 109
2.3.9.1 Locations 109
2.3.9.2 Results 110
2.3.9.3 Comments 110
2.3.10 Comparison of the results and conclusions 110
2.3.11 References 112

2.4 SIMULATION OF RADIO CHANNELS 135
2.4.1 Doppler spectrum types 136
2.4.2 Propagation models 137
2.4.2.1 Typical case for rural (non-hilly) area (RA) 137
2.4.2.2 Typical case for urban (non-hilly) area (TU) 138
2.4.2.3 Typical bad case for hilly urban area (BU) 138
2.4.2.4 Typical case for hilly terrain (HT) 139
2.4.3 Approximation of the delay power profiles by discrete taps 139
2.4.4 Examples for tap settings 141
2.4.4.1 Typical case for rural (non-hilly) area (RA) 141
2.4.4.2 Typical case for urban (non-hilly) area (TU) 142
2.4.4.3 Typical bad case for hilly urban area (BU) 143
2.4.4.4 Typical case for hilly terrain (HT) 145
2.4.5 Hardware fading simulators 146
2.4.6 References 147

2.5 SOFTWARE SIMULATION 148
2.5.1 Introduction 148
2.5.2 Basic of the computer program 149
2.5.3 Analysis of irreducible BER for continuous and smooth spectra 152
2.5.4 Analysis of a two peaks delay power spectrum 153
2.5.5 Influence of different environmental conditions on BER 157
2.5.6 References 158

3 MAN-MADE NOISE 167
3.1 Introduction 167
3.2 Characterization of automotive noise 167
3.3 Summary of existing data 170
3.4 Summary of recent measurements 173
3.4.1 Measurements performed in Italy 173
3.4.2 Measurements performed in France 175
3.5 Simulation techniques 177
3.5.1 Simulators specifications 177
3.5.1.1 Video pulse generators 178
3.5.1.2 Pulse modulated radio frequency carriers generators 180
3.6 Conclusions 182
3.7 References 183

4 ANTENNAS 197
4.1 Introduction 197
4.2 Antenna diversity 198
4.2.1 General aspects of antenna diversity for mobile antennas 198
4.2.2 Base station diversity 200
4.2.3 Diversity antennas 203
4.3 Antenna measurements 205
4.4 Discussion 207
4.5 References 207

5 CONCLUSIONS 209

0. INTRODUCTION

This report summarizes the results of the activities of the Working Group on Propagation. Four subjects related to the signal propagation over the Mobile Radio Channel have been treated and are described in the subsequent sections. The first one reviews the existing and known Radio path loss prediction techniques, based on both empirical methods and approaches based on topographic databases. Their relative accuracy, complexity and weaknesses are determined using data from several measurement campaigns performed in various countries.

The second and largest section deals with the quantitative description of the Mobile Radio Channel characterized by time-variant and frequency selective multipath propagation. A mathematical description provides the theoretical basis for this work. Then, the various measurement techniques used for the measurement campaigns performed in several countries are described. The summary of results contains a considerable amount of new information, especially on the propagation phenomena observed in mountainous terrain. Hardware simulation techniques have been especially developed within this project and the parameters for equipment testing have been determined, based on the experimental work.

Finally, techniques of software simulation of the channel, allowing the prediction of bit error rates have been developed, but could not be included within this report since the examination could not be completed. Experimental data on the level of man-made radio interference in the UHF range have been gathered. The results are compared with the rather sparse data published earlier and it appears that extrapolation of data measured at lower frequencies leads to an underestimation of the interference levels actually observed at UHF. Principles of interference signal generators are also described.

The antennas being the interface between the radio equipment and the transmission channel, some specific problems have also been studied. In particular, diversity antennas for mobile and base stations have been investigated and the observed diversity gain factors are given. Finally, a series of measurements of car-mounted antenna patterns at 900 MHz have been performed and the corresponding vertical and azimuthal diagrams are shown.

For convenience of the reader, the bibliographic references are given at the end of each section or subsection.

1 RADIO PATH LOSS PREDICTION TECHNIQUES

1.1 INTRODUCTION

Land mobile radio services in the VHF/UHF-range are impaired by three different effects resulting from wave propagation:

- temporary superrefraction and ducting,
- rapid fading and
- slow fading.

The meteorological effects occur only in a small percentage of time and then in large areas simultaneously. These effects can be neglected for area coverage but not for interference investigations. However, most prediction models deal only with area coverage.

The received signal consists of the superposition of a direct wave and other partial waves which are scattered and reflected in the vicinity of the mobile: rapid fading. The amplitude is Rayleigh distributed if the direct path is not present. Otherwise Rician statistics apply. A deterministic computation of the instantaneous amplitude is not purposeful because passing vehicles or vegetation moved by wind may change the instantaneous amplitude very rapidly. There are some counter-measures like diversity or error correcting codes against rapid fading.

Therefore, prediction methods have to cope with slow fading caused by changes of the radio path. The models predict either the median or mean of the randomly distributed signal. The propagation curves published in CCIR Rec. 567-3, for example, refer to the field-strength level. In the course of its work COST 207 has decided that "path loss" between isotropic antennas is a better parameter, particularly when data are to be compared. Conversion between path loss (between isotropic antennas) and field strength (assuming 1 kW power feeding a dipole as in CCIR Rep. 567-3) can be made using the relation:

$$L_b = 139.4 + 20 \log f - F \tag{1.1}$$

where: L_b : basic path loss between isotropic antennas in dB,
f : frequency in MHz,
F : field-strength level in dB(μV/m).

Any prediction of path loss must include the effects of
- radio frequency,
- path length between the base station and the mobile,
- antenna height of the mobile,
- base station effective antenna height and
- shadowing and scattering caused by buildings and vegetation (land cover) and mountains.

The influence of land cover and terrain can be estimated by additional correction factors or functions derived from field-strength measurements in different types of land cover like urban, suburban, wooded or open areas and in flat, hilly or mountainous terrain. This category of models is called empirical models.

The application of empirical models yields good results in flat terrain with homogeneous land cover. In hilly and mountainous terrain the prediction can be improved considerably if the additional diffraction loss is computed by means of a path profile taken from a topographical data base. This second category of model is called models based on topographical data bases. The influence of land cover is estimated by empirical correction factors, too.

Common prediction methods belonging to both categories are described very briefly in this chapter. The models are compared with measurements in London and Ipswich. Then, the different influences on prediction accuracy are discussed in more detail, e.g. influences of land cover, urban structure and diffraction. The definition of the base station effective antenna height is an important factor in achieving good accuracy in all types of prediction techniques. Before discussing the various models, two different definitions of effective antenna height are introduced.

1.2 BASE STATION EFFECTIVE ANTENNA HEIGHT

The field strength at the mobile station is roughly proportional to the effective height h_1 of the base station transmitting antenna. This is different from its actual height if the height of the terrain surrounding the mobile station differs from that of the base station. Therefore, whenever the path loss or field strength is calculated, a value for h_1 must be established. When using topographical data bases, h_1 is easily derived for each location of the mobile. However, when using empirical methods it may only be possible to judge the average values for the areas. A common used definition is given in CCIR Rec. 370-4 for broadcasting:

> The height of the transmitting antenna is defined as its height over the average level of the ground between distances of 3 and 15 km from the transmitter in the direction of the receiver.

However, this definition may lead to results without any physical significance under some conditions in land mobile radio, particularly for short distances of only a few kilometers or if the mobile is located higher than the base station. The following definition, which is now also included in CCIR Rep. 567-3, leads to better results on average:

$$h_1 = \begin{cases} h_{0b} - h_{0m} + h_b & \text{for } h_{0b} > h_{0m} \\ h_b & \text{for } h_{0b} \leq h_{0m} \end{cases} \tag{1.2}$$

where: h_1 : base station effective antenna height,

h_{0b} : height of the base station above sea level,

h_b : height of the base station antenna above ground,

h_{0m} : height of the mobile above sea level.

1.3 EMPIRICAL METHODS

Empirical methods are based on a simple power law relationship between path loss and distance and incorporate some empirically derived factors that determine the power law and the influence of the above parameters. In most cases they have been derived from narrow band measurements, where the transmitter was installed at the base station and the receiver was accomodated in a vehicle. The antenna used at the mobile was either a monopole or dipole, i.e. an antenna with omnidirectional pattern. Statistically independent samples were obtained if the distance between consecutive samples was at least a quarter of a wavelength. In order to eliminate the rapid fading, medians or means were computed from ensembles of data measured along runs varying between 20 and 1000 m. Clearly this data can be also used to validate the other category of prediction model described in section 1.4.

1.3.1 Okumura

Okumura's empirical model is derived from a series of measurements made in a variety of environments around Tokyo, Japan. These are published as a number of curves (Okumura et. al., 1968) and form the basis of the CCIR Rep. 567-3. The basic form of Okumura's model makes no concession to the nature of the terrain between base station and mobile. There are, however, additional correction factors for sloping, over water and undulating terrain. These require at least some knowledge of the type of the terrain, and preferably the terrain height profile of the radio path.

A number of authors have fitted equations to these curves, the best known being Hata, 1980, and Reudink, 1974. Hata's equations include the effects of distance, frequency, mobile (h_2) and base station antenna heights (h_1). The application of Hata's formulas is restricted to urban, suburban and open areas and to distances up to 20 km. However, measurements performed in the Fed. Rep. of Germany (Löw, 1986) have shown that Hata's formulas can also be used in forest and for distances up to 40 km. In an unpublished contribution to COST 207, Juul-Nyholm has made

approximations to CCIR Rec. 370-4 and Rep. 567-3. The accuracy of the approximations is better than 2 dB.

Urban or land:

$$F = 10 \log P + k_0 + k_1 \log h_1 - (k_2 + k_3 \log h_1) \log d \qquad (1.3)$$

Sea:

$$F = 10 \log P + k_0 + k_1 \log h_1 - (k_2 + k_3 \log h_1) d \qquad (1.4)$$

where: F : field-strength level in dB(μV/m),

P : effective radiated power (e.r.p.) in W,

$k_0 \ldots k_3$: coefficients (contained in Table 1.1) determined by regression curve fitting to CCIR Rec. 370-4 and Rep. 567-3,

h_1 : base station antenna height in m, 30 m $< h_1 <$ 150 m

d : distance from the base station in km.

Frequency	Mobile ant. height	Path length	Land cover	k_0	k_1	k_2	k_3	CCIR Ref.
450 MHz	1.5 m	1 ... 20 km	urban	27.0	13.0	47.0	-7.0	Rep. 567, Fig. 1
450 MHz	1.5 m	20 ... 100 km	urban	30.0	28.0	50.0	3.6	Rep. 567, Fig. 1
900 MHz	1.5 m	1 ... 20 km	urban	25.0	13.0	47.0	-7.0	Rep. 567, Fig. 2
900 MHz	1.5 m	20 ... 100 km	urban	30.0	27.0	50.0	3.6	Rep. 567, Fig. 2
450 ... 1000 MHz	10 m	10 ... 100 km	land	11.0	45.0	24.0	17.0	Rec. 370, Fig. 9
450 ... 1000 MHz	10 m	10 ... 100 km	sea	4.0	23.0	0.37	0.12	Rec. 370, Fig. 13

Table 1.1: Coefficients $k_0 \ldots k_3$

1.3.2 Blomquist and Ladell

This model (Blomquist and Ladell, 1974) is based upon an empirically derived combination of the path losses calculated according to the "flat earth" formula and from the Epstein and Peterson, 1953, diffraction formula. These are combined by taking the square root of the sum of their squares, the values being expressed in dB. The reference compares calculated path loss at frequencies from 30 to 900 MHz showing good performance over

irregular terrain. The model has not been investigated further within COST 207.

1.3.3 Ibrahim and Parsons (I-P)

In a manner similar to Okumura, Ibrahim and Parsons, 1983, have derived two models based on a series of measurements carried out in central London, UK. Two models are proposed, the essential difference being that method 1 uses a distance power law which is frequency dependent, whilst method 2 uses the "plane earth" distance power law of 40 dB per decade.

In addition to the basic distance dependent path loss, the effect of land cover is included by using two factors denoted by L and U. These are defined as:

L: percentage of area covered by buildings (range 0 to 100 %)

U: degree of urbanisation factor (percentage of buildings having four or more floors, range 0 to 100 %)

Ibrahim and Parsons also include a height correction factor based on the difference between base and mobile stations, derived from a subset of the London measurements. The effect of this is to reduce the path loss as the mobile station height increases.

Generally speaking, the method is limited to relatively flat, urbanised environments such as central London.

1.3.4 Application and performance of empirical models

Since these empirical models are usually presented in the form of a linear, algebraic equation, it is possible, by rearrangement to simply and rapidly calculate any one parameter from a knowledge of the others. It is possible to implement this on a pocket calculator.

Model	Frequency	Antenna heights above ground		Path length	Terrain	Land cover
		Base station	Mobile			
Okumura (CCIR)	150 ...2000 MHz	30 ...1000 m	1 ...10 m	1 ...100 km	all	all
Blomquist and Ladell	30 ...900 MHz	note 1	note 1	1 ...20 km	rugged	rural
Ibrahim and Parsons	160 ...900 MHz	note 2	< 3 m	< 10 km	mainly flat	urban

1. Method compared with measurements made with antenna heights in the range 1 ... 20 m.
2. Method derived from measurements made using an antenna on the roof of a building, 46 m above ground.

Table 1.2: Validity ranges of the empirical prediction models

The validity ranges of the empirical models are given in Tab. 1.2. The major limitation of these models is, however, their inability to invoke diffraction calculations based on the terrain between base and mobile stations. Path loss contours produced by these models tend, therefore, to resemble concentric circles, with some irregularity caused by the various correction factors in the models even in highly irregular terrain.

Land cover	Path length [km]	Measured mean path loss [dB]	Prediction error		Model
			Mean [dB]	Stan. dev. [dB]	
Suburban areas: low density dwellings and modern industrial estates	4 ...31	148.2	-25.8	8.3	I-P, empirical
			-25.5	6.7	I-P, semi-empirical
			-12.1	6.2	CCIR, Hata
			-12.7	6.1	CCIR, Juul-Nyholm
Suburban areas: higher density dwellings, e.g. council estates	2 ...23	144.3	-18.0	6.1	I-P, empirical
			-20.3	5.3	I-P, semi-empirical
			-8.9	6.0	CCIR, Hata
			-8.9	5.9	CCIR, Juul-Nyholm
Urban areas: buildings of up to 4 storeys with some open space between	7 ...10	149.5	-12.7	3.0	I-P, empirical
			-15.0	2.9	I-P, semi-empirical
			-3.5	3.6	CCIR, Hata
			-3.6	3.6	CCIR, Juul-Nyholm

Table 1.3: Comparison of empirical prediction methods with Ipswich data at 941 MHz (Error = measured - predicted path loss)

An example of the prediction ability is given in Tab. 1.3. which compares about 200 measured path loss data at 940 MHz in the Ipswich, UK, area with predictions made using Hata's and Juul-Nyholm's approximations to the CCIR curves for urban area and Ibrahim-Parsons's (I-P) methods. In order to account for the differences in treatment of land cover by various methods, the following procedure has been adopted. First the land cover is defined according to a ten point scale proposed by Gurdenli et. al., 1987. The mean difference between measured and predicted data is then compared with the appropriate correction factor suggested by the author of each method to illustrate the absolute accuracy of the method. The standard deviation of these differences illustrates the reliablility of the method. Whilst in this comparison one method might appear to be better, it must be stressed that comparison with a much larger data set should be undertaken before significant conclusions are reached, and that due account be taken of the effect of terrains that are unsuited to these models which, generally, do not include diffraction calculations.

1.4 METHODS BASED ON TOPOGRAPHICAL DATA BASES

A number of methods for predicting path loss in the VHF/UHF bands have been devised to include the attenuation caused by terrain variations. Simplified flow diagrams of four of these are shown in Fig. 1.1. Specific procedures to make some allowance for the additional loss due to urban clutter can also be applied with three of the methods. Their validity ranges are given in Table 1.4.

Model	Frequency	Antenna heights above ground		Path length	Terrain	Land cover
		Base station	Mobile			
LRC	20 MHz ...1 GHz	No special restrictions	No special restrictions	< 1500 km	flat and hilly	open or built-up
BBC	50 MHz ...1 GHz	No special restrictions	No special restrictions	< 1000 km	flat and hilly	open, trees or built-up
DRT	50 MHz ...1.5 GHz note 2	No special restrictions	No special restrictions	< 1000 km	flat and hilly	open
RAL	20 MHz ...1 GHz	No special restrictions	No special restrictions	< 30 km note 1	flat and hilly	open or built-up
DBP	400 MHz ...1 GHz	10 ...1000 m	1 ...10 m	< 100 km	flat and hilly	open, forest built-up, water
FIN	945 MHz	30 ...200 m	1.5 m	< 30 km	flat, small hills	open, forest built-up water

1. Model only indended for use up to 30 km but may be applicable at somewhat larger distances.
2. An amended program can be used above 1.5 GHz.

Table 1.4: Validity ranges of the models based on topographical data bases

1.4.1 Longley and Rice (LRC)

In the LRC program (Longley and Rice, 1968) horizon obstructions for transmitter and receiver are modelled by knife-edges, and the path loss is calculated combining the diffraction losses computed by the Epstein and Peterson method, 1953, in two points, chosen well beyond the horizon, not coinciding with the receiving site. However, in this program, path losses are also calculated by fitting cylindrical sections to the intervening terrain - two cylinders to represent the sections between the terminals and their horizons, and two further cylinders to fit the central part

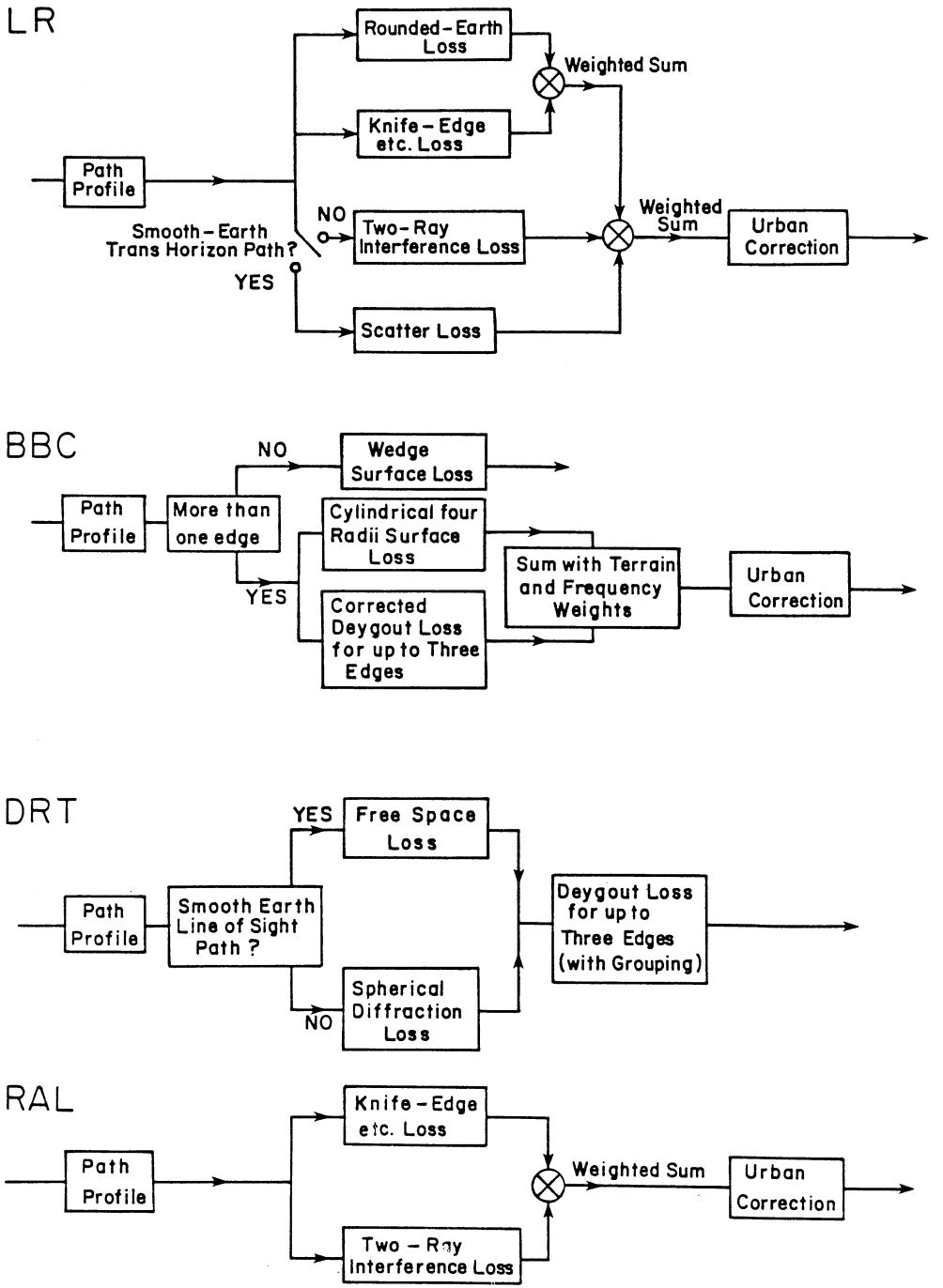

Figure 1.1: Simplified flow diagrams of four prediction methods

of the path between these horizons. This rounded-earth loss and the knife-edge loss may be treated as alternative methods for modelling the diffraction attenuation, and a weighted summation of these is performed.

Longley, 1978, has suggested an empirial correction factor for inclusion as a clutter loss. It is derived by adding the excess loss (relative to the basic Longley-Rice value) obtained from the predictions of Okumura et. al., 1968, for urban conditions. This urban factor is used in both the LRC and RAL programs.

1.4.2 Modifications to the Longley and Rice model

The Rutherford Appleton Laboratory (RAL), UK, have modified the Longley-Rice model to produce a computer-based procedure that could give results of an accuracy comparable with other, more complex methods, but over a limited distance range. The modified version does not consider the rounded earth loss and the Epstein-Peterson result is taken directly as the diffraction contribution to the path loss. The LRC routine for scatter loss is omitted but the two ray absorbtion calculation, representing the optical interference between direct and Earth-reflected rays, is retained. Further details, including a listing, are given in COST 207 TD (87) 44. The method has been used in the prediction of service-area coverage and in producing contour maps of carrier-to-interference ratios for cellular networks (Bowman and Davies, 1987), and some results of a comparison with measured data are given in section 1.5.

British Telecom has also modified the LRC method, as a result of investigations of the methods performance on undulating terrain. The principal modifications are an empirical scaling of the elevation angle, and the incorporation of a single knife-edge diffraction routine for certain types of path profiles. These improve the accuracy for path length up to 30 km, and some results of a comparison with data measured in the Ipswich area are given in a publication by Huish and Gurdenli, 1988.

1.4.3 British Broadcasting Corporation (BBC)

The program due to the BBC (Causebrook et. al., 1982) was developed with the particular aim of evaluating interference at selected locations for VHF and UHF television reception. This program is therefore valid over large distances and also over a wide range of frequencies (see Table 1.4). The general approach to modelling the effect of terrain obstructions is the Deygout construction, 1966, with grouping of adjacent edges. Clutter losses are computed with the BBC program, by considering statistically, the effects of buildings and trees in each 0.5 x 0.5 km^2 in obscuring the first Fresnel zone between the transmitter and receiver. The clutter in each square may be represented by index values for both buildings and trees, and the height distribution may be defined by a statistical probability function. In the present studies, a simple correction, i.e. assuming a 100 %-clutter index for buildings in each square and 0 % for trees, was used.

The BBC program includes routines for calculating a string path profile between the transmitter and receiver using a data base of land heights tabulated for 0.5 x 0,5 km^2. These routines have been used to provide profiles as input not only to the BBC path loss calculations but also to the other programs illustrated.

1.4.4 Division of Radio Technology (DRT)

The program due to the DRT (Division of Radio Technology within the UK Department of Trade and Industry) was, like the BBC program, developed to satisfy a major requirement of evaluating interference at selected locations. This program is therefore valid over large distances and also over a wide range of frequencies (see Table 1.4). Terrain effects are modelled using the Deygout construction.

The DRT program was made available to the Rutherford Appelton Laboratory for research purposes and does not include a clutter correction in the form used in the COST studies.

1.4.5 Deutsche Bundespost (DBP)

This model described briefly by Loew and Lorenz, 1983, and in more detail in COST 207 TD (86) 2 was submitted by the Deutsche Bundespost. The model predicts the median field-strength level. Its validity ranges are given in Table 1.4.

The model is based on Okumura's empirical curves for urban areas (1968) and on the estimation of the knife-edge diffraction loss according to Deygout's model (1966) supplemented by Causebrook's correction (1982). Empirical corrections derived from measurements in forest, built-up and open areas in the Federal Republic of Germany were applied additionally. For determination of the influence of land cover, four different environmental parameters (built-up, forest, open area, water) are computed. The values of these parameters are computed by integration of all areas containing obstructions which are located above the direct line between the mobile and base station antennas. This procedure takes into account areas with mixed land cover and transitions between different types of land cover.

The topographical data base used is organized in mesh grids of 5" x 5", i.e. about 150 x 100 m^2. The data stored for each area element are the maximum height above sea level and a characteristic figure B for land cover (1= built-up, 2= forest, 3= open area, 4= water). Information about street orientation, density of built-up areas or forests are not contained in the data base.

The errors resulting from the comparison with more than 2000 field-strength measurements carried out at 456 and 914 MHz, and path lengths reaching up to 60 km are contained in Table 1.5. The averaged run length was about 1000 m, samples were taken every 20 cm. The measurements were performed

- in flat terrain:
  in the cities of Munich, Frankfurt and Darmstadt and
  in the rural Rhine-Main-area and
- in hilly terrain with mountains reaching up to 700 m:
  Odenwald and Sauerland.

Land cover	Smooth terrain		Irregular terrain	
	Mean	Stand. dev.	Mean	Stand. dev.
Built-up	1.7 dB	6.7 dB	0.7 dB	7.3 dB
Forest	-1.3 dB	7.2 dB	1.0 dB	7.3 dB
Open area	2.8 dB	6.3 dB	2.8 dB	8.1 dB

Table 1.5: Prediction error (Measured - predicted median field-strength level)

The standard deviation is about 7 dB in flat terrain and 8 dB in hilly terrain. In hilly terrain, the standard deviation occurring in open areas is about 1 dB larger than in built-up areas and in forests. The reason is that in the mobile the reflections from far obstacles are received with an omnidirectional antenna but the prediction model considers only the two-dimensional path profile between the base station and the mobile.

1.4.6 Finnish PTT (FIN)

This prediction method was developed for the planning of the NMT900-network in Finland. The prediction method based primarily on measurements (Kajamaa, 1986) includes a median field-strength function, topographical and land cover correction functions.

The median field strength in South-Finland was measured to be

$$F = 59.8 - 34.9 \log d \tag{1.5}$$

where: F : median field-strength level in dB(μV/m),

d : path length (d < 25 km).

Power is 10 W (EIRP), antenna height 50 m, frequency 945 MHz.

The difference between the curve described by Eq. (1.5) and the urban curve of CCIR Rep. 567-3 Fig. 2 is nearly constant with distance.

Two topographical correction functions are available in the programme:

- clearance angle function $F_c(\theta)$
- knife-edge diffraction function $F_c(\nu)$

The clearance angle θ differs from the one defined in CCIR Rep. 239-6 Fig. 2 because the Finnish model has a mobile antenna height of 1.5 m and the CCIR model has 10 m. The diffraction parameter ν is the same as in CCIR Rep. 715-2.

F_c is the measured deviation of the signal strength from the median as a function of θ or ν. In the program F_c is estimated by a linear function, e.g. the equations for $F_c(\theta)$ are:

$$\frac{F_c(\theta)}{\text{dB}} = \begin{cases} -7.6 & \text{for } \theta < -2.75^\circ \\ 2.4\,\theta - 1 & \text{for } -2.75^\circ \le \theta < -0.75^\circ \\ 6.1\,\theta + 1.8 & \text{for } -0.75^\circ \le \theta < 0.25^\circ \\ 3.3 & \text{for } \theta \ge 0.25^\circ \end{cases} \tag{1.6}$$

The difference between the two models is rather small. The function $F_c(\theta)$ seems to be more suitable at long distances (d > 20 km) and $F_c(\nu)$ describes the path better at short distances. The models differ from CCIR Rep. 239-6 probably due to different antenna heights and differences in the topographical data base.

Correction due to the land cover is calculated locally around the mobile station. The topographical data base presents the land cover in 6 classes. The grid size is 200 x 200 m^2. The data base was derived from a coarse roadmap, which had contour lines only at 20 m steps and a scale of 1:200 000. The height values are stored in the data base in a grid of 200 x 200 m^2. The standard deviation from the correct height values is about 10 m. The map does not describe any of the small hills and that is why the values of the θ- and ν-parameters have remarkable errors at some locations. This reduces the prediction accuracy.

1.5 COMPARISON OF DIFFERENT MODELS WITH MEASUREMENTS PERFORMED IN LONDON AND IPSWICH

Comparisons of prediction techniques based on topographical data bases were carried out by the Rutherford Appleton Laboratory using three measurements data sets, having the following characteristics:

(a) Data Set 1 - Ibrahim and Parsons [1983].

Frequencies: 168, 455 and 900 MHz (transmitter at base station).

Base station aerial height: 46 m above local ground level.

Receiver height: 2 m. Receiver operated at approximately fixed ranges of 2, 5 and 9 km from the base station, but no 900 MHz data were collected at 9 km range. The received signals were averaged over all street orientations to provide mean values within selected, and mainly adjacent squares, of side 0.5 km.

Location: Central London.

(b) Data Set 2 - Provided by the Marconi Research Centre to RAL.

Frequencies: 450 MHz (transmitter in mobile).

Base station aerial height: 135 m above local ground level.

Mobile aerial height: 2 m. The operating range was up to 30 km, with routes chosen to investigate radial, circumferential and mixed path situations. Signals were averaged to provide a mean value for each 1 km of travel.

Location: London and Suburbs

(c) Data Set 3 - Provided by British Telecom [Rose, 1982].

Frequencies: 160 and 900 MHz (Transmitters at base station)

Base station aerial height: 55 m above local ground level and 80 m above sea level.

Receiver aerial height: 2 m. The receivers were operated at ranges of between about 5 and 12 km in directions west of the transmitters. The received signals were averaged over all street orientations to provide mean values within 0.5 km squares and within an almost filled grid structure (5.5 x 7 km^2).

Location: Ipswich.

The prime objectives of the studies have been to test the various prediction techniques in a common manner and to assess the effects of environmental clutter, which can be classified into several categories, by making comparisons of the measured data with the predicted values which take into account only the terrain losses. Several limitations were encountered in this process, e.g.

predictions could be made only for areas where terrain data had been made available; the predictions had to be made against the data as it was provided with no possibility of averaging data in a different way, over different areas or different lengths of route. For the common testing of programs, it was necessary to ensure that the same terrain (height-distance) profiles were fed into each procedure. This was, in general, achieved by using a subroutine of the BBC program, together with relevant segments of a UK national terrain data base (Dadson, 1978), to generate the terrain profiles.

In order to test the output predictions against the measured data, it was neccessary to make conversions to programs and to measured data to give a common parameter for purpose of comparison. This was chosen to be the path loss which would be relevant to a link between isotropic transmitting and receiving antennas. Hence, some of the programs which had previously given the result as a field-strength prediction (and sometimes as a field-strength prediction for a dipole transmitting antenna) had to be converted. Likewise, the transmitting and receiving parameters associated with the measurements had to be taken into account to give the equivalent loss between isotropic antennas.

To assess the capabilities of the various prediction techniques, the philosophy adopted for Data Sets 2 and 3 was to compare the measured and predicted results in a common way, using standard routines available in computer libraries. The main format adopted in this regard is to plot measured (y-axis) against predicted (x-axis) data and to evaluate the correlation and regression parameters of the best fit line, in comparison with the ideal line corresponding to the case when measured and predicted values would be equal. Other methods of comparison can involve the use of standard computer library contouring methods, as discussed by Bowman et. al., 1987, and Davies et. al., 1987.

1.5.1 Measurements in London

The results of comparison at 168, 455 and 900 MHz using Data Set 1 are described by Baker et. al., 1983. These comparisons include the computer-based methods of the BBC and of Longley-Rice, together

with results from the empirical models of Okumura (as formulated by Hata, 1980), the CCIR Rep. 567-3, and by Ibrahim-Parsons, 1983. The results indicated that although Central London is fairly flat, terrain losses were largely the cause of location variability at ranges of between 5 and 10 km. For both the BBC and Longley-Rice methods, the urban clutter factors (i.e. difference between the measured and predicted mean path losses) for the three frequencies all fell within the range 26 to 35 dB for distances of 5 km and greater.

The measurements in Data Set 2 for 450 MHz ranged up to 30 km along radial, circumferential and mixed path routes. Results of comparisons with the BBC, DRT and LRC computer-based predictions and with predictions from the Okumura method are described by Baker et. al., 1985. A summary of the regression and correlation analysis for predictions which refer only to terrain loss (i.e. when no allowance is made for urban clutter loss) is contained in Tab. 1.6.

Meas. mean path loss	Radial 133.5 dB			Circumferential 139.9 dB			Mixed 150.4 dB			All 141.6 dB		
Model	DRT	BBC	LRC	DRT	BBC	LRC	DRT	BBC	LRC	DRT	BBC	LRC
Error [dB] meas. - pred.	26.6	20.0	14.9	25.3	15.4	12.3	26.2	12.5	7.3	26.1	15.9	11.4
Correlation coefficient	0.91	0.90	0.91	0.68	0.59	0.58	0.81	0.77	0.71	0.89	0.87	0.84
Regression slope	0.91	0.57	0.81	0.85	0.48	0.38	0.98	0.81	0.50	0.96	0.66	0.60
Regression intercept.	36.1	68.9	37.5	42.3	80.5	91.9	28.5	38.3	78.6	30.7	58.4	63.4

Table 1.6: Summary of analysis for terrain loss predictions at 450 MHz

This shows that the DRT program produced a very good fit with the measured data, with regression slope near to unity, for all kinds of route, but with a consistent underestimate of about 26 dB in path loss. The BBC and LRC programs produced results similar to each other, but with values for regression slope smaller than those for the DRT predictions. It may also be noted that in further analyses which did include a correction for urban clutter the empirical method of Okumura generally compared quite well with the

computer methods with regard to mean error, but exibited considerably poorer correlation.

1.5.2 Measurements in Ipswich

As for Data Set 2, the measurements of Data Set 3 for Ipswich were used for further tests on the BBC, DRT and LRC programs, but at frequencies of 160 and 900 MHz. However, particular emphasis was also placed on the examination of two further prediction methods, namely the DBP method from Germany and the RAL method from the UK. The DBP method requires that a characteristic figure B for the land cover is included for each height/distance point along the terrain profile. Tests were conducted for the cases of open country all along the profile (no clutter), urban clutter all along the profile and thirdly with the actual land cover along the path (mixed mode).

As examples of the results obtained in the analysis, Figs. 1.2 and 1.3 give comparisons at 900 MHz for the DBP program (mixed mode) and for the RAL program (with clutter correction). A detailed summary of all analyses is provided in Tab. 1.7. For the BBC, DRT and LRC results, the regression characteristics are, in general, very similar to those determined in the analysis of Data Set 2. At 900 MHz, both the DBP program in its mixed path mode and the RAL program, with clutter correction, give very satisfactory results, with regression slope close to unity and small mean error, in comparison with this particular set of measurements for Ipswich. The DBP program is not intended for use at 160 MHz, but the RAL program performs very similarly to the DRT program at that frequency. It may also be of interest to note that the simple plane Earth procedure, which does not include diffraction and terrain height effects, has poorer correlation and is generally less satisfactory than the other methods at 900 MHz, but performs quite well at 160 MHz.

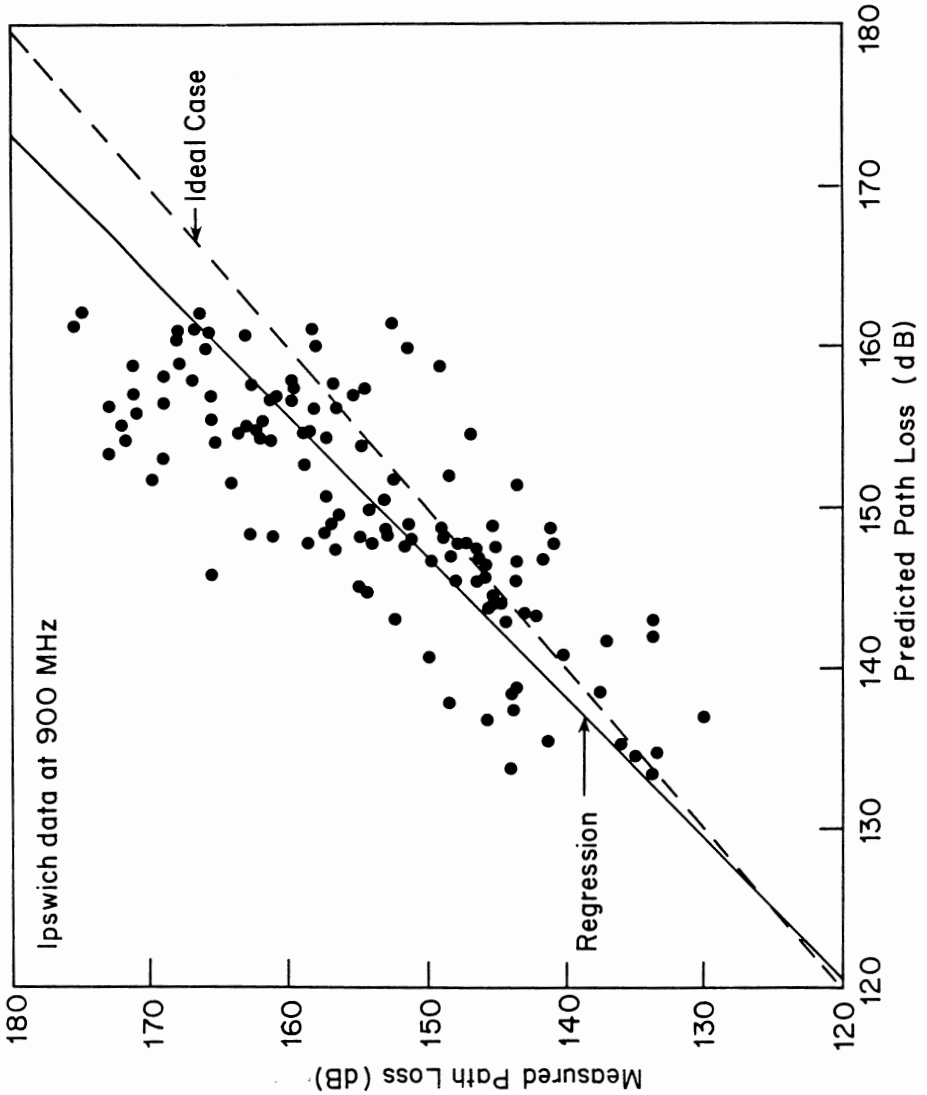

Figure 2: Comparison with the DBP program in the mixed mode

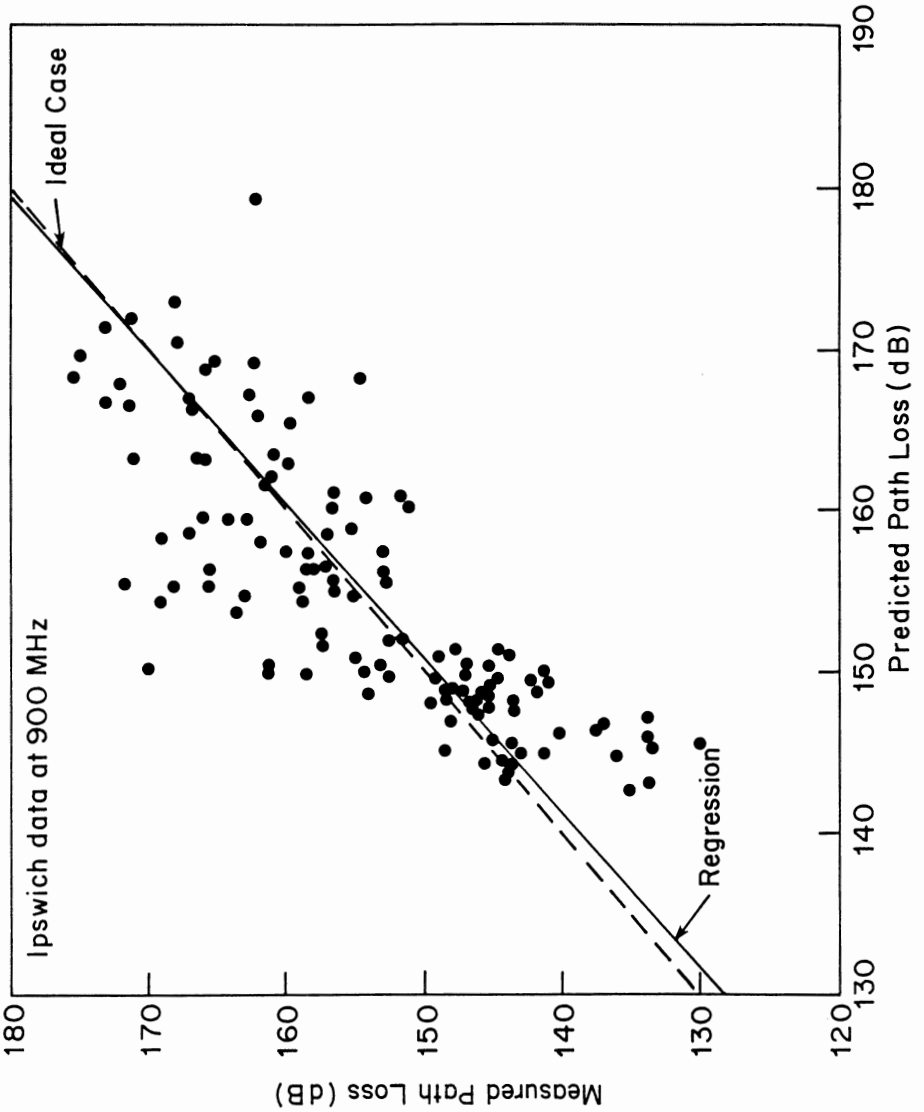

Figure 1.3: Comparison with the RAL program (with clutter correction)

Table 1.7: Summary of Ipswich Data Analysis

900 MHz MEASURED MEAN PATH LOSS ($\bar{Y}$) = 154.01 dB							
METHOD	PRED MEAN PATH LOSS (dB) $\bar{X}$	MEAN ERROR (dB) $\bar{e} = \bar{Y}-\bar{X}$	RMS DEV (dB) FROM REG LINE see note 1	STD DEV (dB) OF ERROR see note 2	REGRESSION SLOPE b	REGRESSION INTERCEPT a	CORRELATION COEFFICENT
BBC	128.03	25.98	5.57	7.44	0.647	71.19	0.853
BBC + CL*	146.22	7.79	5.57	7.62	0.635	61.20	0.853
DRT	116.82	37.19	5.76	5.97	1.224	11.03	0.842
LRC	132.79	21.22	5.81	7.34	0.687	62.73	0.813
LRC + CL	162.56	-8.55	6.29	7.35	0.691	41.68	0.808
LRCM + CL**	163.07	-9.06	6.40	7.26	0.710	38.17	0.800
RAL	124.97	29.04	6.39	6.37	1.029	25.38	0.802
RAL + CL	154.74	-0.73	6.47	6.45	1.039	-6.686	0.796
DBP	132.14	21.87	7.21	7.44	0.803	47.95	0.738
DBP + CL	153.54	0.47	6.42	6.91	1.448	-68.32	0.800
DBP Mixed	150.02	3.99	6.55	6.62	1.153	-19.03	0.790
Plane Earth	112.94	41.07	7.76	8.38	1.802	-49.53	0.687

160 MHz MEASURED MEAN PATH LOSS ($\bar{Y}$) = 130.46 dB							
BBC	120.77	9.69	3.44	4.51	0.635	53.75	0.831
BBC + CL	135.97	-5.51	3.48	4.53	0.635	44.16	0.826
DRT	101.41	29.05	3.03	3.12	1.172	11.63	0.871
LRC	116.26	14.20	3.50	4.14	0.695	49.66	0.824
LRC + CL	134.78	-4.32	3.55	4.11	0.706	35.36	0.818
LRCM + CL**	135.04	-4.58	3.61	4.03	0.733	31.52	0.811
RAL	104.38	26.08	3.37	3.43	1.152	10.21	0.838
RAL + CL	122.90	7.56	3.39	3.48	1.198	-16.81	0.836
Plane Earth	112.94	17.52	4.08	4.11	1.137	2.04	0.750

* CL = with clutter correction ** = Longley Rice with median value for Δh

Note 1 RMS deviation from regression line = $\mathrm{SQRT}\left[\frac{1}{(N-2)}\sum_{1}^{N}(y_i - a - bx_i)^2\right]$

Note 2 Standard deviation error = $\mathrm{SQRT}\left[\frac{1}{(N-1)}\sum_{1}^{N}(y_i - x_i - \bar{e})^2\right]$

1.6 INFLUENCE OF LAND COVER AND CORRECTION FACTORS

The previous sections have shown that improved accuracy can be obtained by considering the diffraction loss along the path between mobile and base station. Different approaches to estimate the diffraction loss due to terrain are discussed in section 1.8. Additional loss will also caused by any obstacles, e.g. forest or buildings, along the path and in the vicinity of the mobile. One solution to this problem is to add a correction factor to the path loss determined by a particular prediction model. This allows curves such as those in CCIR Rec. 370-4 (land and sea) or Rep. 567-3 (urban) to be used in different environments as well as enhancing the accuracy of the prediction models described in section 1.4.

These correction factors can be determined from measurements of radio path loss taken in areas of a uniform type of land cover. The correction factor is usually the difference between the measured and predicted path loss, and is therefore related to the definition of the particular type of land cover and the prediction model used. For example, the correction factor for a village is not the same in Finland and Denmark, because it is customary to surround the houses and gardens with trees in Finland.

The measurements from which the correction due to land cover (land cover factor) are derived, have nearly all been made with narrow-band measuring systems. However, the factors are equally valid for narrow- and wide-band systems, as they deal with the path loss.

The values range from 0 to nearly -30 dB (relative to open areas). The necessary number of land cover factors depends on how large a part of the total range each land cover factor shall represent. For example, the range for the factor for urban areas may be smaller, if the variance caused by street orientation is excluded. The range of the correction will thus put a limit to the accuracy of the prediction.

Most countries use at least four land cover factors, and some use up to ten. A comparison of descriptions of similar land cover categories from three countries which use many land cover factors and the corresponding values has been made, but although the general trend is the same, the result did not show the harmony required to establish a common universal scale. The reason for this seems to be twofold. The nature and interpretation of a specific land cover differ between the countries, and different models for the propagation loss as a function of distance will yield differences in land cover factors.

When the list of land cover categories is being defined, it is natural to match the description of the typical land covers evenly over the total range of the factors. As the standard deviation of the underlying measurements is in the order of 7 to 9 dB, some countries consider four land cover categories to be sufficient, but it could be argued that with more categories the land cover factors may introduce less bias on the result.

Table 1.8 shows the categories considered useful in the United Kingdom (Gurdenli et. al., 1987), and it is typical in structure for the use of many detailed categories. Table 1.9 shows a comparison between the definition of categories from different sources, and the lack of harmony is evident. In Table 1.10 some land cover factors from different sources have been normalized to refer to field strength in open land.

Because of the obvious inconsistency of the values most of the countries or agencies who are using land cover factors, tend to agree that they have to be worked out by the same agency which is going to use them.

Category	Description
0	Rivers, lakes and seas
1	Open rural areas; e.g. fields and heathlands with few trees
2	Rural areas; similar to the above but with some wooded areas, e.g. parkland
3	Wooded or forested rural areas
4	Hilly or mountainous rural areas
5	Suburban areas, low density dwellings and modern industrial estates
6	Suburban areas, higher density dwellings; e.g. council estates
7	Urban areas with buildings of up to four storeys, but with some open space between
8	Higher density urban areas in which some buildings have more than four storeys
9	Dense urban areas in which most of the buildings have more than four storeys and some can be classed as "skyscrapers". This category is restricted to the centre of a few large cities.

Table 1.8: Land-cover categories

Table 1.8	BBC (UK) [Causebrook, 1982]	Denmark	Okumura [1968]
0	-	-	Land/sea
1	1	0/2	-
2	1	1/2	-
3	1	4	-
4	1	-	Undulating
5	2	3	Suburban
6	2	6	Suburban
7	3	7	Urban
8	3	8	Urban
9	4	9	Urban

Table 1.9: Comparison with other land-cover categorisations

Country	Urban	Suburban	Forest	Open land
Denmark	-23.0 dB	-18.0 dB	-15/-20 dB	0 dB
Finland	-22.7 dB	-19.7 dB	-20.0 dB	0 dB
Germany Fed. Rep. of	-23.9 dB	-23.9 dB	-23.7 dB	0 dB
Italy	-24.9 dB	-17.6 dB	-	0 dB
Okumura	-29.0 dB	-19.0 dB	-	0 dB

Table 1.10: Comparison of land cover factors for 900 MHz

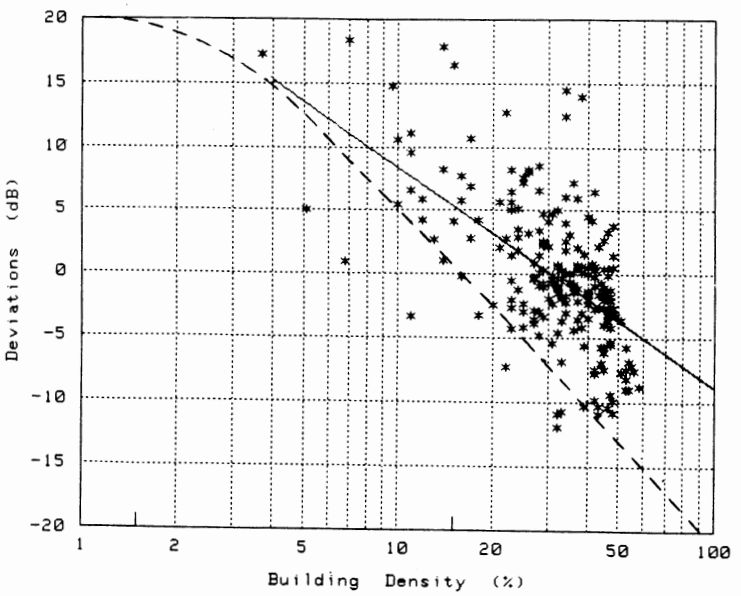

Figure 1.4: 1st order deviations from median field strength values vs building density

——— best fit curve

- - - - - from Kozono and Watanabe

1.7 INFLUENCE OF URBAN STRUCTURE AND STREET ORIENTATION

A number of measurements have been recently performed in Italy (at 900 MHz in Turin and at 450 MHz in Milan), in order to investigate the effects of the urban structure (building density, height of buildings, width of streets, street orientation) on mobile propagation. In this section the most significant results are presented, based on data collected at 900 MHz.

Building densities (i.e. the percentage α of areas covered by buildings) were evaluated on 500 x 500 m^2, according to the definition in CCIR Rep. 567-3, and deviations from the median propagation curve (obtained by interpolation of local mean data, measured on route lengths of about 1 km) have been related to them.

Fig. 1.4 shows such deviations D_1 in dB and the corresponding regression line in log-linear scales.

The regression line results in

$$D_1 = 25.66 - 17.25 \log \alpha \quad . \tag{1.7}$$

A comparison with results of Kozono and Watanabe, 1977, (also reported in CCIR Rep. 567-3) shows similarities both in slope ($\approx$17 dB/decade instead of $\approx$25 dB/decade) and average density ($\approx$30 % instead of $\approx$15 %). Using Eq. (1.7) which is very similar to that obtained from measurements carried out at 450 MHz, a 1.1 dB reduction in the RMS prediction error is achieved.

If a linear regression is established (instead of a logarithmic one), Eq. (1.7) becomes

$$D_1 = 9.84 - 0.29\ \alpha \quad , \tag{1.8}$$

which gives the same RMS prediction error as Eq. (1.7). This confirms that a log-regression seems to provide no advantages versus a simple linear one. Incidentally, the slope coefficient in Eq. (1.8) is very close to the corresponding coefficient (0.265) found by Ibrahim and Parsons, 1983, from measurements at 455 MHz carried out in London.

A slightly better prediction improvement can be achieved if a 2nd order correction factor (the local ratio β of the average height of buildings to the average width of streets) is introduced. In this case, the following regression allows a further reduction of about 0.6 dB in the RMS prediction error:

$$D_2 = -1.22 - 5.98 \log \beta \quad . \tag{1.9}$$

This compares favourably with multiple linear regressions found by Ibrahim and Parsons, in which the degree of "urbanisation factor" U (defined as the percentage of built-up area occupied by buildings with four or more floors) is used, instead of β, for the centre of London.

A number of measurements were performed along routes approximately parallel or transverse to the propagation direction. Relative orientations δ (angles of "line-of-sight"-wave arrival with respect to the direction of vehicle motion, in degrees) were measured, and relative deviations from median values computed, the least squares fit gives:

$$D_3 = 7.14 - 3.72 \log \delta \quad . \tag{1.10}$$

The use of Eq. (1.10) results into an additional improvement of about 0.4 dB in the RMS prediction error.

As a conclusion, a few parameters have been identified: they appear to contribute to local mean deviations from median field strength values with different weights. A number of tentative regressions were established, which allow the RMS prediction error to be considerably reduced with an overall improvement better than about 35 %. Similarities and differences with other results corroborate the hypothesis that correction factors may be strongly related not only to the local, but also to the large scale urban structure. Therefore, caution should be exercised in extensively using the above quoted regressions.

1.8 METHODS TO ESTIMATE DIFFRACTION LOSS

This section deals with the very frequent situation of a receiver placed in a shadow zone, where no ray from the transmitter can be directly received. In such a situation the contribution to the total path loss from the diffraction phenomenon is usually very high.

An accurate evaluation of this effect requires an exact solution of Maxwell's equations and therefore a very detailed description of boundary conditions (i.e. a very high data base solution) as well as an enormous computing time. The big cost of this approach led to the development of several approximate methods providing a tradeoff between accuracy and speed in computing.

Rather than point out the most suitable procedure for inclusion in a prediction model, since this matter is still giving rise to

much controversy in the literature, these comments are aimed at warning the reader that there are differences among the most common solutions. A general classification of these solutions can make reference to the following approaches:

(a) Solutions based on the Huygens-Fresnel theory

The application of the Huygens-Fresnel theory to the evaluation of diffraction losses relies on the assumption that a hill can be represented by a perfectly absorbing "knife-edge". Although this is a quite rough approximation, it allows the use of results developed in the knife-edge case in optics and is, therefore, extensively used.

In addition to the simplest case of a single knife-edge, it is worth mentioning the work by Millington, 1962, dealing with the case of two consecutive knife-edges. The proposed procedure, solving analytically the double Fresnel integral, is quite arduous and the authors themselves advise the reader against the extension to a higher number of obstacles. More recently Vogler, 1982, achieved a theoretical expression with more than two knife-edges.

This expression is in a form that could be easily inserted in a computer program, but the complexity and the computing time are considerable.

(b) Approximated solutions based on the Huygens-Fresnel theory

Some of the most common methods (Epstein-Peterson, 1953, Deygout, 1966, Giovaneli, 1984, CCIR Rep. 715-2) fall within this category. They are characterized by different geometrical approaches, all leading to the total attenuation loss as a sum of the contribution of each obstacle, regarded as a single knife-edge, computed by means of the Fresnel integral.

An extensive comparison among the aforementioned methods with reference to the Millington's results, drew the conclusion that the Deygout's method provides an attenuation estimate higher than expected, whereas the Epstein-Peterson's method

yields lower values. The more recent Giovaneli's method provides more accurate estimates. The complexity of the various methods is quite similar.

(c) Semi-empirical solutions

An empirical approach forms the basis of both the Longley-Rice model, 1968, and the "terrain clearance angle" method (CCIR Rep. 239-6).

The main advantage of these methods lies in their capability to operate without a detailed knowledge of the whole propagation path. The Longley and Rice model requires as input a few characteristic parameters of the terrain-height profile and a statistical parameter (Δh) giving a rough estimation of terrain irregularities (undulation).

The clearance angle method is even simpler requiring just the value of the angle defined by the horizontal line at the receiver and the line which clears all obstacles within 16 km in the direction of the transmitting site.

These methods allow a fast evaluation but a poor accuracy.

(d) Solutions based on ray methods

It should be noted that the previous approaches refer to a two-dimensional description of the radio path, i.e. only the direct radio wave is considered. A more accurate computation should also take into account the reflections of the radio waves at terrain variations occuring beside the direct radio path profile. This possibility is on principle afforded by the solutions based on ray methods.

Among the solutions based on ray methods, the Geometrical Theory of Diffraction (GTD) and its improvements, namely the Uniform Theory Diffraction (UTD) and the Uniform Asymptotic Theory (UAT), seem to be the most suitable for inclusion in a field-strength prediction model. Descriptions of these theories can be easily found in literature. Here it is worth noting

that they can cope with very complex situations (e.g. urban areas) at the cost of a higher computational effort.

A new procedure exploiting both the Huygens-Fresnel theory and the GTD, recently proposed by Whitteker, 1984, seems to occupy a place between the analytical theories and the method of Vogler, both in complexity and accuracy.

1.9 CONCLUSIONS

Various prediction methods have been compared with measurements. The comparisons show that models are available that predict values of radio path loss which are within 6 to 9 dB standard deviation of measured data on the selected test areas. However, four systematic shortcomings of the various models were observed:

- The incorporation of additional loss due to the land cover, which differs from country to country, is particularly important in the UHF-range and can improve the accuracy of the model by up to 30 dB.

- The performance of all models depends strongly on the content of the data bases.

- In hilly terrain, the reflection at obstacles like mountain slopes are not taken into account by a two-dimensional path profile between the mobile and base station.

- Radio path loss calculations of mini and micro cells are generally not possible.

In spite of these shortcomings the prediction models are a powerful tool for radio service planning. Future activities should be concentrated on the reduction of these shortcomings and the harmonizing of the prediction models for Europe by exploiting the huge and rapid advances of data processing in the last years.

1.10 REFERENCES

Baker, P.W., Davies, P.G. and Haley, R., 1983, "Propagation characteristics and prediction techniques relevant to land mobile radio applications", IEE. Conf. Publ., Vol. 224, 61-65.

Baker P.W., Davies, P.G. and Haley, R., 1985, "Propagation path losses at 450 MHz in London relevant to land mobile radio applications: Comparisons of values predicted utilising the UK terrain data base with measured data", ICAP 1985, IEE. Conf. Publ., Vol. 248, 385-389.

Blomquist, A. and Ladell, L., 1974, "Prediction and calculation of transmission loss in different types of terrain", AGARD Conf. Publ., Vol. CP-144, 32/1-25.

Bowman, M. R. and Davies, P.G., 1987, "VHF and UHF signal loss predictions and terrain topography: Application to model development, service area coverage and co-channel interference", ICAP 87, IEE Conf. Publ., Vol. 274, 90-94.

Causebrook, J.H., Davies, B., Eaton, J.L., King, R.W., Knight, P., Lee, R.W. and Tait, B., 1982, "Computer prediction of field strength: A manual on methods developed by the BBC for the LF, MF, VHF and UHF bands", Engineering Division, BBC, 1982.

CCIR, 1986, "Recommendations and Reports of the CCIR, Propagation in Non-Ionized Media", Vol. V, Rep. 239-6, Rec. 370-4, Rep. 567-3, Rep. 715-2.

Dadson, C.E., 1978, "Radio network and radio link survey derived by computer from a terrain data base", AGARD Conf. Proc., Vol. 262, Paper No. 25.

Davies, P.G. and Bowman, M.R., 1987, "Analysis of computer-based prediction methods of propagation path loss for land mobile radio applications at 160 and 900 MHz", Proc. Int. Conf. on Digital Land Mobile Radio Applications, Venice, Italian SIP, 180-189.

Deygout J., 1966, "Multiple knife-edge diffraction of microwaves," IEEE Trans. on Antenna Propagation, Vol. AP-14, 480-489.

Epstein, J. and Petersen, J.W., 1953, "An experimental study of wave propagation at 800 MC", Proc. IRE, Vol. 41, 595-611.

Giovanelli, C.L., 1984, "An analysis of simplified solutions for multiple knife-edge diffraction", IEEE Trans. on Antenna Propagation, Vol. AP-32, 297-301.

Gurdenli, E., Huish, P., King, L.E. and Nicholls, M.J., 1987, "Land usage factors in mobile radio propagation prediction", Fourth International Conference on Land Mobile Radio, Warwick, UK, IEE Conf. Publ. Vol. 78.

Hata, M., 1980, "Empirical formulae for propagation loss in land mobile radio radio services", IEEE Trans. on Vehicular Technology, Vol. VT-29, 317-325.

Huish, P.W. and Gurdenli, E., 1988, "Radio channel measurement and predictions for future mobile radio systems", British Telecom Technology Journal, Vol. 6, No 1.

Ibrahim, M.F. and Parsons, J.D., 1983, "Signal strength prediction in built-up areas, part 1: median signal strength", IEE Proc., Part F, Vol. 130, 377-391.

Kajamaa, T., 1986, "900 MHz propagation measurements in Finland in 1983-85", Nordic Radio Symposium, Stockholm.

Kozono, S. and Watanabe, K., 1977, "Influence of environmental buildings on UHF land mobile radio propoagation", IEEE Trans. on Communication, Vol. COM-25, 1133-1143.

Löw, K., 1986, "UHF Field-strength measurements for determination of the influence of buildings and vegetation in the land mobile radio service", IEEE VTC'86 Conference Record, 40-45.

Loew, K. and Lorenz, R.W., 1983, "Determination of service areas for mobile communication with a topographical data base", IEEE ICC'83 Conference Record, 54-58.

Longley, A.G., 1978, "Radio propagation in urban areas", OT Report 78-144, Office of Telecommunications, Boulder, Colorado.

Longley, A.G. and Rice, P.L., 1968, "Prediction of tropospheric radio transmission loss over irregular terrain - a computer method", ESSA Technical Report ERL79 - ITS67.

Millington, G., Hewitt, R. and Immirzi, F.S., 1962, "Double knife-edge diffraction link loss models", IEE Proc., Part C, Vol. 109, 419-429.

Okumura, Y., Ohmori, E., Kawano, T. and Fukuda, K., 1968, "Field strength and its variability in VHF and UHF land mobile radio service", Review of the ECL, Vol. 16, 825-873.

Reudink, D.O., 1974, "Properties of mobile radio propagation above 400 MHz", IEEE Trans. on Vehicular Technology, Vol. VT-23, 143-159.

Rose, D.J., 1982, "160 and 900 MHz propagation survey in Ipswich", British Telecom Memo. No. R6/003/82.

Vogler, L.E., 1982, "An attenuation function for multiple knife-edge diffraction", Radio Science, Vol. 17, 1541-1546.

Whitteker, J.H., 1984, "Near-field ray calculation for multiple knife-edge diffraction", Radio Science, Vol. 19, 975-986.

2. MULTIPATH PROPAGATION

2.1. INTRODUCTION TO THE MULTIPATH MOBILE RADIO CHANNEL

2.1.1. LIST OF SYMBOLS

α_i	angle of incidence
a	amplitude
d	distance
f	frequency
ω	angular frequency $(2\pi f)$
x	distance,position
ω_x	spatial frequency $(2\pi/x)$
λ	wavelength
β	$2\pi/\lambda$
t	time
ϕ	phase
v	speed
τ_d	group delay
$\dot{\phi}(x)$	spatial random FM
$H(\omega,x)$	frequency transfer function
$h(t,x)$	time transfer function
$H(\omega_x,t)$	spatial frequency transfer function
$P(t,x)$	instantaneous power delay profile $(= \lvert h(t,x)\rvert^2)$
$P(t)$	average power
$P(x)$	instantaneous average power
S	delay spread
$B(t)$	Doppler spread
T_d	mean delay
$\overline{\omega_d(t)}$	mean Doppler frequency

2.1.2. INTRODUCTION

The mobile radio channel acts as a two terminal pair network with characteristics which vary in space, time and frequency. The channel characteristics must be described by statistical parameters because of the variable nature of the propagation path. The characteristics of the channel are divided into slowly varying and fast varying components. The slow variations depend on the general topography and the frequency band chosen. The fast variations depend on the phasor addition of the multipath components and hence vary as the relative path lengths vary within the wavelength. The slow variations give a variation in the median level of the fast variations. It is the latter which limit the bandwidth over which a radio system

can operate. Hence it is the description of these fast variations which has received most attention. Note that here "fast" refers not only to temporal changes or fading but also to the space and frequency variations. Even for static multipath, i.e. when transmitter, receiver, and scatterers are not moving, the e.m. field laid down by the transmitter can vary rapidly in space. Also the field at a particular point may vary rapidly in amplitude and phase as the frequency is altered.

A number of authors have given mathematical descriptions of the multipath radio channel, e.g. (Bello, 1963), (Stein and Jones, 1967), (Clarke, 1968), (Parsons and Bajwa, 1982), (Proakis, 1983). The mathematical descriptions usually take the channel to be a time-varying channel with random characteristics. When the channel is taken to be a WSSUS channel simplifications can be made in its description as demonstrated by (Bello, 1963).

Before going into the mathematical detail it is useful to consider the simple cases of propagation by two or three paths. These give a physical picture of what occurs and illustrate the effects produced.

2.1.3. TWO AND THREE RAY PATH MODELS

2.1.3.1. Two path model

Suppose that a signal can propagate between transmitter and receiver by a direct ray and a second ray travelling by a longer path, Fig.2.1.1. At the receiver the signal is the phasor sum of the two signals. Consider the received signal at a frequency f, wavelength λ. If the path lengths are d_1 and d_2, and the amplitudes of the two signals at the receiver are a_1 and a_2, the received signal is given by

$$s(t) = a_1 \exp[-j\beta d_1] + a_2 \exp[-j\beta d_2] \qquad (2.1.1)$$

in which the phase change coefficient is

$$\beta = \frac{2\pi}{\lambda}$$

If the first signal is taken as the reference the received signal can be written as

$$[\ 1 + \frac{a_2}{a_1}\ exp[-j\beta(d_2-d_1)]\ ]\ a_1\ exp[-j\beta d_1] \qquad (2.1.2)$$

The expression within the large brackets can be regarded as an amplitude and phase modulation of the first arriving signal. To show what happens with changes in relative amplitude and path lengths it is only necessary to show what happens to the terms within the large bracket. So put

$$\begin{aligned} r(t) &= 1 + A\ exp[-j\beta\Delta d] \\ &= 1 + A\ exp[-j2\pi f\Delta\tau] \qquad (2.1.3) \end{aligned}$$

in which

$$A = \frac{a_2}{a_1}$$

$$\Delta d = d_2 - d_1$$

$$\beta\Delta d = 2\pi f\Delta\tau$$

and $\Delta\tau$ is the relative time delay between the signal arriving by the direct path and that arriving by the second path.

Phasor diagrams can be drawn to show how the resultant $r(t)$ will vary with changes in A and $\Delta\tau$. Fig.2.1.2 shows the case in which $A<1$, the second path amplitude is less than the direct path amplitude. In this case as $\Delta\tau$ increases the second signal phasor rotates, the amplitude of the resultant varies between limits of $1\pm A$ and the phase swings between limits of $\pm\pi/2$. Fig.2.1.3 shows the case in which $A>1$. In this case the amplitude varies between $A\pm1$ and the phase rotates

continuously. The amplitude and phase variations are plotted in Fig.2.1.4(a,b). The relative delay is $\Delta\tau = 1\mu s$, the frequency varies between 900-910MHz and the two cases are for $A = 0.9$ and $A = 1.1$. It is seen that in both cases the amplitude variation is the same but in the first case the phase swings about a constant value whilst in the second case the phase swings about a constantly increasing value, plotted mod 2π.

It is well known that the condition for no distortion in transmission is that the amplitude response of a channel should be constant and that the phase response should be a linear function of frequency. Clearly this is not the case. The greatest divergence from the conditions for no distortion occur at the minima in the amplitude response. At these points there are rapid changes in both amplitude and phase response. Near the maxima the amplitude and phase responses are relatively flat so a narrow band signal transmitted at a frequency near a maximum would suffer little distortion.

In general the delay between the two paths is not constant and so the amplitude and phase responses are functions of position and time. The signal distortion then becomes time varying and also, because the phase response is time varying, effects such as Doppler shifts appear.

Clearly even a two path channel can produce severe distortion.

2.1.3.2. Three path model

To give a further illustration the response of a three path model is shown in Fig.2.1.5. In this case the second path is the strongest and the amplitude and phase responses become more complicated. It becomes more difficult to identify the effects of the individual paths and such a model will produce more distortion than the two path model.

It becomes necessary to develop more comprehensive models for the properties of multipath channels and to develop the mathematical tools needed to describe the channel and its effects on signals.

2.1.4. MULTIPATH CHANNELS

The development of the characterisation of multipath channels owes much to the work of (Bello, 1963).

This work has led to the use of the tapped delay line model for multipath channels. Much experimental work has been carried out to characterise radio channels to establish the parameters to be used in such models for system simulation and design.

A multipath channel is one in which the output signal is the sum of a number of signals arriving by different propagation paths. Each path will have its own impulse response or frequency transfer characteristic. For narrow-band signals the impulse responses may be assumed to have attenuations and time delays which are independent of frequency. Use of the term narrow-band may be taken to imply that the signal bandwidth is small enough that this assumption can be made about the response of the channel.

For many channels the attenuation and delay vary with time, e.g. because transmitter, receiver, or scatterers are moving, usually at a rate slow compared with both the carrier frequency and the modulation frequencies. If these assumptions are made about the signal and the channel, the output signal from the channel may be expressed in a reasonably simple form.

2.1.5. DEFINITIONS

It is necessary to define the parameters which should be measured by experiment.

2.1.5.1. Frequency and time domain transfer functions

In a multipath channel, partial signals from a multitude of scatterers at different delays (distances) and directions, arrive at the receiver. Assuming far field scatterers only, the general transfer function in the frequency domain follows from (Andersen, 1988):

$$H(\omega,x) = \sum a_i \exp(j\phi_i) \exp(-j\beta d_i) \qquad (2.1.4)$$

where $a_i \exp(j\phi_i)$ is the complex magnitude of one scatterer and βd_i is the electrical distance from the point of observation to the position of the scatterer. By expressing the electrical distance in terms of a given delay $t_i = \beta d_{oi}/\omega$, spatial doppler shift $\omega_{xi} = \beta \cos(\alpha_i)$, position x, we get eqn.(2.1.4) re-written as:

$$H(\omega,x) = |H| \exp(j\phi) = \sum a_i \exp[j(\phi_i - \omega t_i + \omega_{xi} x)] \qquad (2.1.5)$$

where α_i is the angle of incidence of the ith scatterer. Shifting to the time domain, eqn.(2.1.5) leads to the channel impulse response

$$h(t,x) = \sum a_i \exp[j(\phi_i + \omega_{xi} x)] \; b(t - t_i)$$

$$= |h(t,x)| \exp(j\phi) \qquad (2.1.6)$$

where b(t) is the impulse response of the receiver filter and $P(t,x) = |h(t,x)|^2$ is the instantaneous power delay impulse response. Integrating $P(t,x)$ over the delay axis we get the instantaneous average power $P(x)$ of the channel.

The channel impulse response is measured directly or is derived from the frequency response measurements. In either case there is a finite measurement period and so the 'instantaneous' impulse response cannot be found. However it is usual to treat the measured response as if it were the instantaneous response.

Integrating over a certain distance Δx, we get the average power delay profile (or impulse response) $P(t)$. For general statistical analysis, the second central moment of $P(t)$, called the delay spread S, is used. For many measurements an equivalent delay spread is found for the instantaneous impulse response $P(t,x)$. This is not identical to the original, but it is also useful. In the next sub-chapter the instantaneous delay spread is defined.

The phase derivative functions of frequency and time (distance) are also of importance. In the frequency domain

$$\tau_d(\omega) = \frac{\mathrm{Im}[H(\omega).H'(\omega)^*]}{|H(\omega)|^2} \tag{2.1.7a}$$

is the group delay. Similarly, in the spatial (time) domain:

$$\dot{\phi}(x) = \frac{\mathrm{Im}[H(x).H'(x)^*]}{|H(x)|^2} \tag{2.1.7b}$$

is the random FM.

These follow a Student's t-distribution (Andersen, 1988), (Jakes, 1974). It is noted that the denominator is the instantaneous power, which means that high excursions occur at deep fades. The envelope signal $|H|$ will follow Rayleigh or Rician distributions depending on whether a dominant direct path is present.

The temporal (frequency) and spatial (distance) coherence functions $\phi(\Delta\omega,\Delta x)$ can be found from (Jakes, 1974) as well as the temporal spatial correlation function $C(\Delta\omega,\Delta x)$.

Moving from the spatial domain to the time domain is just a matter of multiplying the spatial frequency ω_x (rads/m) by the vehicle velocity v (m/s). Equivalently the distance $x(\omega)$ is converted to time by division with λ.

2.1.5.2. Definitions of parameters used to describe the impulse response

A number of definitions can be made for parameters of the radio channel which may be derived from the "instantaneous" impulse response, (Lorenz, 1987). In this paper it is assumed that the true impulse response of the channel can be found although it must be remembered that many so-called impulse response measurements are taken over an appreciable period of time and distance and do not represent a true impulse response at a single point.

Referring to Fig.2.1.6, the following terms are used.

In the measuring system

μ_{nf} noise floor

a_n lowest level evaluated, 3dB above μ_{nf}

For line-of-sight measurements

d_{LOS} the geometric path length between transmitter and receiver the 'line-of-sight' distance

μ_{LOS} the peak value of the impulse response the l-o-s measurement should not vary by more than 1dB else multipath propagation prevails

W_o pulse width at the 3dB level below μ_{LOS}

t_{LOS} l-o-s time delay this assumes that time to a common standard is known at transmitter and receiver

r_D dynamic range of the measurement system

$r_D = \mu_{LOS} - \mu_{nf} - a_n$

The l-o-s parameters characterise the performance of the measurement system. The parameters W_o and $r_D(d_{LOS})$ should be reported for several path lengths between 2 and 10 Km. The detection law of the receiver should be reported, e.g. logarithmic, linear, diode.

Because of multipath propagation the energy arriving at the receiver is spread in time, Fig.2.1.7. Referring to Fig.2.1.7. the following parameters are defined.

t_m time of arrival over the geometric path length

t_o time of arrival at which signal first rises through a level $\mu_{nf} + a_n$

t_3 time of arrival at which signal last falls through a level :$\mu_{nf} + a_n$

t_p time of arrival at which signal is a maximum

A delay interval may be defined which includes a certain fraction of the overall energy. In the time interval between t_1 and t_2 the energy received at position x is:

$$\int_{t_1}^{t_2} P(t,x)\ dt = q \int_{t_o}^{t_3} P(t,x)\ dt = q\ P(x)$$

where

$$P(x) = \int_{t_o}^{t_3} P(t,x)\ dt$$

is the total energy in the impulse response.

The delay spread should be evaluated at the following values of the fraction q.

the last decentile	$q = 90\ \%$
the last quartile	$q = 75\ \%$
the median	$q = 50\ \%$

The delay intervals are found from the evaluations:

$$W_q = (t_1 - t_2)_q$$

For reliable measurements the peak amplitude should be more than 20dB above the level $\mu_{nf} + a_n$.

The average delay should be referred to the time of arrival which would occur over the geometric path length.

$$T_D(x) = \frac{1}{P(x)} \int_{t_m}^{t_3} t\ P(t,x)\ dt$$

This definition of the average takes into account the jitter in the time of arrival of the first component of the energy. This delay can only be measured if precise time standards are available.

The delay spread, S, is defined by

$$S^2(x) = \frac{1}{P(x)} \int_{t_0}^{t_3} t^2 P(t,x)\ dt - [\ \frac{1}{P(x)} \int_{t_0}^{t_3} t\ P(t,x)\ dt\ ]^2$$

As mentioned in the previous sub-chapter, the original definition of delay spread is based on the average power delay profile. With the time-frequency duality from (Bello, 1963) in mind, we can shift to the spatial frequency domain where S describes the dispersion in the time domain, i.e. we can find the dispersion in the spatial frequency domain , as the Doppler spread.

$$B^2(t) = \frac{\int \omega_x^2\ H(\omega_x,t)\ d\omega_x - [\overline{\omega_d(t)}]^2}{P(t)} \qquad (2.1.8)$$

where $H(\omega_x,t) = \int h(x,t)e^{-j\omega_x x}dx$ is the Doppler spectrum (spatial Fourier Transform) of the spatial impulse response signal at delay t, while $\overline{\omega_d}$ is the mean Doppler frequency of $H(\omega_x,t)$.

2.1.6. STATISTICAL REDUCTION OF MEASUREMENTS

The various correlation functions derived in the previous section provide a framework for describing the radio channel but the results of measurements require further statistical reduction to provide data useful in design work. This further reduction must take into account the variable nature of the channel with position and the multipath characteristics of the channel which may include both continuous and discrete components. Extreme values must be included in the analysis as the performance of a system depends on what happens for small parts of the time or at a small number of locations.

The presentation of measured results is discussed by Gurdenli, (Gurdenli, 1987), who makes the point that when typical power delay profiles are chosen they should not only represent the range of conditions which may be expected, e.g. for dense urban areas and for mountainous regions, but also in considering the results of tests allowance must be made for the

likelihood of a mobile encountering these conditions. Whilst extreme conditions may be found in certain geographical locations these will matter little if there are to be no subscribers in these areas.

2.1.7 REFERENCES

ANDERSEN, J.BACH, EGGERS, P., ANDERSEN, B.L.,1988, "Propagation aspects of data communication over the radio channel - a tutorial", Eurocon 88, Stockholm, Sweden, June 13-17.

ANDERSEN, J.BACH, LAURITZEN, S.L., THOMMESEN, CHR., 1986, "Short term statistics of phase derivatives in mobile communications", 36th IEE Vehicular Technology Conference, Dallas, Texas, May 1986, pp.228-231.

BELLO, P.A., 1963, "Characterisation of Randomly Time-Variant Linear Channels", IEEE Trans. CS-11, (4), pp.360-393.

CLARKE, R.H., 1968, "A Statistical Theory of Mobile radio Reception", Bell Sys. Tech. Journal, 47, pp.957-1000.

GURDENLI, E., 1987, Wide-band measurements of the land mobile radio channel at 900 MHz", Proceedings of the IERE Int Conf on Land Mobile Radio, Warwick, UK, December 1987.

JAKES, W.C.,1974, "Microwave mobile communications", Wiley, New York.

LORENZ,R., 1985, "Approximation of power delay spectra occurring typically in mobile radio channels for the construction of a wide-band fading simulator", 207TD (85) 30.

LORENZ, R.W., LOW, K., WEBER, M., 1987, "Evaluation of delay profiles in mountainous terrain", 207TD (87) 16.

PARSONS, J.D. and BAJWA, A.S., 1982, "Wide-band Characterisation of Fading Mobile Radio Channels", IEE Proc-F, 129, (2), pp.95-101.

PROAKIS, J.G. 1983, "Digital Communication", McGraw-Hill Book co., New York, pp.454-470.

STEIN, S. and JONES, J., 1967, "Modern Communication Principles with Application to Digital Signaling", McGraw-Hill Book co., New York, pp.329-345.

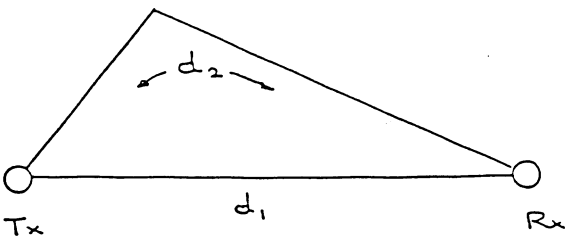

Fig.2.1.1. Two path model.

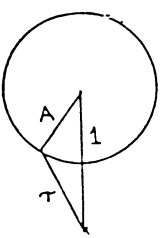

Fig.2.1.2. Two path model phasor diagram, A<1.

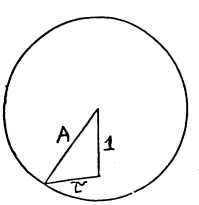

Fig.2.1.3. Two path model phasor diagram, A>1.

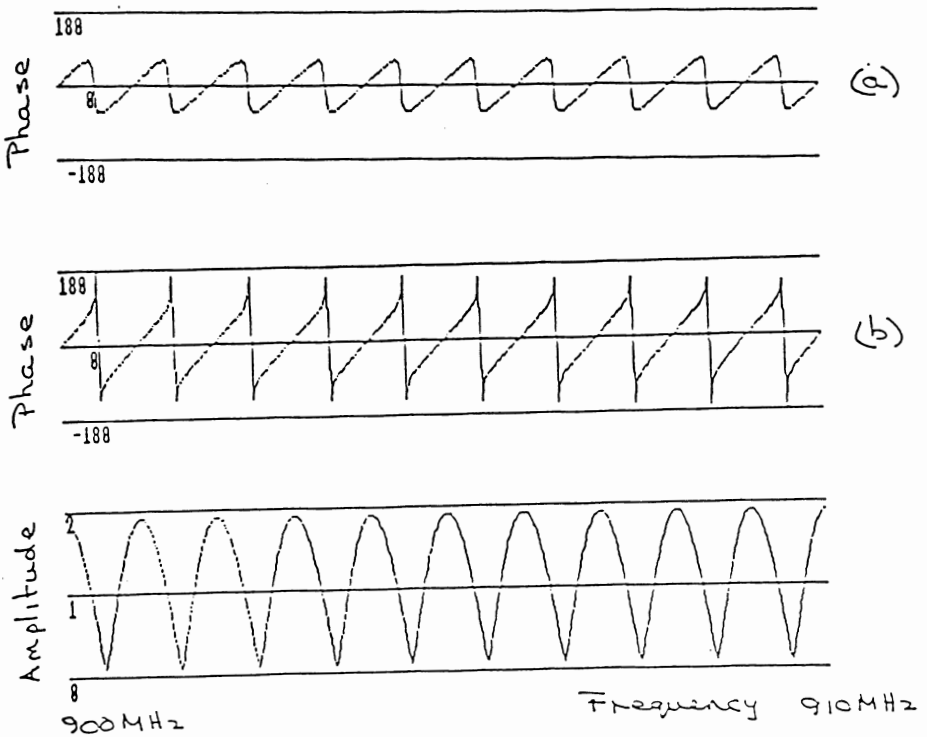

Fig.2.1.4. Amplitude and phase response of two path channel, (a) $A_1 = 1.0$, $A_2 = 0.9$, $\Delta\tau = 1\mu s$ (b) $A_1 = 0.9$, $A_2 = 1.0$, $\Delta\tau = 1\mu s$

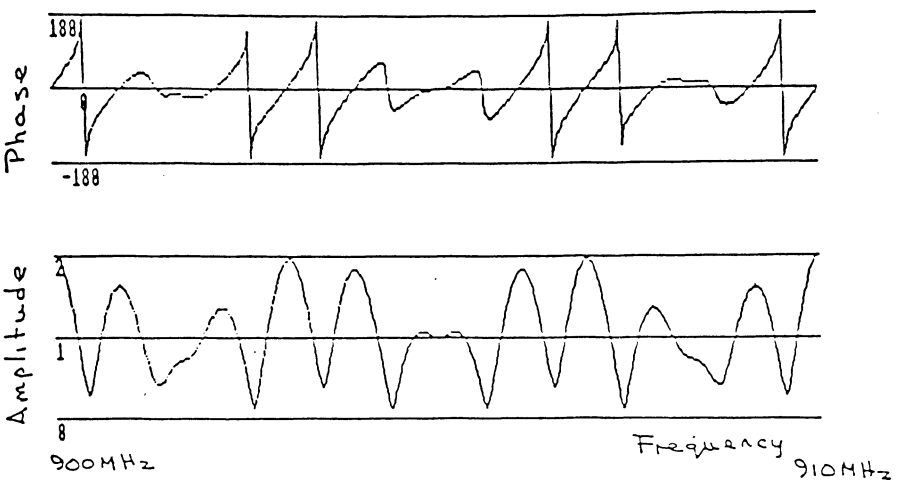

Fig.2.1.5. Amplitude and phase response of three path channel, (a) $A_1 = 0.8$, $A_2 = 0.7$, $A_3 = 0.5$, $\Delta\tau_1 = 1.0\mu s$, $\Delta\tau_2 = 1.3\mu$

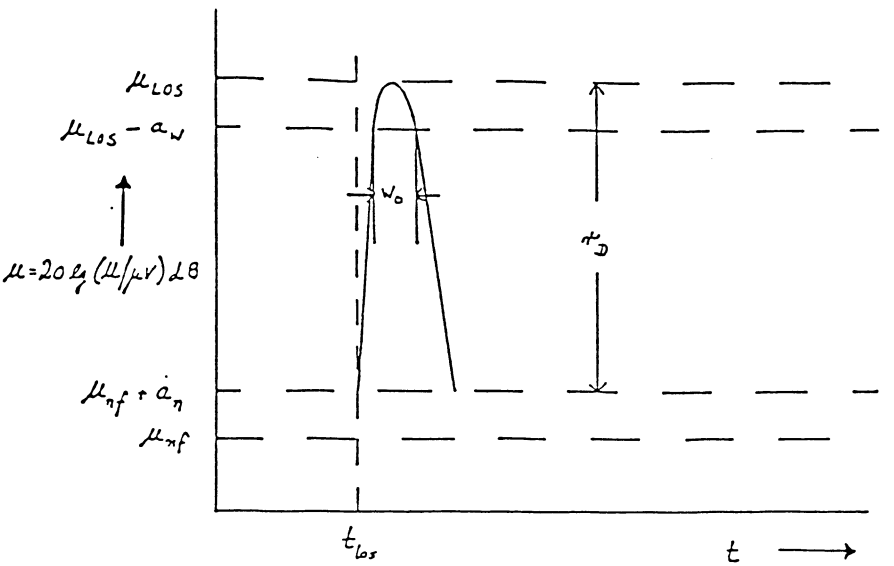

Fig.2.1.6. Definition of impulse response, (Lorenz,1987).

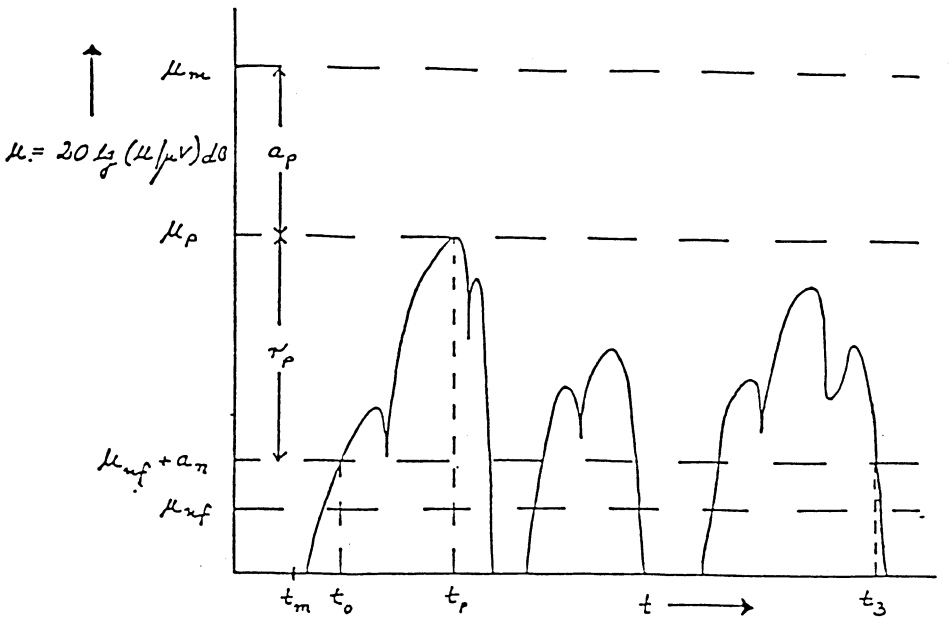

Fig.2.1.7. Definition of delay spread, (Lorenz,1987).

2.2.1 INTRODUCTION

Section 2.1 showed that the wideband channel may be characterised by any one of four system functions. However, in practice, it is only possible to design a measurement system or "sounder" in the time-time delay or frequency-time domains. This section describes the equipment and techniques used to measure the channel characteristics over typical bandwidths of 10 to 20 MHz at or near 900 MHz by contributors to COST207. The information given here covers nine different measurement campaigns carried out in eight countries and embraces three different techniques. All these provide information on the delays associated with the various propagation paths, but differ in their resolution and ability to provide the Doppler spectrum of each path. Section 2.3 gives a selection of results obtained by each method.

2.2.2 METHODS OF MEASURING MULTIPATH DISTORTION

The various techniques used to measure the wide-band channel fall into three categories: pseudorandom sequence techniques, pulse measurements, and frequency domain techniques. The following sub-sections describe the different methods used to gather information on the broadband radio channel characteristics.

2.2.2.1 Pseudorandom sequence sounding

2.2.2.1.1 Correlation techniques.

In the correlation technique the "sounding" signal consists of a carrier frequency modulated with a pseudo-random binary sequence. The receiver uses a series of correlators to extract the impulse response. Early sounders using this technique employed multiple correlators working in parallel (one for each delay).

A time-multiplexed correlator was developed by Bailey, 1970, to characterise the tropospheric channel at 2 GHz obviating the need for a number of correlators in the receiver. A similar type of sounder was used by Cox, 1972, to study multipath propagation at 910 MHz in a mobile radio environment. In this technique, the phase-keyed pseudorandom reference signal runs at a slightly different clock frequency compared to the sounding signal and thus produces a complex (in-phase and quadrature) analogue correlation output which is proportional to the true channel impulse response, but scaled in time. This type of sounder therefore acts in a manner analagous to an interleaved sampling oscilloscope, producing its output from samples of successive impulse responses. It is thus implicit that the multipath structure of the channel should not change significantly during the time required for one measurement (in the British Telecom case, 255 msec). Despite this drawback this type of sounder was chosen by British Telecom for the simplicity of its construction, lower transmitter power and recording bandwidth requirements and the relatively simple data logging and processing involved. A block diagram is shown in fig 2.2.1, and further details are given in appendix I.

The joint Japanese/Swedish Telecom measurements used a similar sounder, shown in fig 2.2.2. However, the receiver correlation sequence does not use a constant frequency offset from the transmitted signal. Instead, the correlation is performed in a stepwise manner by first making a correlation over the full sequence length at the nominal chiprate, and then shifting the receiver sequence in time by one half a chip, before performing a new correlation and so on. This allows the delay window size at the receiver to be chosen in a flexible way.

2.2.2.1.2 Matched filter techniques.

An alternative method, suggested by Bajwa and Parsons, 1982, and used by the French and Swiss PTT, (de Weck, 1988) employs a matched filter to determine the channel impulse response. This allows the impulse responses to be recorded in real time and places no practical limitation on the vehicle speed for collecting Doppler information. In both French and Swiss methods, unlike reference Bajwa and Parsons, the demodulated quadrature output signals pass directly to an A/D converter and are stored in RAM. The data is subsequently transferred to either a hard disk or tape for subsequent processing. A block diagram is shown in fig 2.2.3.

2.2.2.1.3 Comments on correlation and matched filter sounding

Both systems require time and frequency synchronisation between transmitter and receiver. This is achieved by locking all oscillators to high accuracy rubidium frequency standards in both transmitter and receiver. These standards are tuned to a relative accuracy of 1 part in 10^11.

As these frequency standards provide highly stable timing, a knowledge of the receiver's location with respect to the transmitter can be used to remove the line of sight propagation delay from the impulse response. If information on the Doppler spectra for each echo path is not required there is no need to synchronise the RF oscillators in the receiver. Also the quadrature demodulation process is no longer necessary and can be replaced by a simple power detector.

Since the length of SAW matched filters is limited, it is not possible to use PN sequences longer than about 10 to 15 us. Therefore, if longer delays are to be measured, the sequence must be transmitted as a burst and followed by period of no transmission. This "burst mode" introduces correlation side-peaks which limit the usable amplitude dynamic range of the recorded IRs, although this can be minimised by choosing an appropriate sequence. In a similar way the performance of the SAW matched filter is the main determinant of the performance of the convolution sounder. Additional processing is used to remove the side peaks from the results. It is difficult to quantify exactly the influence of this processing upon the precision of the statistical results but experience suggests that it is negligible.

The following improvements are suggested in order to reduce the correlation side- peaks when burst mode transmission is used.

- the optimisation of the ratio between the correlation peak and the most significant side peak can be done by correlating the input signal with a slightly different version of the transmitted sequence. This version differs from the original one by the fact that the bits can take any value between 0 and +1 and 0 and -1 respectively.

- the suppression of the correlation side-peaks can also be made by passing the recorded IRs through an appropriate Wiener filter.

Since the matched filter sounder performs the correlation in real time it is possible to record the IRs with a very high acquisition rate (theoretically up to one IR each time the sequence is transmitted.)

Both techniques offer good robustness against interference due to their inherent processing gain and can operate with reasonably low output power. Furthermore, the signal used does not significantly disturb other services when the measurements are carried out in occupied frequency bands.

2.2.2.1.4 Vehicle Speed and Averaging Distance

In principle the matched filter method has the advantage over the correlation method of being able to record the true instantaneous impulse response of the channel in terms of the power - Doppler - delay profile at all practical vehicle speeds. However, this requires high speed A-D conversion and the handling of vast amounts of data. We now consider the relationships between vehicle speed, averaging distance and the sampling rate.

We observe that the greatest change in the echo delay occurs when the mobile moves along the same or reciprocal bearing as the echo. Since we are concerned with echo delays that are greater than a few hundred nanoseconds (from a comparison of coherence bandwidths with the proposed GSM system bandwith and possible frequency hopping distances), changes in echo delays of a few tens of nanoseconds are of little importance. Therefore, we can assume the channel impulse response to be stationary over distances corresponding to such small variations in the delays as far as the macroscopic multipath structure is concerned. A resolution of 200 ns represents a radial distance of about 60m. This corresponds the averaging distance used to remove the Rayleigh fading leaving the slow fading or shadowing effects unchanged. Taking the British Telecom sounder as the "worst case", recording 4 impulse responses per second, a vehicle speed of up to 30-50 km/hr seems reasonable with between 18 and 27 records averaged over

a distance of 60m. Clearly a higher sampling rate would allow more records to be averaged.

On the other hand, to collect Doppler information accurately, a more severe restriction exists on the mobile speed. For example, a measurement rate of 4 impulse responses per second, restricts the measurement of Doppler frequency to 2 Hz, and limits the vehicle speed to 2.4 km/h at 900 MHz. (the corresponding limit with a matched filter sounder taking a measurement every 12.7 us is about 50,000 km/hr!!!) In this case, the measurements may also include time variant effects which are independent of the speed of the mobile. Therefore care should be exercised in translating these Doppler spectra to realistic vehicle speeds.

Clearly with such restrictions on the speed of the mobile, a practical measurement with the correlation sounder cannot be expected to collect the fast fading information required without risking the safety of the survey team in fast traffic conditions.

However if Doppler spectra are not required, it is possible to travel at reasonable urban speeds provided care is taken in the subsequent processing to remove the effects of fast fading by taking an average over several records. The requirement for locking the receiver oscillators to a frequency standard and for complex demodulation is also removed, as mentioned in 2.2.2.1.3.

2.2.2.2 Pulse measurements

2.2.2.2.1 General

In this method the channel is probed by transmitting a short RF pulse. Limiting the measurement to the received pulse amplitude allows a much simpler configuration to be used and incoherent detection techniques applied. However it is not then possible to obtain the Doppler spectrum.

The characteristics of the sounders used by the Dr Neher Labs in the Netherlands, CSELT in Italy, Swedish Telecom, and the joint campaign by the PTTs of the Federal Republic of Germany and Switzerland are summarised in appendix II.

Swedish Telecom Radio use a fixed transmitter and a transportable receiver mounted in a vehicle. In operation, the impulse response is fed to an oscilloscope, a hardcopy being obtained with an oscilloscope camera. Subsequently data is extracted from these photographs and fed into a computer for analysis. During the measurement the vehicle is stationary; it is then moved a distance of about 25 m and the process repeated.

CSELT transmit from the fixed station to the vehicle which can be moving or stationary. The transmitted signal is about 200 ns wide (at -15 db points), and is repeated at 10 kHz. The mobile unit comprises a low noise amplifier, followed by a logarithmic amplifier with a dynamic range of about 60 dB, and linearity better than +/- 1 dB. The echo profiles are sampled by a two channel digitiser. The data is stored on tape cartridges or hard disk, under the control of a desk-top computer and analysed off line. A block diagram is shown in fig 2.2.4. The system can perform repetitive measurements at time intervals in the range 0.5 to 1.0 ms. However, due to the small computer capacity, only eight consecutive measurements are possible.

In contrast, the Dr Neher Labs, 1987, transmit from the test vehicle. A block diagram of their equipment is shown in fig 2.2.5. The signal is received at the fixed station where it passes through a log amplifier at an IF of 70 MHz before being digitised at a sampling rate of 50 MHz. The digitised data is stored on a hard disk. The data collection system digitises one amplitude delay profile every 20 ms.

The equipment used in the joint German/Swiss measurements, [Lorenz, 1988], is based on aeronautical distance measurement equipment (DME). A block diagram is shown in fig 2.2.6. At the mobile 200ns wide pulses are transmitted at 1050 MHz, with a repetition rate of 10 Hz, and an output power of 57 dBm. As the oscillators are phase locked to rubidium standards, absolute phase measurements are possible. In the receiver at the base station, an AM logarithmic detector with a total dynamic range of 60 dB is used. Each instantaneous impulse response is digitised at 20 M samples/s to produce 2 kbytes of data covering a total delay range of 100 us in 50 ns steps, and an amplitude range from -90 to -30 dBm, quantised into 256 levels. The data is stored on magnetic tape at the rate of one amplitude delay profile every 100 ms, corresponding to a spatial sampling of every 140 cm at 50 km/hr.

2.2.2.2.2 Comments on the Pulse Sounders

Although the equipment is simple to implement and functions reliably, some problems can be encountered.

i. If an absolute reference for the time delay is not available, the starting instant of the delay profile is estimated by setting an amplitude threshold to trigger the acquisition system. A small amount of jitter in the starting instant can be observed and sometimes spurious pulses cause false triggering. The latter phenomenon leads to the corruption of some 5 to 10% of the data. However the corrupted profile can be easily rejected by performing statistical "outlier" tests on the data.

ii. Unless very large transmitter powers are used, the maximum distance from the transmitter is limited, and, on an equivalent power basis, is usually less than the pseudorandom sequence sounders.

2.2.3 FREQUENCY DOMAIN TECHNIQUES

2.2.3.1 Spaced frequency technique

Two frequencies are transmitted. Their amplitude and phase are detected at the receiver to provide an estimation of the degree of correlation between them. The technique has been used for troposperic scatter work by, for example, Oliver and Tiffon, (1987). Jakes, (1974) describes measurements made by Osanna on the UHF mobile channel using this technique, and more recent work has been published by Bultitude, (1983) and Melanc and Lebell, (1986). However it is felt that this technique is not reliable due to the fact that the frequency coherence function is non-monotonic. A better technique, that provides the full information about the correlation characteristics of the channel as a function of frequency, is the "frequency stepping technique", described next.

2.2.3.2 Frequency Stepping Technique

A single frequency is transmitted and the received signal amplitude and phase are detected at the receiver. Repeating this procedure by stepping through a frequency band produces the complex transfer function of the channel. The resolution of the system is directly proportional to the bandwidth over which the transfer function is obtained and the maximum measurable delay is proportional to the stepping frequency. The technique is essentially a static measurement due to the time taken to step through a band of frequencies. Consequently Doppler information is not available in the same way as the measurements described in previous sub-sections. Care is taken to ensure that no time variations are caused by effects such as trees moving in the wind, or road traffic.

A block diagram of the measurement system used by Leeds University, UK, is shown in fig 2.2.7. The synthesisers are locked to rubidium standards, but due to the nature of the synthesisers, their precise phase cannot be predicted following a change of frequency. To overcome this, relative phase measurements are made by modulating the transmitted carrier in a suppressed carrier modulator to produce two sidebands which are transmitted together through the measuring system. The modulating frequency is locked to the standard and remains unchanged throughout the measurement. The step in frequency is equal to twice the modulating frequency, such that the frequencies of the previous upper sideband and current lower sideband are identical. It is thus possible to calculate the phase at each frequency relative to the mean path phase change at that frequency by using suitable off-line signal processing. In simple terms, this joins up the measurements of differential delay across the measurement bandwidth.

Three modulating frequencies are provided, 25, 50, and 100 kHz, which, in principle, allow delays of up to 20, 10, and 5 us respectively to be measured. In practice, due to the signal processing used, the actual values of the maximum calculable delay are somewhat less than these figures.

In the receiver the IF is passed to a square law detector. The output of this contains a component at twice the modulating frequency, which is compared in phase with the same frequency derived from the local standard. Fluctuations in the relative phase between the demodulated signal and the local reference are a measure of the differential phase fluctuations across the band, and may be interpreted in terms of either phase or group delay variations.

To obtain the frequency transfer function the differential phase measurements are adjusted to give a zero mean value across the band of frequencies and then summed sequentially across the band to give the total phase. The frequency transfer function may be converted to the channel impulse response through the Fourier transform.

Further details of the sounder are given in Appendix III.

2.2.4 SUMMARY AND CONCLUSIONS

A variety of techniques have been used, depending on equipment availability and the urgency of the measurement programs to measure the channel characteristics over typical bandwidths of 10 to 20 MHz at or near 900 MHz. The information given here covers nine different measurement campaigns carried out in eight countries and embraces three different techniques. These are pulse measurements, pseudorandom sequence techniques, and frequency stepping techniques.

Pulse measurements are vulnerable to interference, and unless they are limited to short ranges require high peak powers. They are, however, simple to implement, can measure in real time, and, in fact, produced the earliest, and some unique, European data at 900 MHz.

Pseudorandom sequence techniques offer increased sensitivity over the single pulse methods and use lower transmitted powers. They are potentially suitable for measuring close to, or even in, occupied frequency bands due to their low power spectral density. The method using a SAW matched filter has a higher measurement rate and, provided the data flow can be dealt with, can provide an instantaneous measurement of the impulse response and full Doppler information at all realistic vehicle speeds. The correlation sounder eliminates the need for the special SAW filter and is thus more flexible in terms of chip rate and sequence length. It cannot measure the impulse response in real time, and must travel very slowly to record Doppler information. In this case, the measurements may also include time variant effects which are independent of the speed of the mobile. Therefore care should be exercised in translating these Doppler spectra to realistic vehicle speeds.

In terms of complexity, the frequency stepping technique is next to the pulse technique. It is capable of measuring over a wide bandwidth, avoiding segments of occupied spectrum but measurements can be time consuming if stepping rates are low. It is thus limited to static measurements, and the impulse response is derived through the use of the Fourier transform on the complex frequency transfer function.

As a final comment, the authors caution that in addition to constructing the measurement equipment and performing the measurements, the time needed to analyse and present the results of the measurements is not inconsiderable, and generally occupies more time than the measurement itself.

2.2.5 REFERENCES

Bailey C C, Aug/Sep 1970, "Characterization of troposcatter channels by impulse response measurement", AGARD Conference Proc., Part II, Germany, pp 39-1 to 39-11.

Bajwa A S and Parsons J D, April 1982, Wideband characterisation of fading mobile radio channels, IEE Proceedings part F, Vol.129, No.2, pp 95-101.

Bultitude R J C, 1983, A study of coherence bandwidth for frequency selective fading channels, 33rd IEEE Vehicular Technology Conference, Toronto, pp 269-278.

Cox D C , December 1972, Time and frequency domain characterisation of multipath propagation at 910 MHz in a suburban mobile radio environment, Radio Science, Vol 7, No. 12, pp1069-1077.

Jakes W C, 1974, Microwave mobile communications, J Wiley and Sons.

Lorenz R W, Low K, Weber M, Kartaschoff P, Merki P, de Weck J-P, Feb. - March 1988, Excess power delay profiles measured in mountainous terrain, Alta Frequenza, Vol. 57, no. 2.

Melanc P, and Lebell J, July 1986, A characterisation of frequency selective fading of the mobile radio channel, IEEE transactions on Vehicular Technology, vol VT 35, no. 4, pp 153-161

Oliver P, and Tiffon J, April 1987, Transfer function measurements as a characterisation of the urban mobile radio channel, 5th International Conference on Antennas and Propagation, ICAP'87, part 2; Propagation, pp 95-98.

Van Rees J, 1987, Narrow and wideband propagation experiments in the land mobile bands below 1 GHz, DNL Monograph Series 8702, Dr Neher Laboratories/PTT, PO Box 421, Leidschendam, The Netherlands.

de Weck J P, Merki P, Lorenz R W, 1988, Power delay profiles measured in mountainous terrain, Proceedings of the IEEE Vehicular Technology Conference, pp 105 - 112.

APPENDIX I

CHARACTERISTICS OF THE PSEUDORANDOM SEQUENCE SOUNDERS

	France	Switzerland	UK	Japan/Sweden
direction	fixed to mobile	fixed to mobile	fixed to mobile	fixed to mobile
RF	910 MHz	850 MHz	911.125 MHz	775 MHz
IF	70 MHz	70 MHz	70 MHz	142.5 MHz
bandwidth	20 MHz	18 MHz	10 MHz	10 MHz
peak output power	10 W	20 W	1 W	5 W
mean output power	10 W	1.24 W	1 W	5 W
chiprate	10 Mbit/s	10 Mbit/s	5 Mbit/s	5 Mbit/s
sequence length	127 bits	127 bits	255 bits	1023 bits
modulation	BPSK	BPSK	BPSK	BPSK
repetition rate	1 seq every 12.7 us	1 seq every 204.8 us	1 seq every 51 us	1 seq every 204.6 us
time resolution	100 ns	100 ns	200 ns	200 ns
duration of the recorded IRs	12.7 us	71.44 us	51 us	25 us (var.)
max acquisition rate of the IRs	140 Hz	12 Hz	4 Hz	19.6 Hz (var.)
sample rate	20 MHz	25 MHz	2 kHz	4.89 kHz
quantization	8 bits lin.	8 bits lin.	8 bits lin.	12 bits lin.
noise floor		-111 dBm	-105 dBm	-132 dBm
total dynamic range		90 dB (AGC)	60 dB	>70 dB (AGC)
instantaneous dynamic range	30dB max		60 dB	25 dB approx
ratio peak to spurious in correlator	32 dB	21 dB	34 dB	>30 dB
cut off level		-107 dBm		

APPENDIX II

CHARACTERISTICS OF THE PULSE SOUNDERS

	Sweden	Netherlands	Italy	Germany/ Switzerland
direction :	fixed to mobile	mobile to fixed	fixed to mobile	mobile to fixed
RF :	847.25 MHz	910 MHz	895 MHz	1050 MHz
IF :	38.9 MHz	70 MHz	70 MHz	70 MHz
bandwidth :	5 MHz	10 MHz	10 MHz	8 MHz
peak output power :	10 W	10 W	10 or 20 W	500 W
Pulse length :	500 ns	200 ns	200 ns	200 ns
repetition rate :	10 kHz	10 kHz	10 kHz	10 Hz
time resolution :	500 ns	200 ns	5 ns	50 ns
duration of the recorded IRs :	20 us	10 us	20 or 40 us	100 us
max acquisition rate of the IRs :	N/A	1 every 20 ms	1 every 0.5 or 1 ms	1 every 100 ms
no of IRs recorded consecutively :	N/A	20000	8	2000
sample rate :	N/A	50 MHz	200 MHz	20 MHz
quantizaton :	N/A	8 bits	8 bits	8 bits
noise floor :	-100 dBm	-100 dBm	-94 dBm	-89 dBm
total dynamic range :	25 dB	-95 to -35 dBm	30 dB	60 dB
sensitivity :	-80 dBm*	-95 dBm	-94 dBm	-89 dBm

* for 20 dB SNR

APPENDIX III

CHARACTERISTICS OF THE FREQUENCY STEPPING SOUNDER

direction	: fixed to mobile (mobile stationary)
RF	: 852 to 888, 917 to 923, 952 to 958 MHz
IF	: 21.4 MHz
bandwidth	: 3 kHz
peak output power	: 39 dB EIRP (8 dB gain antenna)
mean output power	: as above
modulation	: DSBSC
time resolution	: Depends on analysed bandwidth - typically 125 ns for 8 MHz bandwidth
duration of the recorded IRs	: 5, 10, 20 us depending on modulating freq and step size
max acquisition rate of the IRs	: 8 mins to cover 110 MHz band at 50 kHz steps size
sample rate	: 2 Hz
no. samples/sweep	: 960, 480, 240
agc time const	: 60 ms
phase comprator time const	: 12 ms
averaging time per sample	: 100 ms
quantizaton	: 8 bits (dB scale)
noise floor	: -110 dBm in 3 kHz BW / -94 dBm in 10 MHz BW
total dynamic range	: -90 to -20 dBm
instantaneous dynamic range	: -90 to -20 dBm
ratio peak to spurious in signal processing cut off level	: 30 dB

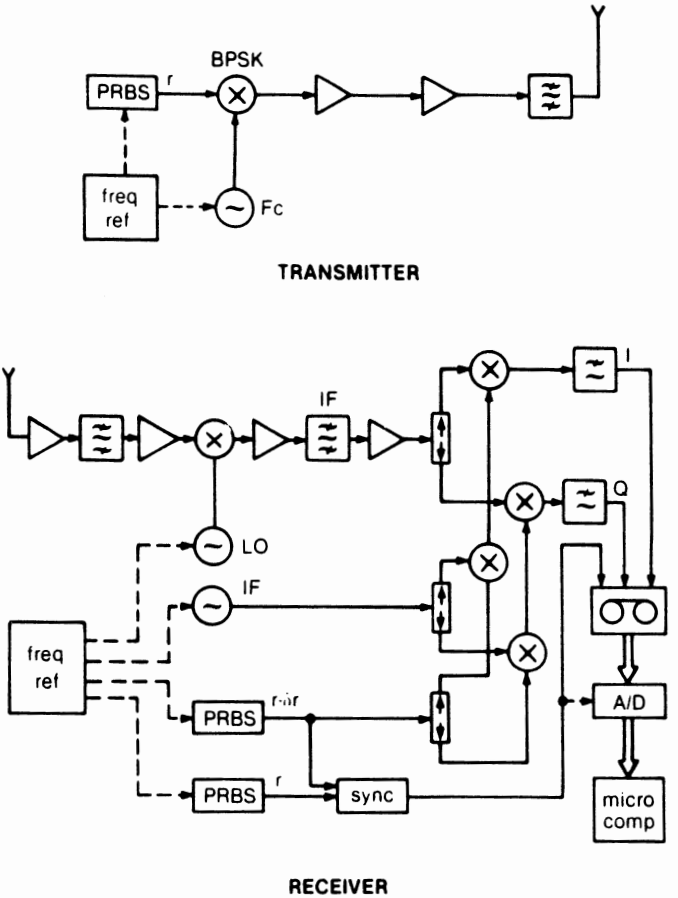

Fig. 2.2.1 The British Telecom channel sounder.

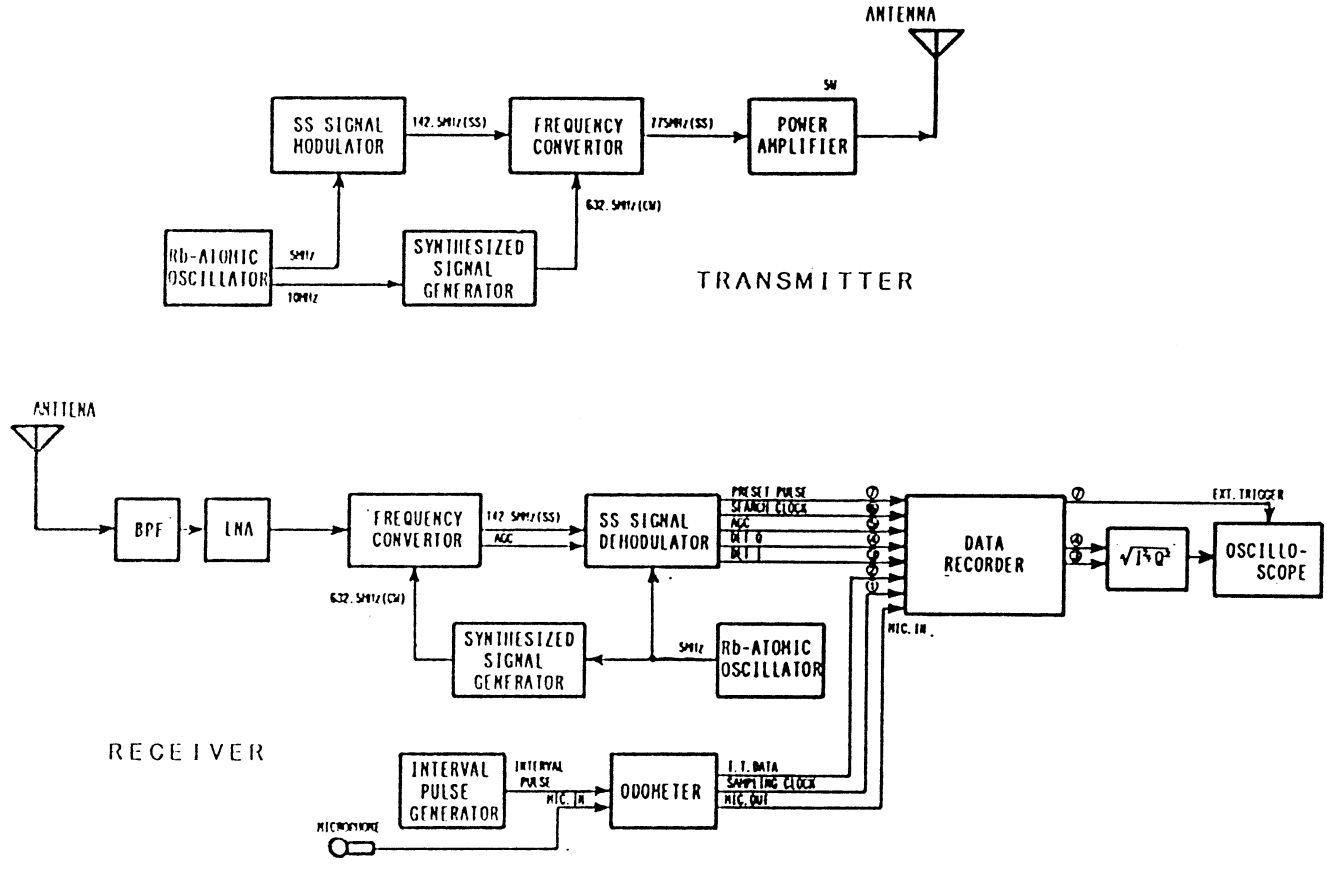

Fig. 2.2.2 Correlation type sounder used for the measurements in Japan.

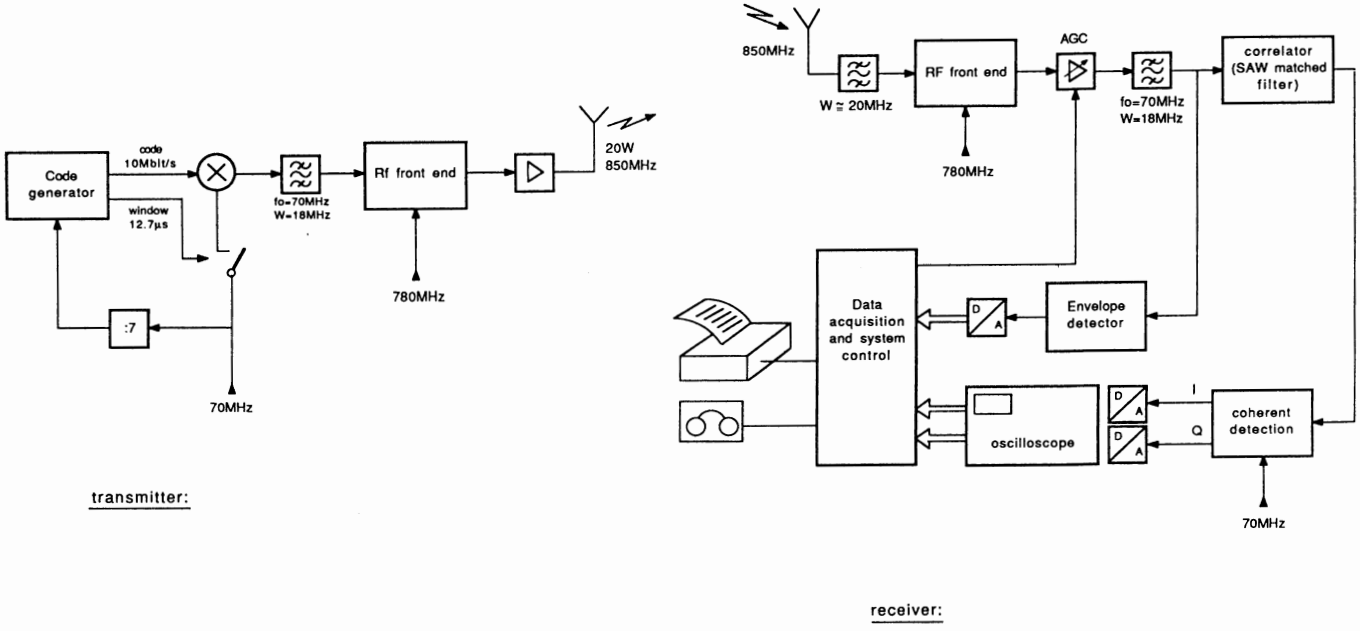

Fig. 2.2.3 Matched filter channel sounder as used by the Swiss PTT.

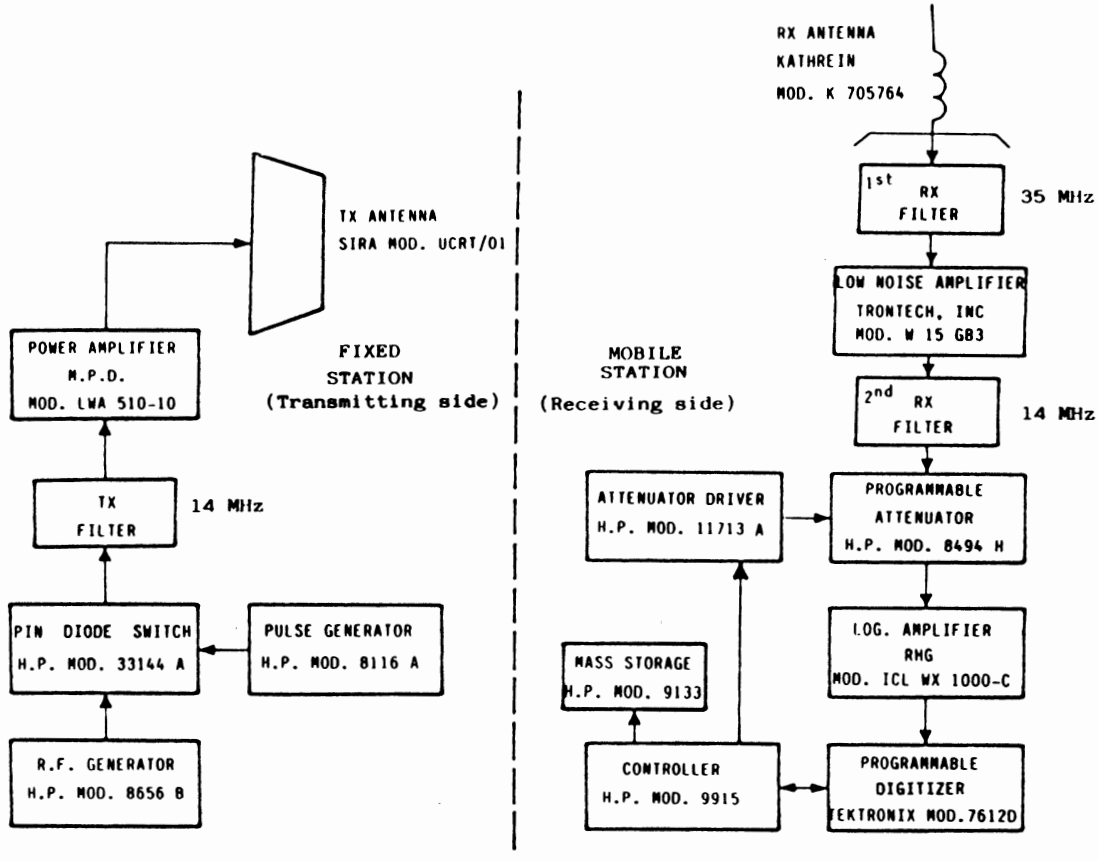

Fig. 2.2.4 Pulse channel sounder used by CSELT (Italy).

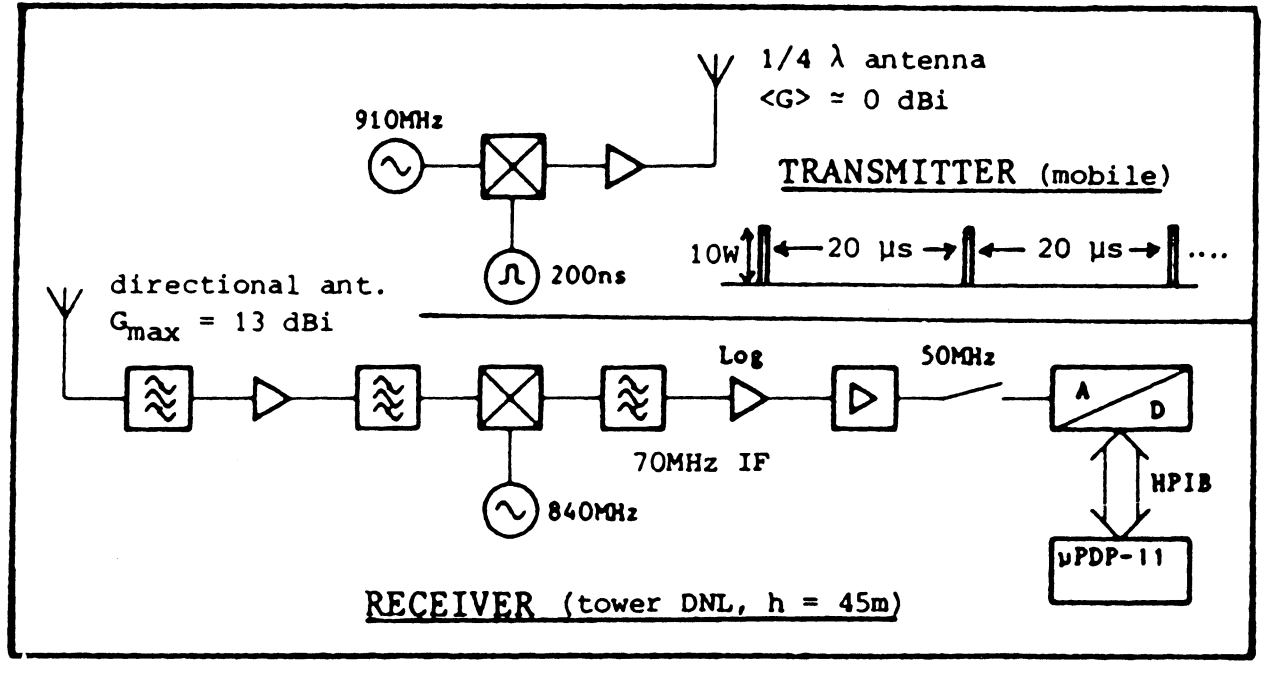

Fig. 2.2.5 Pulse channel sounder used by the Dr Neher Labs (The Netherlands PTT).

Mobile station (transmitter)

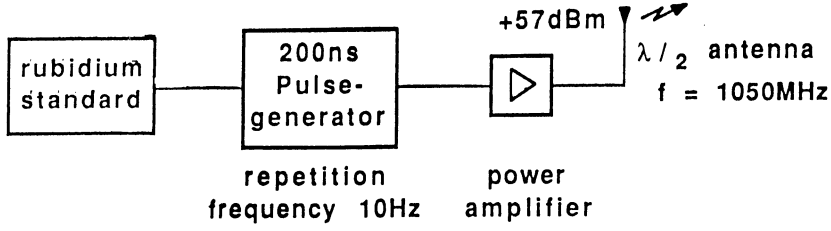

Base station (receiver)

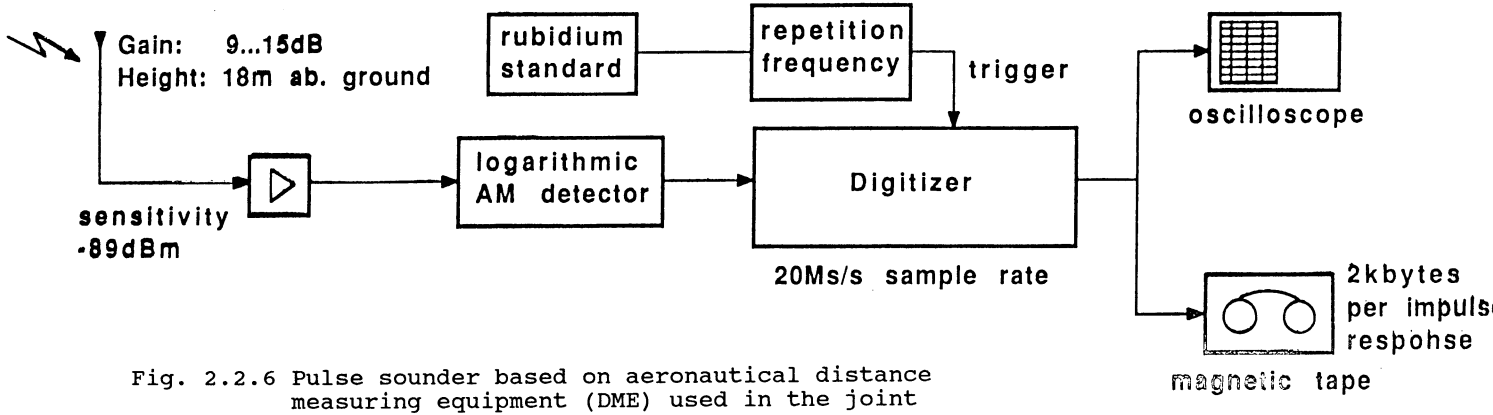

Fig. 2.2.6 Pulse sounder based on aeronautical distance measuring equipment (DME) used in the joint German/Swiss measurements.

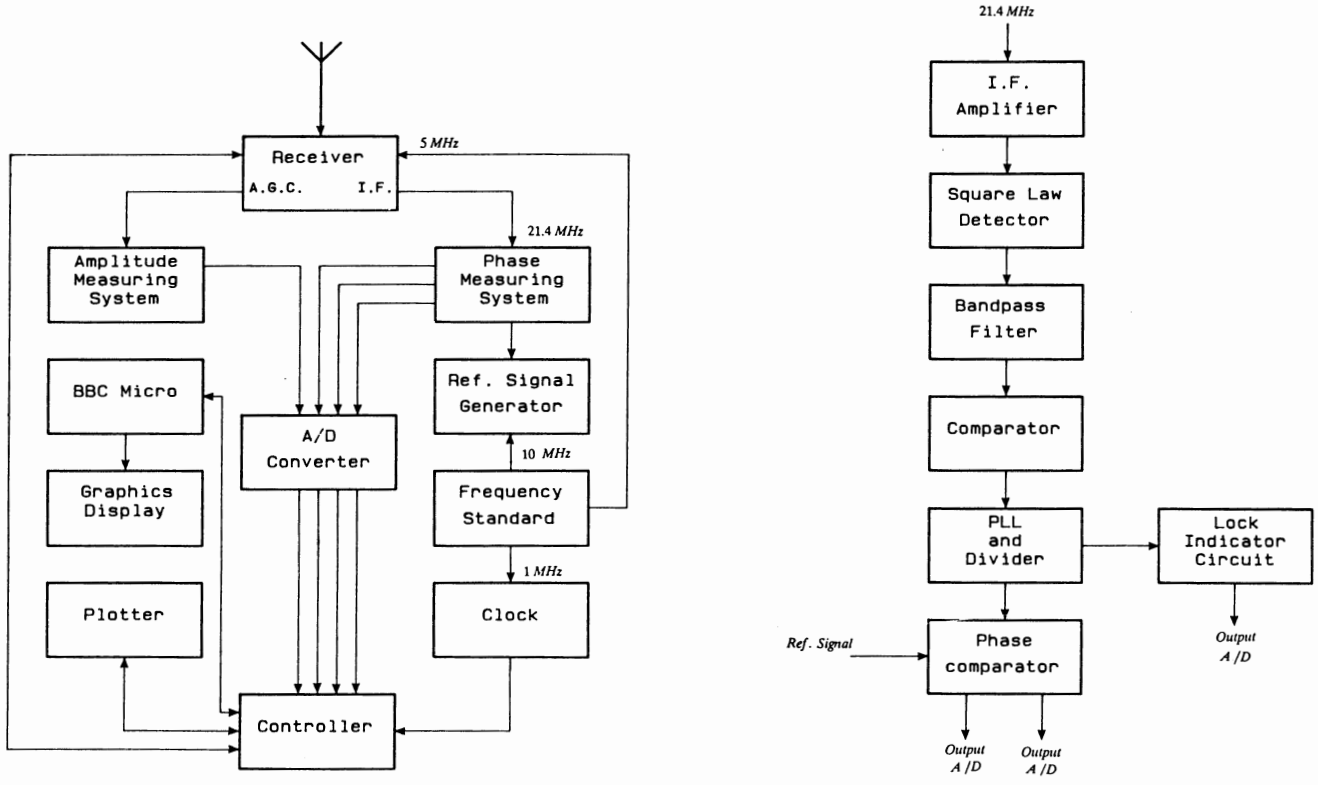

Fig. 2.2.7 Frequency swept channel sounder used by the University of Leeds (UK).

2.3.1 INTRODUCTION

The previous section described three different techniques used to measure the wideband characteristics of the mobile radio channel at or near 900 MHz. These equipments were used in a number of measurement campaigns to provide information to facilitate the specification, optimisation and planning of the Pan European digital mobile telephone system. Thus care had to be taken to ensure they represented realistic conditions of use. The most important considerations were:

i) the transmitter power and the receiver sensitivity had to be compatible with the proposed system;

ii) the base station antennas had to be placed at realistic heights i.e. not too low, or too high;

iii) the measurement locations would cover a range of terrain types and land cover variations;

iv) the size of the measurement area had to be appropriate for the location and land usage, for example smaller in urban areas than in rural.

The measurement of even a few km of route produces a considerable amount of data that requires some statistical analysis to characterise the area in an understandable and meaningful way. The parameters agreed by COST 207 for summarising and comparing data were discussed in section 2.1. These have been used here to present a selection of the results gathered by the various measurement campaigns. It must be emphasised that these are, necessarily, a sample from many such measurements, chosen on a subjective basis. They should not, therefore, be interpreted as a complete description of all the channel characteristics encountered in practice.

During the course of the measurements described here, interest became focussed on the channel characteristics found in hilly

or mountainous rural terrain, where long echo delays were expected. Whilst the emphasis placed on different environments should, of course, be related to the expected mobile radiotelephony traffic density, the hilly terrain was expected to provide a worst case condition for the radio equaliser subsystem. Thus in addition to measurements being performed in urban areas, further measurements were made in hilly terrain.

The parameters for the transmitters and receivers used for the measurements together with details of the routes and locations are summarised in appendix I. A summary of the main statistical results is given in appendix II.

2.3.2 MEASUREMENTS IN FRANCE

The transmitting antenna had a 3dB beamwidth of 60 degrees and was located on the roof of the CNET building, which is located to the south west of central Paris, (Issy-les-Moulineaux). Measurements were made on six routes in central Paris and the suburbs. On all these routes the average received signal strength was within +/- 8dB of that predicted from Okumura's method. The results were presented to COST 207 and also appear in a conference publication (Berthoumieux et al, 1987). The summary below gives details of delay profiles, obtained by averaging 20 instantaneous complex impulse responses, and scattering functions.

a) Delay profiles: about 250 delay profiles have been measured (corresponding to 5000 complex impulse responses), on six different routes. These have produced the following statistical results:

	Mean Value (us)	Standard Deviation (us)
Mean delay	0.9	0.7
Delay spread	0.75	0.4
Maximum delay (-15dB)	2.7	1.7

The maximum delay is defined by the longest delayed path with a power higher than -15 dB from the strongest path. This definition must be considered with care, as the result of the measurement depends on the maximum time delay that can be measured by the equipment.

For each of the three variables, the cumulative distributions are shown on fig 2.3.1.

b) Scattering functions: The 100 scattering functions already processed, measured on 10 different routes around CNET are not sufficient to produce reliable statistical data. However, we show three examples:

Fig 2.3.2a: scattering function measured on the right bank of the river Seine facing towards CNET. This is one of the measurements that show some of the longest delays.

Fig 2.3.2b: scattering function measured on the left bank along the river Seine (on the same side as CNET). Like most of the measurements made on the left bank, it does not show very long delays and may be considered to be typical of most of the measurements made in Paris.

Fig 2.3.2c: scattering function measured at Vanves. This includes the effects of moving scatterers which were observed in about 30% of cases, but only for short delays.

The initial conclusion is that the results found are very much as we expected, and confirm the validity of the channel models used for GSM tests. The delays measured in Paris are generally shorter than previously published measurements, and this is probably due to the relatively low height of the BS antenna.

2.3.3 MEASUREMENTS IN THE UK.

Measurements have been made using two methods in the UK. The correlation technique was used in London and NW England, whilst the swept frequency technique was used in Leeds. Full details of these measurements have been presented to COST 207, reported in the literature (Gurdenli et al, 1987, Huish and Gurdenli, 1988, Matthews 1987 (ICAP and IERE)), and as a PhD thesis in the University of Leeds, (Molkdar, 1988). A summary of the measurements is given below.

2.3.3.1 Measurements in London

The transmitter was located at a height of 58m above ground, on the roof of a 15 storey building near Old Street station in north-east central London. The ERP from the omni-directional antenna was 14 dBW (including an antenna gain of 8 dB). A 5.2 dB gain receiver aerial was mounted about 1.2 m above ground, on the roof of a saloon car carrying the receiver. The route, lying in a dense urban area, varied between 1.6 and 3.2 km in distance from the transmitter.

One section of the route runs along the Embankment between its junctions with Blackfriars Bridge and Waterloo Bridge and is just under 1 km long. Most of this section is bordered on one side by the River Thames (>200 m wide) and on the other (transmitter side) by tall buildings and rising ground. The majority of this section is characterised by a relatively high signal strength comprising an attenuated direct path due to

shielding and a strong source of echoes from the far side of the river. A sample impulse response is shown in figure 2.3.3. The CDs of the mean delay, delay spread, delay window and delay interval as defined above are also shown for this section of the route.

A second section of the route, (not shown here), runs from Waterloo Bridge to the Houses of Parliament and is just over 1 km long. It is similar to the first section but lies almost radially to the transmitter. Consequently, a strong direct signal is observed and the delay spread reduces although a strong echo from the other side of the river is occasionally present.

2.3.3.2 Measurements in Cumbria

Measurements were also made in the hilly/mountainous terrain of Cumbria, in NW England, near the town of Keswick. The transmitter site was to the SE of the town, using the local television transmitter site. The 45 m lattice tower for the TV transmitter was about 10 m SW of the test transmitter, and the surroundings were mainly farmland, sloping down to Derwent Water with partial blockage due west and north because of trees. The vertical beamwidth of the antenna was 18 degrees with a 6 degree down-tilt. During the measurements the weather was overcast, breezy but dry on the first day and wet with frequent rain showers on the second. The route, around 50 km long, lay in an area about 10 km by 15 km mostly within 5 km of the transmitter, the furthest point being around 12 km away. There were two lakes (70-80 m ASL) in the area surrounded by hills and mountains generally 200-500 m ASL with some peaks in the range 700-900 m ASL. The more gentle slopes were covered by farmland whereas the steeper hills were afforested. Most of the route lay on low ground, frequently along the edge of Lake Bassenthwaite and Derwent Water. Height contours for the area were used to check the path profiles for line-of-sight from the

transmitter to the points along the route. A total of approximately 50% of the route was found not to have line-of-sight. However, it should be pointed out that some of the distant parts of the route which did not have line-of-sight to the transmitter did not yield useable data either.

Data from the whole route was analysed in 500 record blocks representing up to 2.2 km of road distance travelled (for a maximum vehicle speed of 40 mph). The data has been divided into three categories representing 'better than typical', 'worse than typical' and 'typical' parts of the route. This categorisation is based on a subjective assessment made from a study of the impulse responses observed and the CDs obtained following the statistical analysis of the data. The typical category represents approximately 50% of this route whilst 20% is better and 30% worse than typical.

The 'better than typical' part of the route exhibits few echoes which are usually much smaller than the direct signal. The 75%-window and -12 dB delay interval CDs, (not shown), show that almost all excess delays are under 1 us. The channel can, at times contain a large number of echoes, some ranging up to 30 us although the amplitudes of such echoes are rarely large compared with the direct signal. These have been classified as 'worse than typical'. The CDs, (not shown) reveal 90% of 75%-windows to be under 18 us and 90% of -12 dB intervals under 14 us.

On average, this route may best be characterised by the CDs of figure 2.3.4. The sample impulse response shows most of the energy to be concentrated near the direct signal, nominally within 10 us. The mean and spread CDs show 90% of the mean delays to be under 2 us and 90% of the delay spreads under 5 us. The 75% delay windows as well as -12 dB delay intervals indicate values under 3 us for 90% of the time.

2.3.3.3 Comments on the data processing

In the analysis of the results reported here, minimum peak-to-spurious ratios of 15dB for Keswick and 10dB for London were used as acceptance criteria for a record to be included in the statistics. It should be pointed out that the highest-percentage delay window CDs and the lowest threshold delay interval CDs should be interpreted with care, as these CDs contain entries closest to the spurious threshold of the system. The lowest- threshold delay intervals are particularly sensitive in this respect because of the peak-to-spurious acceptance criterion mentioned above.

2.3.3.4 Measurements in Leeds

2.3.3.4.1 Description of the Environment

Measurements have been made at over 100 sites in the city of Leeds using the frequency swept system. The sites at which measurements were made were selected by reference to the OS grid and were the nearest accessible points to the 500m points on the grid. The transmitter was located at the University of Leeds on the Engineering Faculty building. Further details are given in appendix I. It was not possible to make measurements at all sites because of variation in the terrain and buildings leading to low signal strengths. Over the area covered the terrain varies in height from 14m at the river Aire in the centre of the city to a maximum of 190m at points on the outskirts of the city.

The sites at which measurements were made included suburban areas with a low density of building, surburban areas with a higher density of building including flats and some industrial premises, and urban areas. The reception sites were classified

according to the scheme presented in section 1.2.4. In this scheme the sites fell into the categories 5, 6, 7 and 8, but as there were few sites in category 8, (urban with high rise buildings), these were grouped with those of category 7.

2.3.3.4.2 Results

In more than 100 sets of measurements taken, only one set could be described as a single path, as shown by a flat amplitude and phase response. In all other cases the variability of the response showed that only a small or medium number of paths were contributing to the received signal even though there may have been an optical l-o-s between transmitter and receiver.

In attempting to reduce the many and varied characteristics of the channels measured to a few simple numbers, the detail of the characteristics are liable to be suppressed. The measured characteristics often have a quasi-periodic form which is the reason for saying that only a few paths account for the received signal. This is unlike the case of a randomly scattering medium which leads to monotonically decreasing functions for the frequency coherence and power delay profile functions.

The results presented here include the statistical parameters of the frequency coherence function and power delay profile for the band 869-877 MHz. These parameters are frequency coherence bandwidth, average delay, delay spread, number of discrete paths, and excess delay. These measurements of the invidual channel responses have been reduced to cumulative probability distributions to show the probability of occurrence of the different parameters.

The cumulative distributions of the coherence bandwidth at 0.37, 0.5 and 0.8 coherence levels has been evaluated for the three different categories of receiving sites. The cumulative distributions are noticeably different for different coherence

levels. This is because of the quasi periodic shape of the frequency coherence function. From the distributions it can be said that at 30% of the locations the coherence bandwidth measured at the 0.5 level is less than 1.1 MHz, 600 kHz, and 200 kHz for the categories 5, 6 and 7. In simple terms the coherence bandwidth decreases as the building density increases.

Distributions of the average delay and the delay spread have also been evaluated. The delay spread distributions show that at 90% of locations most of the energy arrives within 0.6, 1.1, and 1.3 us for categories 5, 6 and 7 respectively.

The number of discrete paths by which the signal arrives is of interest because a small number of paths producing deep nulls in the frequency transfer characteristic is more difficult to equalise than a response with a large number of random components. The number of peaks including the main peak were counted using the rule that a subsidiary peak was present if it rose more than 5 dB above the level on either side and that it was within 10, 15 or 20 dB of the maximum.

The excess delay is a measure of the maximum delay at which any significant component arrives, and for this analysis, was selected as the delay beyond which a discrete path never exceeded a level which was chosen as 10, 15 or 20 dB below the maximum.

The cumulative distributions of the number of discrete paths and excess delay are shown in figures 2.3.5 to 2.3.7. These show that for 50% of locations the number of paths with amplitudes within 20 dB of the maximum is 2, 3 and 6 for category 5, 6 and 7 respectively. For the excess delay taken at the -20dB level, at 90% of locations the corresponding excess delay is not more than 2, 5 and 6 us.

2.3.4 MEASUREMENTS IN THE NETHERLANDS

The measurements presented here were obtained in the vicinity of the Dr Neher Laboratories in Leidschendam, giving some 120,000 power-delay profiles corresponding to some 12 km of distance. The initial analysis of this data was focussed on characterising a number of "standard" power delay profiles for the evaluation of the "candidate" GSM systems in Paris. Recently more emphasis has been placed on the modelling aspects and this section shows the first results of a simple analysis of the data obtained from a 0.5 km test route. The line of sight paths between the mobile unit and the transmitter were completely blocked by numerous tall buildings and dwelling houses near the test route. The signals received must, therefore, arrive through scattering by the tall buildings. This is confirmed by the observed delay profiles which exhibit a number of peaks at several different delay times. A typical power delay profile, averaged over a distance of 10 m to remove fast fading, is shown in fig 2.3.8. The upper part trace shows the standard deviation of the amplitudes of each echo path. Fig 2.3.9 shows the average power delay profile for the whole 0.5 km route and has a mean delay of 1.33 us and delay spread of 0.75 us.

2.3.5 MEASUREMENTS IN SWEDEN

The measurements reported here were made in three different locations in Stockholm. The first is a suburban area with single family dwellings. The second is in the city centre with many tall buildings 5-8 storeys high, whilst the third includes the Stockholm waterfront where large stretches of open water intersperse the urban development. In all environments there is frequently no direct line of sight path between transmitter and receiver. Three examples corresponding to suburban, urban and urban with open water are shown in figure 2.3.10. The values of mean delay and delay spread were calculated for each power delay profile and their average value and standard

deviation are given below:

TABLE 1 Summary of results from measurements in Stockholm

Category	Mean delay		Delay Spread		No of Samples
	Average	Std Dev	Average	Std Dev	
Suburban	0.15	0.11	0.15	0.07	18
Urban	0.29	0.19	0.38	0.34	17
Urban (open water)	3.41	0.70	1.60	0.51	22

2.3.6 MEASUREMENTS IN SWITZERLAND : FIRST CAMPAIGN

2.3.6.1 Locations

A joint measurement campaign was conducted by the Swiss and German PTTs during May 1987, using the pulse sounding equipment described in section 2.2.2.2.1. The results have been reported to COST 207, and also in the literature, (Lorenz et al, 1988).

The receiver was installed at the base station and the transmitter in the mobile. The vehicle speed was about 50km/h on normal roads and 80 km/h on motorways. One impulse response was acquired every 100 ms, giving a spatial separation between two consecutive impulse responses of 1.4 and 2.2m respectively. The mean length for collecting data was about 1 km. In total about 70,000 IRs were recorded, representing 40 km of motorway, 29 km normal rural roads, and 24 km of normal roads in built up areas such as cities, towns and villages. The measurements were taken at six different sites, two sites being measured twice with different base station antennas to produce eight sets of data as indicated in appendices I and II.

Measurements were carried out at the following locations:

1. Vevey: The BS was located 220m above the level of Lake Geneva, and directed towards the south east to cover a motorway and a main road along the lakeside. The maximum path length was 12.9 km.

2. Geneva-Lancy : The BS was located on a hill south west of the centre of Geneva, and directed towards the south east to cover industrial and residential areas. It was expected that the steep rocky slope of Mt. Saleve, 6.5 km away, would produce significant reflections. The maximum path length was 4.6 km.

3. Yvorne: The BS was located on a 140m above the level of the River Rhone, close to the east end of Lake Geneva. The valley is about 5 km wide with very steep slopes on both sides.

4. Lucerne: The BS was located on a hill 210 m above the level of Lake Lucerne, with the antenna directed towards the city of Lucerne, some 2.5 km away. The maximum path length was 5.6 km.

5. Stockmatt: The BS was located 360 m above the plain of Stans in the southeast of Lucerne. The motorway from Basle to Lugano traverses the plain.

6. Stans: This site was 110m above the plain of Stans, opposite Stockmatt and covering the same motorway.

2.3.6.2 Data processing and results.

The cut-off level was chosen 6 dB above the noise floor. Impulse responses were only retained for statistical evaluation if the peak exceeded the cut off level by at least 12 dB.

As an example, the CDF of the delay spread for the Vevey site using a horn antenna is shown in fig 2.3.11. This is based on

14,386 impulse responses. CDFs of the delay intervals W50, W75, and W90 for the same site are shown in fig 2.3.12.

Data for the this and the other sites are summarised in appendix II. The results from Yvorne and Lucerne show that both delay spread and delay interval can be reduced in hilly terrain by the use of the "DME" antenna. This is believed to be due to the reduced illumination of the upper parts of the mountain slopes, since the antenna has a narrow radiation pattern that directs the energy down into the valley.

2.3.7 MEASUREMENTS IN SWITZERLAND : SECOND CAMPAIGN

2.3.7.1 Locations

A second measurement campaign was carried out during October 1987 in Switzerland with the equipment described in 2.2.2.1.2, and in [de Weck,1988]. The receiver was located in a measuring van whilst the transmitter was left unattended at the base station. The vehicle speed was about 40km/h and the acquisition rate was one impulse response every 210ms. Thus the spatial separation between two consecutive impulse responses was about 2.3m. Runs of about 1.2km in length were measured. Each run contains 560 impulse responses.

The measurements were carried out at the following locations :

1. Berne : This site is located within an urban and suburban area with some hills in its surroundings. The base station antenna was located on a high building, 80m above ground. The maximum LOS path length was 5.5km. The data of 7 runs (3293 impulse responses) was used for the statistical evaluations. Three runs were measured in urban areas and four in suburban ones.

2. Krattigen : The base station was located on a hill, 170m above the level of the lake of Thun, 10km away from Interlaken. On the opposite shore (ab. 4km), very steep mountains act as reflectors. The maximum LOS path length was 6.5km. The data of 4 runs (1474 impulse responses) was used for the statistical evaluations. Three runs were located on the same shore of the lake as the base station.

2.3.7.2 Description of the processing

2.3.7.2.1 Cut-off-level

The cut-off-level was chosen between 3dB and 8dB above the noise floor which was defined as three times the noise r.m.s. voltage.

In order to compensate for the offset drifts, quantizer noise, etc., the cut-off-level was always set higher than 2 to 4 quantization steps.

A given impulse response was kept for the statistical evaluations only if the peak to cut-off-level was at least 10dB. This condition is less severe than that proposed by COST 207 but seemed sufficient since careful attention was given to reject noise and interference.

2.3.7.2.2 Correlation side-peaks

As mentioned before, the finite autocorrelation function of a maximum PN-sequence contains not only a main peak but also side-peaks which reduce the dynamic amplitude range. If an impulse response contains only one reflection, a threshold has to be set 22dB (POP-ratio) below the main peak and 12.8us to each side of it in order to get rid of the side-peaks. Now, in a general case, an impulse response contains several reflections. In this case, the side-peaks of the reflections

will add with random phase. It is possible, for each point along an impulse response, to evaluate the level of the side peaks and to compute a variable threshold which indicates that the peaks appearing under it should be considered as suspect and therefore have to be removed. This processing was done for each impulse response before computing the parameters for the statistical evaluations.

2.3.7.3 Results

Fig 2.3.13 shows two sample impulse responses measured in Krattigen, on the shore of the lake of Thun. They were measured very close to the base station, but the direct path was obstructed. The very steep mountain slopes located on the opposite shore of the lake produce impulse responses characterised by long delays and exhibit extreme values of delay spread and delay intervals.

Figs 2.3.14 a and b show the cdf's of the delay spread S and the delay windows W50, W75 and W90 for the measurements carried out in Berne. Appendix II gives some important values of the cdf's. It is interesting to mention that in 90% of the cases the delay spread is smaller than 4.9us and the window containing 90% of the impulse response energy is smaller than 6.2us.

Figs 2.3.15 a and b show the same cdf's as fig 2.3.14 but for the measurements carried out in Krattigen. The values given in appendix II are always larger than those given for Berne. For example, in 10% of the cases, the delay spread can be greater than 9.1us and in 20% of the cases the window containing 90% of the impulse response energy can be greater than 19.8us! Although these values seem unbelievable, they still can be explained. The situation which was measured in Krattigen is certainly one of the worst which can be encountered and therefore one of those which should be avoided by network planners. The base station was installed on a hill, 500m away

from the shore of a lake and 170m above its level. The base station antenna had an omnidirectional pattern with a beamwidth of 15 degrees in elevation. The measurements were carried out along the same shore of the lake as the base station. The direct path was often obstructed but there was almost always a good view to very steep mountain slopes on the other shore of the lake, about 3 to 4 km away. These slopes were well illuminated by the base station antenna and thus scattered a significant amount of energy towards the mobile station.

Figs 2.3.16 a and b are scattergrams showing the dependence between the peak path loss and the delay spread for Berne and Krattigen respectively. This dependence can be approximated by a mean curve :

$$S_m\ (L_p) = S_{mo} + a_1\ (L_p - 80dB)^2$$

and by an envelope curve containing 90% of the points :

$$S_e\ (L_p) = S_{eo} + a_2\ (L_p - 80dB)^2$$

Table 2, below, gives the values of the parameters S_{mo}, S_{eo}, a_1 and a_2 for Berne, Krattigen and for the site measured during the first campaign (2.3.6).

Other measurements were carried out in order to investigate the stability of the echo structure. Impulse responses were collected every quarter wavelength. Then the magnitude of a given impulse response was correlated with the following ones. Fig 2.3.17a shows the typical behaviour of the correlation coefficient in urban areas. The echo structure is often stable in the long-term, but short fluctuations can occur due for example to moving vehicles or abrupt shadowing. Fig 2.3.17b shows the same for a mountainous region. The correlation coefficient value decreases very rapidly (generally in less than one wavelegth). This seems due to the fact that in such

Table 2

Coefficients for the approximation of S vs. L_p

Site	S_{mo} [us]	a_1 [us/(db)^2]	S_{eo} [us]	a_2 [us/(db)^2]
Vevey	0.5	$2.8 \cdot 10^{-3}$	0.8	$6.3 \cdot 10^{-3}$
Lancy	1	$12.5 \cdot 10^{-3}$	2	$25 \cdot 10^{-3}$
Yvorne Horn 15 dB	1.25	$15 \cdot 10^{-3}$	1.7	$18 \cdot 10^{-3}$
Yvorne DME antenna	0.5	$3.9 \cdot 10^{-3}$	1	$6.1 \cdot 10^{-3}$
Luzern Horn 15 dB	0.5	$2.8 \cdot 10^{-3}$	0.8	$5 \cdot 10^{-3}$
Luzern DME antenna	0.2	~0	0.3	$0.6 \cdot 10^{-3}$
Stockmatt Corner reflector	0.5	$3.7 \cdot 10^{-3}$	0.8	$8 \cdot 10^{-3}$
Stans	0.5	$4 \cdot 10^{-3}$	1.2	$6 \cdot 10^{-3}$
Berne	2.7	~0	1.1	$1.5 \cdot 10^{-3}$
Krattigen	0.7	$1.4 \cdot 10^{-3}$	0	$3 \cdot 10^{-3}$

regions a significant amount of power comes from scatterers rather than from discrete reflectors.

Statistical evaluations of the distances on which the correlation coefficient remains above 0.8 were made. These evaluations show that in urban and montainous regions, the median value of the distance is about 1.5 wavelengths and in residential areas about 4 wavelengths. The longer value for residential areas is probably due to the fact that, as the buildings are generally small, the direct path is less obstructed.

2.3.8 MEASUREMENTS IN ITALY

2.3.8.1 Description of the Environment

Measurements have been performed in the Aosta Valley and along the Mt. Blanc and St. Bernard highways, using three base stations, placed at St Vincent, Aosta, and Courmayeur, which, although mountainous, are characterized by rather different terrain configurations.

The St Vincent base station is located on a side of the valley, at a level of about 75 m above the bottom where the Dora Baltea river flows. Both north and east directions are characterised by a number of hills close to the town of St Vincent which are covered by grass and scrub. To the south (towards Turin), the valley is very narrow; a long stretch appears to be blocked by reliefs which are placed in the middle of the valley; therefore, the first part of the highway toward Turin (characterized by many tunnels, particularly in the Montjovet zone) is not in line-of-sight (LOS). The westerly direction (highway towards Aosta) is, on the contrary, characterized by a rather wide valley, (at least for a few kilometers), with fairly gentle slopes, covered at a low altitudes by grass and woods, while near the top there are rock faces. The highway runs in the middle of the valley, in an elevated position with

respect to the Dora river to a great extent, and, apart from a single tunnel (placed at about 5 km from St Vincent), is in LOS with the base station.

The Aosta station is placed in the Northern zone of the urban centre of the town (590 m asl), at a height of 35 m above the ground. The main valley runs from east (Turin) to west (Courmayeur); in the North direction there is another valley, towards the Great St Bernard mountain. Aosta town lies at the crossing of the two valleys, very close to the north edge. All the neighbouring zone is characterized by slopes covered by grass and forests, up to a height of about 2000 m. Above this level, rocky walls exist, up to about 3000m; the width of both valleys ranges from 5 to 10 km. Unlike the measurements performed at St. Vincent, most Aosta measurements were carried out in locations where line of sight was obstructed, and propagation by diffraction took place.

The Courmayeur transmitter was placed at a level of 20 m above the ground (1225 m asl); in this zone, the valley is rather narrow (not exceeding 5 km), and most locations in the South direction are sheltered near Pre St. Didier. Moreover, in the Nort-west direction, a 1 km wide and a few hundred meteres high rocky wall rises at a distance of about 1.5 km from the base station. Finally, in the north direction the Mt Blanc walls (covered by glaciers) overhang the valley at a distance ranging from 5 to 10 km from the transmitter.

2.3.8.2 Results

A typical profile of the St Vincent area is reported in fig 2.3.18; the response length is rather long, due to the decrease of the signal level under the effect of diffraction losses : delays up to about 15 us (differing by less than 10 dB from the top of the delay profile) may be pointed out.

Unlike the measurements performed at St. Vincent, most Aosta measurements were carried out in locations where LOS was

obstructed, and propagation by diffraction took place. Fig 2.3.19 is representative of a situation encountered at Aosta, even more critical than that depicted in fig 2.3.18; several peaks are present (of about the same amplitude), in the range 1 to 8 us.

Examples of delay windows statistics for the three localities, are reported in Figs 2.3.20 (a, b, c), where the curves corresponding to the 90%, 75% and 50% of the total energy are shown. As a general comment, notice the fact that for 95% of cases the 90% energy delay window does not exceed values of about 15 us.

Similar conclusions may be drawn from Figs 2.3.21 (a, b, c), where the statistics of delay intervals, measured at -10 and -15 dB from the peak of the responses, are reported for St Vincent, Aosta and Courmayeur, respectively. These results show that, although in most cases the irregularities in the channel transfer function may be adequately counteracted by fairly simple equalizers, in a not completely negligible percentage of situations the performance of the system would be unsatisfactory, particularly when severe variations in radio path attenuation, due to diffraction by obstacles, exist. In these cases, however, it has been found that a proper selection of the antenna pattern could overcome the problem. Figs 2.3.22 (a, b) show the scattergrams of the average delays and delay spreads, measured at the same site (St Vincent), with the directional and the omnidirectional antenna, respectively. Although such results must be considred with caution, due to the very small data sample size, they do indicate that the use of a directional antenna generally results in a slight reduction in the average delays of the profiles and a greater reduction in the delay spreads, in some cases by a factor of two.

2.3.9 MEASUREMENTS IN JAPAN

Measurements have been carried out in Japan during the spring of 1987 by the Communication Research Laboratory of the Ministry of Posts and Telecommunications and with the participation of Swedish Telecom Radio. The measurements utilised a frequency of 775 MHz, and formed part of Japanese research activities on digital mobile radio. The results have been reported to COST 207, and a brief summary is included here.

2.3.9.1 Locations

Three test routes were chosen, one in mountainous terrain, and two in dense urban areas.

1. Yamanashi: The BS was located on top of a hill in the small village of Katsunuma at one end of a valley several km wide and 25 km long. The surrounding mountains are between 300 and 500 m above the valley floor and are covered with trees. The mobile height varied from 100m above the base station to 250m below it.

2. Tokyo: The same base station was used for two measurement routes both located in the "down town" area of Tokyo. The first test route, (Kasumigaseki), was in an area including a mixture of very high buildings and a compact distribution of lower houses. The effect of reflections from the high buildings combined with blockage from the houses suggests a higher probability for observing longer delay profiles than in other urban environments. The second route, (Tukiji), was close to the harbour area and was included to study the effects of the open areas of water on the delay power profiles.

2.3.9.2 Results

The -10 dB delay profile widths (with respect to the strongest signal) have been calculated for the three test routes. The CDFs of these are shown in figs 2.3.23 to 2.3.25.

2.3.9.3 Comments

The mountainous and hilly terrain results show a polarised behaviour. On one hand, the line of sight case was frequently observed giving a high probability of very short delays. On the other hand, very long delays were observed where the direct path was obstructed, such as fig 2.3.23.

The dense urban measurements produced slightly longer delay power profiles than expected. Thet are, however, not extreme, and are similar to those obtained along the Stockholm waterfront. (see section 2.3.5).

2.3.10 COMPARISON OF THE RESULTS AND CONCLUSIONS

Considering the differences of equipment and the measurement environments there is remarkable consistency between the various results obtained in both urban and rural hilly environments. It is thus possible to draw some comparative conclusions and to offer a subjective assessment of the mobile radio channel at 900 MHz.

One application of the measured data is to compare it with the delay power profiles proposed by COST 207 for radio channel simulations, and discussed in a later section. A comparison with the statistical results obtained in Switzerland for the delay interval and especially for W90 show good agreement with the characteristics of the delay profiles defined by COST 207. This indicates that the length of the power profiles has been chosen correctly. For the delay spread, the agreement is a little worse. However the 90% values of the statistical results

for Berne and Krattigen are approximately twice the delay spread of the power profiles defined respectively for the typical poor urban case and the typical poor case in mountainous regions. This is probably due to the fact that the energy distribution within the measured impulse responses is different from the COST 207 defined power delay profiles.

The Italian results suggest that the average delay profiles may, in general be well fitted by a single or two slope exponential decay, as previously recommended by COST 207. A more accurate comparison with the average profiles for urban (or typical bad-urban), suburban and rural terrains, shows that the best agreement is obtained for rural terrain. For suburban and urban areas COST 207 profiles appear, in general, fairly pessimistic. This is contrary to the Swiss findings and clearly demonstrates the difficulty of finding a pofile that is both typical and representative of the variety of environments found in Western Europe.

Even so, it seems that on the limited data available the "COST 207 profiles" are a reasonable approximation to practical situations and, provided the comments above are remembered, can be used with confidence in system simulations and tests.

A significant feature of these results is the variability of the channel over relatively short distances (1-2 km). This means that the planning of the operational systems will require more location-specific information on the channel.

Although long delays have been seen in Stockholm, London and Tokyo, in the majority of cases, the delays are of the order of a few microseconds. The delay spread is usually greater in urban areas than in suburban areas, the coherence bandwidth is smaller in urban areas, and the number of paths is greater in urban areas. This might be expected because of the larger number of buildings to scatter the signal in urban areas.

As expected, longer delays are generally more prevalent in the hilly and mountainous environments than in urban areas. In moderately hilly areas, such as that in NW England, a figure of 10 us is typical despite the presence of longer echoes sometimes reaching 30 us. Longer delays can be found in truly mountainous areas, such as Switzerland, eg Krattigen, and Italy. The Italian and UK (hilly) results show that for 95% of cases the 90% energy delay window does not exceed values about 15 us, whereas those for Krattigen have a corresponding value of about 25 us.

We conclude that, although in most cases the irregularities in the channel transfer function may be adequately counteracted by fairly simple equalizers, there remain some situations where the performance of the system could be unsatisfactory, particularly when severe variations in radio path attenuation, due to diffraction by obstacles, exist. In these cases, however, it has been demonstrated (in the Italian and Swiss measurements) that careful selection of the base station locations as well as the antenna heights and radiation patterns can reduce the multipath distortion and thereby improve the quality of service.

2.3.11 REFERENCES

Berthoumieux D, et al, 1987: Wideband Mobile Radio Channel Characterisation, Proceedings of the International Conference on Digital Land Mobile Radiocommunications, Venice, June 1987.

Gurdenli et al, 1987: Wideband measurement of the land mobile radio channel at 900 MHz, Proceedings of the IERE International Conference on Land Mobile Radio, Warwick, UK, December 1987.

Huish and Gurdenli, 1988: Radio channel measurement and predictions for future mobile radio systems, British Telecom Technology Journal, Vol 6, No 1, January 1988.

Lorenz et al, 1988: Excess power delay profiles measured in mountainous terrain, Alta Frequenza, Vol 57, No 2, April 1988.

Lorenz R W et al,1987: "Evaluation of delay profiles in mountainous terrain", COST 207 technical document, COST207 TD(87)#16, May 1987

Lorenz R W,1987: "12th report of the working group on propagation", COST 207 technical document, COST207TD(87)#30, May 1987

Matthews P and Molkdar D, 1987 (ICAP), Wideband measurements of the UHF mobile radio channel, Proceedings of the IEE International Conference on Antennas and Propagation, ICAP'87, York, UK; March/April 1987.

Matthews P and Molkdar D, 1987 (IERE): Frequency coherence function and power delay profile statistics of the UHF mobile radio channel and their effect on system performance, Proceedings of the IERE International Conference on Land Mobile Radio, Warwick, UK, December 1987.

Van Rees J, 1987: Narrow and wideband propagation experiments in the land mobile bands below 1 GHz, DNL Monograph Series 8702, Dr Neher Laboratories/PTT, PO Box 421, Leidschendam, The Netherlands.

de Weck et al, 1988: Power delay profiles measured in mountainous terrain, Proceedings of IEEE Vehicular Technology Conference, 1988, pp 105 - 112.

APPENDIX I

DETAILS OF WIDEBAND MEASUREMENTS

	Fixed station				Mobile station				
Country	Location	Gain dBi	Ht m	ERP dBW	Gain dBi	Ht m	ERP dBW	Range km	Environment
F	CNET, 5.5km SW centre of Paris	19	28	29	3	2	-	1-3.5	Urban
UK	5 km NE centre of London	8	58	14	5	1.2	-	1.6-3.2	Dense Urban
	1.5 km SE Keswick, Cumbria, UK	5	10[1]	11	5	1.2	-	1-12 km	Hilly
	Leeds University UK		35[2]					8 km	Urban
NL	Leidschendam	13	45	-	2	2	10	1.8	Urban/ suburban
S	Stockholm	7.5	60	17.5	2	2	-	1-2.5 1.5-4.5	Urban Suburban
CH	Berne	6[3]	80	13	[4]	2.8		5.5 km	Urban/ suburban
	Krattigen (10 km from Interlaken)	6[3]	[5]	13	[4]	2.8		6.5 km	Hilly
I	St Vincent	11			1				Hilly
	Aosta	11	35 [5]		1				Hilly
	Courmayeur	11	20		1				Hilly
J	Yamanashi	2	-100 to +250	9	2	2.5		0.1 to 10 km	Hilly/ mountainous
	Tokyo	2	40	9	2	2.5		0.08 to 3.9 km	Dense urban

APPENDIX II SUMMARY OF THE MAIN STATISTICAL RESULTS

(See notes at end for explanation of symbols)

Site	no of impulse responses	dmax km	L80 dB	L90 dB	$T_{D90}-T_{D10}$ us	S80 us	S90 us	W90 us	80% W75 us	W50 us	W90 us	90% W75 us	W50 us
United Kingdom:													
London													
Blackfriars Br. to Waterloo Bridge		1.6	N/A	N/A	N/A	1.8	2.5	4.9	3.6	2.3	9	4.3	3.2
Waterloo Bridge to House of Parliament		3.2	N/A	N/A	N/A	0.5	0.6	1.1	0.7	0.4	1.3	0.8	0.5
Long Acre		1.6	N/A	N/A	N/A	0.2	0.4	0.7	0.5	0.2	0.8	0.6	0.3
Keswick (total)	7500	12	N/A	N/A	N/A	10.7	12.4	N/A	N/A	N/A	N/A	N/A	N/A
"typical"	~50%	N/A	N/A	N/A	N/A	10.1	11.1	16	1.5	0.4	23	3.5	0.7
"better than typical"	~20%	N/A	N/A	N/A	N/A	6.4	7.3	3.5	0.5	0.4	11.5	0.6	0.5
"worse than typical"	~30%	N/A	N/A	N/A	N/A	13	14	29	12	0.8	31	18.5	1
Leeds:													
open suburban	34	8	N/A	N/A	0.4	0.35	0.5	N/A	N/A	N/A	N/A	N/A	N/A
dense suburban	57	8	N/A	N/A	0.65	0.8	1.2	N/A	N/A	N/A	N/A	N/A	N/A
urban	24	8	N/A	N/A	0.8	1.2	1.4	N/A	N/A	N/A	N/A	N/A	N/A
The Netherlands, Leidschendam													
Rural	14500	2.6	104.	108	0.29	0.55	0.73	0.48	0.3	0.18	0.89	0.45	0.2
Residential	9700	2.5	123	125.	0.28	0.53	0.66	0.65	0.46	0.28	0.8	0.57	0.34
High rise dwellings 1	17600	2.3	126.	129	1.1	1.04	1.29	1.81	1.38	0.65	2.65	1.87	1.24
High rise dwellings 2	10400	1.8	121.	124	0.73	0.95	1	1.98	1.26	0.77	2.35	1.81	1.01
Sweden, Stockholm:													
Suburban	90	4.5	N/A	N/A	0.6	0.5	0.8	N/A	N/A	N/A	N/A	N/A	N/A
Urban	199	2.5	N/A	N/A	3	1.3	1.9	N/A	N/A	N/A	N/A	N/A	N/A

(continued)

APPENDIX II SUMMARY OF THE MAIN STATISTICAL RESULTS

(continued)

Site	no of impulse responses	dmax km	L80 dB	L90 dB	$T_{D90}-T_{D10}$ us	S80 us	S90 us	W90 us	80% W75 us	W50 us	W90 us	90% W75 us	W50 us
Switzerland 1													
Vevey (horn, 17dBi)	14386	12.9	143	145	5	7.5	10	8.5	4	1.8	18.5	8	3.5
Lancy (horn, 17dBi)	9034	4.6	126	128	28	9	10	21.5	19	7.5	23	21.5	19
Yvorne (horn, 17dBi)	3595	4.6	117	122	6	6.7	7.7	19.5	13.3	1	21.2	16.3	4.7
Yvorne (DME, 11dBi)	11740	4.6	120	125	4.6	3.5	4.6	5.7	3	0.7	10.5	5	2
Lucerne (horn, 17dBi)	4970	5.6	130	133	5.4	3.6	6.1	3.5	2.3	1	7	3.8	2.3
Lucerne (DME, 11dBi)	3426	5.6	128	130	1.7	0.5	0.8	1.3	0.8	0.4	2	1.3	0.7
Stockmatt Corn. (12 dB)	18147	7	118	126	5.6	2.3	4	1.7	0.4	0.2	6.5	3.2	1.2
Stans (DME, 11dBi)	5289	7	126	132	7.2	5.3	7.1	10	6.2	2.5	14	8	4.8
Switzerland 2													
Berne	3296	5.5	140	146	2.6	3.7	4.9	4.2	2.2	0.7	6.2	4.4	1.9
Krattigen	1474	6.5	148	150	7.5	7.9	9.1	19.8	14.3	2.7	23.8	18.1	9.4
Italy													
St Vincent	160	15	122	123	N/A	2.5	4	3.6	2	0.9	5.1	2.5	1.1
Aosta	N/A	N/A	119	123	N/A	4.5	6.5	4	1.8	1	6	3.3	1.5
Courmayeur	N/A	N/A	N/A	N/A	N/A	N/A	N/A	6.2	4.3	2.1	9	5.3	3.6
Japan:												80%	90%
Yamanashi	60247	10	N/A	N/A	For the measurements in Japan only the -10 dB delay interval (I10), has been computed. These results are given opposite instead of the delay window.							13.5	20.5
Kasumigaseki	31467	1.8	132	135								4	5.3
Tukiji	15385	3.9	147	149								6.3	9

NOTES

1. On hill, 170m AOD above lake (70m AOD). Measurement area contained hills generally 200-500 m AOD with peaks up to 900m. Route was generally around 100 m AOD.

2. On hill, 110m AOD; measurements taken in area varying from 14 to 190m AOD.

3. A 6dB gain collinear antenna with omnidirectional horizontal pattern and a beamwidth of 15 for the vertical radiation pattern at the transmitter. It was mounted on a mast, 10m above ground.

4. A broad $\lambda/4$ ground-plane antenna at the mobile receiver. It was mounted on the roof of the measuring van, 2.8m above ground.

5. On hill, 170 m above lake Thun. Very steep mountains rise from opposite lake shore, about 5 km away.

NOTES:

1. dmax is the longest line of sight path length measured.

2. L80 and L90 are the 80% and 90% CDF values of the basic transmission loss defined according to CCIR rec 841-2, as:

   $L = P_o - P_{in} + G_t + G_r$

   P_o = transmitted power

   P_{in} = received power

   G_t = transmit antenna gain with respect to isotropic

   G_r = receive antenna gain with respect to isotropic

3. $T_{D90} - T_{D10}$ is the difference between the 90% and 10% values of the mean delay CDF. The value of the mean delay should be referred to the direct path delay to eliminate the effect of the distance between transmitter and receiver changing during the measurement.

4. S80 and S90 are the 80% and 90% values of the delay spread CDF.

5. W90, W75 and W50 are the delay "windows" containing, respectively, 90%, 75% and 50% of the impulse response energy, and evaluated at the 80 and 90 percentiles of the CDF.

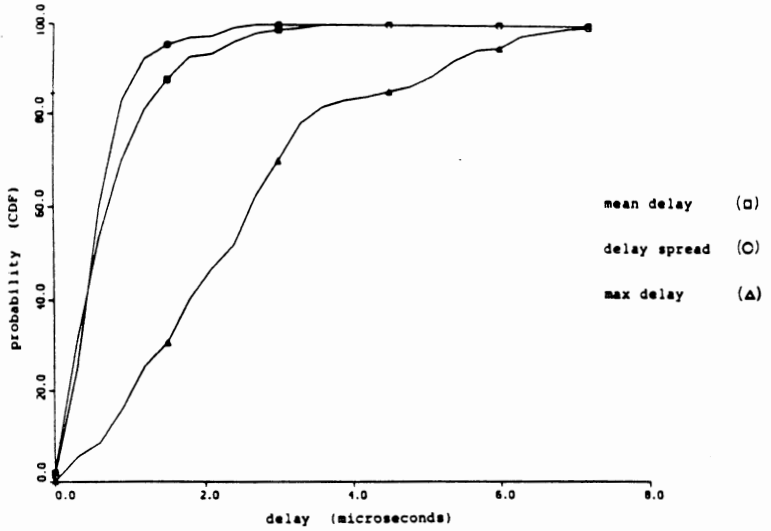

Fig. 2.3.1 Cumulative distributions of the mean delay, delay spread, and the maximum delay.

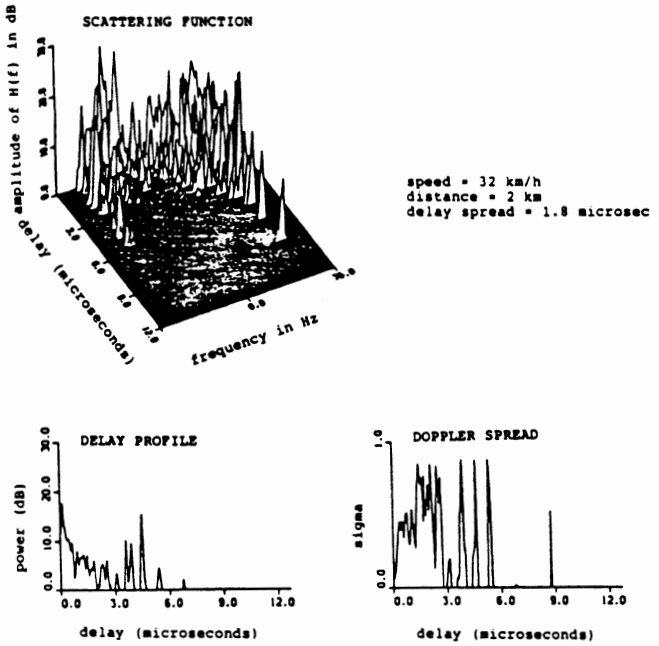

Fig. 2.3.2 (a) Scattering function, delay profile, and Doppler spread for the RH bank of the R. Seine

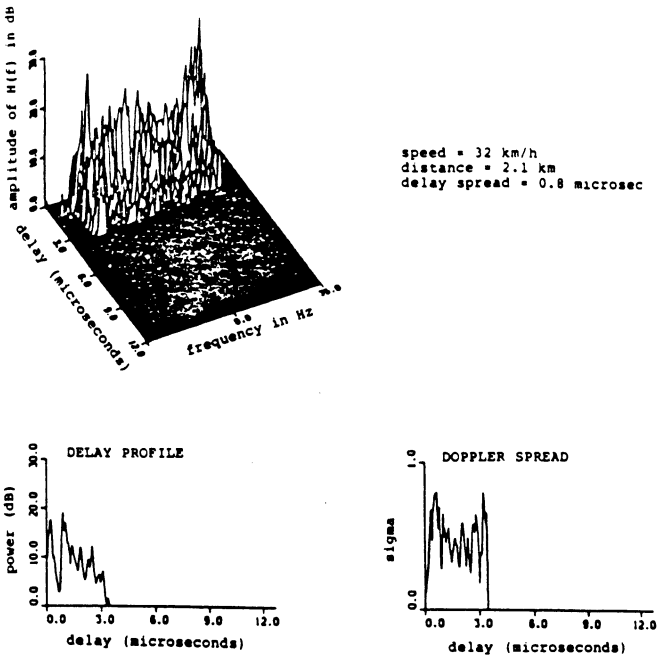

Fig. 2.3.2 (b) Scattering function, delay profile, and Doppler spread for the LH bank of the R. Seine

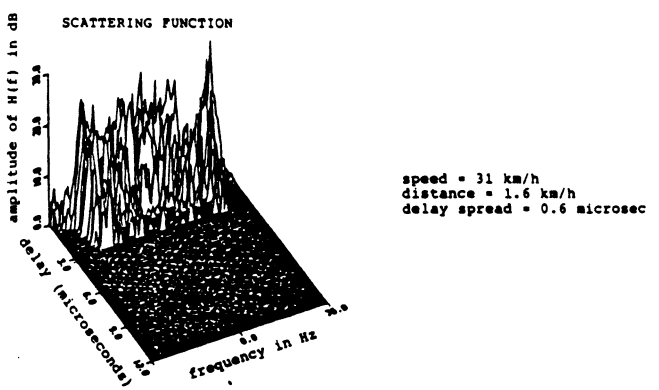

Fig. 2.3.2 (c) Scattering function, delay profile, and Doppler spread for Vanves.

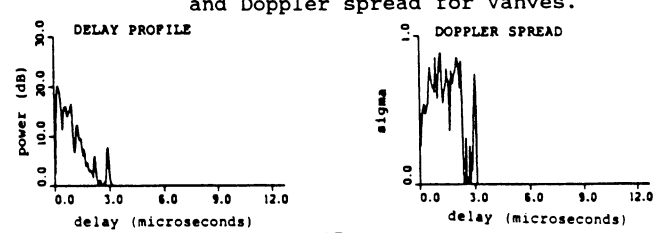

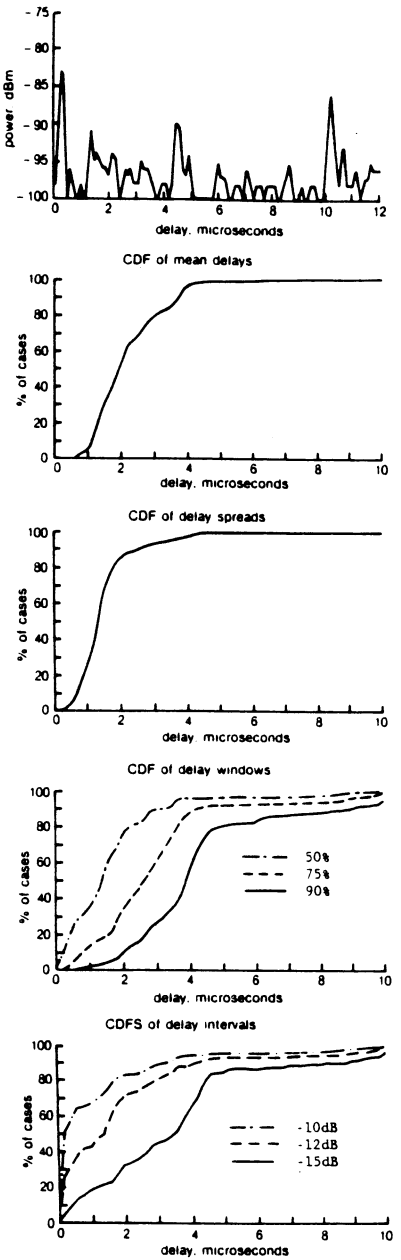

Fig. 2.3.3

Sample impulse response and cumulative distribution for London between Waterloo and Blackfriars bridges.

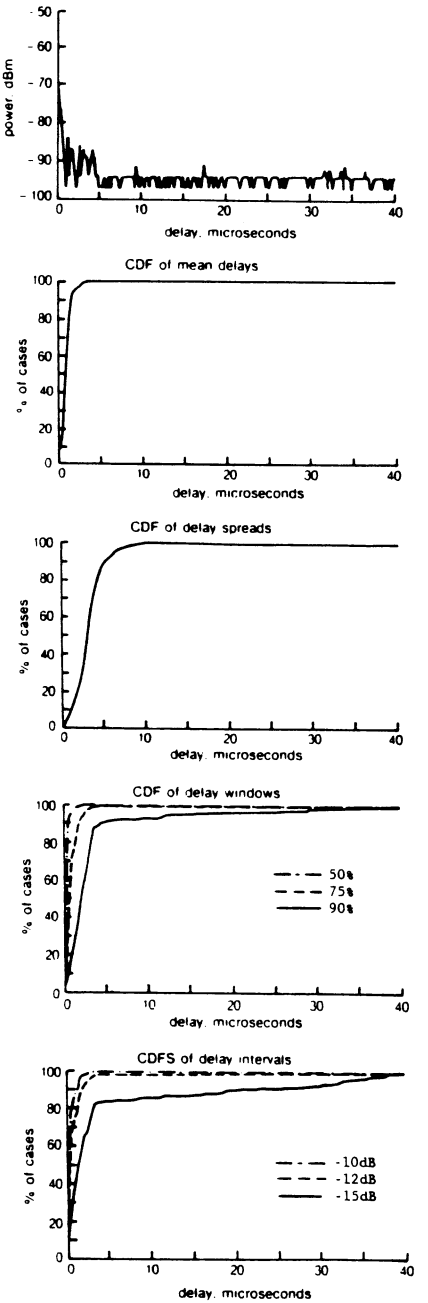

Fig. 2.3.4

Sample impulse response and cumulative distribution for Keswick, representing "typical" sections of the route.

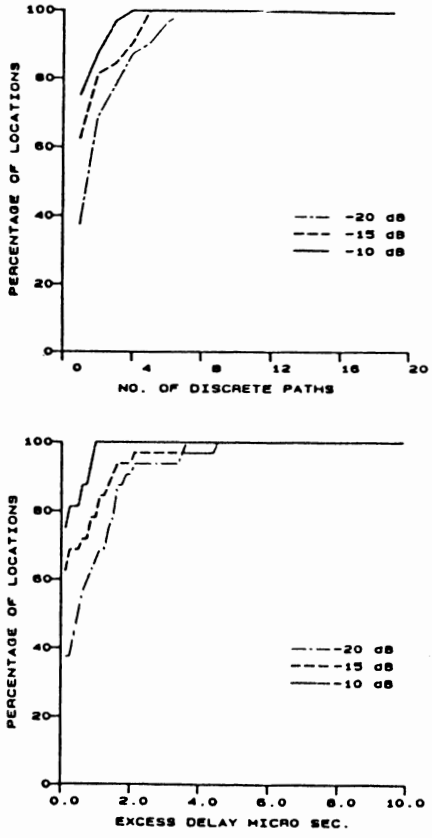

Fig. 2.3.5

CDF of number of discrete paths, and excess delay for Leeds, cat. 5.

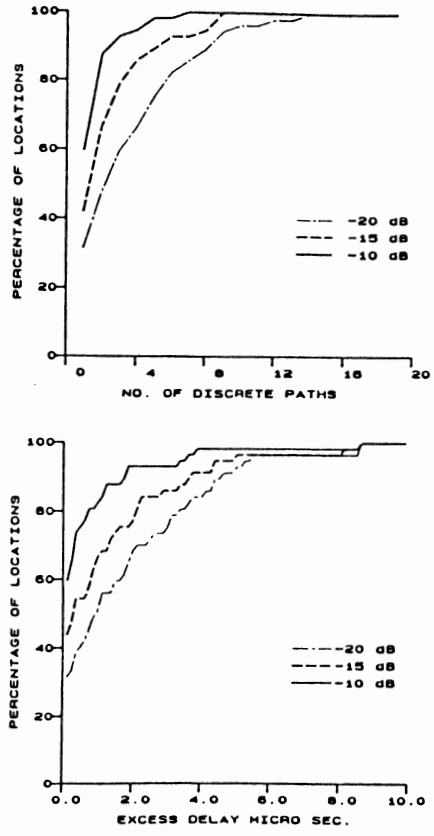

Fig. 2.3.6

CDF of number of discrete paths, and excess delay for Leeds, cat. 6.

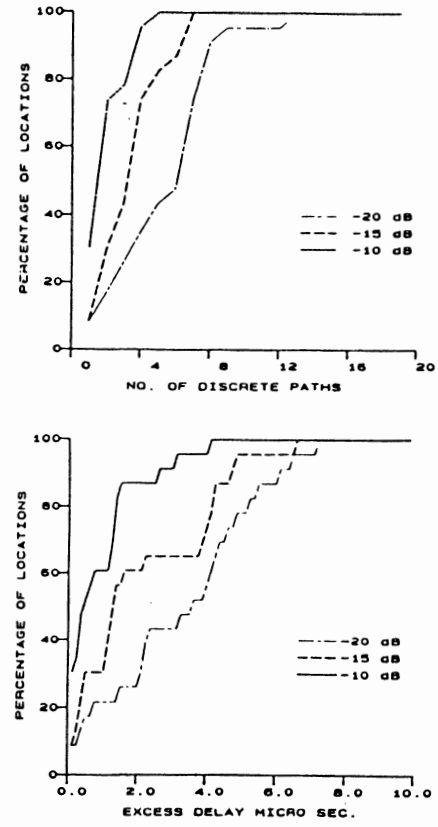

Fig. 2.3.7

CDF of number of discrete paths, and excess delay for Leeds, cat. 7

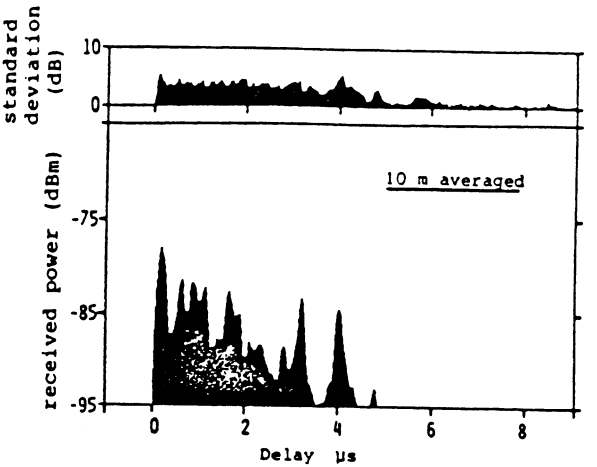

Fig. 2.3.8 Delay profile from first 10 km of route near Leidschendam.

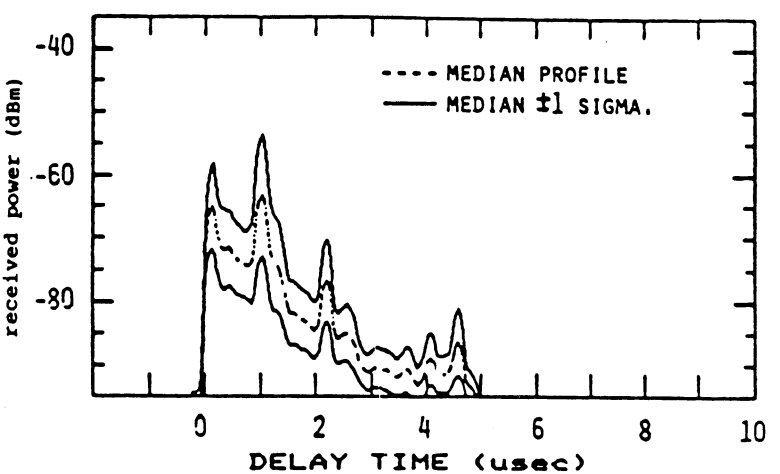

Fig. 2.3.9 Average delay profile from whole of route near Leidschendam.

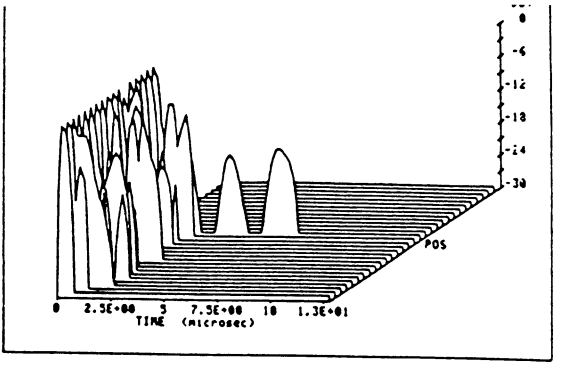

Urban area

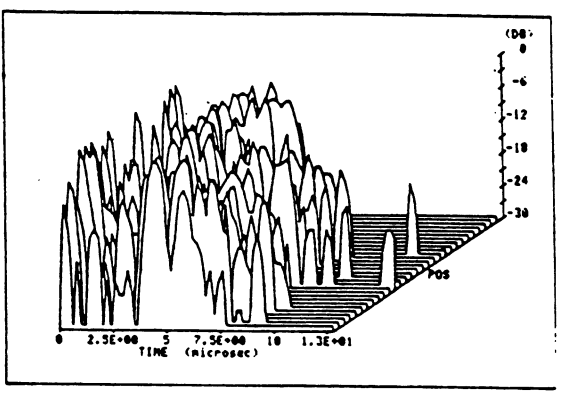

Urban, waterfront

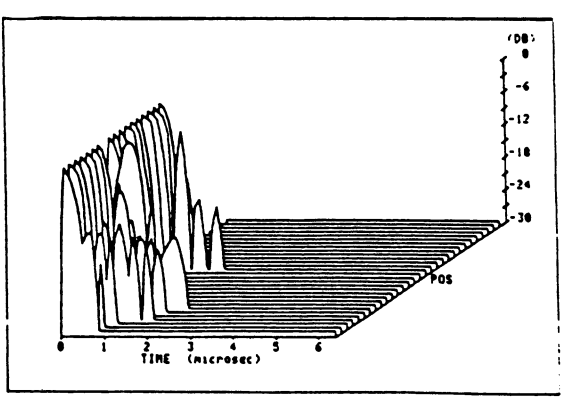

Suburban

Fig. 2. 3. 10 Instantaneous power delay profiles at different positions in Stockholm.

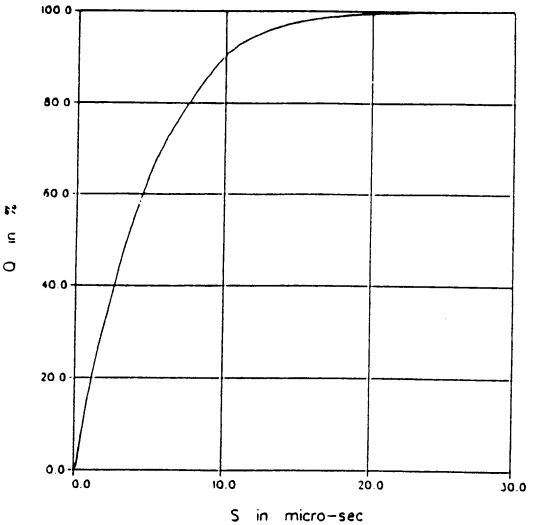

Fig. 2.3.11 CDF of the delay spread for Vevey.

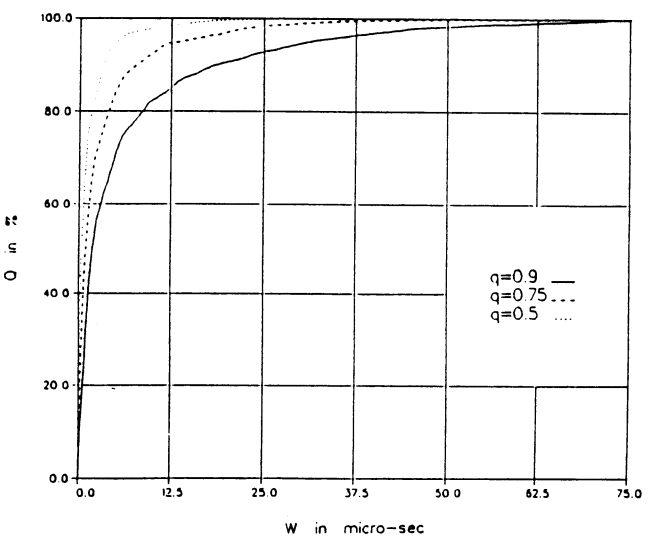

Fig. 2.3.12 CDF of the delay window containing a portion (q) of the impulse response energy for Vevey.

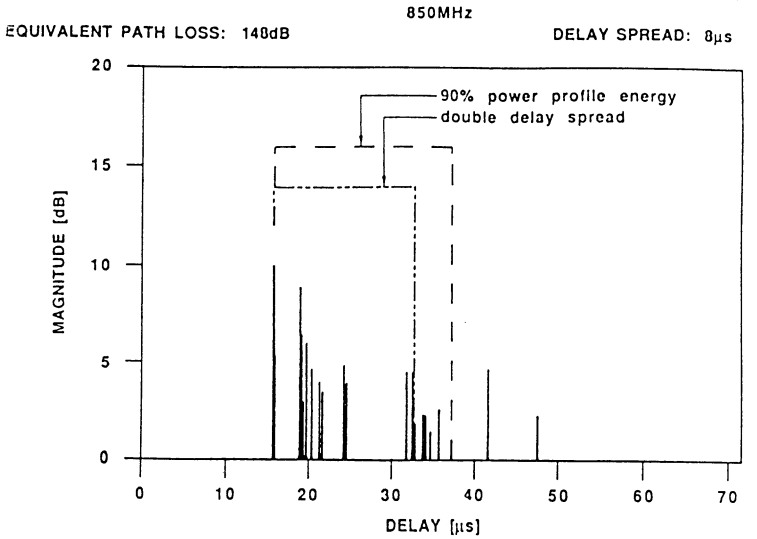

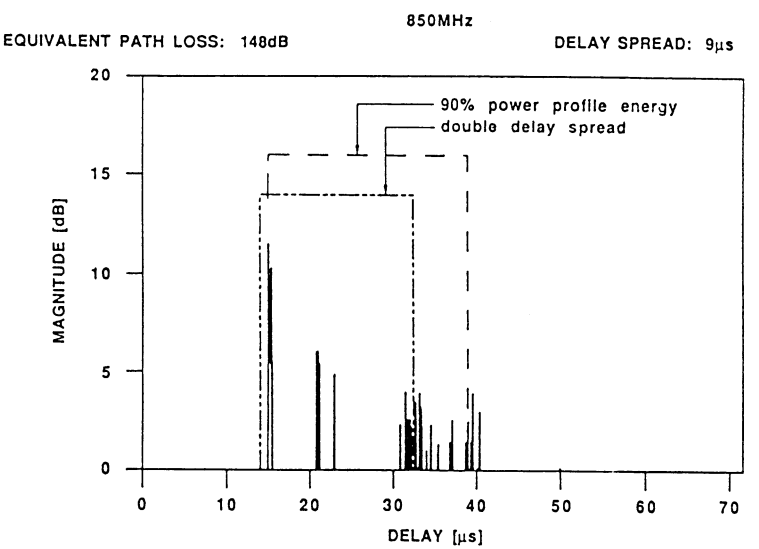

Fig. 2.3.13 Sample impulse response for Krattigen.

note: noise and side peaks have been removed
these examples show extremes of delay spread and delay window.

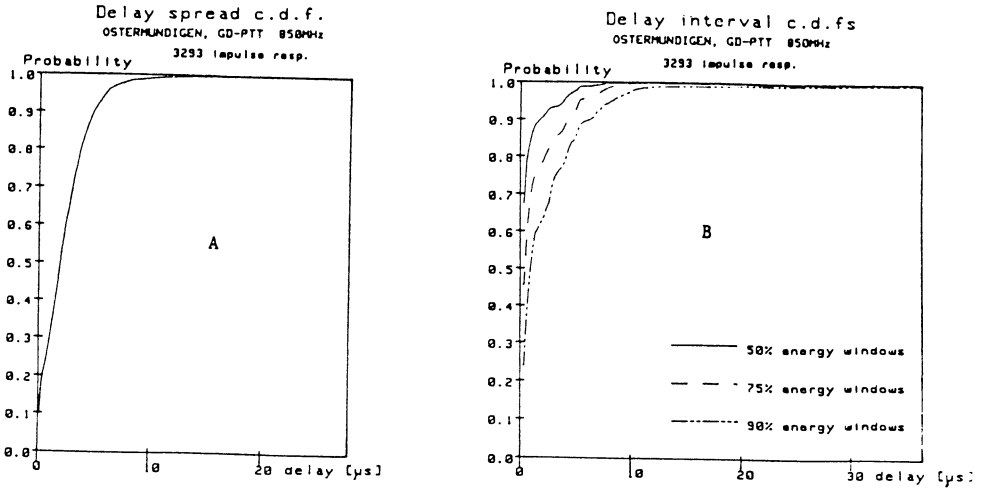

Fig. 2.3.14 CDFs of delay spread and the delay windows for Berne.

a. cdf of the delay spread S.
b. cdf of the delay intervals W_{50}, W_{75} and W_{90}, containing respectively 50%, 75%, and 90% of the energy.

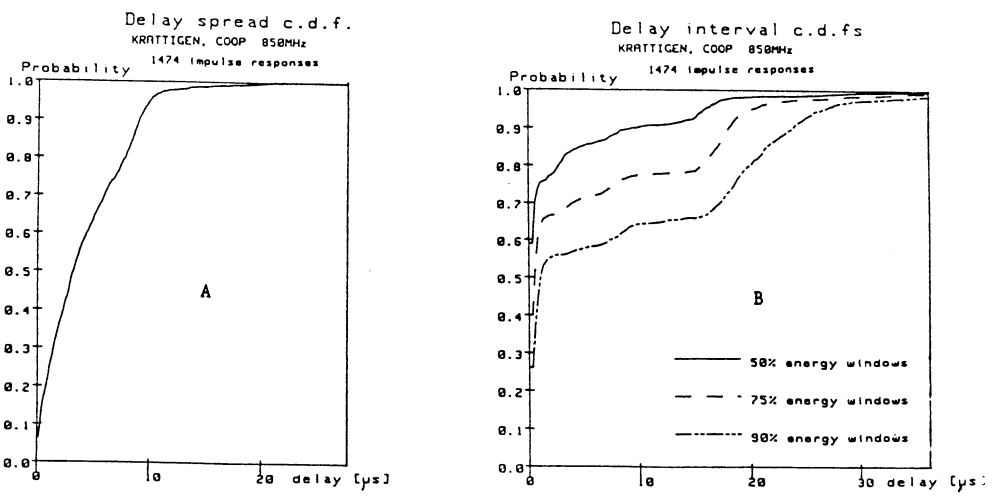

Fig. 2.3.15 CDFs of delay spread and the delay windows for Krattigen.

a. cdf of the delay spread S.
b. cdf of the delay intervals W_{50}, W_{75} and W_{90} containing respectively 50% ,75% and 90% of the energy.

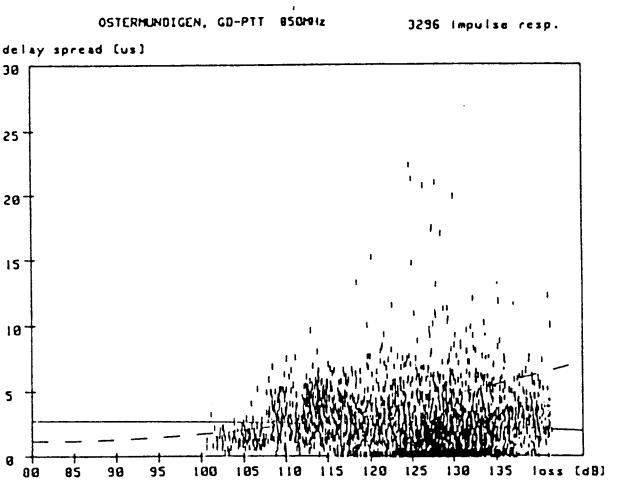

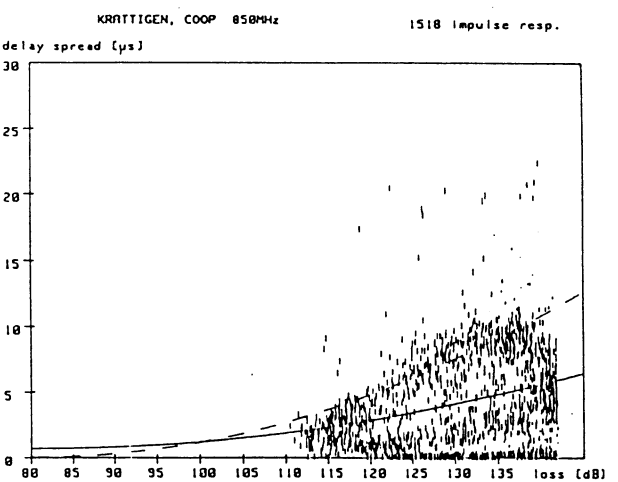

Fig. 2.3.16 Scattergram of the delay spread against peak path loss for Berne (top) and Krattigen (bottom).

The mean curve and the envelope curve are shown.

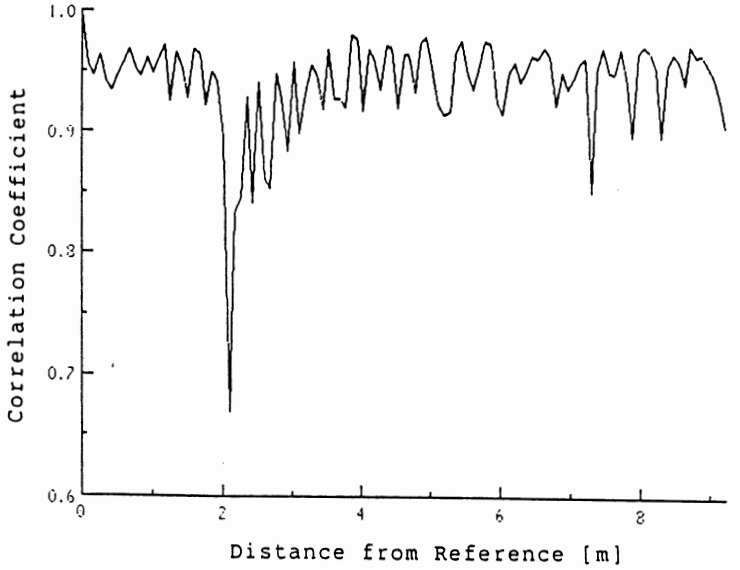

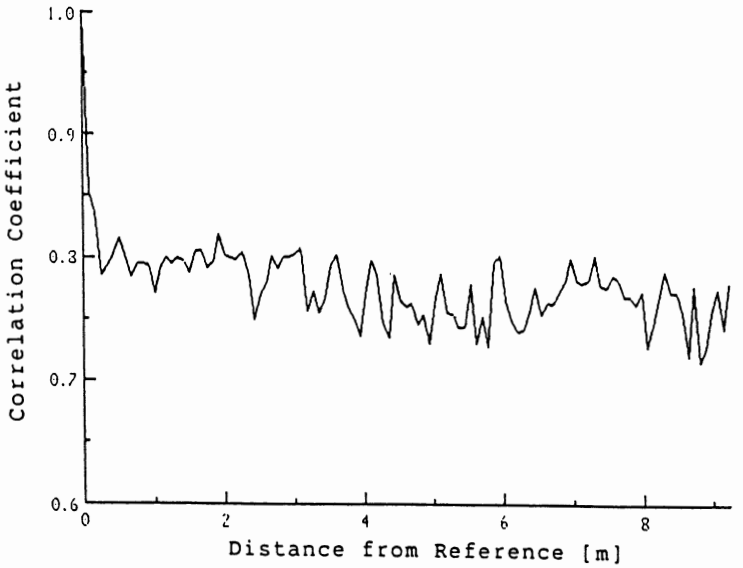

Fig. 2.3.17 Typical behaviour of the correlation coefficient with distance.

top: Berne

bottom: Krattigen

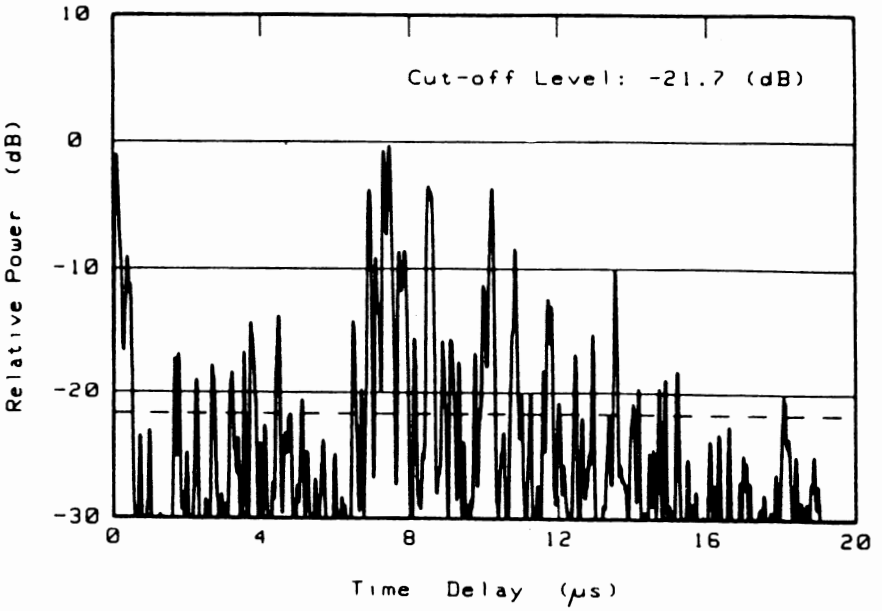

Fig. 2.3.18 Example of the impulse response in the St Vincent area.

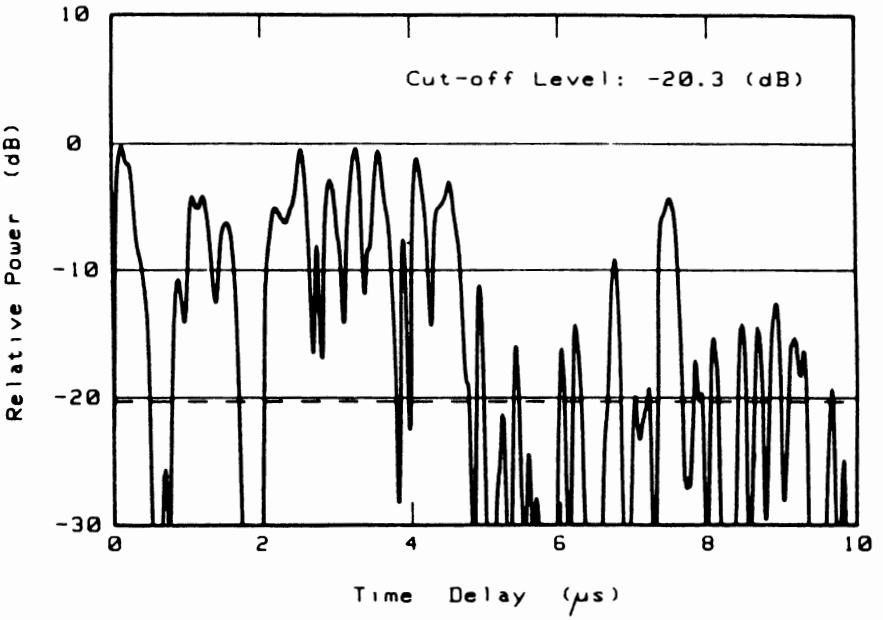

Fig. 2.3.19 Example of the impulse response in the Aosta area.

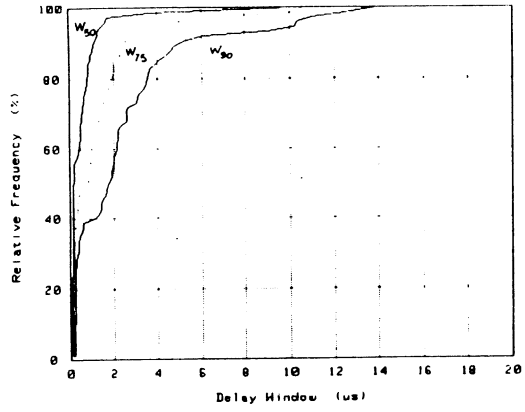

Fig. 2.3.20 (a) CDF of delay window for St. Vincent.

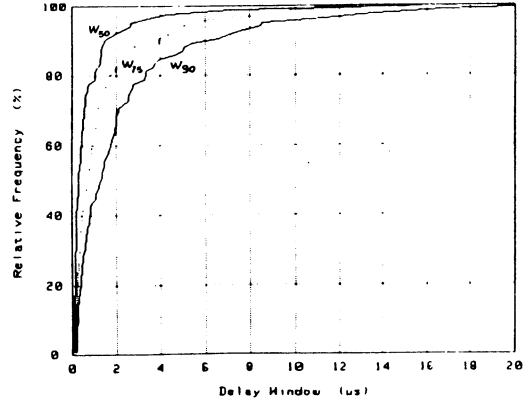

Fig. 2.3.20 (b) CDF of delay window for Aosta.

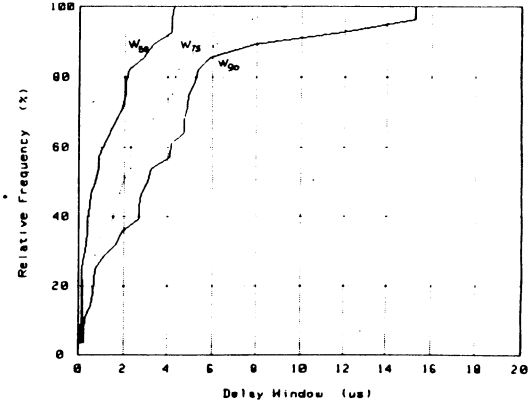

Fig. 2.3.20 (c) CDF of delay window for Courmayeur.

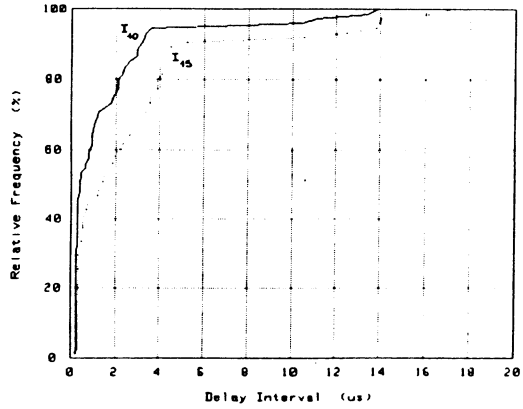

Fig. 2.3.21 (a) CDF of delay interval for St Vincent.

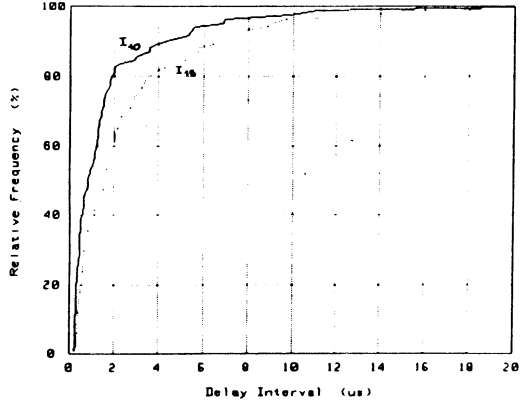

Fig. 2.3.21 (b) CDF of delay interval for Aosta.

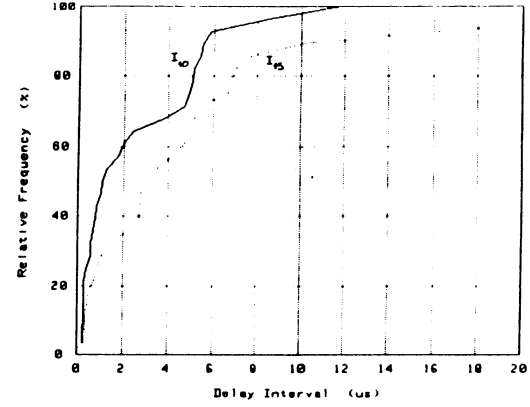

Fig. 2.3.21 (c) CDF of delay interval for Courmayeur.

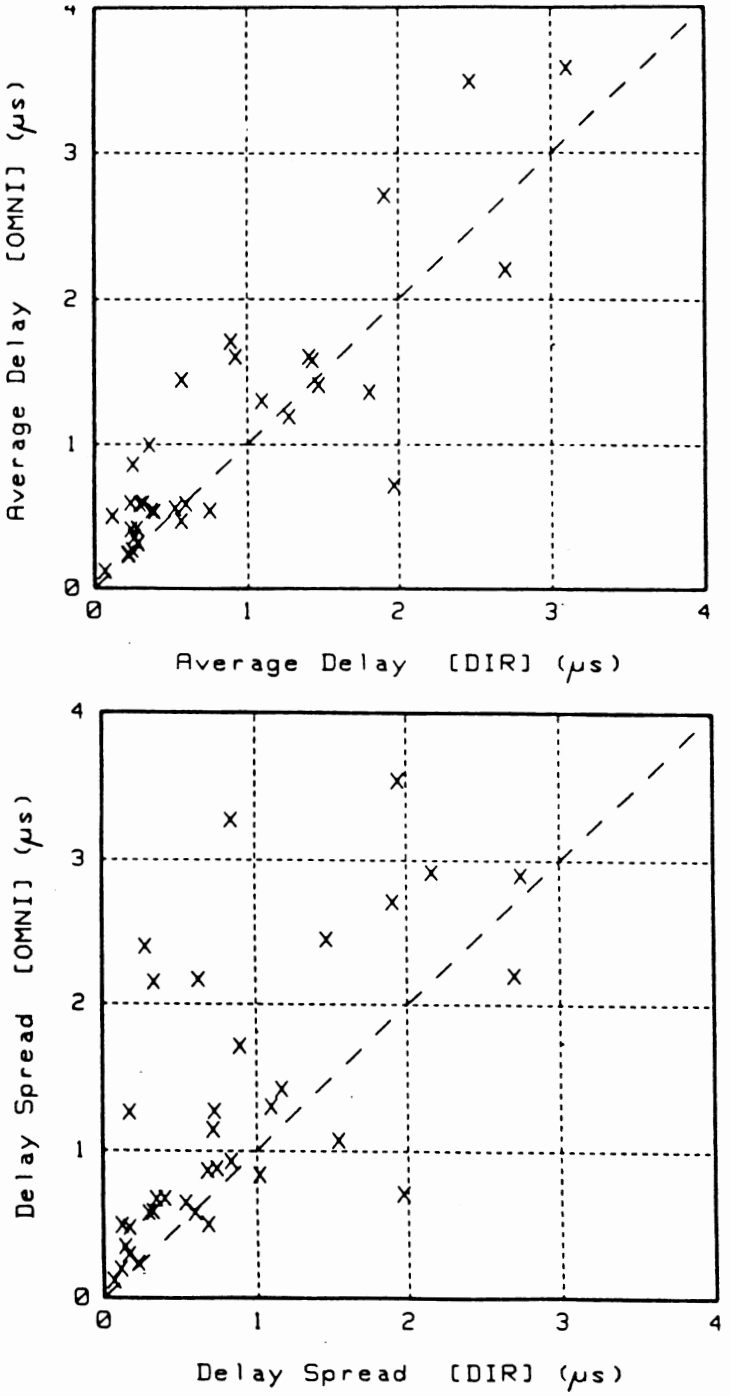

Fig. 2.3.22 Scattergram of average delay (top) and delay spread with omni-directional and directional antennas.

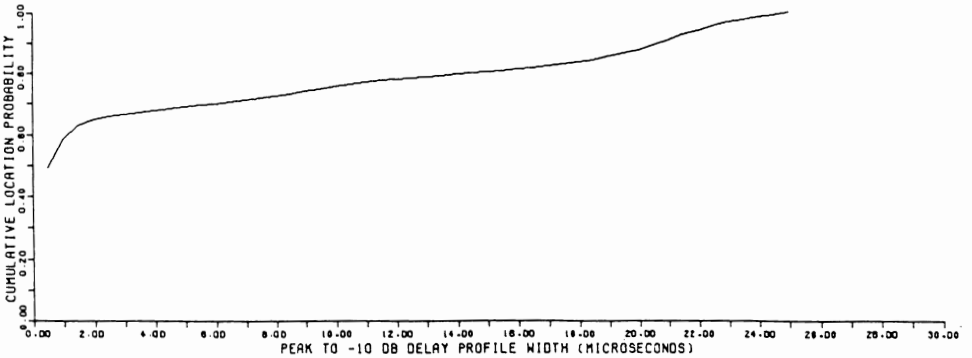

Fig. 2.3.23 CDF for 10db delay profile width for Yamanashi.

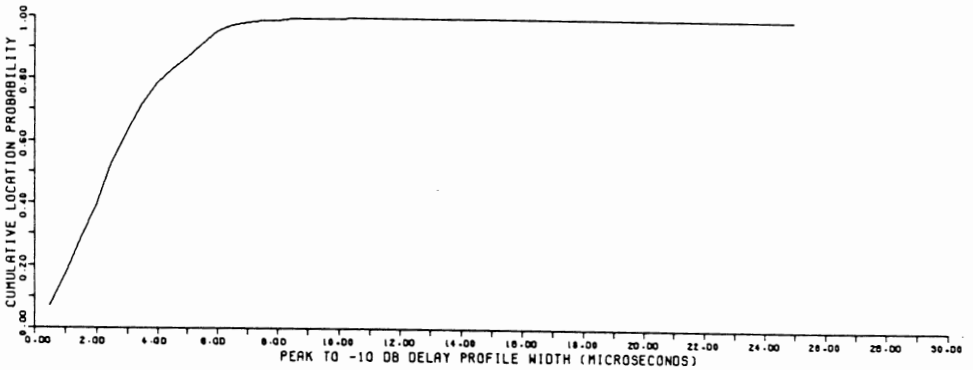

Fig. 2.3.24 CDF for 10db delay profile width for urban area, Tokyo.

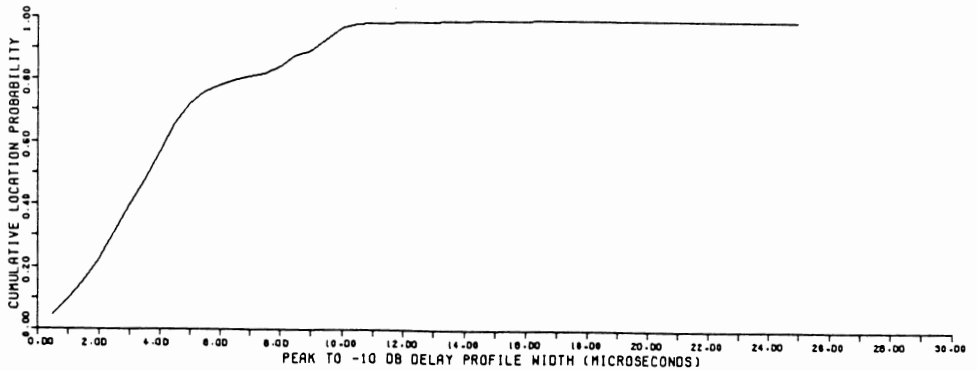

Fig. 2.3.25 CDF for 10db delay profile width for waterfront area, Tokyo.

2.4 SIMULATION OF RADIO CHANNELS

Radio propagation in the mobile radio environment is described by highly dispersive multipath caused by reflection and scattering. The paths between base station and mobile station may be considered to consist of large reflectors and/or scatterers some distance to the mobile, giving rise to a number of waves that arrive in the vicinity of the mobile with random amplitudes and delays.

Close to the mobile these paths are further randomised by local reflections/diffractions. Since the mobile will be moving, the angle of arrival must also be taken into account, since it affects the Doppler shift associated with a wave arriving from a particular direction. Echos of identical delays arise from reflectors located on an ellipse.

The multipath phenomenon may be described in the following way in terms of the time delays and the Doppler shifts associated with each delay:

$$z(t) = \iint_{R^2} y(t-\tau)\, S(\tau, f) \exp(2i\pi f \tau)\, df\, d\tau \qquad (2.4.1)$$

where the terms on the right-hand side represent the delayed signals, their amplitudes and Doppler spectra.

It has been shown that the criterion for wide sense stationarity is satisfied for distances of about 10 meters. Based on the wide sense stationarity uncorrelated scattering (WSSUS) model, the average delay profiles and the Doppler spectra are necessary to simulate the radio channel.

In order to allow practical simulation, the different propagation models will be presented here in the following terms:

1) a discrete number of taps, each determined by their time delay and their average power;
2) the Rayleigh distributed amplitude of each tap, varying according to a Doppler spectrum $S(\tau_i, f)$, where i is the number of the tap.

2.4.1 DOPPLER SPECTRUM TYPES

In this section, we define the four types of Doppler spectra which will be used for the modelling of the channel. Throughout this section the following abbreviations will be used:

- $f_d = v/\lambda$, represents the maximum Dppler shift, with v (in m/s) representing the vehicle speed, and λ (in m) the wavelength
- $G(a,f_1,f_2)$ is the Gaussian function

$$G(f) = A\exp\left(-\frac{(f-f_1)^2}{2f_2^2}\right). \tag{2.4.2}$$

The following types are defined:

a) CLASS is the classical Doppler spectrum and will be used for paths with delays not in excess of 500 ns; ($\tau_i \leq 0.5\,\mu s$)

$$\text{(CLASS)} \qquad S(\tau_i,f) = \frac{A}{\sqrt{(1-(f/f_d)^2)}} \qquad \text{for } f \in]-f_d,f_d[; \tag{2.4.3}$$

b) GAUS1 is the sum of two Gaussian functions and is used for excess delay times in the range of 500 ns to 2 μs; ($0.5\,\mu s < \tau_i \leq 2\,\mu s$)

$$\text{(GAUS1)} \qquad S(\tau_i,f) = G(A,-0.8f_d,0.05f_d) + G(A_1,0.4f_d,0.1f_d) \tag{2.4.4}$$

where A_1 is 10 dB below A;

c) GAUS2 is, also, the sum of two Gaussian functions and is used for paths with delays in excess of 2 μs; ($\tau_i \geq 2\,\mu s$)

$$\text{(GAUS2)} \qquad S(\tau_i,f) = G(B,0.7f_d,0.1f_d) + G(B_1,-0.4f_d,0.15f_d) \tag{2.4.5}$$

where B_1 is 15 dB below B;

d) RICE is the sum of of a classical Doppler spectrum and one direct path, such that the total multipath contribution is equal to that of the direct path. This spectrum is used for the shortest path of the model for propagation in rural areas;

$$\text{(RICE)} \qquad S(\tau_i,f) = \frac{0.41}{2\pi f_d\sqrt{(1-(f/f_d)^2)}} + 0.91\,\delta(f-0.7f_d) \tag{2.4.6}$$

for $f \in]-f_d,f_d[$.

2.4.2 PROPAGATION MODELS

As a general principle the propagation models are refered to as NAMEx, where NAME is the name of the particular model, which is defined hereunder, and x is the vehicle speed (in km/h) which impacts on the definition of f_d (see section 2.4.1) and hence on the Doppler spectra.

The models are defined by the delay power profiles

$$P(\tau_i) = P_0 \int_{-f_d}^{f_d} S^2(\tau_i, f)\, df \qquad (2.4.7)$$

where P_0 is a normalising power and $P(\tau_i)$ is the power transmitted by tap i of a transversal filter.

The discrete possibilities for parameter settings of hardware fading simulators may differ. Therefore, propagation models for different types of terrain are defined by continuous delay power profiles which are to be approximated according to rules which are given in section 2.4.3.

The continuous delay power profiles $P(\tau)$ are defined as follows:

2.4.2.1 Typical case for rural (non-hilly) area (RA)

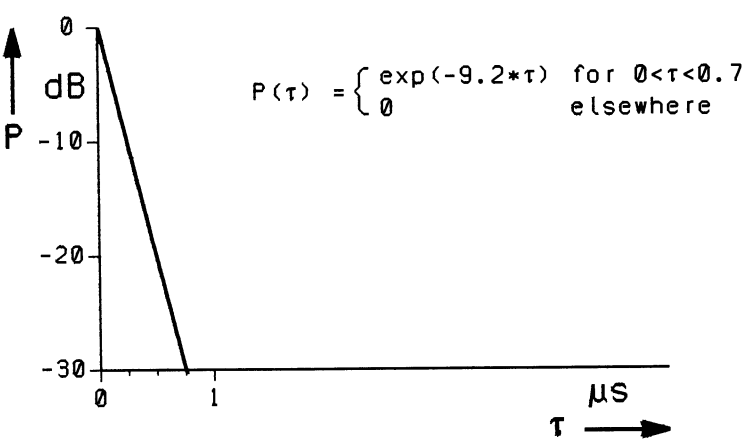

Figure 2.4.1

2.4.2.2 Typical case for urban (non-hilly) area (TU)

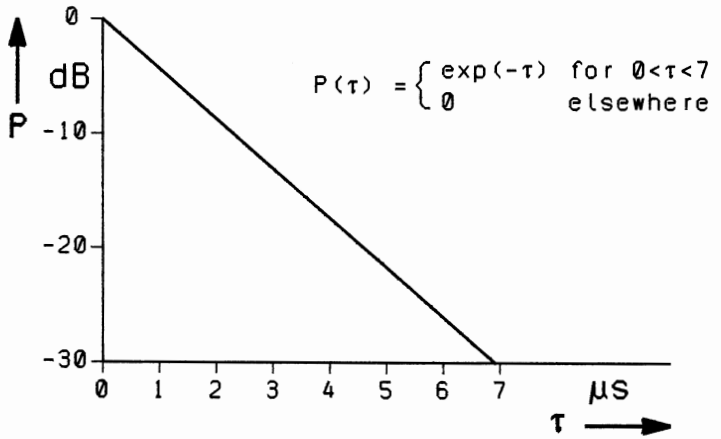

Figure 2.4.2

2.4.2.3 Typical bad case for hilly urban area (BU)

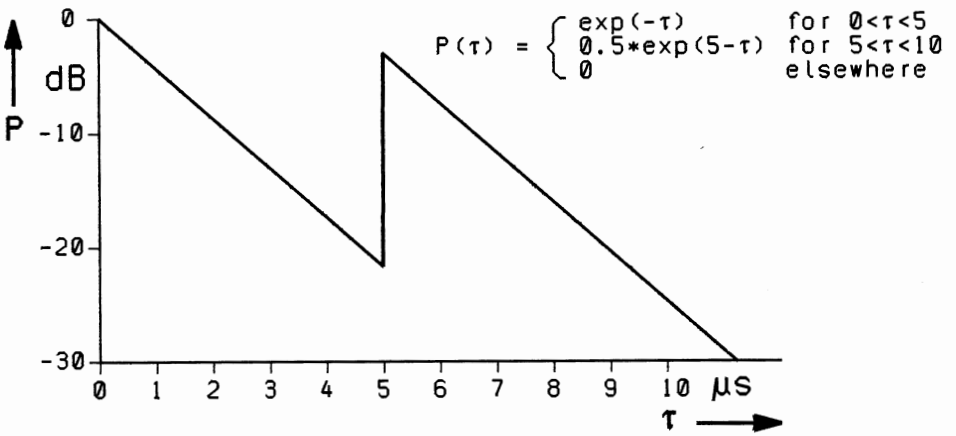

Figure 2.4.3

2.4.2.4 Typical case for hilly terrain (HT)

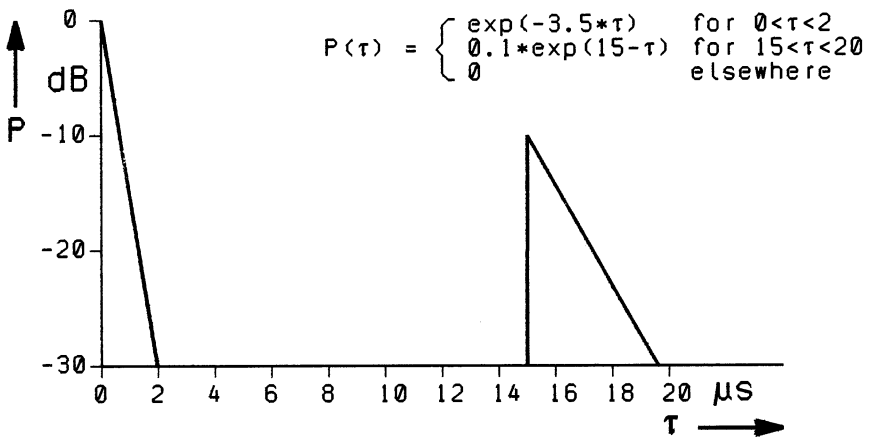

Figure 2.4.4

2.4.3 APPROXIMATION OF THE DELAY POWER PROFILES BY DISCRETE TAPS

Hardware multitap fading simulators can be set only to discrete values of $P(\tau_i)$ in both, amplitude and delay. Different types of fading simulators may differ in the parameters to be set. The approximation of the delay power profiles given in section 2.4.2 is to be performed according to the following rules:

<u>RULE I:</u>

The delay spread

$$S_D^2 = \frac{1}{P_m}\sum_{i=1}^{I}\tau_i^2 P(\tau_i) - \left[\frac{1}{P_m}\sum_{i=1}^{I}\tau_i P(\tau_i)\right]^2, \qquad (2.4.8)$$

where I is the total number of taps and

$$P_m = \sum_{i=1}^{I} P(\tau_i) \qquad (2.4.9)$$

is the total transmitted power, should be within the tolerances:

RA: $S_D = (0.1 \pm 0.02)\,\mu s$

TU: $S_D = (1.0 \pm 0.1\ )\,\mu s$

BU: $S_D = (2.5 \pm 0.2\ )\,\mu s$

HT: $S_D = (5.0 \pm 0.2\ )\,\mu s$

RULE II:

The delay interval W_{90} defines the period of time within which 90 % of the total received energy of a short pulse is detected. W_{90} is defined by

$$\int_{t_0}^{W_{90}} P(\tau)\,d\tau = 0.9 \int_{t_0}^{\infty} P(\tau)\,d\tau \qquad (2.4.10)$$

where t_0 is the delay along the direct line of sight. For discrete taps W_{90} is usually not existing. Therefore, it must be linearily interpolated between the delays of the tap where a value is just below 90 % of the energy and the next tap where the energy is above 90 %.

The value of W_{90} should be within the following tolerances:

RA: W_{90} = (0.25 ± 0.15) μs
TU: W_{90} = (2.3 ± 0.6) μs
BU: W_{90} = (6.6 ± 1.0) μs
HT: W_{90} = (15.5 ± 1.0) μs

RULE III:

The total number of taps should not be smaller than

RA: 3
TU: 4
BU: 6
HT: 6

Future study is needed to compare the performance between continuous power delay profiles and approximation based on a discrete number of taps from a system simulation point of view.

RULE IV:

The delay spacing between the taps should be chosen to avoid a regular spacing. This will ensure the frequency transfer function of the radio channel will not have large periodicities. (This is particularly important for frequency hopping.)

2.4.4 EXAMPLES FOR TAP SETTINGS

For three different types of fading simulators tap settings were defined according to the rules given in section 2.4.3 to approximate the delay power profiles in section 2.4.2. They are given for simulators with up to 12 taps and for simulators for reduced model settings with up to 6 taps.

2.4.4.1 Typical case for rural (non-hilly) area (RA)

Tap No	Delay [μs]	Power (lin)	Power [dB]	Doppler category	s_D [μs]
1	0	1	0	RICE	
2	0.2	0.63	-2	CLASS	0.1
3	0.4	0.1	-10	CLASS	
4	0.6	0.01	-20	CLASS	

Table 2.4.1a

or

Tap No	Delay [μs]	Power (lin)	Power [dB]	Doppler category	s_D [μs]
1	0	1	0	RICE	
2	0.1	0.4	-4	CLASS	
3	0.2	0.16	-8	CLASS	0.1
4	0.3	0.06	-12	CLASS	
5	0.4	0.03	-16	CLASS	
6	0.5	0.01	-20	CLASS	

Table 2.4.1b

Note: There are no parameter settings for rural areas with more than 6 taps to be recommended.

2.4.4.2 Typical case for urban (non-hilly) area (TU)

Tap No	Delay [μs]	Power (lin)	Power [dB]	Doppler category	S_D [μs]
1	0	0.4	-4	CLASS	
2	0.2	0.5	-3	CLASS	
3	0.4	1	0	CLASS	
4	0.6	0.63	-2	GAUS1	
5	0.8	0.5	-3	GAUS1	
6	1.2	0.32	-5	GAUS1	1.0
7	1.4	0.2	-7	GAUS1	
8	1.8	0.32	-5	GAUS1	
9	2.4	0.25	-6	GAUS2	
10	3.0	0.13	-9	GAUS2	
11	3.2	0.08	-11	GAUS2	
12	5.0	0.1	-10	GAUS2	

Table 2.4.2a

or

Tap No	Delay [μs]	Power (lin)	Power [dB]	Doppler category	S_D [μs]
1	0	0.4	-4	CLASS	
2	0.1	0.5	-3	CLASS	
3	0.3	1	0	CLASS	
4	0.5	0.55	-2.6	CLASS	
5	0.8	0.5	-3	GAUS1	
6	1.1	0.32	-5	GAUS1	1.0
7	1.3	0.2	-7	GAUS1	
8	1.7	0.32	-5	GAUS1	
9	2.3	0.22	-6.5	GAUS2	
10	3.1	0.14	-8.6	GAUS2	
11	3.2	0.08	-11	GAUS2	
12	5.0	0.1	-10	GAUS2	

Table 2.4.2b

Examples for 6-tap reduced TU:

Tap No	Delay [μs]	Power (lin)	Power [dB]	Doppler category	S_D [μs]
1	0	0.5	-3	CLASS	
2	0.2	1	0	CLASS	
3	0.6	0.63	-2	GAUS1	1.1
4	1.6	0.25	-6	GAUS1	
5	2.4	0.16	-8	GAUS2	
6	5.0	0.1	-10	GAUS2	

Table 2.4.2c

or

Tap No	Delay [μs]	Power (lin)	Power [dB]	Doppler category	S_D [μs]
1	0	0.5	-3	CLASS	
2	0.2	1	0	CLASS	
3	0.5	0.63	-2	CLASS	1.0
4	1.6	0.25	-6	GAUS1	
5	2.3	0.16	-8	GAUS2	
6	5.0	0.1	-10	GAUS2	

Table 2.4.2d

2.4.4.3 Typical bad case for hilly urban area (BU)

Tap No	Delay [μs]	Power (lin)	Power [dB]	Doppler category	S_D [μs]
1	0	0.2	-7	CLASS	
2	0.2	0.5	-3	CLASS	
3	0.4	0.79	-1	CLASS	
4	0.8	1	0	GAUS1	
5	1.6	0.63	-2	GAUS1	
6	2.2	0.25	-6	GAUS2	2.5
7	3.2	0.2	-7	GAUS2	
8	5.0	0.79	-1	GAUS2	
9	6.0	0.63	-2	GAUS2	
10	7.2	0.2	-7	GAUS2	
11	8.2	0.1	-10	GAUS2	
12	10.0	0.03	-15	GAUS2	

Table 2.4.3a

or

Tap No	Delay [μs]	Power (lin)	Power [dB]	Doppler category	S_D [μs]
1	0	0.17	-7.7	CLASS	
2	0.1	0.46	-3.4	CLASS	
3	0.3	0.74	-1.3	CLASS	
4	0.7	1	0	GAUS1	
5	1.6	0.59	-2.3	GAUS1	
6	2.2	0.28	-5.6	GAUS2	2.5
7	3.1	0.18	-7.4	GAUS2	
8	5.0	0.72	-1.4	GAUS2	
9	6.0	0.69	-1.6	GAUS2	
10	7.2	0.21	-6.7	GAUS2	
11	8.1	0.1	-9.8	GAUS2	
12	10.0	0.03	-15.1	GAUS2	

Table 2.4.3b

Examples for 6-tap reduced BU:

Tap No	Delay [μs]	Power (lin)	Power [dB]	Doppler category	S_D [μs]
1	0	0.5	-3	CLASS	
2	0.4	1	0	CLASS	
3	1.0	0.5	-3	GAUS1	2.4
4	1.6	0.32	-5	GAUS1	
5	5.0	0.63	-2	GAUS2	
6	6.6	0.4	-4	GAUs2	

Table 2.4.3c

or

Tap No	Delay [μs]	Power (lin)	Power [dB]	Doppler category	S_D [μs]
1	0	0.56	-2.5	CLASS	
2	0.3	1	0	CLASS	
3	1.0	0.5	-3	GAUS1	2.5
4	1.6	0.32	-5	GAUS1	
5	5.0	0.63	-2	GAUS2	
6	6.6	0.4	-4	GAUs2	

Table 2.4.3d

2.4.4.4 Typical case for hilly terrain (HT)

Tap No	Delay [μs]	Power (lin)	Power [dB]	Doppler category	S_D [μs]
1	0	0.1	-10	CLASS	
2	0.2	0.16	-8	CLASS	
3	0.4	0.25	-6	CLASS	
4	0.6	0.4	-4	GAUS1	
5	0.8	1	0	GAUS1	
6	2.0	1	0	GAUS1	5.0
7	2.4	0.4	-4	GAUS2	
8	15.0	0.16	-8	GAUS2	
9	15.2	0.13	-9	GAUS2	
10	15.8	0.1	-10	GAUS2	
11	17.2	0.06	-12	GAUS2	
12	20.0	0.04	-14	GAUS2	

Table 2.4.4a

or

Tap No	Delay [μs]	Power (lin)	Power [dB]	Doppler category	S_D [μs]
1	0	0.1	-10	CLASS	
2	0.1	0.16	-8	CLASS	
3	0.3	0.25	-6	CLASS	
4	0.5	0.4	-4	CLASS	
5	0.7	1	0	GAUS1	
6	1.0	1	0	GAUS1	5.0
7	1.3	0.4	-4	GAUS1	
8	15.0	0.16	-8	GAUS2	
9	15.2	0.13	-9	GAUS2	
10	15.7	0.1	-10	GAUS2	
11	17.2	0.06	-12	GAUS2	
12	20.0	0.04	-14	GAUS2	

Table 2.4.4b

Examples for 6-tap reduced HT:

Tap No	Delay [μs]	Power (lin)	Power [dB]	Doppler category	S_D [μs]
1	0	1	0	CLASS	
2	0.2	0.63	-2	CLASS	
3	0.4	0.4	-4	CLASS	5.0
4	0.6	0.2	-7	CLASS	
5	15	0.25	-6	GAUS2	
6	17.2	0.06	-12	GAUS2	

Table 2.4.4c

or

Tap No	Delay [μs]	Power (lin)	Power [dB]	Doppler category	S_D [μs]
1	0	1	0	CLASS	
2	0.1	0.71	-1.5	CLASS	
3	0.3	0.35	-4.5	CLASS	5.0
4	0.5	0.18	-7.5	CLASS	
5	15.0	0.16	-8.0	GAUS2	
6	17.2	0.02	-17.7	GAUS2	

Table 2.4.4d

Classical Doppler spectra <u>may</u> be used for all taps instead of RICE, GAUS1 and GAUS2. This approach is a worst case of the time variance of the mobile radio channel.

2.4.5 HARDWARE FADING SIMULATORS

Within the framework of COST 207 three different types of fading simulators were developed, tested and used for test measurements of radio subsystems.

An analog fading simulator is described by Berthoumieux, 1986. The delays are performed by coaxial cables of different length and by SAW elements. A large multitude of delays can be set. The maximum delay is 31.2 μs. The noise sequences with specified Doppler spectra are stored in RAMs. The length of the sequences is specified for a period of measurement of 30 s for simulation of a vehicle speed of 300 km/h. After that time interval the

noise sequence is repeated. At lower speeds the periodicity is longer according to the speed ratios.

A digital fading simulator is described by Schüßler, 1986. The radio signal is down-converted to baseband, digitized, delayed in up to 15 taps and modulated by random sequences separated by signal processors in real time. The delays can be set in 0.1-μs steps with a maximum delay of 200 μs.

Both fading simulators were tested in their performance carefully and found suitable to be used for the GSM tests of different radio subsystems in 1986. They suffered, however, from some technical drawbacks so that it was not recommendable to reproduce one of them. Therefore, a third fading simualtor was developed, which is described by de Brito et. al., 1988. The radio signals are down converted to 10 MHz, digitized and delayed in 0.2-μs steps. The maximum delay is 51 μs and 12 taps are available. The noise sequences are stored in EPROMs and modulated analogically at each tap. Also this fading simulator was tested by COST 207 and found to be suitable for simulation of mobile radio path. Its performance was in all characteristics improved with respect to the purely analog and digital devices.

2.4.6 REFERENCES

Berthoumieux, D. and Pertoldi, J.M., 1986, "Hardware propagation simulator of the frequency-selective fading channel at 900 MHz", Proceedings of the Second Nordic Seminar, Stockholm, 214-217.

de Brito, G., Failli, R., Lorenz, R.W. and Swain, R.S., 1988, "An Overview of the COST 207 Programmes in Support of the GSM", Proceedings of the Third Nordic Seminar, Copenhagen, 3.2.

Schüßler, H.W. and Thielecke, J.M., 1986, "A Digital frequency fading simulator", Proceedings of the Second Nordic Seminar, Stockholm, 331-336.

2.5 SOFTWARE SIMULATION

2.5.1 INTRODUCTION

The topic we shall discuss in this section is the simulation of the signal distortion due to severe conditions which radio propagation in mobile communication has to cope with and his impact in terms of Bit Error Rate on performance of digital system.The presented matter is based on the COST Document [8], successivly published [11].

In the previous paragraph "Mathematical description of the multipath mobile radio channel", it has been deeply discussed a suitable stochastic model for mobile radio links, known in literature as GWSSUS (**G**aussian **W**ide-**S**ense **S**tationary **U**ncorrelated **S**cattering) model [1], [2]. Here only the matter relevant for understanding the simulation performed in the frame of COST 207 is discussed.

Although the characteristics of a mobile radio channel can change abruptly, for example when the mobile enters a city from the country, nevertheless a stationary model can be assumed valid for times which are adequate for B.E.R. estimation. The differences among the various environments, which primarily determine the abrupt changes, can be taken into account by repeating the computations for the different environments. Bearing this in mind, the GWSSUS model can be adopted for the simulation of the channel .

As the transmission channel has to be described by means of a random process, the problem arises of how determining the parameters and the functions which give a suitable description of the phenomenon.

For the adopted stochastic model the environmental conditions enter mainly by means of two functions: the "Delay Power Spectrum"(DPS) and the "Doppler Power Spectrum". These functions describe respectively the

dispersion due to the channel in the time or frequency domain.

The experimental results obtained in the COST 207 research activity are the basis for the computations [10].

In order to investigate the importance of the shape of these functions and of the parameters which are involved in their expression, a flexible tool like a software simulation turned out to be interesting and useful.

The main goal of the work was to emphasize the correlation between propagation and demodulation errors; the emphasis was not on the precise evaluation of the BER for a given and well-defined mo-demodulation scheme, but rather on the general influence of the channel; therefore only the irreducible probability of error was estimated in order to separate the influence of the channel from the other sources of error like random noise or interference and to point out the effect of the time and frequency selective behaviour of the channel. Among the implemented mo-demodulation schemes, the non coherent 2-FSK system was chosen as the most adequate for this purpose. Due to the flexibility of the computer program, several environmental conditions were explored and the main parameters of the above defined functions were changed in their proper range.

The analysis was able to individuate which parameters are really important in order to characterize the real channel and must be experimentally evaluated.

2.5.2 BASIC OF THE COMPUTER PROGRAM.

Hereinafter only the aspects relevant for the understanding of the computer program are summarized; for further details, you may refer to [1] [2] [3] [4].

The basic formula used for the computation of the output signal y(t) is:

$$y(t) = \mathrm{Re}\left\{ v(t)\ e^{j2\pi f_o t} \right\} =$$

$$= \mathrm{Re}\left\{ \sum_{i=1}^{N} \rho_i u(t-t_i) \bullet e^{(j2\pi t(f_o-f_i)-j2\pi f_o t_i - j\vartheta_i)} \right\} \quad (2.5.1)$$

where $v(t)$ represents the complex envelope of $y(t)$, $u(t)$ the complex envelope of the input signal $s(t)$; f_o represents the central frequency of the pass-band signal and N discrete scattering points are assumed generating the received signal, each determined by four random variables: an amplitude f_i, a relative delay t_i, a Doppler shift f_i and phase ϑ_i (in the range $0 \div 2\pi$).

The number N can be assigned as a specification (discrete scattering model) or determined in such a way to approximate a continuous distribution of scattering. All the simulations we present were obtained with 100 scattering points in order to have a good approximation of a continuous spectrum of scattering points. In the real life some isolated multipath signals can be present: the computer program is able to simulate also this situation.

We have to introduce also two statistic functions; the function $Q(t_r)$ is known as Delay Power Spectrum (DPS) and yields the average delay distribution of the scattering points, no matter which Doppler shift they introduce. The function $P(f_d)$ is known as Doppler Power Spectrum whose meaning is easily understood by duality. Related to these functions, there are also the two parameters:

$$B = \sqrt{\frac{\int f_d^2 \, P(f_d) \, df_d}{\int P(f_d) \, df_d} - \left[\frac{\int f \, P(f_d) \, df_d}{\int P(f_d) \, df_d} \right]^2} \qquad (2.5.2)$$

$$L = \sqrt{\frac{\int f_d^2 \, Q(t_r) \, dt_r}{\int Q(t_r) \, dt_r} - \left[\frac{\int f \, Q(t_r) \, dt_r}{\int Q(t_r) \, dt_r} \right]^2} \qquad (2.5.3)$$

The parameter L is known as the delay spread, B as the Doppler spread. It is readily understood that they yield a measure of the extension in time or frequency of the function which they are related to.

The quantity:

$$K = 4 \, BL \qquad (2.5.4)$$

is a measure of the overall spreading of the channel in time and frequency and is usually known as spread factor.

A first choice in generating the random variables for eq. (2.5.1), was to interpret the $P(f_d)$ and $Q(t_r)$ functions, suitably normalized, as the probability density function for a distribution of scattering points having equal amplitude.

In such a way $Q(t_r) \, dt_r$ represents the probability of a SP occurring with delay between t_r and t_r+dt_r. In the computer program the N scattering points are distributed, following the given $P(f_d)$ and $Q(t_r)$, with a Rayleigh amplitude having equal rms P_r.

This approach is equivalent to assume that, for istance, $Q(t_r)$ is the average power distribution at any generic Doppler shift f_d.

This is not an intrinsec limitation of the program, but it is a useful simplification and a reasonable hyphotesis

The block diagram of the program is sketched in Fig. 1.

2.5.3 ANALYSIS OF IRREDUCIBLE BER FOR CONTINUOUS AND SMOOTH SPECTRA.

A first analysis was performed assuming some classical functions for $Q(t_r)$ ad $P(f_d)$, theoretically derived.

An example of such a computation is shown in Fig. 2 where these functions were used:

$$P(f_d) = \begin{cases} 0 & |f_d| > \sqrt{2B} \\ \dfrac{1}{\pi\sqrt{2B^2 - f_d^2}} & |f_d| < \sqrt{2B} \end{cases} \qquad (2.5.5)$$

$$Q(f_d) = \begin{cases} 0 & t_r < 0 \\ \dfrac{1}{L} e^{-\frac{t_r}{L}} & t_r \geq 0 \end{cases} \qquad (2.5.6)$$

The spread factor K can be assumed as a constant parameter for the curves. In Fig. 2 plots are referred to the irreducible BER versus the normalized bit rate d:

$$d = \frac{1}{T}\sqrt{\frac{L}{B}} \qquad (2.5.7)$$

and are related to a classical non-coherent binary CPFSK modulation scheme with limiter-discriminator detection.

Fig. 2 shows two regions where the BER increases; the first one on the left, where the main responsible is the time variation of the channel. The second one, on the right, where the frequency selectivity due to the multipath propagation plays the most important role.

For the digital mobile radio system under definition this is the most interesting area as it will be shown in the following.

For continuous and smooth spectra a first question is related to the importance of the shape of the functions; some investigations [5], [6], [7] suggested the possibility that the only relevant parameters are B and L, no matter what shape the functions have. Simulations performed with different spectra, but with the same B and L, confirmed that in the case of smooth functions the BER are negligibly different. Fig. 2 can be assumed to present results valid for any type of smooth spectrum, and the way of presentation is, in this case, adequate for characterizing the performance of a given mo-demodulation scheme.

Furthermore, in the region were the frequency selectivity of the channel is important, the variation of the frequency selectivity characteristics during the transmission is important in averaging the results, but in the range of values found useful in practice, the shape and the characteristics of the Doppler spectrum is not a critical matter.

Our attention was then focused on the delay power spectrum, not only because it is the responsible for the frequency selectivity, but also because the experimental work in progress showed the necessity to characterize some environments with spectra particularly sharp and with a two peak structure.

2.5.4 ANALYSIS OF A TWO PEAKS DELAY POWER SPECTRUM.

The experimental activity conducted in the propagation group of COST 207, brought to the conclusion that in some cases for hilly terrain, a delay power spectrum with two peaks can arise. ([8], [9]).

This situation is the mobile radio analogue to the two path model frequently used in radio relay links outage predictions. Of course more than two peaks can be present, but it is of great interest to analyze first the irreducible BER of that case when different relative

amplitude and delay are considered for the peaks, with the aim of connecting this particular environmental situation with BER performance and to control if the knowledge of B and L is enough also for this case.

A function $Q(t_r)$ is introduced in such a way that:

$$Q(t_r) = Q_1(t_r) + R\, Q_1(t_r - T_2) \qquad (2.5.8)$$

In eq. (2.5.8) $Q_1(t_r)$ represents the shape of the first peak; while the second one is delayed by a time T_2 and reduced in amplitude by a factor R. With the previous hypothesis it is possible to show that:

$$R_{\Omega\tau}(\Omega,\tau) = R_1(\Omega,\tau)\left[1 + Re^{-j\pi\Omega T_2}\right] \qquad (2.5.9)$$

(where $R(\Omega,\tau)$ is the single peak time-frequency correlation function related to $Q_1(t_r)$).

In a first set of simulation each peak was assumed with the same exponential shape; this yielded the following delay power spectrum:

$$Q(t_r) = e^{-t_r/r} + Re^{-(t_r - T_2)/r} \qquad (2.5.10)$$

for which the delay spread L follows from eq. (2.5.3).

If we want to maintain constant delay spread, this relation must be satistified by the three parameters r, R, T_2 appearing in eq. (2.5.10):

$$L = \sqrt{R^2 + \frac{R}{(1+R)^2}T_2^2} = r\sqrt{1 + R\left[\frac{T_2}{r(1+R)}\right]^2} \qquad (2.5.11)$$

$$L = \left(R^2 + \frac{R}{(1+R)^2}T_2^2\right)^{1/2} = r\left(1 + R\left(\frac{T_2}{r(1+R)}\right)^2\right)^{1/2} \qquad (2.5.11)$$

Some particular cases according to eq. (2.5.10) and

eq. (2.5.11) are shown in Fig. 3.

Because of eq. (2.5.11), if two parameters are fixed the third one is implicitly determined. Moreover the BER can be plotted versus each parameter, determining curves with one of the other kept constant. As r is a measure of the extension of each peak and T_2 represents the delay between them, interesting plots can be obtained versus the ratio T_2/r. If this ratio is low the peaks are overlapping and the spectrum is a smooth function; if the ratio increases, the shape with two peaks becomes more evident. The results of BER vs. T_2/r are shown in fig. 4. There is a substantial merging of the curves for different values of R, for low T_2/r; this corroborates the conclusion that the delay spread is the most important parameter for smooth spectra. On the contrary for high values the curves are quite different and higher values of R yields higher BER. Moreover the asymptotic behaviour shows that after a certain value the effect of the second peak does not change. Then for high values of T_2/r the most important parameter is the ratio R between the peaks amplitudes. In order to better understanding the physical interpretation we have investigated the performance of the system when we let the distance T_2 between the two peaks increase. The results are shown in fig. 5 and 6 which differs for the different values of r we used. A comparison of the two figures suggests a poor influence of this parameter.On the contrary the asymptotic behaviour is still present and the asymptotic values is determined by R. The figures allow to emphasize a sharp increase of the BER after a certain value; keeping in mind that we operate with a standard pulse duration of 1 ms., the saturation is reached when the peak separation is beyond a period interval. The interpretation can be as follows.

Since here the value of r is small, if compared to the symbol period, the paths belonging to the same peak do not

produce a significant frequency selectivity within the signal band, but only a flat fading. The channel produces two signals, whose median amplitude ratio is strictly related to the corresponding ratio R and whose phases are rapidly changing because of Doppler shifts in the carrier that sum up to produce the total signal. When the delay of the second signal exceedes the symbol period, it acts as a disturbance on the first one, no matter which is the delay. In this condition the final effect on the multipath is similar to the generation of a cochannel interferer. A more general interpretation is possible if one considers that in our demodulation scheme only the energy of the impulse response contained in one symbol period can be considered useful for the decoding. This energy spread inside the symbol period yield a distortion, greater as long as the delayed paths have greater energy. The energy outside the symbol period is considered as an uncorrelated interfering signal, whose effect is not dependent on the delay of the different paths. If more involved demodulation schemes are adopted, with adaptive equalizers or **M**aximum **L**ikelihood **S**equence **E**stimation (MLSE), the useful time duration can be extended, but this behaviour should be qualitatively present: in practice the energy of the impulse response is divided in two parts, the first one approximately useful and the second one interfering. Having this in mind it is of great importance for a given DPS the percentage of power beyond the time duration considered by demodulation/ decoding circuitry. Since this parameter is dependent on the complexity acceptable for the receiver, it is important to estimate the complete shape of the spectrum. Alternatively, for the presentation of the experimental results, one can estimate the percentage of the impulse energy distribution corresponding to multipaths whose delay does not exceed a certain value. Examples of this experimental work are shown in [9].

2.5.5 INFLUENCE OF DIFFERENT ENVIRONMENTAL CONDITIONS ON B.E.R.

Experimental work (see [8] [9]) conducted in the frame of COST 207 propagation group showed that different environments have quite different delay power spectra.[10]. It was then necessary to repeat the B.E.R estimation for the different environments, in order to examine if the specifications are reached. We did not test the proposed systems, but once again the goal was to highlight the problems the system designers are faced by.

Then the already discussed 2-FSK scheme was used in the different environments. In the figs. 7 a, b, c the delay power spectra experimentally found for the quoted situations are presented. It is possible to realize that two peak spectra are present in two typical bad cases. One can expect for these environments a sharp increase of B.E.R. beyond a certain bit-rate.

The results of the simulations are presented in fig. 8. A sharp increase is found for the typical bad case for hilly terrain. It ranges from 30 to 50 Kbit/s which is in correspondance with the delay between peaks. A similar behaviour was found for the typical bad case for suburban and urban areas where the values are approximately 200 Kbit/s and 5 μs. At low bit rates the B.E.R does not depend on the bit-rate or on the environment, but these values (10÷20 Kbit/s) are very low indeed. The values where the B.E.R. increases are in sequence as one can expect looking at the different spectrum shapes.

The Doppler spectrum was not found a critical point of the analysis in the bit-rate range in which we are interested. Simulations were performed with the Doppler spectrum defined by eq.(2.5.2).

2.5.6 REFERENCES

[1] Bello P.A. - "*Characterisation of randomly time variant linear channels*" - IEEE Trans. on Comm. Sys. - Vol. 11 Dec. 1963.

[2] Parson J. D. - "*Wideband characterisation of fading mobile radio channels*" - IEE Proc. Vol. 129, PK F N° 2 April 1982.

[3] G. Falciasecca, G. Riva - "*Software evaluation of BER in GWSSUS channels*" COST 207 - TD(87) N° 9 January 1987.

[4] G. Falciasecca, G. Riva, "*Programma di simulazione di un canale GWSSUS utilizzabile nei sistemi radiomobili*" F.U.B. , Rel. 40 Dec. 1983 Rif. 1B6483 (in Italian).

[5] Bach Andersen, "*Short term statistics of phase derivative in mobile communications*" COST 207 - T(85) 27.

[6] R.W. Lorenz, "*Impact of frequency-selective fading on binary and quadrature phase modulation in mobile radio communication demostrated by computer simulation using the Gwussus Channel model*", COST 207 - TD(86) 1, Darmstadt, Jan. 1986.

[7] C.I. Chuang - "*Simulation of Digital Modulation on Portable Radio Communication Channels with Frequency - Selective Fading*" GLOBE Com. '86. Dec. 1-4, 1986.

[8] E. Damosso - " *Wide-Band Propagation Measurements at 900 MHz in Mountainous Regions (Aosta Valley)*. COST 207 - TD(87) Doc. 35. May 1987.

[9] R.W. Lorenz, P. Kartaschoff et alii - *"First results of Delay Profile Measurements in Mountainous Area of Switzerland"* COST 207 - TD(87) Doc. 38. May 1987.

[10] *"Proposal on channel transfer functions to be used in GSM tests late* "1986" COST 207 - TD(86) N° 51 Rev. 3 Sept. 1986.

[11] *"B.E.R. simulation on wideband mobile radio channels and its correlation with the environmental parameters"* AEI Alta frequenza - Vol. LVII-N.2 - Febbraio/Marzo 1988

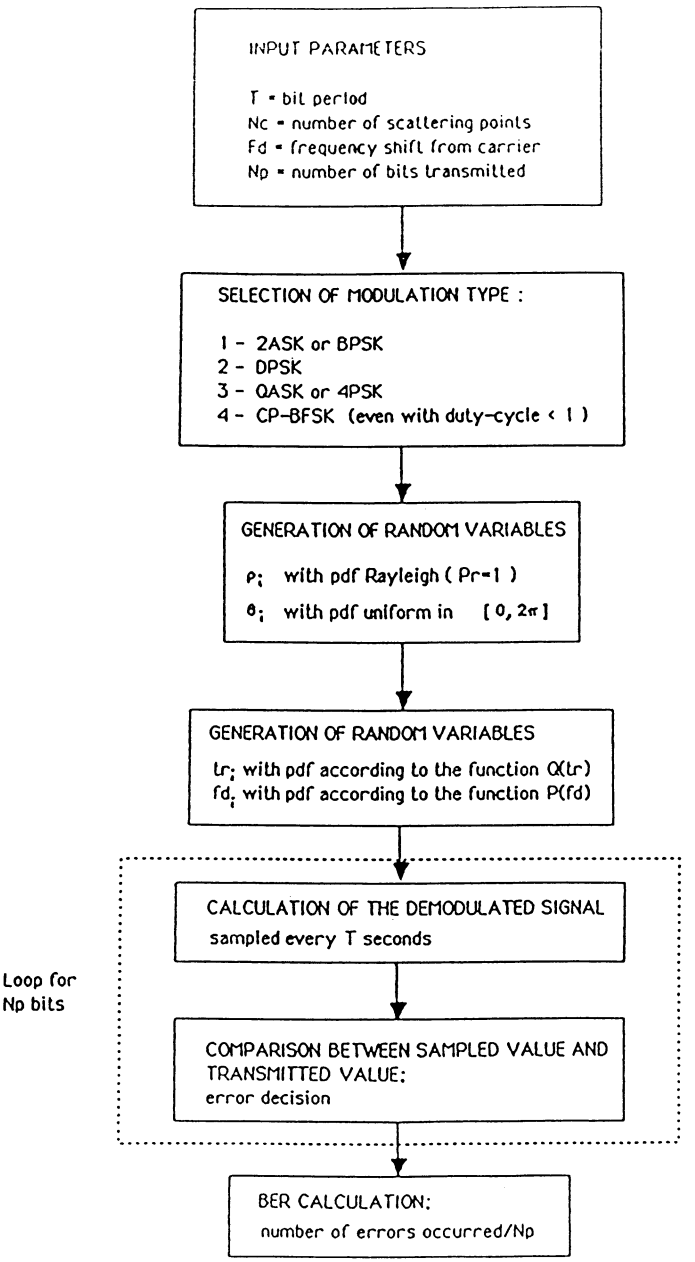

Fig.2.5.1 - Block diagram of the computer program.

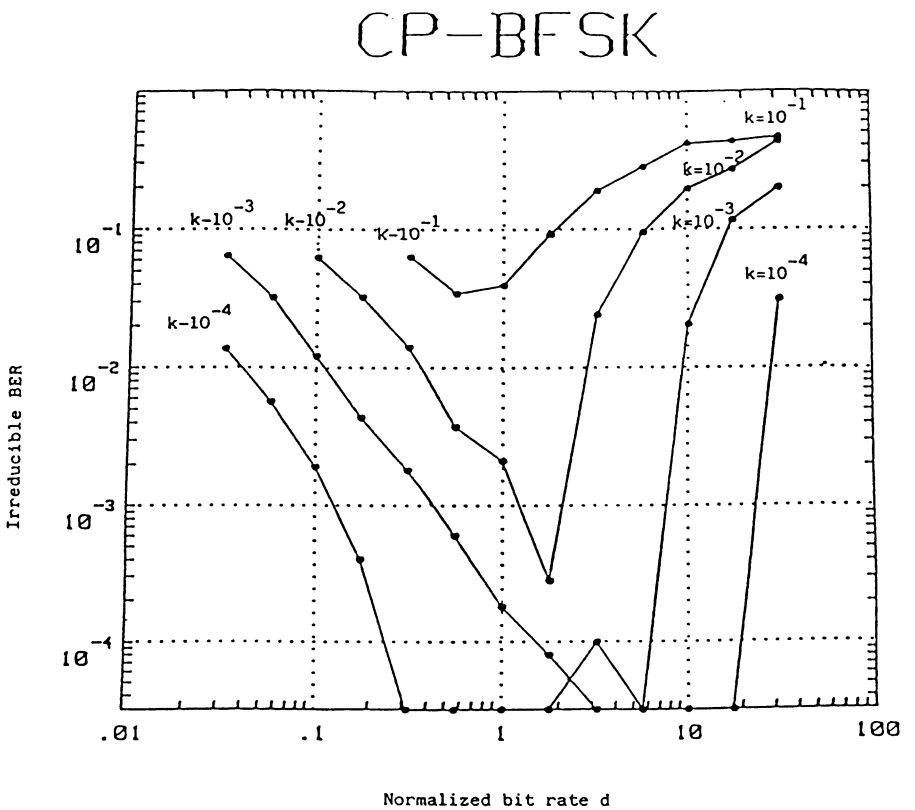

Fig.2.5.2 - Irreducible BER against the normalized bit-rate $d = (L/B)^{1/2}/T$ for different value of $K = 4BL$ (spread factor)

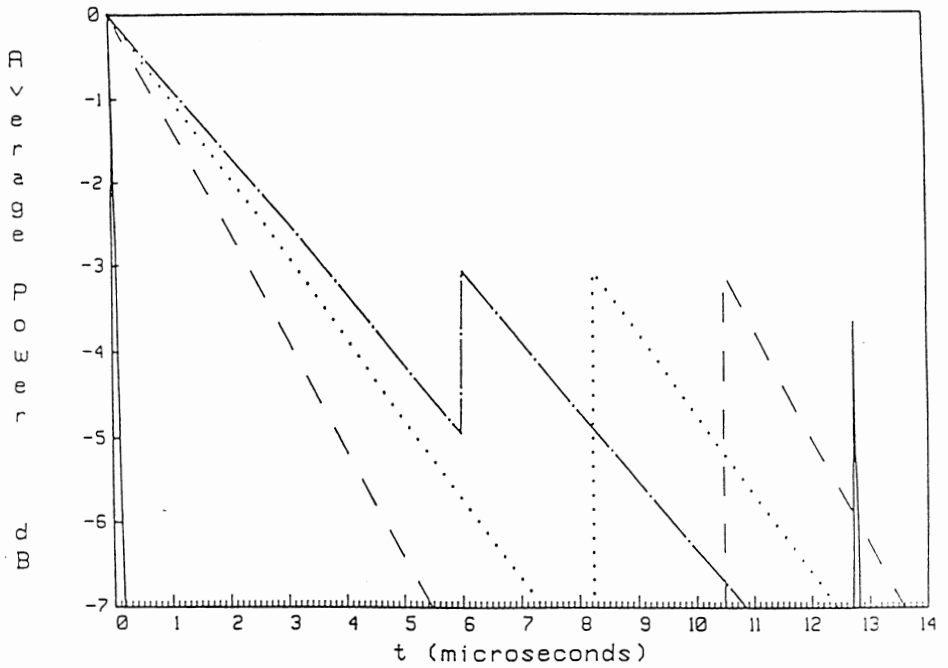

Fig.2.5.3 - Two peaks spectra with the same value of delay spread L = 6μs and for distance T_2 between peaks ranging from 6.0 to 12.72μs
Relative amplitude R = 0.5; 0.011 ms < r < 5μs

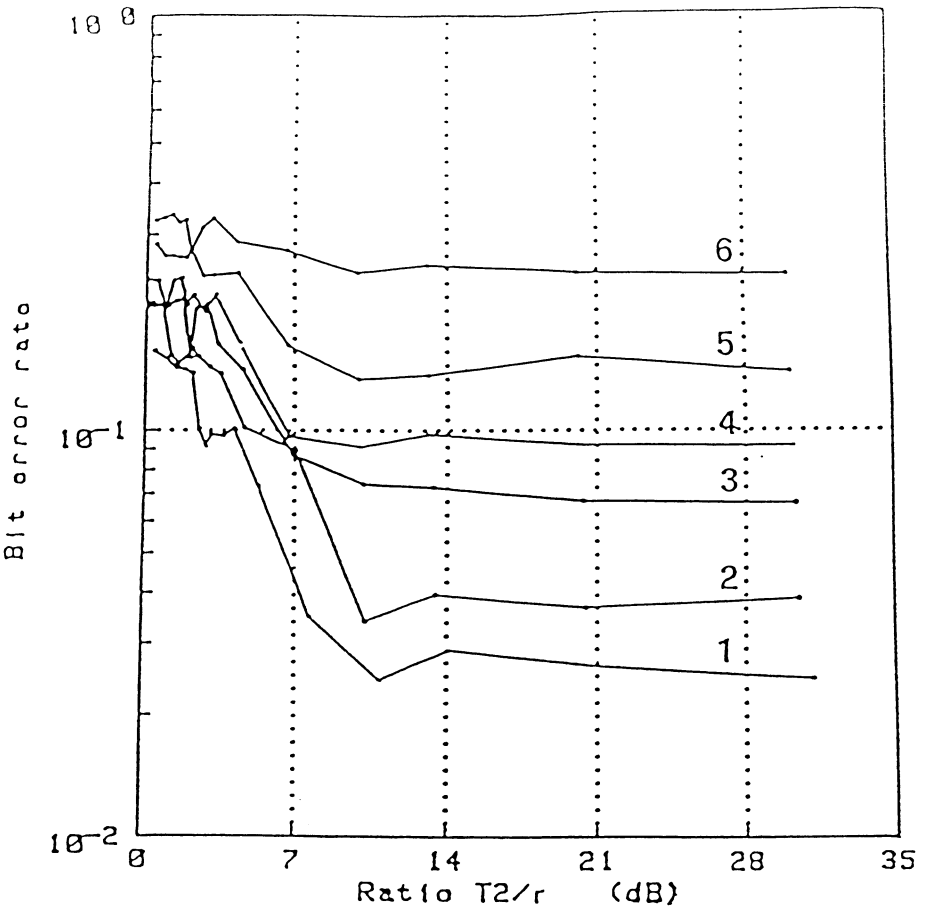

Fig.2.5.4 - Performance of CPFSK modulation in GWSSUS channels characterized by delay power spectra with two peaks of equal shape but different relative amplitude.
Simulation obtained with the following values: spread factor k=0.4; B=100 Hz; L=1000 ms; plots are related to the R values:
1-R=1/19; 2-R=3/17; 3-R=1/4; 4-R=1/3; 5-R=3/13; 6-R=1

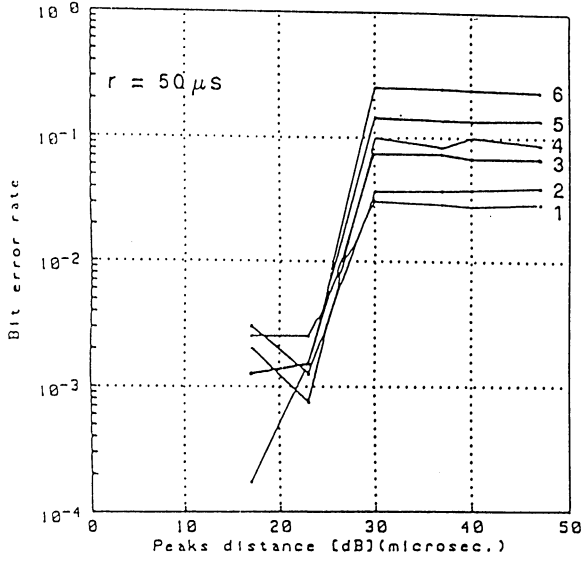

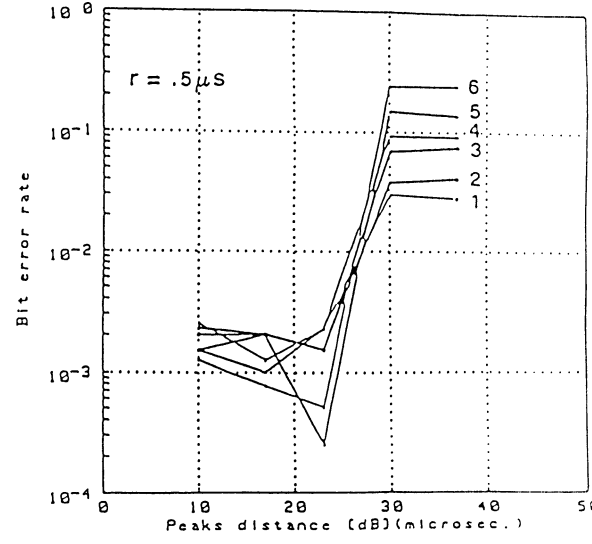

Fig.2.5.5-6 Performance of CPFSK modulation in GWSSUS channels characterized delay power spectra with two peaks of equal shape but different relative amplitude. Simulation obtained for the same value of fig.4 for B and R and with a costant value of r and T=1ms.

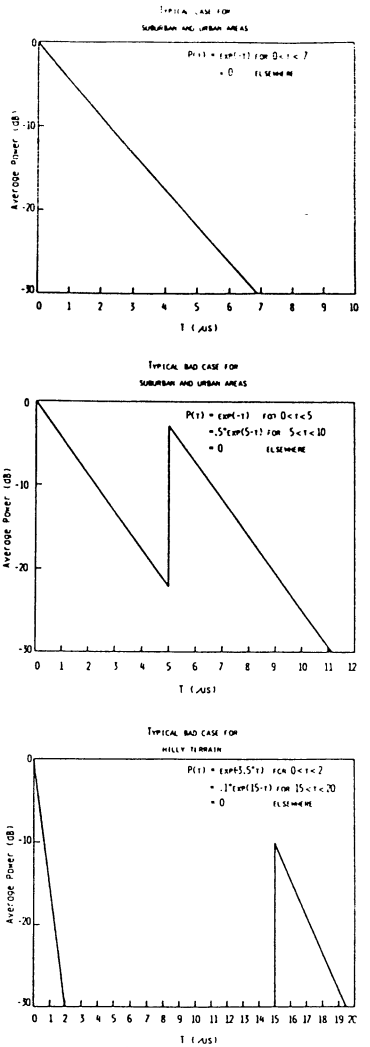

Fig.2.5.7a,b,c - DPS in typical cases as quoted in the various figures; for rural areas the DPS has the same shape but this expression:

$P(t)=\exp(-9.2\bullet t)$ for $0<t<0.7\mu s$

$P(t)=0$ elsewhere.

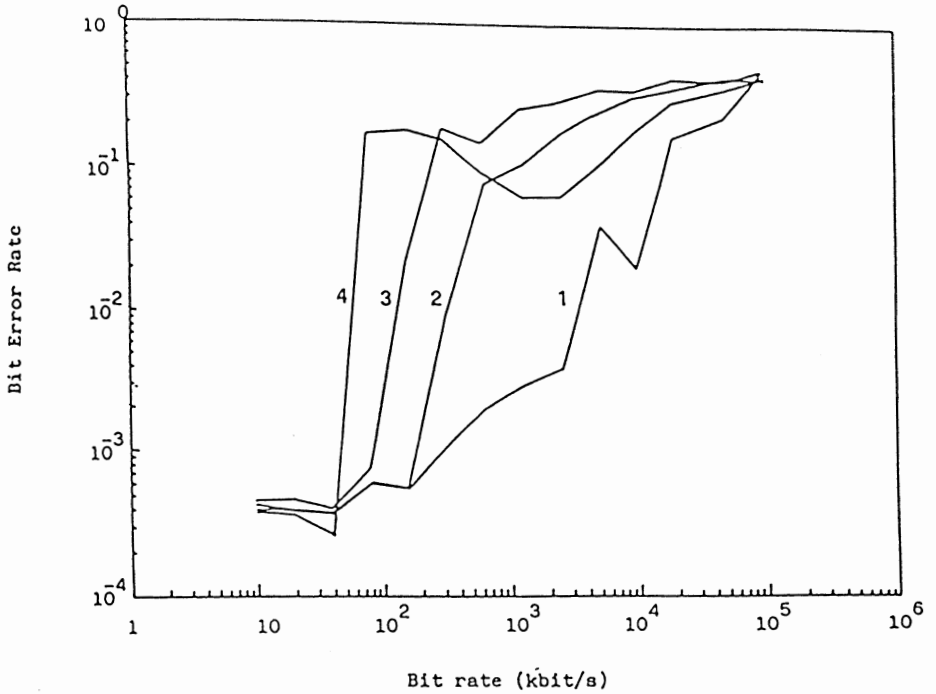

Fig.2.5.8 - BER performances of CP-BFSK in different environmental situation:

1 - Typical case for rural areas;

2 - Typical case for suburban and urban areas;

3 - Typical bad case for suburban and urban areas;

4 - Typical bad case for hilly terrain.

3 MAN MADE NOISE

3.1 INTRODUCTION

The man-made radio interference environment of a metropolitan area is the composite emission from different classes of human-produced radio noise sources. Apart from intentional noise contributions and natural sources (such as atmospheric, solar and galactic noise), which are beyond the scope of this analysis, unintentional man-made sources may be grouped according to the following ranking [Skomal, 1978]:

I) Automotive sources
II) Power transport and generating facilities
III) Industrial equipment
IV) Consumer products
V) Lighting systems
VI) Medical equipment
VII) Electric trains and buses

Among the above quoted sources the automotive ones, i.e. noise contributions due to car ignition systems, are the most important for land-mobile communications and will be examined in the following.

3.2 CHARACTERIZATION OF AUTOMOTIVE NOISE

As known, this type of noise, being impulsive in nature, has characteristics quite different from thermal noise (which is completely defined by the rms value), and its characterization is not a plain matter. In particular [Parsons et al., 1979], "one unfortunate aspect of man-made noise characterization is the apparent lack of any agreement among various research workers about the techniques of measurement and the relative usefulness of the parameters for characterization".

Such a phenomenon is emphasized by the typical non stationarity of the noise random process, which causes particular difficulties in establishing statistical models valid even only for most usual situations which may be encountered in practice.

Moreover, there is a variety of parameters which may be measured and used for the characterization of man-made noise (and related simulators), listed as follows:

a) mean or average value
b) peak value
c) quasi-peak value
d) rms value
e) impulsiveness ratio
f) amplitude probability distribution (APD)
g) noise amplitude distribution (NAD)
h) level crossing rate (LCR)
i) pulse duration distribution (PDD)
j) pulse interval distribution (PID)

The above quantities are self-explanatory; it is only to be reminded that:

- the rms values are commonly converted into the corresponding average noise power and referred to an ideal lossless antenna (typically, a grounded monopole antenna);
- the impulsiveness ratio is defined as the difference (in dB) between the rms and average noise envelope values;
- the APD is the cumulative amplitude probability distribution function of the noise envelope;
- the NAD is defined as the curve giving the number of noise impulses per second which exceed a given amplitude, usually expressed in dB[μV/MHz].

According to these definitions, the APD gives the first-order statistics of noise, in that it allows a determination of the overall fraction of time for which the noise exceeds a particular value, whereas the NAD gives information about how this time was made up (2nd order statistics).

The relative usefulness of the above quoted quantities depends on the type and characteristics of the communication system to be analyzed; for example, quasi-peak measurements have been extensively used for evaluating the performance of radio and television receivers in that they have been shown to have some correspondence with the subjective annoyance; mean or average measurements, together with amplitude probability distribution, appear to be useful for the characterization of atmospheric noise, especially in the HF band [CCIR Rept. 322-3, 1986]; the impulsiveness ratio seems useful in comparing noise contributions from different kinds of sources, etc.

For digital transmissions, in which BER provides a good indication of the system performance, recent works based on the impulsive nature of man-made noise generated and radiated by motor ignition systems [Nakamura, 1986], seem to show that a satisfactory representation of the bit error generation mechanism can be obtained in terms of the knowledge of both average noise power and peak values of the impulsive noise (or, equivalently, its impulsiveness ratio), together with information about NAD and its occurrence rate (noise amplitude distribution and level crossing rate). In fact, no single parameter, such as APD alone, appears to be sufficient to provide a complete evaluation of digital system performance, since communication quality is strongly influenced by the noise waveform as well: in particular, some information about the time of arrival of the impulses is actually needed (the majority of the theoretical models of impulsive interference recently developed [Middleton, 1974 and 1975], assumes that

urban noise may be adequately described by a random Poisson process, as far as pulse arrival times are considered).

3.3 SUMMARY OF EXISTING DATA

As above mentioned, man-made noise data are rather difficult to organize and compare, due to the existing large variety of types of possible measurements, measuring equipment and way of presentation of results.

In this section summary data are presented, relative to different enviroment types, obtained from a work [Spaulding and Disney, 1974] (as arranged by Skomal), which, at present, seems to be the most comprehensive one. In their report, all data coming from various experiments were first of all converted into average noise power, and then expressed in terms of an effective antenna noise factor f_a, as defined by:

$$f_a = p_n / kT_o b \qquad (1)$$

where:

- p_n is the noise power available from the antenna
- k is the Boltzmann's constant (1.38·10(-23) J/K)
- T_o is the reference temperature, taken as 288 K
- b is the effective receiver noise (pulse) bandwidth

Furthermore, for comparison purposes, the noise power p_n has been referred to an ideal loss free short monopole grounded antenna ($h \ll \lambda$), according to CCIR definitions [CCIR Rep. 670, 1986], using the following relationship:

$$F_a = E_n - 20 \log F - 10 \log b + 95.5 \qquad (2)$$

where $F_a = 10 \log f_a$, E_n is the field strength in dB(μV/m), F is the frequency in MHz and b is the noise bandwidth in Hz. Similar expressions can be derived for other antennas [Lauber,

1977], provided that the appropriate gain is known.

Data collected by Spaulding and Disney come from many different locations of USA and are assembled into three broad general categories, characterized by different degrees of urbanization and industrialization: business, residential and rural areas (which, at least in principle, correspond to the urban, suburban and open (or rural) areas, usually considered in studying mobile propagation characteristics).

Figs. 3.1(a,b,c) show median values of F_a, as a function of frequency, for the three areas previously identified. The upper and lower hourly deciles are shown by the range bars; to each set of median values a least squares regression line is fitted. In any case, the fitting curves exhibit an approximate slope of -27.7 dB/decade; however, it is interesting to note that median values at frequencies above about 300 MHz lie above the regression lines. This reveals a probable change in the rate of decrease of noise power with frequency, consistent with the presence of a localized maximum in the UHF-band spectrum of vehicular ignition interference and is confirmed by more recent measurements, as it will be examined later on. The associated standard errors of estimates obtained from curves of Figs. 3.1(a) through 3.1(c), as reported by Skomal, are 7 dB for Business, 5 dB for Residential and 6.5 dB for Rural areas. The estimate error is defined as the standard deviation of the median values of F_a about the mean squares regression line, within the indicated frequency interval.

It is to be recalled that the work of Spaulding and Disney was the basis for CCIR Reports and Recommendations on man-made noise characteristics [CCIR Repts. 258-4 and 322-3, 1986], as it will be examined in detail in the following.

Since a performance analysis of a radio system requires also a knowledge of the randomness existing in the level of man-made noise to which a receiver is exposed, it is interesting to associate to the previously mentioned median figures, a statistical measure of variability, for example the standard deviation of noise power levels distributions. Results are reported in Fig. 3.2; no systematic variation of σ with frequency is evident, for any class of environments.

Finally, Spaulding and Disney also provided some information about the impulsiveness ratio V_d, which, as above stated, may be considered as a measure of the deviation of the noise envelope distribution from a Rayleigh distribution; in fact, when purely Gaussian noise is observed (as for example in the case of atmospheric noise), V_d = 1.05 dB. When V_d increases above such limit, the impulsive character of the observed interference increases. However, notice that measurement results are strongly depending on the receiver bandwidth; in fact, as the filter detection bandwith decreases, pulse overlapping occurs and the output noise envelope approaches that of purely thermal noise, i.e. a Rayleigh distribution. Therefore, the knowledge of the detection bandwidth is essential in the interpretation of impulsiveness measurements. Fig. 3.3 shows variations of mean values of V_d with frequency and environment, as reported by Skomal, using a 10 kHz detection bandwidth; notice that higher V_d measurements correlate quite closely to higher F_a values, i.e. high noise levels usually mean high "impulsive" noise levels. An example of cumulative distribution of V_d, obtained at a single location (residential) during a period of 1 hour is presented in Fig. 3.4. Time variations in V_d, for a given location, appear to be very large, in comparison with the average value (see Fig. 3.3) which could be considered as representative of that location. This is a further confirmation of the extreme variability (both in space and time) of man-made noise contributions, and is a clear indication of the difficulty in

assessing and modelling the phenomenon.

3.4 SUMMARY OF RECENT MEASUREMENTS

In this section the main results of two measurement campaigns (carried out in Italy and France in the recent past, with different measuring techniques) will be examined, and principal differences with data usually found in the literature will be emphasized. In particular, the former allowed to corroborate the hypothesis that the existing data seem to underestimate, when extrapolated around 1 GHz, the actual noise power levels for the various possible environments and traffic intensities; the latter allowed to separate the influence of the noise generated by the mobile unit engine (intrinsic noise) from that of the surrounding traffic and served as a calibration tool for the development of a noise simulator, which will be dealt with in section 3.5.

3.4.1 Measurements performed in Italy

The block-diagram of the equipment is shown in Fig. 3.5. A calibrated antenna, placed at about 2.5m above the ground and at about 5m from the vehicles flow was used, connected to a low-noise broadband pre-amplifier (G33dB, NF2 dB) and to a test receiver. By knowing the antenna factor, voltage (or power) measurements at the receiver input were translated into the corresponding field strengths. Measurements were performed in Turin, at 3 frequencies, for comparison purposes: 139 MHz, 439 MHz and 914 MHz, according to the following procedures:

- peak measurements, using a peak detector
- quasi-peak measurements, according to CISPR standards
- average measurements, using an envelope detector.

In any case, an IF bandwidth of 120 kHz (corresponding to an effective pulse bandwidth of 126 kHz) was used; man-made noise was sampled every two seconds, within time intervals of a few minutes, during approximately steady traffic conditions.

Statistical results at 914 MHz, obtained in conditions of moderately high traffic density (40 to 50 vehicles/min) are reported in Figs. 3.6(a,b,c), which refer to peak, quasi-peak and average field strengths, respectively, measured at the same time and the same location. Notice that all distributions are approximately log-normal; their most significant parameters (mean, median, standard deviation values, lower and upper deciles) are reported in Table I.

	Mean dB(μV/m)	Median dB(μV/m)	Std. Dev. dB	Lower Decile dB(μV/m)	Upper Decile dB(μV/m)
Peak	51.7	52.6	4.7	44.6	57.0
Quasi-Peak (CISPR)	39.1	38.7	3.4	35.2	43.9
Average	11.7	11.5	1.5	10.1	13.9

Table I - Man-Made Noise Characteristics at 914 MHz Field Strength in dB(μV/m)

Average noise power results have then been expressed in terms of antenna noise factor, according to Eqs. (1) and (2), in order to compare them with existing data. Fig. 3.7 shows the probability distribution curves obtained in this way, at the 3 frequencies; it can be pointed out that, whereas a quite

conspicuous difference exists between 139 and 439 MHz results (about 10 dB, on average), the difference reduces down to about 2 dB from 439 to 914 MHz. Median effective antenna noise factors, together with range bars from the lower to the upper deciles are then reported in Fig. 3.8, where the curves suggested by CCIR on the basis of Spaulding and Disney work, for the above quoted environmental conditions, are also drawn (linearly extrapolated beyond 300 MHz). It can be seen that noise power figures actually measured, in traffic conditions which tentatively may be considered corresponding to the "residential" ones, display a rate of decrease considerably less than that can be obtained from existing data, as already inferable from an examination of Figs. 3.1. In particular, present results seem to indicate that noise values at 900 MHz are practically at the same levels of those expected in the 450 MHz band.

Finally, as far as time variations of noise levels are concerned, Fig. 3.9 shows a 10 min concurrent recordings of peak measurements at 914 MHz and 139 MHz, respectively; very high fluctuations occur in both cases (within a range of about 30 dB), and an average difference of about 15 dB seems to exist between the two frequencies (in agreement with Fig. 3.8).

3.4.2 Measurements performed in France

Various sets of measurements have been carried out at 900 MHz in different locations of the city of Paris, according to the system reported in Fig. 3.10. A quarter-wave antenna is mounted on the front hood of a car, connected to a spectrum analyser via a pre-amplifier. At each sweep, the spectrum analyser stores 1000 samples of the received power and transfers this block to a microcomputer. One set of measurements is composed of a sequence of 112 blocks, and takes about 6 min to be performed; the interval between two consecutive samples is 0.75 ms. Various bandwidths were used, in order to

investigate this effect on the received noise level; in most cases a bandwidth of 1 MHz was adopted, which allowed to extract noise pulses from the plafond of thermal noise, with a good dynamic range. These measurements were repeated twice at the same place, both with the vehicle engine on (at 1700 revolutions per minute) and with the engine off.

Figs. 3.11 (a,b) show two examples of measurements, in the two above said conditions; it appears that the intrinsic noise is sometimes predominant, in spite of the existing RFI suppressor located at the spark plug; a quasi periodic component in the intrinsic noise, related to the engine number of revolutions, can be pointed out.

The two types of measurements (engine on and off) led to a rather complete description of the two overlapping phenomena (intrinsic noise and traffic noise, respectively) which must be accounted for by a realistic noise simulator. As far as traffic noise is concerned, measurements revealed a mutual independence between pulse inter-arrival times and amplitudes, which allowed them to be studied separately. Inter-arrival times were found to be exponentially distributed (see Fig. 3.12), while the distribution law for the amplitudes was obtained by fitting the experimental histogram; this suggests to model the pulse trains of the traffic noise by a compound Poisson measure. On the other hand, the most important characteristics of the intrinsic noise is that the signal is pseudo-periodic, depending on the engine number of revolutions; therefore, corresponding inter-arrival times can no longer be considered as random variables (see Fig. 3.13): for an usual four-stroke engine, one can expect a pulse every 5 to 50 ms, depending on the number of revolutions (700 rpm to 7000 rpm). The different behaviour with respect to Fig. 3.12 does not need to be emphasized.

Moreover, it is to be recalled that amplitude and duration of each pulse are strongly related to the receiver filter bandwidth; Fig. 3.14 shows the effect on received peak amplitudes: these appear to increase with increasing bandwidth (from 300 kHz to 3 MHz) at a rate of about 17 dB/decade. Finally, an average noise level reduction of about 10 dB was experienced when moving the car antenna from front to rear.

3.5 SIMULATION TECHNIQUES

This section is intended to provide some information on the characteristics which a man-made noise simulator (either hardware or software) should have, in order to perform measurements and test equipments, possibly according to well established domestic or international specifications.

A large number of national standards exist (military, commercial or consumer): among the former perhaps the US Department of Defense rules (commonly referred to as MIL Standards) are well known. Among the latter, the US FCC, German VDE and SAE (Society of Automotive Engineers) rules appear to be widely acknowledged [EMC Handbook, 1976]. In the international field, a position of paramount importance is held by CISPR (International Special Committee on Radio Interference), which is organized under the general framework of the IEC (International Electrotechnical Commission); in presenting the characteristics of noise simulators, it seems therefore appropriate to refer to CISPR specifications for radio interference measuring apparatus and measurement methods [CISPR, 1977 and 1980].

3.5.1 Simulators specifications

From the above discussions, it appears that a noise simulator must consist of a more or less sophisticated pulse generator, capable of giving sequences of pulses resembling as

much as possible the "real" pulse trains generated by ignition systems.

As mentioned above, CISPR Publications provide guidelines for radio interference measuring equipment and related calibration procedures; therefore, they do not actually deal with specifications for hardware simulators of man-made noise. However, it is obvious that such specifications, which refer to pulse generators to be used for calibration of EMI receivers, may be actually interpreted, with some judgement, also as the specifications for the pulse generators to be used as noise simulators.

Simulators may be fundamentally grouped into two classes:

- Video pulse generators;
- Pulse modulated radio frequency carriers generators;

CISPR specifications mainly refer to the former (see Publication No. 16), and are briefly summarized in the following paragraph, but some directions are also given for the latter (see Appendix Q of the same Publication). Notice, however, that video pulse generators provide deterministic (periodic) pulse sequences, i.e. the typical randomness of the traffic noise is not accounted for by these simulators; so, their use can lead to misleading results, especially when BER generation mechanisms in digital systems are to be investigated.

3.5.1.1 Video Pulse Generators

According to this measurement philosophy, a possible equipment configuration for static man-made noise measurement is reported in Fig. 3.15; the characteristics of the impulse generator are contained in Appendix D of Publication No. 16, which says:

" The generator should be capable of producing pulses with the characteristics given in Table II; the spectrum should be substantially constant up to the upper limit of the frequency band under consideration. The generator should have a variable frequency repetition rate, giving at least the frequencies indicated in the Table. The amplitude of the spectrum should be known within ±1 dB, and the repetition frequency to within 1 %. The spectrum may be regarded as satisfactorily uniform within a given frequency band if, within this band, the variation of the spectrum amplitude is not greater than 2 dB relative to its value for the lower frequencies within the band."

Band (MHz)	Pulse area (µs·V)	Repetition frequency (Hz)
0.01-0.150	13.5	1,2,5,10,25,60,100
0.15-30	0.316	
30-300	0.044	1,2,10,20,100,1000
300-1000	(See note)	

Note: This generator should be capable of producing pulses of adequate amplitude with as uniform spectrum up to 1000 MHz as possible

Table II - Pulse generator characteristics

In order to obtain a very flat spectrum up to 1 GHz (which is the frequency of interest for the GSM system), pulses must have an exceptionally short duration. For example, since the spectral pattern for exactly rectangular pulses follows the familiar sin(x)/x curve, pulses with a duration of 1 ns have their first zero crossing in spectral pattern already at 1 GHz: such pulses can be safely used up to about 250 MHz only for noise simulations. In fact, practical time

domain pulse envelopes lie between rectangular and triangular (or exponential) shape; as a result, using particular tricks to compensate for spectral roll-off, relative spectral flatness can be increased [EMC Handbook, 1978] up to about 0.4/0.5 times the first null. As a conclusion, pulse generators capable to operate up to 1 GHz must be able to produce pulses with a duration of 250 ps, or less.

An example of generator which complies with the above specifications is the Schwarzbeck Mess-Elektronik Type IGU-2912. Due to the very short pulses generated (250 ps), with a repetition rate up to 200 pulses/s, a very good spectral flatness is achieved; it can therefore be safely used for testing wideband receivers, at least in analog systems.

Appendix D continues: " For checking compliance with the requirements on the limitation of intermodulation effects, the spectrum above the upper limit of the frequency band under consideration must be limited (10 dB down at twice the upper frequency). This is necessary to standardize the severity of tests, since cross-modulation products of all components of the spectrum separated one from the other by the tuned frequency will contribute to the response".

3.5.1.2 Pulse Modulated Radio Frequency Generators

As said before, video pulse generators are typically capable of generating constant period trains of pulses at a fixed repetition frequency, which must be fixed before each measurement. In the same way also the amplitude of the pulses has to be settled in advance; both variables can then be changed only from one measurement to another. This, of course, is not the case of the "real" world, where the pulse sequences, generated by multiple ignition systems, belonging to a random process, are continuously evolving in time, as far as both amplitudes and arrival times are concerned. According

to previous considerations, the use of video pulse generators is only capable to account for the first order statistical parameters of the noise random process.

More recent generators, which may be considered as "ad hoc" developed for noise simulations, allow to overcome such difficulties by generating reproducible radio noise signals closely resembling field noise signals; they are capable of generating pulse trains with randomly variable amplitudes and pulse arrival times, which modulate an RF external signal. In this way, thanks to the modulation process, less stringent requirements are imposed to the pulse width (i.e., in the frequency domain, to the corresponding spectral flatness), which may be tailored to the bandwith of the receiver under test. If this solution is adopted, a possible configuration for laboratory measurements can be as in Fig. 3.16: the wanted signal for the receiver under test is generated by a signal generator (1); an RF (interfering) signal is generated by another device (2) and is fed into the simulator, where it is modulated with the baseband noise by a product modulator. The RF noise signal is then mixed with the desired one (this latter eventually passed through a proper fading simulator) and the resulting signal is fed into the receiver under test.

An example of generator/simulator of this type is manufactured by JRC (Japan Radio Company); the Noise Simulator Type NJZ-317C is capable of generating both constant period and Poisson's trains with average repetition frequencies in the range 1 Hz to 10 kHz. In both cases the pulses may be amplitude modulated by a Gaussian noise process which accounts for a log-normal distribution of pulse amplitudes. Unfortunately, the pulse width is about 1 us; the flatness of the spectrum is then limited to approximately ± 100 kHz around the carrier. This renders such a particular equipment quite suitable for testing narrowband systems, but not immediately usable for a wideband one.

The description of a more complete noise simulator, particularly suitable for testing wideband systems, is reported in Appendix 1; the device was developed at CNET and is capable of generating pulse trains of very complex nature, whose structure has been experimentally studied, as outlined in section 3.4.2. The simulator may be roughly divided into three parts, according to the scheme of Fig. 3.A.1:

- synthesis of traffic noise
- synthesis of intrinsic noise
- combining and mixing unit

The intrinsic and the traffic noises are generated separately. With respect to traffic noise, both amplitudes and inter-arrival times are synthesized from measured data stored in EPROMS. As far as the intrinsic noise is concerned, the amplitudes are obtained in the same way as for the traffic noise ones, while the arrival times are generated by a variable clock driven by an external potentiometer. The adopted configuration of the combining and mixing unit allows to obtain very sharp pulses and a satisfactory peak dynamic range with respect to the thermal noise. Fig. 3.A.2 shows the spectra of the two generated signals; as it can be seen, for this simulation the intrinsic noise was calibrated at about -30 dBm, while the traffic noise was adjusted about 12 dB below; however, according to performance specifications of Table A.I, both amplitudes can be varied in a rather broad dynamic range. It is also clear that both spectra are quite flat within a 6 MHz band.

3.6 CONCLUSIONS

A brief discussion on automotive noise characterization has been presented, with particular reference to the parameters which appear most effective in determining the performance of digital transmission systems. A summary of recent

results, obtained during two measurement campaigns carried out in Italy and France, has then been outlined, and differences with existing data pointed out. One of the two quoted campaigns also allowed to identify more precisely the structure of noise due to car ignition systems. This served as a tool for the development and calibration of a new type of broadband noise simulator, whose characteristics have been described in a section devoted to man-made noise simulation techniques.

3.7 REFERENCES

CCIR Rept.258-4 [1986] XVIth Pl. Assy., Vol. 6, Dubrovnik (Yu)

CCIR Rept.322-3 [1986] XVIth Pl. Assy., Vol. 6 (Suppl. No. 1), Dubrovnik (Yu)

CCIR Rept.670 [1986] XVIth Pl. Assy., Vol. 1, Dubrovnik (Yu)

CISPR Publ. No. 16 [1977] IEC, Geneva, (CH)

CISPR Publ. No. 16 [1980] (Amdt. No. 1), IEC, Geneva (CH)

EMC HANDBOOK [1976] Vol. 1 (Electrical noise and EMI specifications), Don White Consultants, Germantown (USA)

EMC HANDBOOK [1978] Vol. 2 (EMI test methods and procedures), Don White Consultants, Germantown (USA)

LAUBER, W.R. [May 1977] Radio noise surveys at canadian HF communication sites, IEEE Trans., Vol. EMC-19, No. 2

MIDDLETON, D. [1974] Statistical-physical models of man-made radio noise, Part I, Office of Telecommunications Technical Report, Washington (USA)

MIDDLETON, D. [1975] Statistical-physical models of man-made radio noise, Part II, Office of Telecommunications Technical Report, Washington (USA)

NAKAMURA, S. [1986] The effects of urban impulsive noise on mobile digital radio communications, Trans. of the IECE, Vol. E69, No. 1

PARSONS, J.D. and SHEIKH, A.U.H. [1979] The characterization of impulsive noise and considerations for a noise measuring receiver, The Radio and Elec. Eng., Vol. 49, No. 9

SKOMAL, E.N. [1978] Man-made radio noise, Van Nostrand Reinhold Co., New York (USA)

SPAULDING, A.D. and DISNEY, R.T. [June 1974] Man-made radio noise, Part I, Estimation for Business, Residential, and Rural areas", U.S. Dept. of Commerce, O.T. Rep. 74-38

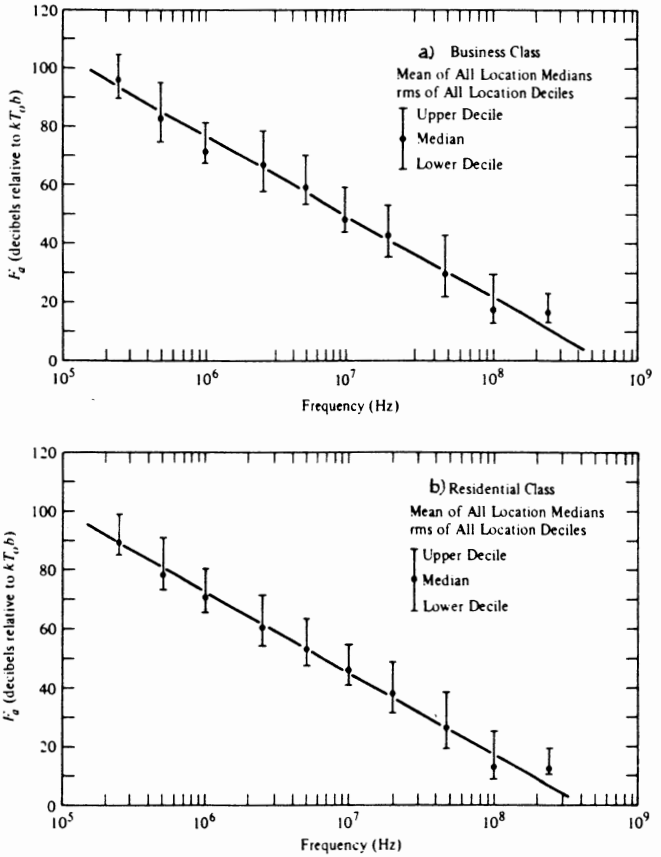

Figs. 3.1 - Median values of Fa vs frequency [Skomal,1978] for Business (a) and Residential (b) Areas

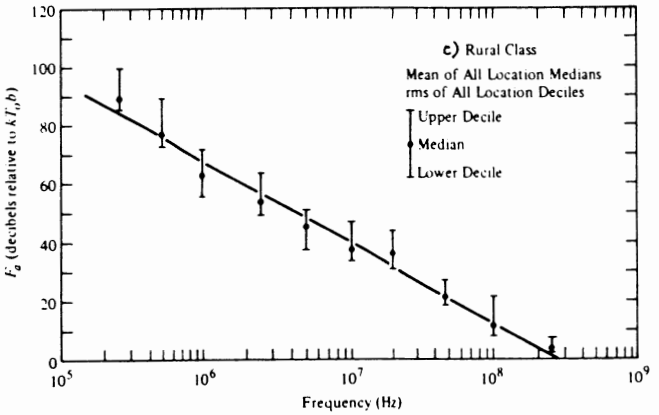

Fig. 3.1 (c) - Median values of Fa vs frequency [Skomal,1978] for Rural Areas

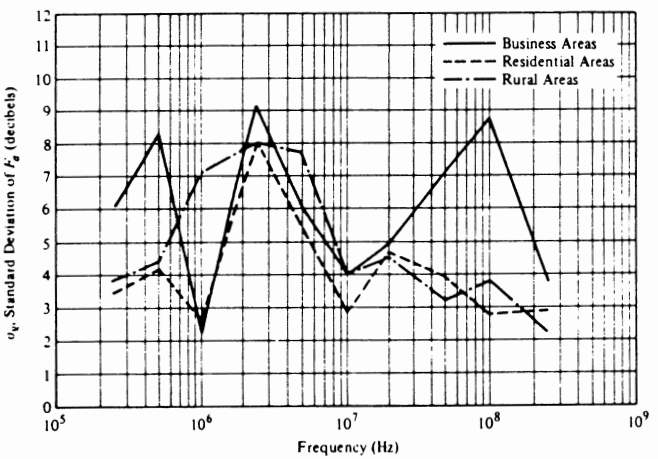

Fig. 3.2 - Standard deviations of Fa versus frequency [Skomal,1978] for each area of Figs. 3.1

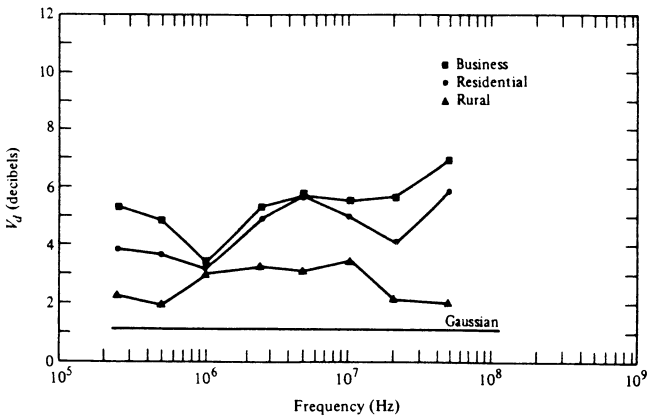

Fig. 3.3 - Variation of Vd versus frequency [Skomal,1978] for each area of Figs. 3.1 - (10 kHz detection bandwidth; Gaussian noise ref. level is shown)

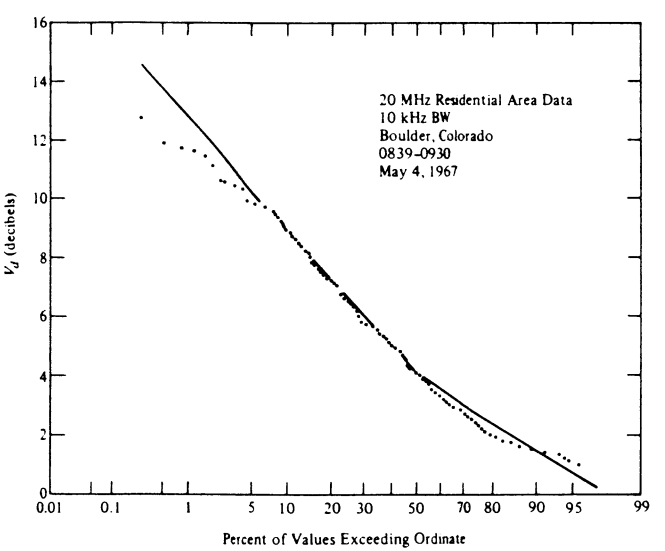

Fig. 3.4 - Cumulative distribution of Vd for a residential area, observed at 20 MHz (50 s integration time)

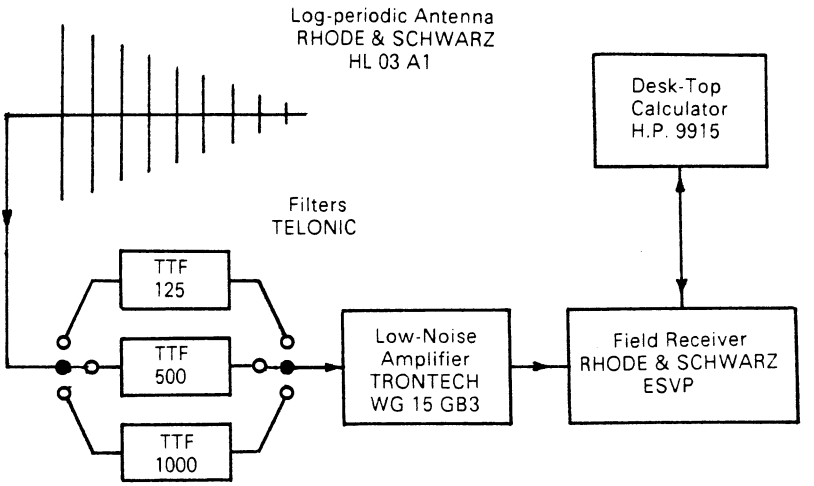

Fig. 3.5 - Block diagram of the measurement set-up (ITALY)

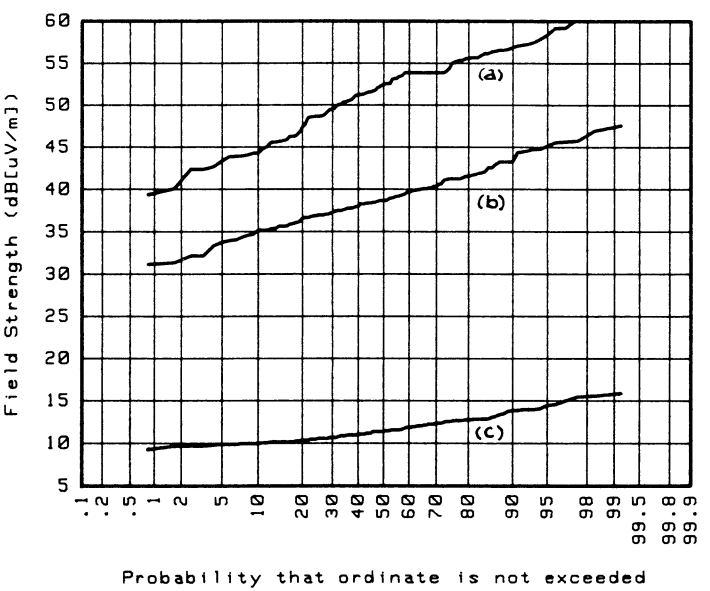

Fig. 3.6 - Peak (a), Quasi-Peak (b) and Average (c) noise statistics measured at 914 MHz in moderately high traffic conditions

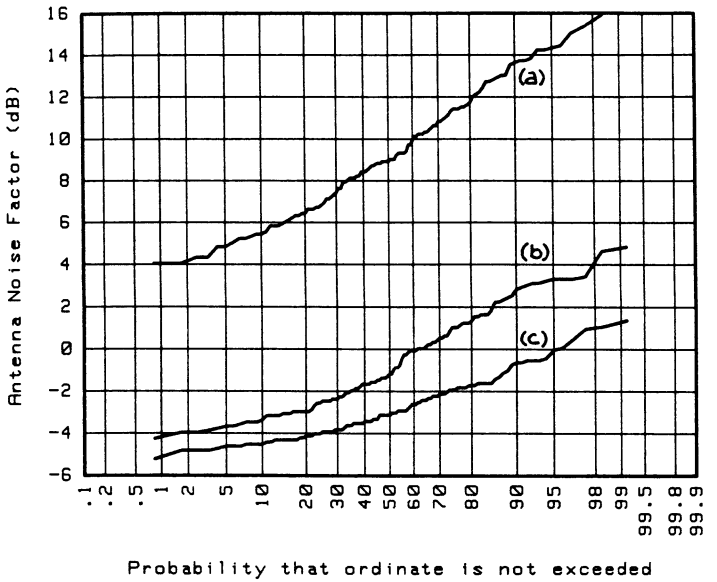

Fig. 3.7 - Antenna Noise factor statistics for a short vertical loss free grounded monopole at 139 (a), 439 (b), 914 (c) MHz in moderately high traffic conditions, as in Fig. 3.6

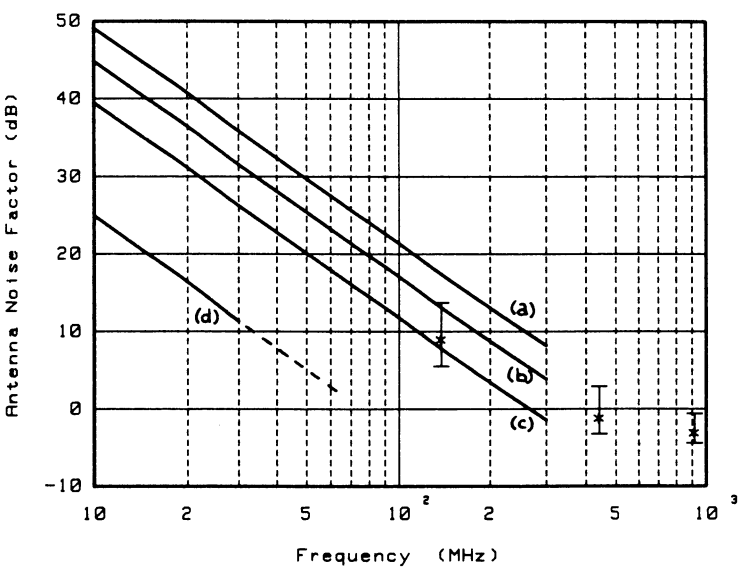

Fig. 3.8 - Median values of antenna noise factors measured at the 3 frequencies of Fig. 3.7 and CCIR curves for Business (a), Residential (b), Rural (c) and Quiet Rural locations (d)

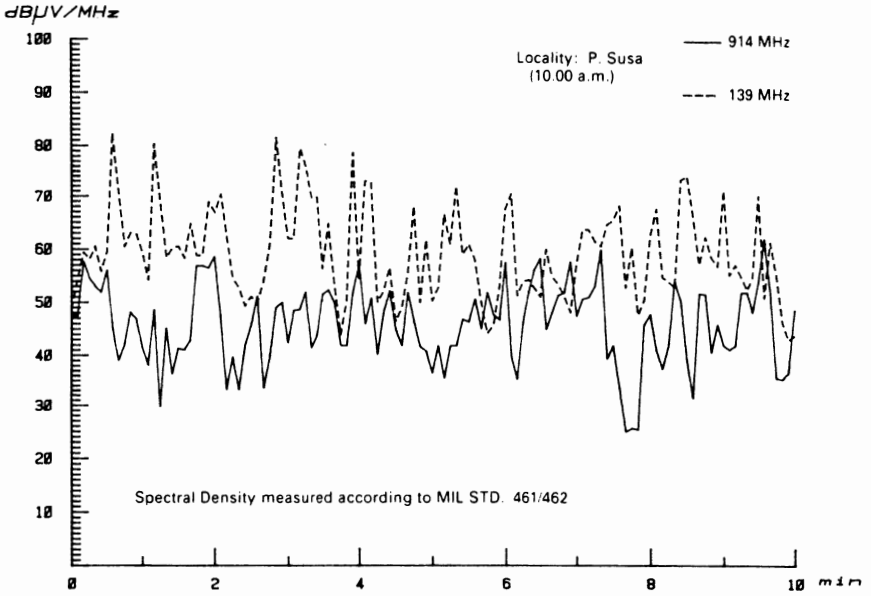

Fig. 3.9 - Comparison between 900 and 150 MHz measurements (10 a.m.)

laboratory van

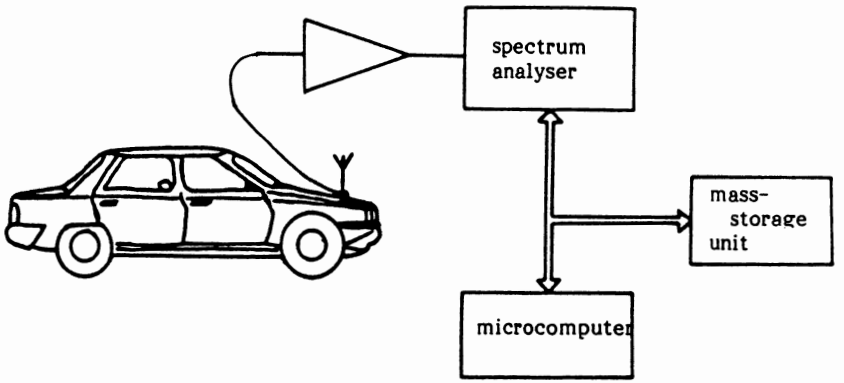

Fig. 3.10 - Block diagram of the measurement set-up (FRANCE)

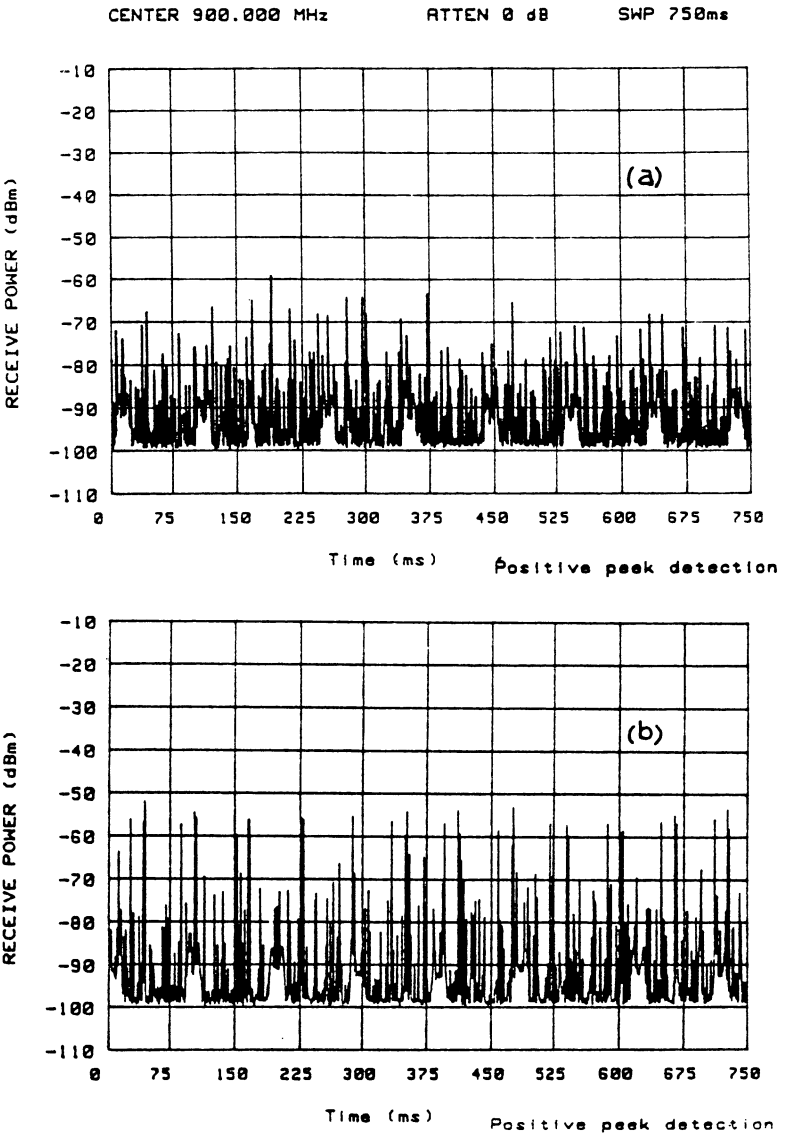

Fig. 3.11 - Man-made noise measured in high traffic conditions (a= traffic noise, engine off; b=intrinsic noise, engine on)

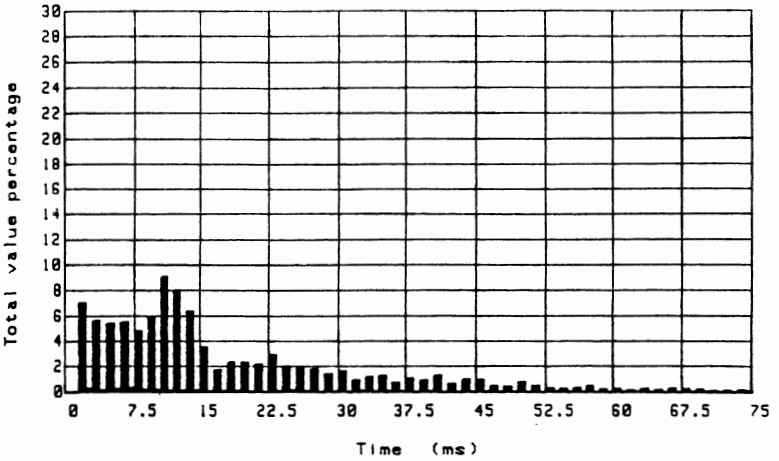

Fig. 3.12 - Distribution of time intervals between two successive pulses (traffic noise)

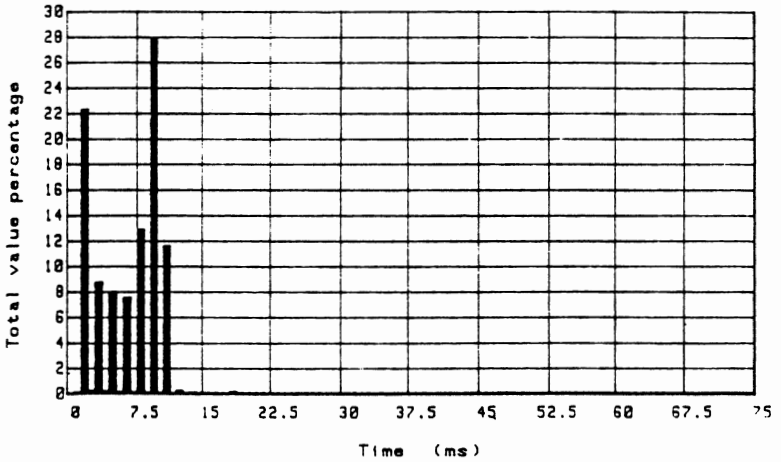

Fig. 3.13 - Distribution of time intervals between two successive pulses (intrinsic noise)

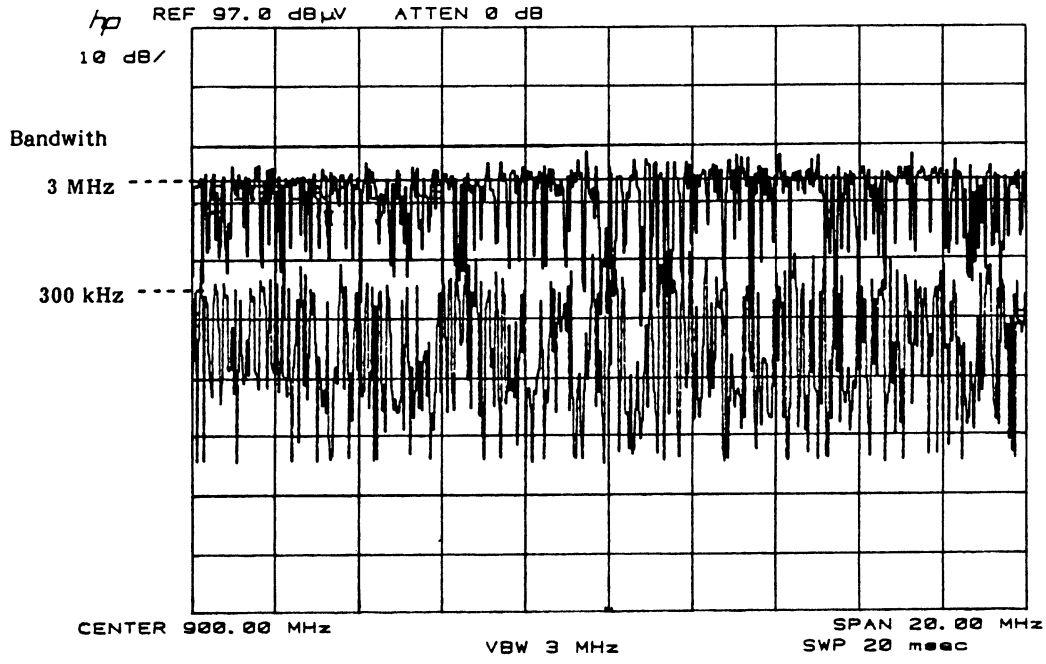

Fig. 3.14 - Effect of the bandwidth on noise level

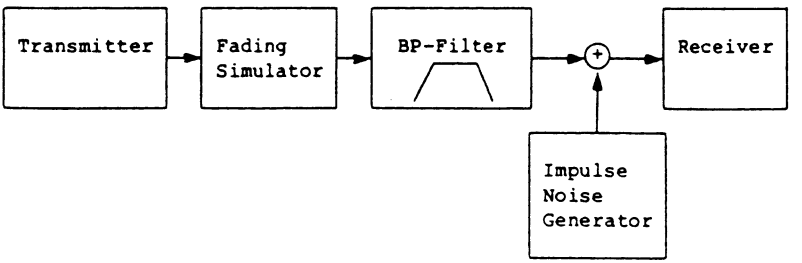

Fig. 3.15 - Simulator block diagram using a video pulse generator

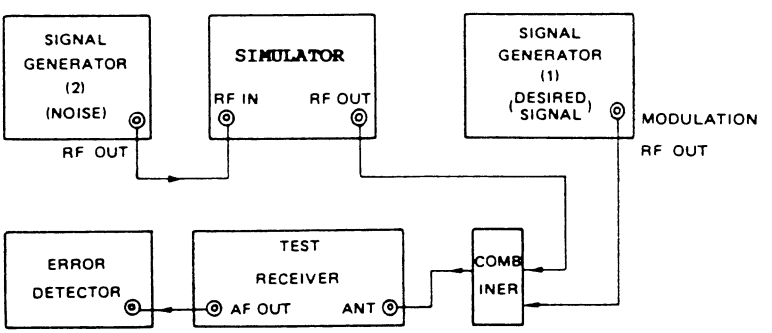

Fig. 3.16 - Simulator block diagram using a pulse modulated radio frequency generator

SUMMARY OF TECHNICAL DATA FOR
A BROADBAND NOISE SIMULATOR
TABLE A.1 - PERFORMANCE SPECIFICATIONS

- MAXIMUM PEAK AMPLITUDE (INTRINSIC) : -30 dBm
  (in a 1 MHz bandwidth) (TRAFFIC) : -42 dBm

- 3 dB BANDWIDTH : 6 MHz
- SIGNAL DYNAMIC RANGE (MAX/MIN LEVEL) : 42 dB
- SIGNAL TO NOISE RATIO : 65 dB
- POISSON PULSES INTER-ARRIVAL TIMES : .5 to 127 ms
- QUASI-PERIODIC PULSES REPETITION TIME : 4 to 40 ms
  (engine revolutions : 700 to 7000 rpm)

- DURATION OF A SIMULATED PULSE SEQUENCE: 5 to 10 min

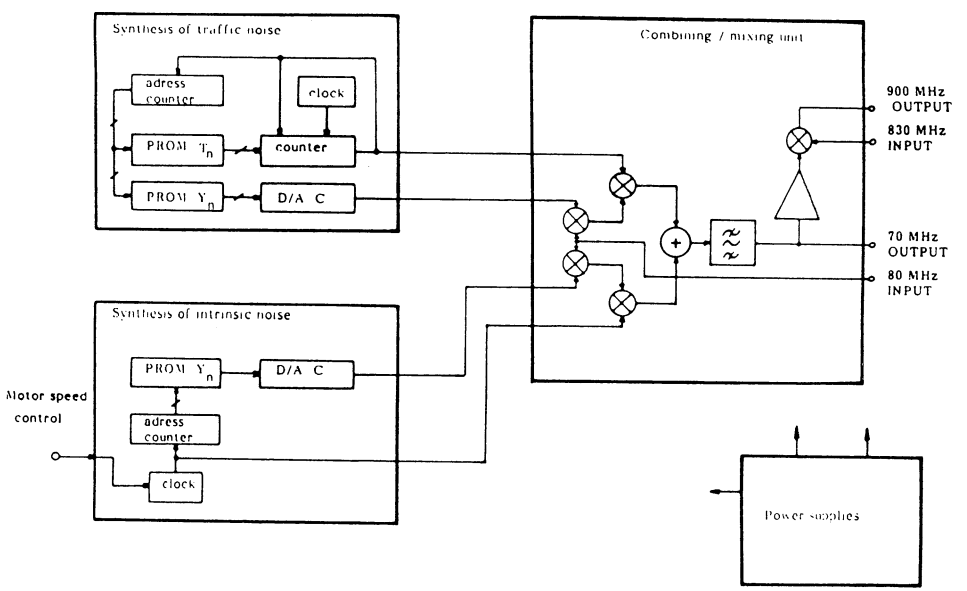

Fig. 3.A.1 - Block diagram of the broadband noise simulator

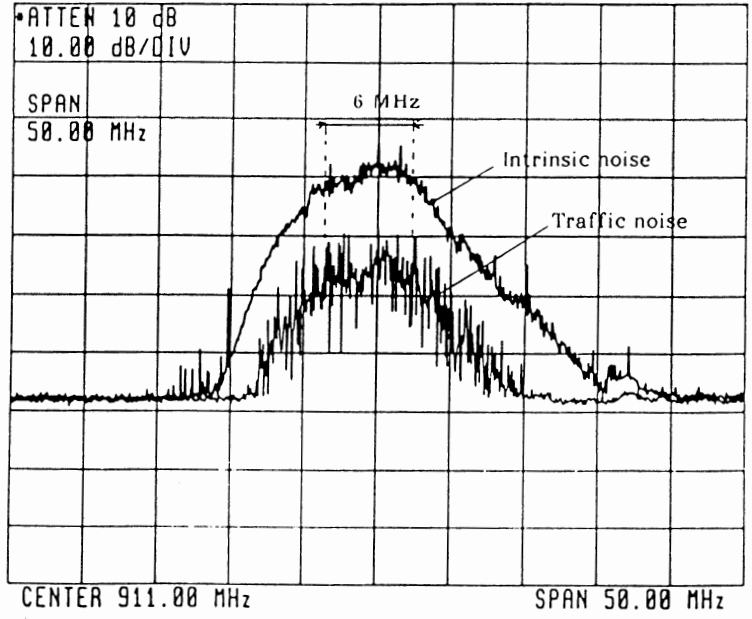

Fig. 3.A.2 - Comparison of the spectra of traffic and intrinsic noise

4. ANTENNAS

4.1 INTRODUCTION

There are essentially two types of antennas in a mobile communications network: base station antennas and mobile antennas, which again may be classified into vehicular and portable antennas. The demands on the different types are different, although they all in theory should be well matched over the frequency band and have the proper polarisation.

The base station antennas will for reasonably large cell sizes be elevated high above the ground and have some beam-shaping in the vertical plane in order to cover the cell as well as possible, and also some beam-shaping in the horizontal plane, if the base stations are placed at the edges of cells (sector coverage). Usually the polarisation will be vertical.

The vehicular antennas are in principle less critical, usually a whip antenna placed as a monopole above the metal structure of the car is sufficient. The horizontal pattern should be omnidirectional since the dominant energy may come from any direction, and the vertical pattern should have its maximum as close as possible to zero elevation (some experimental results will be shown in a later section). Since 900 MHz is almost in the microwave region there are other possibilities of antenna design, slot antennas, microstrip etc, they will be partially discussed in the section on antenna diversity.

The hand-portable antennas have an additional requirement of light weight and small volume.

In practical use most mobile antennas are single element and rather simple. If the antenna gain is maximum transverse to the direction of motion the Doppler spread will be reduced, but there is of course a danger of having a reduced direct ray from a direction of minimum gain.

It is worth stressing that an adaptive multi-element array may have a profound influence on the received signal quality, but it is often considered to be too costly for the general user. In principle those directions giving most delay spread would be nulled out, and the general flat fading would be minimised. The future will show whether there is a market for these more specialised antennas.

4.2 ANTENNA DIVERSITY

4.2.1 General aspects of antenna diversity for mobile antennas.

The advantages of antenna diversity in mobile communications have been discussed in detail in a recent paper [1]. As shown in a previous section one of the worst effects of multipath propagation is the destructive interference between waves from different directions giving rise to deep fades at different frequencies. Not only will the energy be small at such a fade, but frequency-selective effects will be enhanced as well. The effect on the communication link will depend on the speed of the vehicle, but in the present TDMA system the channel may be considered reasonably constant over the length of the burst.

The effect of antenna diversity in the pan-European system will depend on the environment, especially the size of the delay spread, and we can distinguish between a narrowband and a wideband case.

A narrowband case may be defined as the situation where the product of bandwidth and delay spread is small. Even in the case of the GSM-system this will occur in many situations, especially in the urban environment where the delay spread will be small. The fading will be flat, i.e. all frequency components will fade simultaneously, and the main purpose of an antenna diversity

system will be to restore the energy. The only condition is that the two or more antenna ports are uncorrelated, in which case the chance of a simultaneous fade at both ports is small. The benefit of diversity is especially clear at small or zero speeds, where one antenna port may be in a deep fade for a long time.

The level of improvement achievable with two-branch switched diversity in digital mobile radio was studied at the Technical Research Centre of Finland [Närhi, 1986]. At first, simulation measurements were made to demonstrate that by using switched diversity, a significant improvement in the transmission of digital signal in a Rayleigh-fading mobile radio channel is obtained. Especially at low vehicle speeds the BER is clearly better, when diversity is used, as the figure shows. At higher vehicle speeds the improvement is smaller because of impulse noise caused by switching, but still marked.

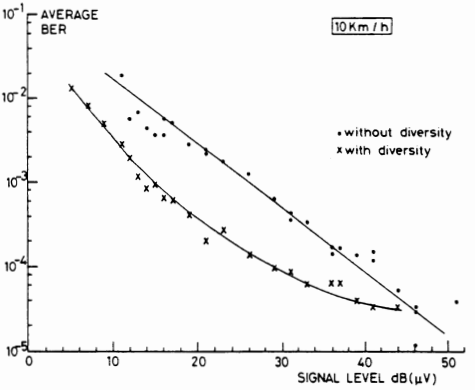

Also burst error characteristics of the digital mobile radio channel were studied. A Rayleigh-fading 900 MHz channel with 16 kbps data rate was measured with switched diversity. A considerable reduction of burst error lengths was achieved. Again, this effect is most notable with a slowly moving vehicle. Also it turned out that the improvement is rather insensitive to imperfections in the diversity system, such as correlation or gain difference between the two diversity branches. This makes diversity attractive also to hand portable receivers, where the small size imposes strict limitations on the antennas.

The feasibility of switched diversity in a narrow band TDMA system was also demonstrated. Here the system works well at high vehicle speeds, too, because all switching happens outside the active receive time-slot of the receiver.

A wideband case is characterised by a bandwidth-delay spread product of the order one or greater. The fading will be frequency-selective, so the energy situation will be improved in the sense that only part of the frequency spectrum will disappear in a fade. Also in this case will antenna diversity be an advantage, since the frequency of the fade (usually just one in the band) will be different in the two branches, so one branch will usually be superior to the other. There will still be a need for equalisers etc., but the resulting bit error rate is a function of the position of the frequency fades.

4.2.2 Base station diversity.

The situation for base stations is slightly different from the mobile case since the angular spread of the incoming waves is much smaller. This leads to a choice of different possibilities of antenna positioning on the mast, including the use of polarisation diversity. This has been studied at Aalborg University, Denmark. Several antenna arrangements were measured in different environments, transmitting both speech and frames in the NMT900 system. The receivers were equipped with a post detection equal gain combiner. The base to mobile separation were 15 to 25km. A compact combination of horisontal (5-6 lambda) separation and vertical separation (12 lambda) gave generally correlation coefficients below 0.7. Polarisation arrangements with orthogonally tilted antenna arrangements (45 degrees around axis and referred to the ground) gave correlation coefficients below 0.7 for environments with dense population of scatters (typical urban environment). A mean power loss of 2 to 3 dB must be encountered though, when referring to ordinary space diversity. A combination of space and polarisation diversity will work well over a wide range of environments, though still giving a mean loss of 2-3 dB.

The diversity gain on the analog speech transmission on NMT900 was found to be around 0.2 MOS (Mean Opinion Score, scale 1 to 5) in mean and up to 0.7 MOS maximum. This corresponded to mean power gain of more than 5dB. The diversity gain vanished when the received mean power level exceeded 5 to 10 dBuV, as well as for mobile speeds over 40 km/h. The diversity gain on cochannel interference was found to 3 to 6dB (correlation coefficient=0.7, down to zero).

The diversity gain for the NMT900 frame transmission was also found to be around 5dB for FER (Frame Error Ratio =probability of receiving an erroneous frame) and FNAR2 (Frame Not Accepted Ratio =propability that neither of 2 successive frame are accepted). Diversity reduced FER and FNAR2 down below 0.2 of the value encountered without diversity. Generaly FER was below 5% for mean signal levels down to -3dBuV. For mean signal levels over 10dBuV FER dropped to nearly 0%. The absolute level of FNAR2 was generally well below a 1/3 of FER. The diversity gain on cochannel interference was found to be around 3 to 6 dB. Burst distributions based on accepted frames have been produced. Generally diversity did not change the cumulative burst distribution, which was centered on burstlengths below 2 frames. The diversity gain on the cumulative gap distribution is large, giving higher propabilty for large gaps between errors. In the Fig. 1 an example is shown for a mobile speed of 65km/h in an suburban area.

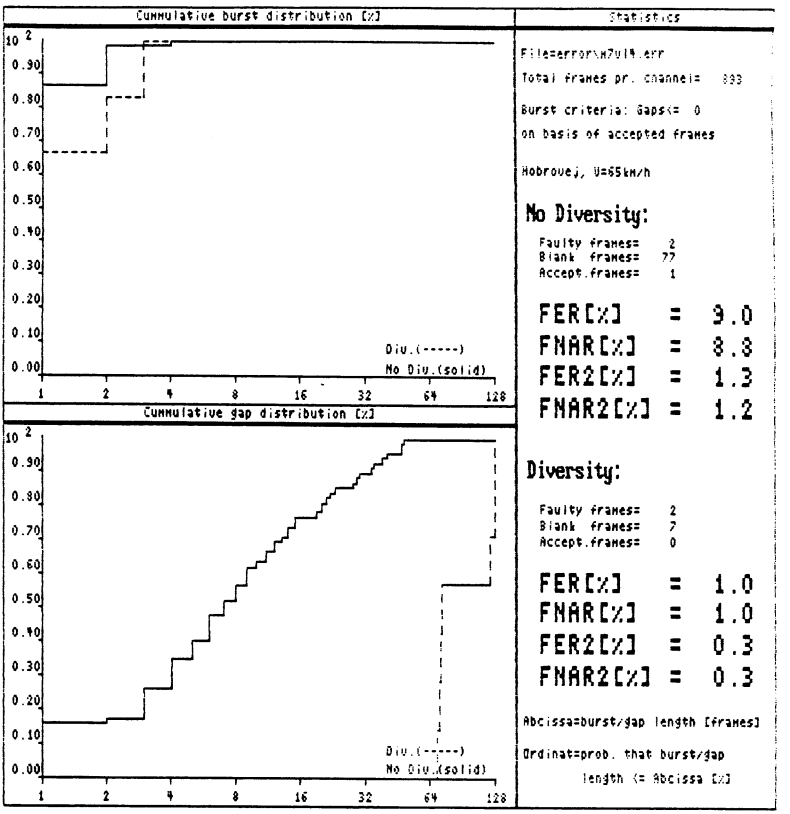
Cummulative burst distribution [%]
Statistics
File=error\H7u19.err
Total frames pr. channel= 833
Burst criteria: Gaps<= 0
on basis of accepted frames
Hobrouej, U=65km/h
No Diversity:
Faulty frames= 2
Blank frames= 77
Accept.frames= 1
FER[%] = 9.0
FNAR[%] = 8.8
FER2[%] = 1.3
FNAR2[%] = 1.2
Diversity:
Faulty frames= 2
Blank frames= 7
Accept.frames= 0
FER[%] = 1.0
FNAR[%] = 1.0
FER2[%] = 0.3
FNAR2[%] = 0.3
Abcissa=burst/gap length [frames]
Ordinat=prob. that burst/gap
length <= Abcissa [%]
Div.(-----)
No Div.(solid)
Cummulative gap distribution [%]
Div.(-----)
No Div.(solid)

Fig. 1

4.2.3 Diversity antennas.

In the simplest case antenna diversity may be achieved by standard space diversity, which for the mobile case corresponds to a separation of half-a-wavelength or more. It is interesting that much more compact antennas may be achieved, and some of

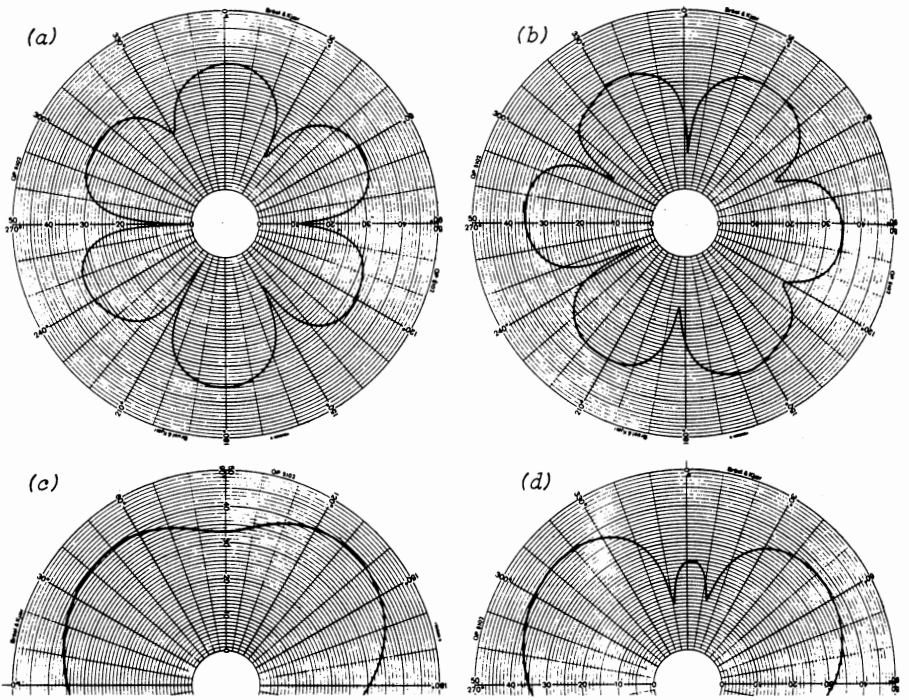

Figure a. Experimental patterns for a patch with parameters listed with fig. 3. The frequency was 894 MHz, the first n=3 mode resonance. 5a and 5b are Ø-patterns for feeds at Ø=0° and Ø=90° respectively. 5c is at θ-pattern of $E_{Ø}$ for a cut between two nulls of fig. 5a. 5d is a θ-pattern of E_{θ} for a cut between two maxima of fig. 5a. The ground-plane was 50 x 50 cm. All scales are in dB but the powers are not equalized.

Figure b. A stacked multiport patch offering the possibility of diversity reception as well as duplexer action.

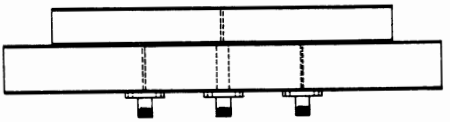

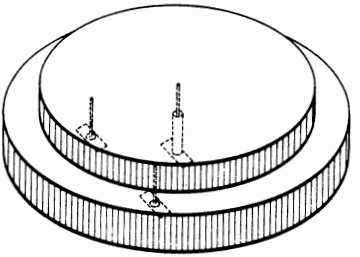

these have been studied at Aalborg University. One case is an arrangement of two or three sloping monopoles with a common base, another is a multiport patch antenna utilising higher order modes in the patch to obtain uncorrelated port signals [Vaughan 1987] og [Vaughan 1984]. Illustrative examples of the patch radiation patterns are shown in the figure

For the portables a study into the possibilities of using antenna diversity was carried out at the Technical Research Centre of Finland [Laukkanen, 1986]. The configuration shown in the figure was found to work very well. A whip antenna is used for both transmitting and receiving and a microstrip antenna operating at quarter-wavelength-resonance above groundplane is the second branch for diversity reception. The two antennas work as a combination of space diversity, pattern diversity and polarization diversity, as can be seen from the figure below. The figure gives the radiation patterns of each antenna for two perpendicular polarizations.

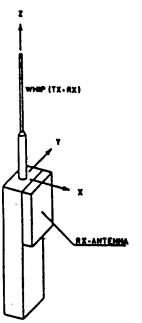

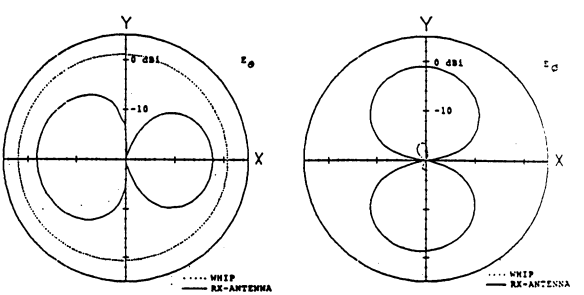

One problem with a hand-held unit is the effect of the user on the antenna performance. In this case the VSWR of both antennas is less than 2 on a 25 MHz band even when the radio unit is held in talking position.

4.3 ANTENNA MEASUREMENTS.

Azimuth and elevation patterns of 900 MHz mobile antennas mounted on the roof of a typical passenger car were measured in the anechoic chamber of the Technical Research Centre of Finland [Koivumäki, 1988]. Six different antenna positions were used, as shown in the figure.

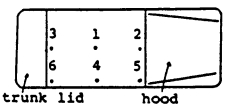

Quarter-wavelength, 5/8-wavelength whip antennas, and a half wavelength dipole were measured. The whip antennas were attached directly to the roof, while the feed point of the dipole was 45 cm above the roof.

The main objective of these measurements was to answer a question raised in a COST 207 meeting, namely how much effect the radiation pattern of the measurement antenna may have on the result of e.g. a delay profile measurement. The car roof may have quite a large effect on the elevation pattern if the antenna, so especially in a mountaineous region, where multipath signals come from different elevation angles, the measured amplitudes of different delayed signals may be somewhat in error. Whether this error of some dBs has very much significance, depends on the situation.

The measurements showed that the direction of the pattern maximum in the elevation plane varies somewhere between about 10 and 30 degrees, depending on the antenna position and the azimuth angle of the pattern cut. The measured patterns of each antenna at the centre of the roof is shown on the following page.

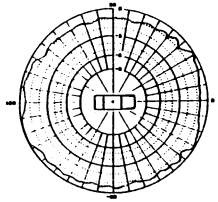

λ/2-dipole. Azimuth pattern.

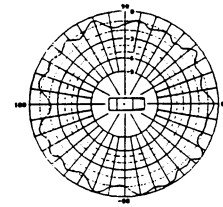

λ/4-monopole. Azimuth pattern.

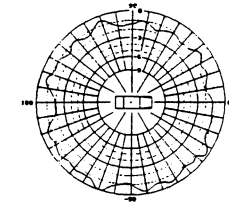

5λ/8-monopole. Azimuth pattern.

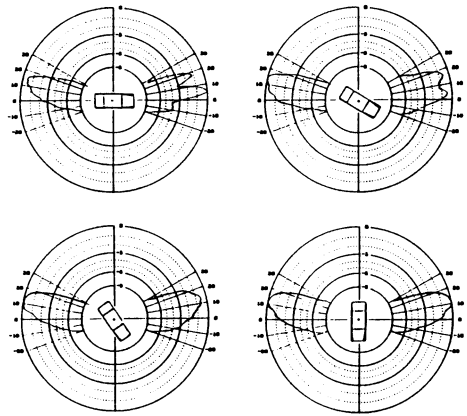

λ/2-dipole. Elevation patterns.

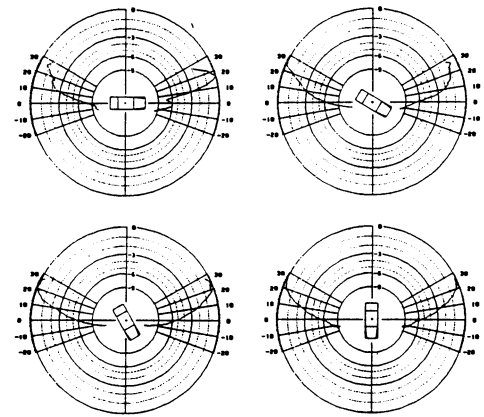

λ/4-monopole. Elevation patterns.

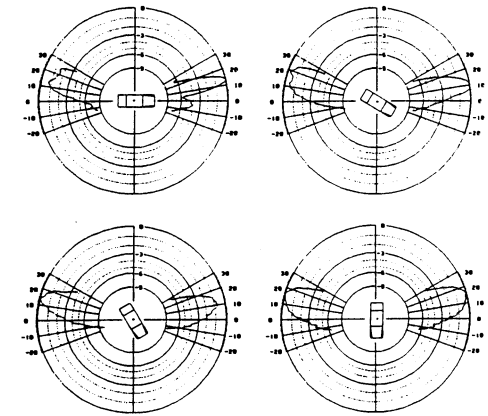

5λ/8-monopole. Elevation patterns.

In elevation pattern diagrams, the position of the car shows the azimuth angle of the elevation cut.

4.4 DISCUSSION.

In the present COST-project only limited work has been done concerning antennas namely on design of diversity antennas for base station and car- and hand held antennas, effect of these antennas on errors and their distribution. Radiation patterns for antennas on a car including the effect of the car.

Future work might be directed towards using more sophisticated antennas, including those with adaptive gain in the horizontal plane. This has been shown to reduce errors in some circumstances [Olsson, 1988], especially at low speeds.

4.5 REFERENCES.

R.G. Vaughan and J. Bach Andersen, 'Antenna diversity in mobile communications', IEEE Transactions on Vehicular Technology, VT-36, No 4, November 1987, pp 149-172.

R.G. Vaughan and J. Bach Andersen, 'A multiport patch antenna for mobile communications' in Proc. 14'th European Microwave Conference, Sept. 1984, pp 607-612.

B. Olsson, 'Antenna pattern diversity test with a 250 kbit s/s radio modem at 900 MHz', Eurocon 88, Stockholm, Sweden, June 1988, R.1.5, p. 306-309.

T. Närhi. 'Experimental results on diversity in digital mobile radio'. Second Nordic Seminar on Digital Land Mobile Radio Communcation, Stockholm, 1986.

K. Laukkanen, 'A diversity antenna for portable radio unit', URSI XII National Convention on Radio Science, Otaniemi, Finland, 1986.

A. Koivumäki, private communication, 1988.

5. CONCLUSIONS

The work described in the preceding sections has been stimulated by the urgency to create a sound basis for the development of digital land mobile radiocommunication services using transmission bit rates of a few hundred kbit/s. Before the start of this project, the known published literature described propagation characteristics for the urban environment only.

The channel properties for all other possible environments had to be investigated. Wideband hardware channel simulators were not generally available. Man-made interference such as that from automobile ignition systems was known only up to 500 MHz and these data were recorded before the widespread introduction of electronic ignition controls. During this project, these gaps in our knowledge have been closed to a large extent. Multipath propagation characteristics for signal bandwidths up to 15 MHz have been recorded for all possible environments, i.e. urban, suburban, hilly and mountainous terrain configurations, using various measurement methods.

Two generations of hardware wideband channel simulators have been developed.

Two prototypes have been used in autumn 1986 for tests of candidate equipment for the GSM. The results of these tests were used to chose the basic system parameters of the future digital mobile radio service defined by GSM. The experience acquired with the prototypes has led to the development of a commercially available channel simulator.

Efforts in developing software simulation techniques have also been pursued with the aim to create design tools for system and hardware developments.

The man-made radio interference levels, mainly due to automobile ignition systems is now known for actual traffic environments.

Antennas for diversity reception and the influence of car antenna mounting position on the radiation characteristics have been investigated.

Further work remains to be done in Radio path loss prediction techniques. Moreover, the knowledge acquired about digitally modulated radio signal propagation in the mobile radio applications should provide a good basis for further work along the lines defined in the proposals for the COST 231 project.

ANNEX 2

Final Report of the Working Group 2 on Baseband Processing

CONTENTS

1. GENERAL 215

2. SUMMARY OF THE FINAL RESULTS 216

3. DETAILS CONCERNING THE WORK DONE 216

3.1 STEPS IN DEFINING THE GSM SPEECH CODEC 216

3.2 RESULTING ALGORITHM AND CORRESPONDING CHANNEL CODING 223

3.3 FINAL ADAPTATION OF THE RPE-LTP TO THE RADIO ENVIRONMENT 224

1. GENERAL

Although some contributions were presented to COST 207 concerning 64 kb/s video-codecs, WG2 concentrated on speech coding, after decision of GSM, not to include higher bit rate channels than 9.6 kb/s (data) - 13 kb/s (speech).

The work that led to the technical approval by GSM of a low bit rate codec was carried out in sequence, in two periods of time, by :

- COST 207 WG2 ,
- Joint TM3 (TR3)/COST 207 SCEG.

During the first period of time, the design goals of the codec were clarified and a number of codecs were studied in laboratories with the participation of Industry, University and Administrations.

During the second period of time, the rules for the selection were established, a final solution was optimized and proposed to the GSM. This solution, a Regular Pulse Excited Linear Predictive Coder with Long Term Prediction (RPE-LTP), was proposed together with a channel coding scheme defined together with GSM/WP2. The corresponding Recommendation (GSM Rec. 06-10 or TM3 T/L/03/11) was writen and tested (Hardware Verification Tests). A number of implementations of this codec are operational (on TMS 320 C 25, PCB 5011, etc). As an example of the level of detail provided in the GSM Rec. 06.10, Table 1 indicates the relative importance of the bits produced by the RPE-LTP codec.

Following a later request of the GSM, non continuous operation (DTX) was studied by a sub-group of SCEG : SCEG/DTX. The first results showed that, in the mobile environment, a great amount of noise was coded together with the speech, and that an unacceptable quality impairment would result from simply switching on and off the mobile transmitter under the control of the voice activity detector (VAD). Therefore, it was decided to insert "comfort noise" at the receiver. Quality impairment could also result from loss or stealing of speech frames : another recommendation was therefore proposed concerning "speech extrapolation/frame replacement". The Figure 1 shows the relations between the various functional blocs involved with the processing of the speech.

Finally, GSM asked SCEG to define the rules of the selection of a "half- rate codec". Since GSM/WP2 has defined the characteristiques of the "half-rate channel", it has been decided that the "half-rate codec" will be provided with corresponding channel coding, corresponding therefore to a global bit rate of 11.4 kb/s. SCEG document 88/39 gives the corresponding details.

The conditions under which this new "half-rate" competition will take place are not yet known, but non European manufacturers claim to have available codecs offering very good quality at 8 kb/s. A follow-on COST project could therefore help European manufacturers to cope with this new threat.

2. SUMMARY OF THE FINAL RESULTS

The quality of the RPE-LTP codec, finally proposed by the SCEG to the GSM, was shown by the subjective tests to be far better than that of the analog channels. Therefore, the GSM decided to use digital speech.

As a consequence of this choice, the SCEG proposed to the GSM the following recommendations :

- 06.01
- 06.10
- 06.11
- 06.12
- 06.31
- 06.32 .

Recommendation numbers 06.2x were left open for the "half-rate codec" recommendations.

The tables of contents of these recommendations can be found as appendices to the present report (as drafted to this date).

Recommendations GSM 06.10 has also been proposed for the transmission of speech in other radio systems. In his last meeting, CEPT /T/R/RES has approved its usage for the "DSRR" system ("CEPT Digital Short Range Radio). Obviously, a particular channel coding mechanism has to be studied for each new application of this recommendation (Table 1 suggests the bits to be carefully protected).

The results of this work have been in particular presented at CCITT (SG XVIII), CCIR (SG 8, IWP 8/13) and at a number of conferences dealing with signal processing and (digital) mobile radio.

3. DETAILS CONCERNING THE WORK DONE

3.1 STEPS IN DEFINING THE GSM SPEECH CODEC

The sharing of both resource allocation and performance between radio equipments and speech coder/decoders has in fact always been very critical and demanding. Furthermore the work was progressing simultaneously and independently (or almost) in both fields. The work of the SCEG had therefore to be divided into

Figure 1

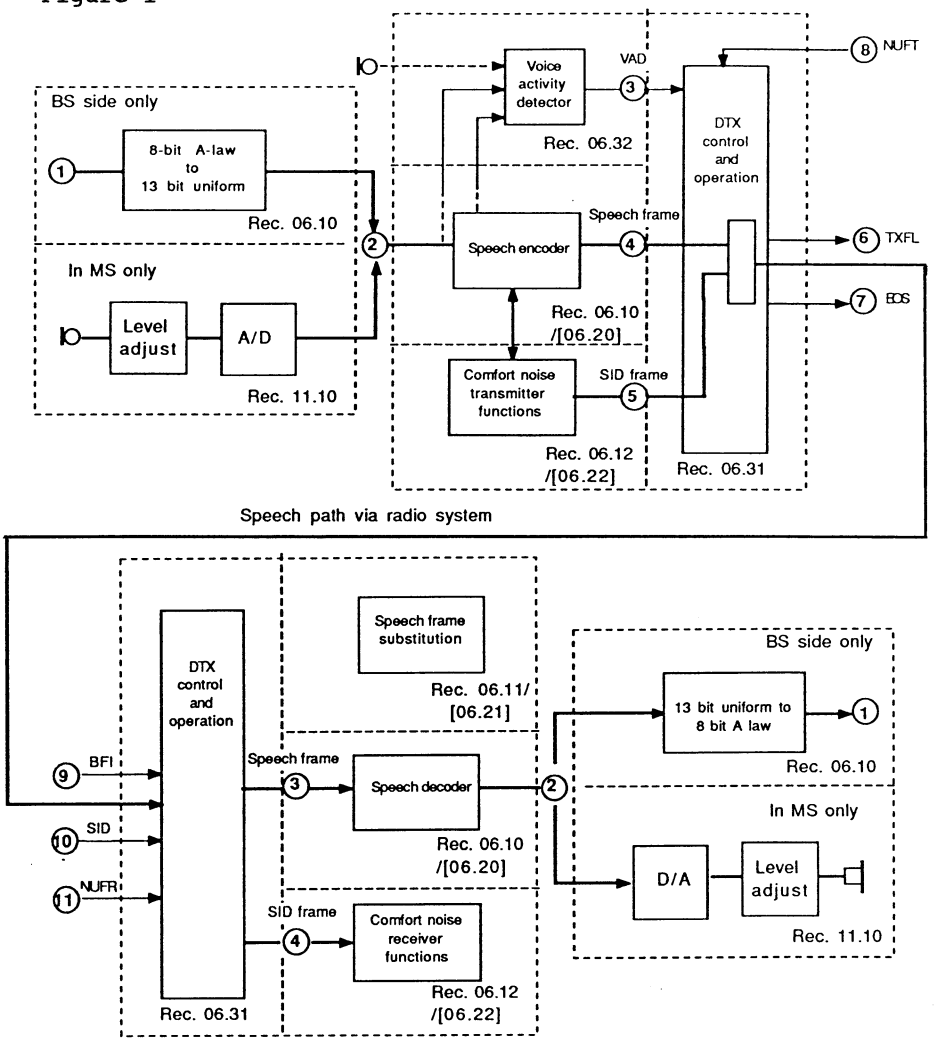

Interfaces and definitions:

Information path →

Flag →

(1) 8 bit/A-law PCM (CCITT G.711), 8000 samples/s
(2) 13 bit uniform PCM, 8000 samples/s
(3) Voice activity flag
(4) Encoded speech, 50 frames/s, 260 bit/frame
(5) SID frame: Special speech frame containing comfort noise updating information
(6) Transmit flag
(7) End of speech flag
(8) Noise update flag (transmitter)
(9) Bad frame indication flag
(10) Silence descriptor flag
(11) Noise update flag (receiver)

Table 1 Subjective importance of encoded bits.

Importance class	Parameter name	Parameter number	Bit index
1	Log.area ratio 1	1	5
	Block amplitude	12,29,46,63	5
2	Log.area ratio 1	1	4
	Log.area ratio 2	2	5
	Log.area ratio 3	3	4
3	Log.area ratio 1	1	3
	Log.area ratio 2	2	4
	Log.area ratio 3	3	3
	Log.area ratio 4	4	4
	LTP lag	9,26,43,60	6
	Block amplitude	12,29,46,63	4
	Log.area ratio 2,5,6	2,5,6	3
	LTP lag	9,26,43,60	5
	LTP lag	9,26,43,60	4
	LTP lag	9,26,43,60	3
	LTP lag	9,26,43,60	2
4	Block amplitude	12,29,46,63	3
	Log.area ratio 1	1	2
	Log.area ratio 4	4	3
	Log.area ratio 7	7	2
	LTP lag	9,26,43,60	1
	Log.area ratio 5,6	5,6	2
	LTP gain	10,27,44,61	1
	LTP lag	9,26,43,60	0
	Grid position	11,28,45,62	1
5	Log.area ratio 1	1	1
	Log.area ratio 2,3,8,4	2,3,8,4	2
	Log.area ratio 5,7	5,7	1
	LTP gain	10,27,44,61	0
	Block amplitude	12,29,46,63	2
	RPE pulses	13..25	2
	RPE pulses	30..42	2
	RPE pulses	47..59	2
	RPE pulses	64..76	2
	Grid position	11,28,45,62	0
	Block amplitude	12,29,46,63	1
	RPE pulses	13..25	1
	RPE pulses	30..42	1
	RPE pulses	47..59	1
	RPE pulses	64..76	1
6	Log.area ratio 1	1	0
	Log.area ratio 2,3,6	2,3,6	1
	Log.area ratio 7	7	0
	Log.area ratio 8	8	1
	Log.area ratio 8,3	8,3	0
	Log.area ratio 4	4	1
	Log.area ratio 4,5	4,5	0
	Block amplitude	12,29,46,63	0
	RPE pulses	13..25	0
	RPE pulses	30..42	0
	RPE pulses	47..59	0
	RPE pulses	64..76	0
	Log.area ratio 2,6	2,6	0

Note: For bits appearing on the same line, the order of importance is from left to right.

several phases which are presented below.

Codec Requirements

In mid-1985, a first attempt to fix the requirements of the coding scheme was achieved. "Phase 1" of the work of SCEG had started. SCEG had its first meeting in Paris in Autumn 1985.

Methodology Used for the Selection

During phase 1, the basic requirements of the codecs were known. But the radio channel had not yet been defined. The aim of this phase was to compare the speech quality of the "candidate" codecs and their resistance to transmission errors. Therefore a scenario, somewhat artificial, had to be defined for the comparison : a 16 kbit/s channel with random errors.

The number of candidate codecs known by the group was over 20. A first step was to reduce this number to a manageable value allowing formal listening tests to be made. For phase 1, an international, multi-lingual subjective experiment had been planned. It was therefore decided to limit the number of candidates at the SCEG level to 6, a maximum of one per country. National tests and selections had thus to be made.

The CSELT of Italy organized a common processing laboratory session for the international test. This laboratory ran speech material through the 6 hardware models of the candidate codecs and through reference systems, under the agreed test conditions, and recorded stimulus tapes for the subsequent subjective testing. In addition to the codecs, a FM mobile radio reference system was included to enable the verification of the GSM voice quality requirements.

The listening tests were carried out with speech material in the native languages of the participating countries.

The design of the experiments was a compromise between, on one hand, the need to evaluate each codec under a minimum number of relevant conditions, and, on the other hand, the need to limit the experiment to a practical size.

Each test condition was assessed using 2 speech samples spoken by 2 male speakers and 2 samples spoken by 2 female speakers. Two different opinion scales were used. The listening effort scale results were used to verify that the minimum requirements were satisfied (average scores of the codecs better than those of the companded FM reference system). On the basis of this evaluation, two of the six codecs were withdrawn.

Candidate Codecs

The 4 remaining codecs were grouped in 2 classes:

- 2 Sub-band coders ;
- and 2 Pulse-excited coders.

Details concerning the pulse-excited coders are given below.

MPE-LTP
- multipulse-excited LPC with long-term prediction;
- net bit rate 13.2 kbit/s, FEC 2.8 kbit/s.

RPE-LPC
- regular-pulse excited LPC;
- net bit rate 14.77 kbit/s, FEC 1.23 kbit/s.

These 2 codecs had similar framing, LPC analysis and inverse filtering. The main differences could be found in the pulse modelling and quantization methods.

The residual signal is represented, when using the MPE algorithm , by a small number of pulses. Positions and amplitudes are optimized to minimize the weighted error. This algorithm includes a long-term prediction loop around the quantizers to increase coding efficiency.

The residual signal is represented, when using the RPE algorithm, by a train of pulses. The positions are chosen among a restricted set of positions, using more pulses than in the case of the MPE.

First Results

Three basic criteria were used to compare the 4 codecs:

- speech quality and robustness against transmission errors;
- transmission delay (theoretical and practical);
- ease of implementation and expected power consumption.

The results showed that the quality of these 4 codecs exceeded the quality of the analog system under medium or high error probabilities conditions.

The average MOS taken over all test conditions was :

- RPE-LPC 3.54
- MPE-LTP 3.27
- SBC-APCM 3.14
- SBC-ADPCM 2.92
- FM 1.95 .

The sensitivity to random and burst errors of the different solutions did not seem to be very different and did not justify the development of two compromise solutions. As a conclusion it was decided by GSM to work on only one compromise solution based on the 2 pulse-excited codecs, providing therefore a "RPE-LTP" (Regular-Pulse Excited LPC with Long-Term Prediction) .

Codec Optimization

The RPE-LTP was based on the two "best" codecs. The target was to design a codec based on the RPE-LPC scheme using a long-term prediction loop (LTP), hopefully more robust to transmission errors than the RPE-LPC.

The bulk of this work was performed by the "Franco-German Codec Optimization Team", bringing together the two Administrations and the two manufacturers that had proposed the corresponding coding schemes.

The first subjective tests involving the RPE-LTP showed that the goal had been reached. It was then necessary to adapt it closely to the radio environment. By that time, the radio sub-system had been defined and some simulations were available.

Channel Coding Optimization

This task was also performed by the Codec Optimization Team, based on simulations of the radio channel provided by GSM/WP2.

The 260 bits produced by the speech coder for each speech frame were sorted according to their sensitivity to transmission errors. Pair comparison tests were used to rank all the bits.

The 4 time slots corresponding to the transmission by radio of a speech frame provide some 456 bits. The question was finally to select the good coding scheme able to protect very strongly some bits and not as much the others. A great number of possibilities were tested, for instance, codes protecting selectively 2 and 3 classes of bits.

Formal and unformal listening tests were used to make this choice.

Hardware Verification Tests

The Codec Optimization Team had also produced a detailed specification of the RPE-LTP. It includes computational details to allow the implementation of bit exact versions of the codec. The resulting GSM recommendation is GSM Rec 06.10 and it also has as the reference CEPT/TM3 T/L/03/11.

In order to verify the specification, several hardware models were implemented based only on the draft of Rec 06.10 . Different DSP were used (TMS 320C25, PCB 5011, a semi-custom, a proprietary DSP, etc.). Test sequences have been prepared for comparison of the results of the processing by the various codecs (these test sequences are now available for further use).

The results did show the accuracy of the GSM draft recommendation 06.10 . This recommendation has been technically approved by the GSM.

Characterization Tests

Objective tests were performed on those hardware models, eg delay, frequency response, linearity were measured.

Finally, subjective characterization tests were performed in a manner similar to that used for the tests of phase 1.

The errors, resulting from the simulations of the radio channel under different conditions, were inserted between coder and decoder using an Error Insertion Device (EID).

The conditions assessed in phase 2 tests were the following:

- transmission channel quality : "C/I"(simulated) 4, 7, 10, and excellent channel ;

- speech input level : -12, -22, -32 dB below codec overload ;

- four transcoding situations : coder decoder back to back, tandeming of 2 codecs (with errors), and RPE-LTP to CCITT G 721 and CCITT G 721 to RPE-LTP ;

- MNRU reference : 6, 12, 18, 24, 30, 36 dB and direct ;

- listening levels : preferred (P), P-10 dB, P+10 dB ;

- two environmental noises : <30 dB(A) and lorry noise ;

- in addition two input circuits used : commercial A-law PCM and linear PCM (high quality).

Two different opinion scales (using scores from 1 to 5) were used :

- listening effort scale (optional)
- quality scale (mandatory).

All Administrations used the quality scale, two used additionally the listening effort scale.

Each test condition was assessed using 2 male speakers and 2 female speakers.

Using all possible combinations of these parameters would have resulted in an experiment of impractible size. Therefore a limited subset of parameters was allocated to three smaller experiments.

There were at least 16 listeners (8 male, 8 female).

As two opinion scales were used, 2 separate sets of data were obtained. The scores obtained in the various countries were processed by CSELT. The results, in terms of M.O.S. using both scales were similar.

3.2 RESULTING ALGORITHM AND CORRESPONDING CHANNEL CODING

Performance of the RPE-LTP

Results of the subjective experiments of phase 2

- under good conditions, the RPE-LTP (Regular-Pulse Excited LPC with Long-Term Prediction) had a score over 4 in the M.O.S. scale (up to 4.3);

- on the average a slightly lower score was obtained by female talkers;

- it performed well at all input levels (poorer performance at -32 dB);

- at "C/I" of 10 dB the degradation is noticeable (degradation of 0.2 to 0.8 M.O.S.); at "C/I" of 4 dB the breakdown in voice quality is clear (scores down to a value of 2 M.O.S.).

Objective Results

The following values were found:

- delay : theoretical = 20 ms ; practical implementation = 22.65 to 28 ms;

- "smoothed" audio band-width up to 3300 Hz (but oscillations of the frequency response above 2 000 Hz);

- total distorsion (CCITT G 712) acceptable (sinewaves of 422 Hz and 813 Hz).

Characteristics of the RPE-LTP (GSM Rec 06.10)

The coding scheme can be described as follows:

- the sampling rate is 8 kHz;

- the frame length is 20 ms; the frame is coded into 260 bits; it is divided in 4 sub-blocs of 5 ms each;

- the net bit rate is 13 kbit/s;

- the bits are divided into 2 classes; the first class (182 bits) is very strongly protected (182 redundancy bits used by a convolutionnal code plus a 3 bit CRC), the second class is not protected at all;

- the maximum delay allocated to the codec is 30 ms; the maximum end-to-end delay in the system is in the order of 75 ms (more than 40 ms are allocated to the interleaving of the time slots and to channel decoding).

3.3 FINAL ADAPTATION OF THE RPE-LTP TO THE RADIO ENVIRONMENT

Speech Extrapolation (GSM Rec 06.11)

One purpose of the work is to enable the coding scheme to cope with transmission errors erasing a complete speech frame. An extrapolation procedure has been proposed. It would make "hand-overs" virtually non-noticeable.

This work is based on the particular characteristics of the RPE-LTP coding scheme.

Voice Activity Detection (VAD) (GSM Rec 06.32)

Another area under study is the implementation of voice activity detectors (VADs) that could enhance the spectral efficiency of the system and reduce the power consumption of the hand held stations. A "data base" with speech plus noise samples is needed to compare such VADs and selection/acceptability methodology must be agreed.

Proposals for reference VAD have been made and corresponding simulations appear to offer acceptable performance.

Discontinuous Transmissions (DTX) (GSM Rec 06.31)

Various DTX mechanisms have been discussed. They have been described using a couple of State Diagramms, one for the transmitter, one for the receiver. Listening to speech tapes produced while using DTX showed that an important impairment of the speech quality would result of using a basic DTX in a noisy background. Therefore Comfort Noise had to be added.

Rec 06.31 is a general recommendation that describes the various actions/decisions to be taken when DTX has been activated in a link transmitter/receiver.

Comfort Noise (GSM Rec 06.12)

Comfort Noise is supposed to fill the gaps between speech fragments. The parameters of the noise to be inserted (spectrum and level) are calculated by the transmitter at the end of the talkspurts (to be detected by the VAD). They are transmitted using a special frame, the "SID" frame ("SIlence Descriptor frame"). If speech is not detected during a long period of time, an updated value of the same parameters is transmitted at regular intervals (eg every 24 frames or every 480ms, in the middle of the interval between two transmissions of the SACCH).

At the receiver, comfort noise is generated using the decoder algorithm : the RPE samples are replaced by pseudo-random values generated locally, and normal use is made of the parameters transmitted in the SID-frame ("LARs" and "Block Maxima"). Smoothing may be introduced at the transitions between the processing of a SID-frame and the processing of the next one.

The SID frames can be recognized with a good reliability since all non used parameters are set to fixed (and unusual) values.

GSM RECOMMENDATION: 06.01

Title: SPEECH PROCESSING FUNCTIONS: GENERAL DESCRIPTION

Date: 1.03.88

Draft: 0.2.0

Editor: Norway

List of contents

1 Introduction

2. Full rate speech transcoding

3. Half rate speech transcoding

4. Discontinuous transmission (DTX)

5. Voice activity detection

6. Comfort noise insertion

7. Speech frame substitution

8. List of terms used in the 06-series

Language of original: English

GSM recommendation: 06.10

Title: GSM full rate speech transcoding

Date: 29 August 1988

List of contents:

1. General

2. Transmission characteristics

3. Functional description of the RPE-LTP codec

4. Computational details of the RPE-LTP codec

5. Digital test sequences

Annex 1. Codec performance

Annex 2. Subjective relevance of the speech coder output bits

Annex 3. Format for test sequence distribution

Note: This Recommendation is a reproduction of recommendation T/L/03/11 "13 kbit/s Regular Pulse Excitation - Long Term Prediction - Linear Predictive Coder for use in the Pan-European Digital Mobile Radio System".

Floppy disks containing the digital test sequences described in section 5 can be distributed by GSM/PN on request.

Language of original: English

Number of pages: 86

Detailed list of contents
****

1. GENERAL

1.1. SCOPE
1.2. OUTLINE DESCRIPTION
1.3. FUNCTIONAL DESCRIPTION OF AUDIO PARTS
1.4. PCM FORMAT CONVERSION
1.5. PRINCIPLES OF THE RPE-LTP ENCODER
1.6. PRINCIPLES OF THE RPE-LTP DECODER
1.7. SEQUENCE AND SUBJECTIVE IMPORTANCE OF ENCODED PARAMETERS

2. TRANSMISSION CHARACTERISTICS

2.1. PERFORMANCE CHARACTERISTICS OF THE ANALOGUE/DIGITAL INTERFACES

2.1.1. Discrimination against out-of-band input signals
2.1.2. Spurious out-of-band signals (receiving)

2.2. TRANSCODER DELAY

3. FUNCTIONAL DESCRIPTION OF THE RPE-LTP CODEC

3.1. FUNCTIONAL DESCRIPTION OF THE RPE-LTP ENCODER

3.1.1. Offset compensation
3.1.2. Preemphasis
3.1.3. Segmentation
3.1.4. Autocorrelation
3.1.5. Schur Recursion
3.1.6. Transformation of reflection coefficients to Log.-Area Ratios
3.1.7. Quantization and coding of Log.-Area Ratios
3.1.8. Decoding of the quantized Log.-Area Ratios
3.1.9. Interpolation of Log.-Area Ratios
3.1.10. Transformation of Log.-Area Ratios into reflection coefficients
3.1.11. Short term Analysis Filtering
3.1.12. Sub-segmentation
3.1.13. Calculation of the LTP parameters
3.1.14. Coding/Decoding of the LTP lags
3.1.15. Coding/Decoding of the LTP gains
3.1.16. Long term analysis filtering
3.1.17. Long term synthesis filtering
3.1.18. Weighting Filter
3.1.19. Adaptive sample rate decimation by RPE grid selection
3.1.20. APCM quantization of the selected RPE sequence
3.1.21. APCM inverse quantization
3.1.22. RPE grid positioning

3.2. DECODER

3.2.1. RPE decoding section
3.2.2. Long Term Prediction section
3.2.3. Short term synthesis filtering section
3.2.4. Postprocessing

4. COMPUTATIONAL DETAILS OF THE RPE-LTP CODEC

4.1. DATA REPRESENTATION AND ARITHMETIC OPERATIONS
4.2. FIXED POINT IMPLEMENTATION OF THE RPE-LTP CODER

4.2.0. Scaling of the input variable
4.2.1. Downscaling of the input signal
4.2.2. Offset compensation
4.2.3. Preemphasis
4.2.4. Autocorrelation
4.2.5. Computation of the reflection coefficients
4.2.6. Transformation of reflection coefficients to Log.-Area Ratios
4.2.7. Quantization and coding of the Log.-Area Ratios
4.2.8. Decoding of the coded Log.-Area Ratios
4.2.9. Computation of the quantized reflection coefficients

4.2.9.1. Interpolation of the LARpp[1..8] to get the LARp[1..8]
4.2.9.2. Computation of the rp[1..8] from the interpolated LARp[1..8]

4.2.10. Short term analysis filtering
4.2.11. Calculation of the LTP parameters
4.2.12. Long term analysis filtering
4.2.13. Weighting filter
4.2.14. RPE grid selection
4.2.15. APCM quantization of the selected RPE sequence
4.2.16. APCM inverse quantization
4.2.17. RPE grid positioning
4.2.18. Update of the reconstructed short term residual signal dp[-120..-1]

4.3. FIXED POINT IMPLEMENTATION OF THE RPE-LTP DECODER

4.3.1. RPE decoding section
4.3.2. Long term synthesis filtering
4.3.3. Computation of the decoded reflection coefficients
4.3.4. Short term synthesis filtering section
4.3.5. Deemphasis filtering
4.3.6. Upscaling of the output signal
4.3.7. Truncation of the output variable

4.4. TABLES USED IN THE FIXED POINT IMPLEMENTATION OF THE RPE-LTP CODER AND DECODER

5. DIGITAL TEST SEQUENCES

5.1. INPUT AND OUTPUT SIGNALS
5.2. CONFIGURATION FOR THE APPLICATION OF THE TEST SEQUENCES

5.2.1. Configuration 1 (encoder only)
5.2.2. Configuration 2 (Decoder only)

5.3. TEST SEQUENCES

5.3.1. Test sequences for configuration 1
5.3.2. Test sequences for configuration 2

ANNEX 1. CODEC PERFORMANCE

A1.1. INTRODUCTION
A1.2. SPEECH PERFORMANCE

A1.2.1. Single encoding
A1.2.2. Speech performance when interconnected with coding systems on an analogue basis

A1.2.2.1. Performance with 32 kbit/s ADPCM (G.721)
A1.2.2.2. Performance with another RPE-LTP codec
A1.2.2.3. Performance with encoding other than RPE-LTP and 32 kbit/s ADPCM (G.721)

A1.3. NON-SPEECH PERFORMANCE

A.1.3.1. Performance with single sine waves
A1.3.2. Performance with DTMF tones
A1.3.3. Performance with information tones
A1.3.4. Performance with voice-band data

A1.4. DELAY
A1.5. REFERENCES

ANNEX 2. SUBJECTIVE RELEVANCE OF THE SPEECH CODER OUTPUT BITS

ANNEX 3. FORMAT FOR TEST SEQUENCE DISTRIBUTION

A3.1. TYPE OF FILES PROVIDED
A3.2. FILE FORMAT DESCRIPTION

GSM recommendation: 06.11

Title: Speech extrapolation

Date: 2 AUGUST 1988

Editor: The Netherlands

Language of original: English

Number of pages: 4

GSM recommendation: 06.12

Title: Comfort noise aspects

Date: 28, June 1988

Editor: Italy

Language of original: English

Number of pages: 8

GSM Recommendation : 06.31

Title : DISCONTINUOUS TRANSMISSION (DTX) FOR FULL RATE SPEECH TRAFFIC CHANNELS

Date: 28 June 1988

Editor: FRANCE

List of contents:

0. Scope

1. General

2. Transmitter

2.1. Input and output signals

2.2. Transmitter states

2.3. Transitions between states at the transmitter

3. Receiver

3.1. Input signals

3.2. Receiver states

3.3. Transitions between states at the receiver

Language of original: English

Number of pages: 7

ANNEX 3

Final Report of the Working Group 3 on Modulation Methods

ANNEX 3

DIGITAL LAND MOBILE RADIO COMMUNICATIONS :

FINAL REPORT OF WORKING GROUP 3

CONTENTS

1. PREAMBLE 241

2. MODULATION METHODS 243

2.1 INTRODUCTION 243

2.2 MODULATION TECHNIQUES 244

2.2.1 General Definition of Phase Modulation 244

2.2.1.1 Gaussian Minimum Shift Keying 246

2.2.1.2 Generalised Taming Frequency 246

2.2.1.3 Amplitude Imbalance and Quadrature Error 246

2.2.2 General Definition of Frequency Modulation 246

2.2.2.1 Pulse Amplitude Modulation/Frequency Modulation (PAM/FM) 247

2.2.2.2 PAM/FM Power Spectrum 247

2.3 SIMULATION CONDITIONS AND DEFINITIONS 247

2.3.1 Definitions 248

2.3.2 Receivers GMSK and GTFM 249

2.3.3 Receiver PAM/FM 249

2.4 PERFORMANCE COMPARISON : IN A NON-FREQUENCY SELECTIVE CHANNEL 250

2.4.1 Adjacent Channel Interference 250

2.4.2 Co-Channel Interference 250

2.4.2.1 Discriminator Detection 250

2.4.2.2 Coherent Detection 251

2.4.3 Urban Environment Performance 251

2.4.4 Transmission Error Statistics 252

2.4.5 Experimental Confirmation 253

2.4.6 Performance Summary 253

2.5 NARROWBAND TDMA SYSTEMS : FREQUENCY SELECTIVE CHANNEL 254

2.6 CONCLUSIONS 256

REFERENCES 256

FIGURES 258

3. ADAPTIVE EQUALISERS 277

3.1 INTRODUCTION 277

3.2 THEORETICAL BACKGROUND 278

3.2.1 Adaptive Linear Transversal and Decision Feedback Equalisers 278

3.2.1.1 The CFKA Algorithm 281

3.2.2 Equalisers based on Maximum Likelihood Sequence Estimation (MLSE) 284

3.2.2.1 GMSK as an Offset QAM Modulation 284

3.2.2.2 Channel Effects 285

3.2.2.3 The Likelihood Function 286

3.2.2.4 The Viterbi Algorithm and MLSE Detection 287

3.2.2.5 Equalisation based on a Whitened Matched Filter 290

3.2.2.6 Comparison between the two Equaliser Structures 291

3.2.2.7 Variations of Equaliser Structure 292

3.3 PROPAGATION CHANNEL MODELS 293

3.3.1 Channel Model 1 (Static Two-Path) 293

3.3.2 Channel Model 2 (Rayleigh Two-Path) 294

3.3.3 Channel Model 3 (Flat Rayleigh Fading) 294

3.3.4 Channel Model 4 (Hilly Terrain) 295

3.3.5 Channel Model 5 (Rural Area) 296

3.3.6 Channel Model 6 (Typical Urban Area) 296

3.3.7 Channel Model 7 ('Equaliser Model') 296

3.3.8 Channel Model 8 (Simplified Hilly Terrain Model) 297

3.4 GSM SYSTEM CHARACTERISTICS 297

3.4.1 Time Slot Structure and Transceiver 297

3.4.2 Synchronisation Techniques 299

3.4.3 Channel Impulse Response (CIR) Estimation 301

3.5 PERFORMANCE RESULTS OF LTE AND DFE AS APPLIED TO CEPT/GSM SYSTEM 303

3.5.1 Signature Curves 303

3.5.2 BER in a Static Frequency Selective Channel 303

3.5.3 BER in a Flat Rayleigh Fading Channel 304

3.5.4 BER in a Frequency Selective Fading Channel 304

3.5.5 Discussion 304

3.6 PERFORMANCE RESULTS OF VITERBI EQUALISERS AS APPLIED TO THE CEPT/GSM SYSTEM 306

3.6.1 Introduction 306

3.6.2 Signature Curves 306

3.6.3 BER in a Static Frequency-Selective Channel 307

3.6.4 BER in Flat and Frequency Selective Rayleigh Fading Channels 307

3.6.5 BER in Multipath Rayleigh Fading Channels (Channels 4-8) 308

3.6.6 Error Statistics for Channel 2 309

3.6.7 Discussion 310

3.7 CONCLUSIONS 311

3.7.1 Overview of Results Obtained 311

3.7.2 Future Developments 313

3.8 REFERENCES 314

FIGURES 317

4 REED-SOLOMON FORWARD ERROR CORRECTING CODES 345

4.1 Introduction 345

4.2 FEC Coding Specifications 346

4.2.1 Correcting Capability 347

4.2.2 Specification of a Reed-Solomon Code with Interleaving 349

4.2.3 Performance Results 350

4.3 Error and Erasure Correction Concept 350

4.3.1 Erasure Detection 352

4.3.2 Results and Comparisons 353

REFERENCES 355

FIGURES 356

1. PREAMBLE

COST 207 Working Group 3 started its task by identifying current research programmes in signatory countries that would assist in the characterisation, definition, choice and optimisation of modulation methods and related functions. On the basis of contributions from participating members the Working Group was able to study and produce output documents on modulation performance, channel equalisation techniques, forward error-correction and interleaving.

Each study programme is reported in the following sections 2, 3 and 4 respectively.

Each section is self-contained having an individual Introduction and Conclusion thereby focusing on the considerable information reported.

2. MODULATION METHODS

2.1 INTRODUCTION

At the beginning of COST 207 action it was not clear whether narrow-band or wide-band transmission systems would be adopted in the CEPT/GSM specification for a pan-European, digital, cellular, mobile radio system. Consequently both single-channel per carrier (SCPC) and time-division multiple access (TDMA) systems were considered in detail, and the results are reported here.

In these systems the transmitters need to produce signals with low spectral tails and the radio frequency (RF) carrier must be electronically tunable over a number of channels. Moreover, to minimise complexity, cost and power consumption the RF amplifiers should be allowed to operate at saturation implying minimal linearity requirements. These constraints demand modulation methods that produce constant-envelope, compact spectrum, signals without need for additional filters after the modulation process. Typical of this class of modulation are; Gaussian minimum-shift keying (GMSK), generalised tamed frequency modulation (GTFM), pulse amplitude modulation/frequency modulation (PAM/FM).

A number of studies can be found in literature that deal with particular aspects and applications of such methods but comprehensive performance comparisons under the same conditions are not easily found, particularly with reference to the radio environment envisaged for the pan-European system under study. In this regard performance will be compared in terms of sensitivity to thermal noise, co-channel interference, adjacent-channel interference and random FM noise, noting that SCPC systems are not sensitive to frequency-selective channel distortion. When narrowband TDMA systems were first proposed it was said they also would not suffer from channel distortion due to multipath propagation since the width of their power spectrum would be less than the so-called coherence bandwidth in a typical urban environment. Now, however, it is known that digital signals with bit rates of the order of 270 kbit/s, like those currently envisaged for the pan-European narrowband TDMA system, can be significantly distorted. To compare the relative robustness of the considered modulation schemes to channel distortion signature curves have been used as a means of indicating performance.

Before presenting the results for SCPC and TDMA systems it is appropriate to define more closely the modulation techniques, the evaluation parameters and some more-general performance data.

2.2 MODULATION TECHNIQUES

In this section the three modulation methods investigated are categorised either as phase modulation (GMSK, GTFM) or frequency modulation (PAM/FM).

2.2.1 General Definition of Phase Modulation

A modulation method is classified as Phase Modulation (PM) if the amplitude of the signal at the modulator output is constant and if the phase of the carrier wave is forced to reach, at the end of each signalling period, one of the values of a given set of phase states, apart from some intersymbol interference which can arise because of filtering effects. According to fig 2.2.1 such a signal may be produced by adding two quadrature components of the carrier, which are amplitude modulated by the sine and cosine functions of the signal phase, respectively; the modulating waveforms are produced by digital circuits, through D/A (Digital-to-Analogue) converters.

The PM modulation methods usually proposed for land mobile applications (GMSK, GTFM) belong to the general class having the following characteristics:

(a) The number of distinct phase states of the signal constellation is 12; four of them are placed on the axes of the signal plane, while the position of the others depends on a parameter which will be called ϕ (see fig 2.2.2).

(b) The phase shift occurring during each signalling period depends on the logical value of three consecutive bits, according to Table 1 and can take six distinct values: $\pm 90^{\circ}$, $\pm \phi$ and $\pm(2\phi - 90^{\circ})$;

(c) The above phase shifts take place according to four different sets of paths, called f_1, ..., f_4 in Table 1, plus their opposite shapes.

b_{i-1} b_i b_{i+1}	Phase shift	Path set
1 1 1	90	f_1
0 0 0	-90	$f_{1'}$
1 1 0	$\emptyset$	f_2
0 0 1	$-\emptyset$	$f_{2'}$
0 1 1	$\emptyset$	f_3
1 0 0	$-\emptyset$	$f_{3'}$
0 1 0	$2\emptyset - 90$	f_4
1 0 1	$-2\emptyset + 90$	$f_{4'}$

Table 1 - Phase shifts and selection of the path sets for the PM modulation class.

As shown in fig 2.2.3, in general each set of paths includes more than one phase trajectory with slightly different shape. The selection of a particular phase path of a given set is done on the basis of the logical value of the bit which comes before and the bit which follows the three bits determining the set (phase shift). This additional degree of freedom allows different shapes of the power spectra to be obtained without altering the selected phase shifts at the end of the signalling periods.

The PM methods having the above characteristics are called 12PM3 (1,2) modulations (12 phase states, PM for Phase Modulation, 3 consecutive bits used to choose the phase shift in each signalling period). To define a modulation method belonging to this class it is necessary to specify $\emptyset$ and the phase-transition path. This latter item can be specified either mathematically or, more conveniently, as a filter with an appropriate response to produce the necessary controlled intersymbol interference.

2.2.1.1 Gaussian Minimum Shift Keying (GMSK)

GMSK is essentially a frequency-shift keyed modulator (3) in which the input non-return-to-zero binary signal is passed through a Gaussian low-pass filter and the output is then applied to a voltage controlled oscillator with a modulation index (M_f) of 0.5. By setting the bandwidth of the filter, controlled amounts of inter-symbol interference may be introduced. The greater the inter-symbol interference the more compact the radiated spectrum. One parameter is used to define this trade-off; a product of the 3dB filter bandwidth (B) and the bit interval (T). The product BT and phase parameter ϕ are related by the curve of fig 2.2.4.

2.2.1.2 Generalised Tamed Frequency Modulation (GTFM)

GTFM differs from GMSK in the shape of the pre-modulation filter; which is a raised-cosine defined by its roll-off factor (ρ). The phase-change parameter is ϕ. Performance is not very sensitive to changes in ρ about the value 0.42 but the value of ϕ is significant. Note, fig 2.2.4 shows that $\phi = 60^{\circ}$ is equivalent to the GMSK BT product of 0.315.

2.2.1.3 Amplitude Imbalance and Quadrature Error

Both modulation schemes discussed are critically dependent on the value of ϕ and consequently amplitude imbalance and quadrature (angle) error between the quadrature components can cause a deterioration in out-of-band emission. Fig 2.2.5., shows the significance of such imperfections to spectral shaping and adjacent channel interference.

2.2.2 General Definition of Frequency Modulation

A digital modulation method is classified as Frequency Modulation (FM) if the amplitude of the signal at the modulator output is constant and if the instantaneous frequency of the carrier wave is forced to reach, at the end of each signalling period, one of the values of a given set

of frequency states, apart from some intersymbol interference due to filtering and implementation imperfections. The phase of the carrier wave is not required to reach any particular value at any instant.

2.2.2.1 Pulse Amplitude Modulation/Frequency Modulation (PAM/FM)

In this modulation scheme (4,5) the bits of the input stream (duration T) are serial-to-parallel grouped n-by-n and coded into a rectangular multi-level signal of 2^n, equally spaced, gray coded levels. Rectangular pulse duration is nT. Before the frequency modulation process, the multi-level baseband signal undergoes a pre-modulation filtering in order to reduce its spectrum occupancy. The transfer function of the pre-modulation filter will include any linear process (spectrum shaping, partial-response coding, if any, etc.), required to produce the desired modulating signal. The characteristics of the modulated signal will depend on the number of modulation levels, the transfer function of the pre-modulation filter and the frequency deviation. This last parameter is defined as the ratio of the steady-state frequency deviation corresponding to the highest modulating level to the bit rate of the input signal.

PAM/FM signals have the same characteristics as FSK signals but the baseband shaping of the modulating signal causes both phase and frequency transitions of the modulated signal to be continuous.

2.2.2.2 PAM/FM Power Spectrum

The power spectrum for a 4-level PAM/FM signal is shown in fig 2.2.6. The pre-modulation filter frequency response was equivalent to the square root of a raised-cosine characteristic (ρ = 0.2) with a (x/sin x) whitening factor. This spectrum characteristic should be compared with those given in fig 2.2.5 with zero impairments; the differences between them are insignificant for signal spectral density above -75dB.

2.3 SIMULATION CONDITIONS AND DEFINITIONS

The large majority of results presented in this report have been derived

through simulation (1,2,4,6). In order to contain the range of variables and test parameters within manageable proportions the following conditions were adopted as being representative of operational status expected to be found in practice.

- Static performance is represented by the addition of white Gaussian noise (AWGN).

- Co-channel and adjacent-channel, multiple, interfering signals are simulated by signals with Gaussian amplitude probability-density and a spectrum shape equal to that of the wanted signal.

- Dynamic performance is represented by the introduction of flat Rayleigh fading in which the channel is fully identified by the vehicle speed.

- To assess system behaviour in the presence of frequency-selective distortion a static two-path channel model is swept across the occupied band and a system-signature obtained.

- The 3dB bandwidth (B) of the pre- and post-detection filters are normalised to the bit rate (B_r).

- Channel spacing is also normalised to the bit rate.

- Channel spacing is assumed to be 1.56 B_r, however, adjacent channel interference has been evaluated with a carrier-spacing of 1.44 B_r to account for frequency drift of oscillators.

2.3.1 Definitions

C/I = carrier-to-interference power ratio (dB).

E_b/N_o = energy per bit to noise power spectral density ratio (dB).

B = 3dB bandwidth of filter.

B_{eq} = noise equivalent bandwidth of the pre-discrimination filter (Hz).

B_r = bit rate (bit/s).

$$E_b/N_o = \text{SNR} + 10 \log \frac{B_{eq}}{B_r} \text{ dB}$$

2.3.2 Receivers GMSK and GTFM

GMSK and GTFM modulation schemes have been evaluated both with non-coherent (discriminator) and coherent detection.

The non-coherent receiver uses an ideal frequency discriminator, preceded and followed by filters. The pre-discrimination filter accounts for all the selectivity of the receiver from the RF front-end to the discriminator and is represented by a 7-pole ideally equalised Butterworth filter, $B = B_r$. The post-discrimination filter represents all the linear processes between discriminator and decision circuit, and is represented by a low-pass 8-pole ideally equalised Butterworth filter with $B = 0.38\ B_r$. A typical eye-diagram at the decision input is shown in fig 2.3.1. A hard decision, bit-by-bit, circuit can be used to regenerate the digital signals. In this the received signal is compared against two decision thresholds at time instants at which the eye displays three levels ($t = 0$ in fig 2.3.1). The three-level eye has a zero-level which raises an error propagation problem, overcome in this case by the use of differential encoding of the binary signal.

Since both GMSK and GTFM introduce memory to the transmitted signal (or correlation between transmitted symbols) then it is possible to use this to improve the bit-error ratio (BER) performance. One suitable algorithm is known as maximum likelihood sequence estimation (MLSE, see section 3.2.2). In the process used in these results the sequence estimation is performed over an interval of 16 bits.

The coherent receiver uses a pre-detection filter consisting of a 7-pole ideally equalised Butterworth filter with $B = 1.56\ B_r$. The post-detection filter is a 5-pole Butterworth filter of $B = 0.5\ B_r$. Due to the well-known uncertainty of multiples of $\pi/2$ radians in the phase of the recovered carrier, differential encoding in the transmitter and the corresponding decoding in the receiver is assumed.

2.3.3 Receiver PAM/FM

This receiver differs from those in section 2.3.2 because the

post-discrimination filter represents a square-root of a raised cosine filter with a 0.2 roll-off factor. This complements an identical filter in the modulator. The pre-discrimination filter is a 7-pole ideally equalised Butterworth filter with a 3dB bandwidth equal to the bit-rate.

2.4 PERFORMANCE COMPARISON: IN A NON-FREQUENCY SELECTIVE CHANNEL

2.4.1 Adjacent Channel Interference

In figs 2.4.1, 2.4.2 and 2.4.3 the performance in an AWGN channel of GMSK, GTFM and PAM/FM modulating schemes are shown for a bit-error ratio (BER) of 10^{-2}, discriminator detection, and bit-by-bit hard decision with results for MLSE in the cases of GMSK and GTFM. Noting that the GMSK parameter BT = 0.315 is equivalent to GTFM parameter $\emptyset = 60^{o}$ then it can be seen that the difference in performance for these systems is negligible irrespective of the decision process. Close affinity also exists between BT = 0.25 and $\emptyset = 55^{o}$ with similar conclusion to be drawn. In the COST 207 project it has been found that in general the performance of GMSK and GTFM are quite similar. Regarding the decision process it is clear that the adoption of MLSE can raise the immunity to thermal noise in the presence of adjacent-channel interference by 1dB.

The PAM/FM result of fig 2.4.3 indicates significant improvements, in terms of adjacent channel and concurrent thermal noise sensitivities, with respect to GMSK and GTFM both using MLSE decision.

A representative result for GTFM and coherent detection is given in fig 2.4.4 but, noting the above comment, it is also indicative for GMSK performance.

2.4.2 Co-Channel Interference

2.4.2.1 Discriminator Detection

Sensitivity to co-channel interference is indicated in the form shown in fig 2.4.5. Once again this result shows the close similarity between GMSK and GTFM.

In terms of bit-error ratio performance in the presence of additive white Gaussian noise and co-channel interference it is possible to present the results of simulation in one graph. Fig 2.4.6 is one such graph for GTFM and GMSK assuming a stationary transmission environment. Clearly to assume a stationary situation is unrealistic in practice and so fig 2.4.7 shows the performance in the presence of multipath propagation on both wanted and interfering signals, for slowly moving vehicles. From this latter figure some deductions can be made.

- For low interference a considerable increase in signal power (~10dB) is required to achieve a 10 times improvement in BER. However, channel coding is expected to mitigate this effect.

- If the system is co-channel interference limited then it is seen that BER = 10^{-2} can be achieved with very low carrier-to-interference ratios of the order 9dB.

Although bit-by-bit decision has been used in these cases fig 2.4.2 implies that MLSE would raise C/I, for BER = 10^{-2}, by about 1dB.

Once again the corresponding figure for PAM/FM (figs 2.4.8, 2.4.9 and 2.4.10) show a generally better performance for bit-by-bit decision but the application of MLSE decision to the GMSK/GTFM results offsets this advantage in the interference limited case. Under thermal noise limited conditions (low interference) the PAM/FM advantage is maintained.

2.4.2.2 Coherent Detection

Fig 2.4.11 is representative of GMSK and GTFM data for coherent detection and bit-by-bit decision. Comparing this result with fig 2.4.5 shows, under thermal noise-limited conditions, approximately a 3dB E_b/N_o advantage. This advantage is maintained until the threshold value for C/I is approached.

2.4.3 Urban Environment Performance

In previous sections vehicle speeds have been kept very low, obviously

higher speeds need considering and speeds up to 100 km/h have been evaluated. Such speeds introduce doppler frequency shifts and random FM noise resulting in an irreducible BER. Since GMSK and GTFM have displayed similar performance only GMSK is shown, fig 2.4.12, together with that for PAM/FM in fig 2.4.13. The trends between these to figures are consistent with previous observations but their differences, in terms of irreducible BER, are small. Irreducible BER depends on the ratio of vehicle speed to transmitted bit rate, consequently increasing bit-rate from 16 kbit/s, the value used in these simulation results, to another value X kbit/s changes the value of the vehicle speed according to the following;

$$V_x = \frac{V.X}{16} \text{ km/h}$$

Changes in the key modulation parameters of BT and $\emptyset$ for GMSK and GTFM have little effect on the value of irreducible BER.

2.4.4 Transmission Error Statistics

This sub-section presents some statistics on transmission error based on a definition of error burst which is widely used (5).

According to this definition, two transmission errors separated by less than g error-free bits are considered to belong to the same error burst. Conversely, two consecutive transmission errors separated by g or more error-free bits are considered to belong to different error bursts. This is not the only possible definition for identifying bursts of transmission errors and possibly distinguishing error burst from random errors (5). Perhaps more suitable definition could be found for giving statistical description of digital channels and anticipating performance of FEC codings, but for the time being, we will use only the above definition.

Fig 2.4.14 shows the cumulative distribution of burst-errors length (BEL), for two values of parameter g, for GTFM modulation ($\emptyset = 60^{o}; f = 0.42$) and alternative decision techniques. The results were obtained by simulating three narrowband channels, without channel coding, at a BER = 10^{-2}. The corresponding cummulative distributions of error-free interval length (the number of error-free bits between two errors),

(EFIL) are given in fig 2.4.15.

Equivalent results for PAM/FM modulation are presented in fig 2.4.16.

2.4.5 Experimental Confirmation

All participants in the modulation performance simulation were keenly aware of the need to confirm the results using a practical modem. One opportunity of doing so produced the results given in figs 2.4.17 and 2.4.18. The first figure indicates performance with added white Gaussian noise with bit-by-bit (3-level) decision. The difference between simulation and practical model results are in a range of 1 to 2 dB. This may be due to the fact that simulation does not take into account all the actual characteristics of the modem (eg. in simulation a perfectly constant group delay has been associated with the selectivities, while some distortion was probably present in the experiment). In the case of the MLSE decision the differences are a little greater, probably because of some additional implementation imperfection of the MLSE algorithm.

The same can be said about the comparison of performance in an urban environment (fig 2.4.18), but noting that the simulation did not take into account the actual behaviour of the implemented clock recovery circuit.

Overall the order of agreement is considered to be very good and confirms the validity of the simulation procedure.

2.4.6 Performance Summary

For non-dispersive channel conditions it was concluded that:

- GMSK performance is very similar to that for GTFM.

- In the case of GMSK and GTFM, MLSE decision generally performs better than, bit-by-bit decision under both fading and non-fading conditions.

- PAM/FM, by suitable choice of filtering and modulation index, can produce a range of characteristics and performance. In the

typical conditions considered in this paper it was concluded that PAM/FM was the better choice.

- Coherent detection for GMSK, or GTFM, offers some performance advantage over discriminator detection but requires extra receiver complexity. This advantage is maintained until the threshold value of C/I is approached.

2.5 NARROWBAND TDMA SYSTEMS: FREQUENCY SELECTIVE

In digital transmission with multipath propagation, when symbol rates are of the order of the coherence bandwidth, frequency selective (dispersive) phenomena occur. To assess their effect on the performance and practical implementation of modulation schemes in land mobile radio systems the "signature curves" widely used in digital radio-relay systems (7) have some value. Such curves are obtained by simulating the propagation conditions as the sum of two components coming from different paths. According to such a model the channel transfer function exhibits a periodic shape with maxima and minima (notches) defined by the following.

B^1 = notch depth of the simulated channel transfer function amplitude characteristic.

f_n/f_{bit} = notch and carrier frequency difference normalised to bit rate.

$\tau.f_{bit}$ = delay of the weaker signal with respect to the stronger normalised to bit rate (when τ is positive the channel is said to be minimum phase conditions, and non-minimum phase when τ is negative.

The signature curves are produced by scanning the periodic channel transfer function through the occupied bandwidth noting the value of B^1 at which channel collapse occurs as a function of f_n/f_{bit}, with $\tau.f_{bit}$ a parameter. The criterion defining collapse of the system may be, in the absence of noise, closure of the eye diagram or reaching a BER threshold. Results of simulation have verified that both give substantially the same curves. The smaller the area under the signature curves the lower the system sensitivity to channel distortions.

Signature testing is a static test that does not fully exercise the dynamic properties of a mobile receiver's adaptive channel-equaliser, carrier recovery, clock recovery circuits; when implemented. In mobile-radio communications the fading mechanism is far more dynamic and presents a relatively wider-ranging delay characteristics than found in radio-relay systems. However, in the absence of a representative dynamic channel-simulation model, it is concluded that two-path signature testing does offer a means of comparatively judging mobile system performance by noting the respective areas under the signature curve. Caution is required in coming to conclusions from such tests because:

- Signature curves may change shape for minimum and non-minimum phase conditions.

- Signature curves measured for deteriorating signal conditions may often differ from that for signal recovery conditions (a function of system implementation).

- When signal condition are such as to cause a change from minimum to non-minimum phase conditions (or vice versa) at the instant of change the group-delay characteristic changes sign.

Nevertheless two-path signature testing was the only means quickly available to us to introduce dispersive effects to our results thereby making them more relevant to narrow-band TDMA systems.

Figs 2.5.1 to 2.5.4 show signature curves assuming perfect bit timing and reference carrier synchronisation (where needed). It was concluded from these results that;

- once again GMSK and GTFM performance is quite similar,

- for narrowband TDMA systems, PAM/FM has a wider signature and is, therefore, more sensitive to channel distortion,

- Comparison of figs 2.5.2 and 2.5.3 shows the MLSE decision process to have a very significant advantage,

- The fig 2.5.4 results for coherent detection and bit-by-bit decision, show a better performance than non-coherent detection with MLSE

decision (fig 2.5.3).

This latter results arises because for coherent detection the receiver bandwidth is dominated by the low-pass baseband filter which has a bandwidth about a quarter of that of a bandpass pre-discrimination, non-coherent, system filter. Hence the signature is reduced in width, and longer delays can be tolerated. In figs 2.5.1, 2.5.2 and 2.5.3 the longest delay curves seem not to decrease. This is the result of the channel model assuming a simple, stable, two-path propagation condition which results in the notches (minima) falling at regular frequency intervals and spaced by less than the receiver bandwidth. Such regularity would not be expected in practice.

2.6 CONCLUSIONS

The COST 207 project concluded from its studies that:

- For systems operating with a transmission rate less the coherence bandwidth amplitude modulation/frequency modulation (PAM/FM) functions better than GMSK and GTFM,

- For systems with a transmission rate larger than the coherence bandwidth the optimum would seem to be coherent detection GMSK or GTFM, based on the conclusions from two-path signature evaluations. MLSE decision will further enhance performance.

REFERENCES

[1] P. Porzio Giusto and R. S. Swain, "Digital Modulation Schemes for Narrowband Mobile Radio : An Overview by COST 207". Proc. International Conference on Digital Land Mobile Radio Communications, Venice, Italy. June 30-July 3 1987.

[2] G. D'Avia et alli, "Narrowband Modulation Methods for Land Mobile Radio", Proc Digital Land Mobile Radiocommunications Workshop, Pontechhi Marconi, Italy, pp 41-42. September 1985.

[3] Murota, K. and Hirade, K. (July, 1981) GMSK modulation for digital mobile radio telephony. IEEE Trans. Comm., vol COM-29, No 7, pp. 1044-1050. July 1981.

[4] G. D'Avia and V. Zingarelli, "Pulse Amplitude Modulation/Frequency Modulation (PAM/FM) techniques for Digital Mobile Radio", Proc. IEEE Globecom '86, Houston, TX, pp.31.3.1.-31.3.5. Dec 1-4 1986.

[5] G. D'Avia, G. Taricco, and V. Zingarelli, "Performance and Burst Error Characteristics of PAM/FM modulations in Mobile Radio Channels", Proc IEEE Globecom '86, Houston, TX, pp.31.4.1-31.4.5. Dec 1-4 1986.

[6] G. D'Avia et alli, "Performance of GMSK and Comparison with the Modulation Methods of the 12PM3 Class", IEEE Vehicular Technology Conference, Tampa, Florida. June 1987.

[7] A. J. Giger and W. T. Barnett, "Effects of multipath propagation on digital radio" IEEE Trans. Comm, vol COM-29, No 9, pp 1345-1352. Sept. 1981.

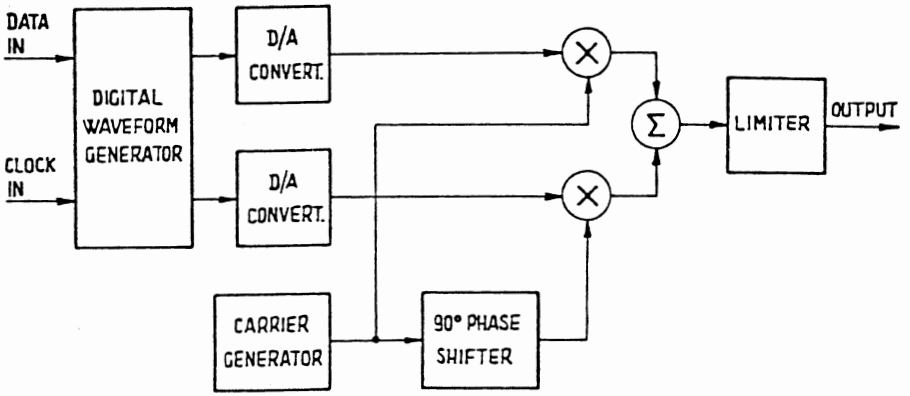

Fig 2.2.1 - Simplified block diagram of a general PM modulation scheme.

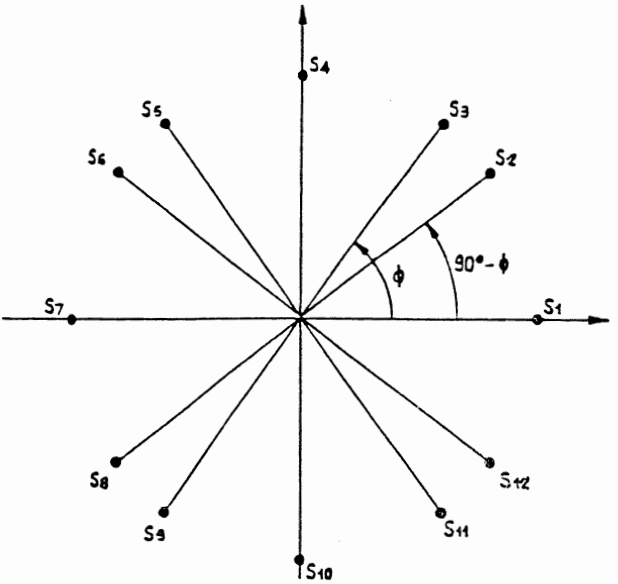

Fig 2.2.2 - Signal constellation of the PM modulation class.

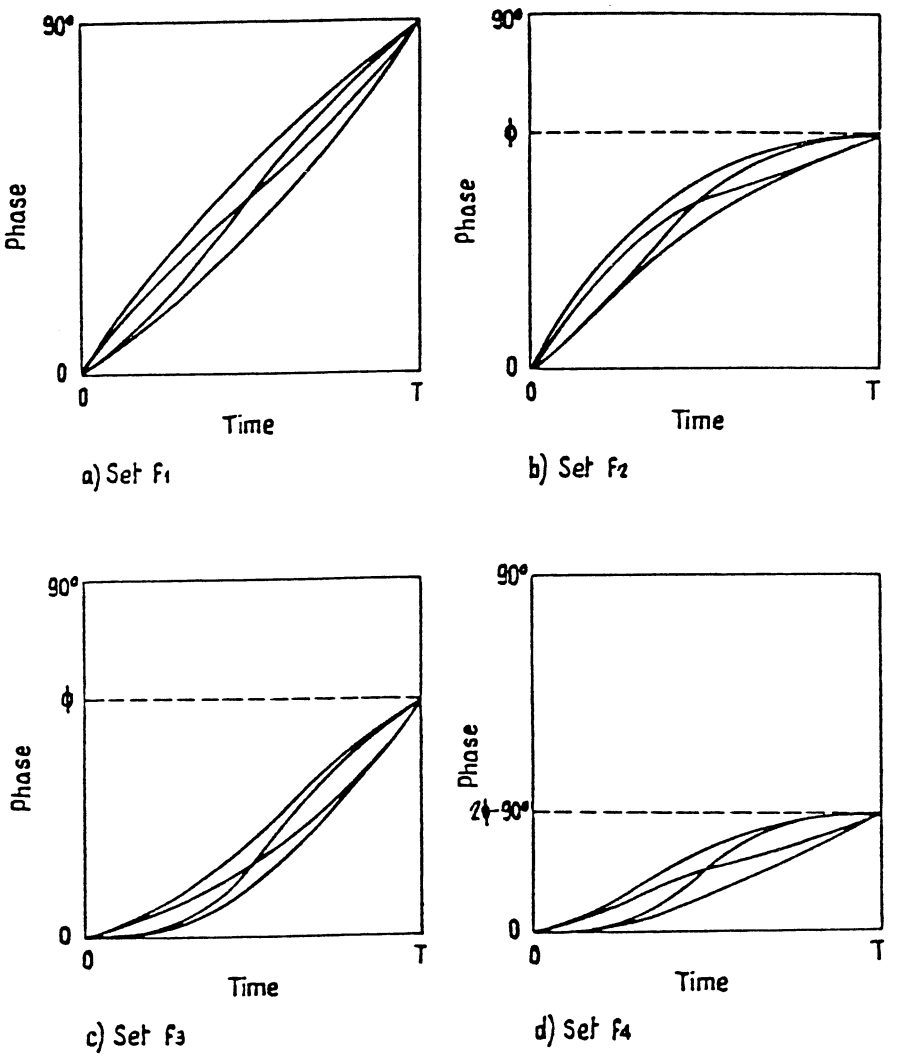

Fig 2.2.3 - Qualitative shapes of the phase paths for each set selected according Table 1 (for example with four phase-paths per set).

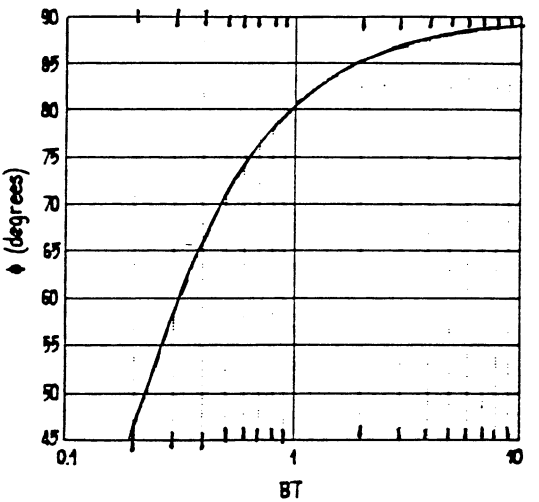

Fig 2.2.4 - Relationship between parameters Ø and BT for GMSK modulation.

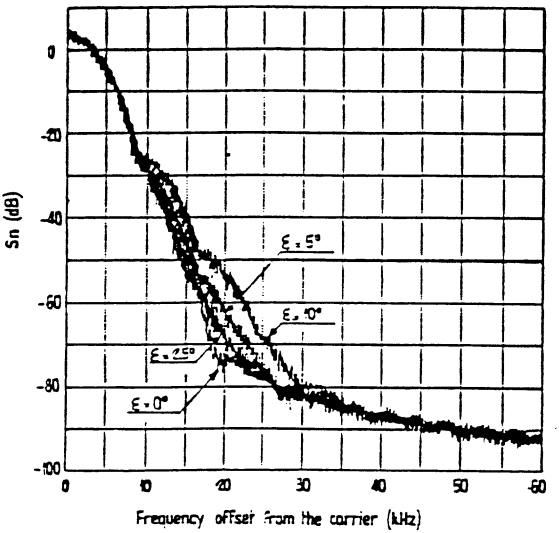

Fig 2.2.5a - Effect of a quadrature error between the components of the carrier.

Variable Parameter = quadrature error on degrees.
Modulation = GTFM; ϕ 47.3°, P = 0, and bit-rate = 16 kbit/s.
Sn = Signal spectral density relative to energy per bit.

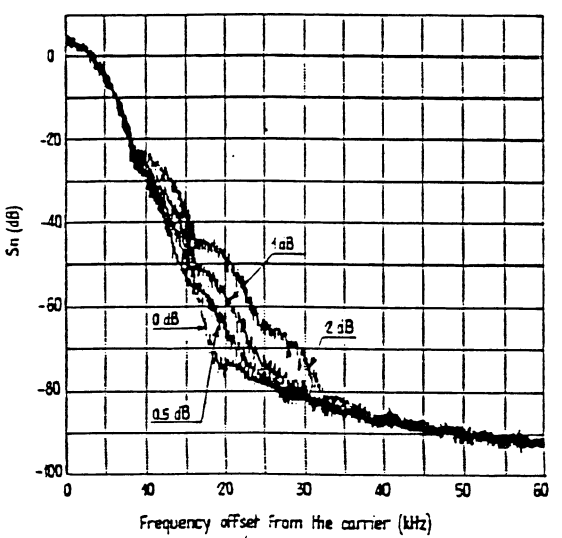

Fig 2.2.5b - Effect on an amplitude imbalance between the quadrature components.

Parameter = amplitude imbalance in decibels.
Modulation = GTFM, ϕ = 47.3°, P = 0 and bit-rate = 16 kbit/s.
Sn = Signal spectral density relative to energy per bit.

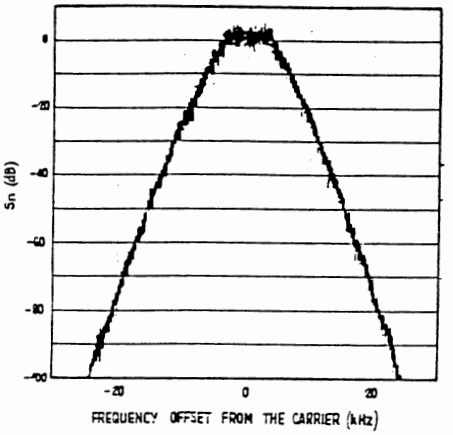

Fig 2.2.6 - Power spectrum of a 4-level PAM/FM signal.

Modulation = 4-level PAM/FM,
Bit rate = 16 kbit/s and M_f = 0.25

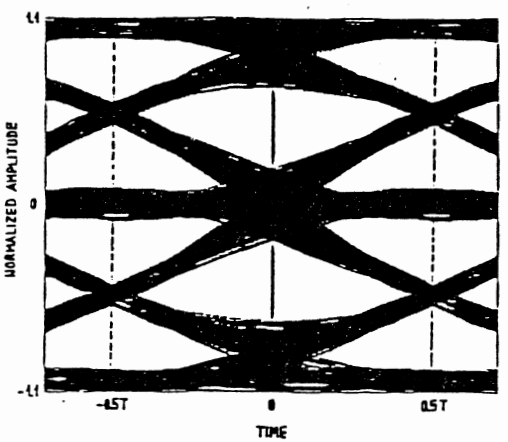

Fig 2.3.1 - Typical eye diagram of a GMSK or GTFM signal at the input of the decision circuit.
The vertical scale is normalised with respect to the amplitude coming out when at the discriminator input a continuous carrier wave arrives at a frequency greater than the nominal carrier frequency by 0.25 of the bit rate.

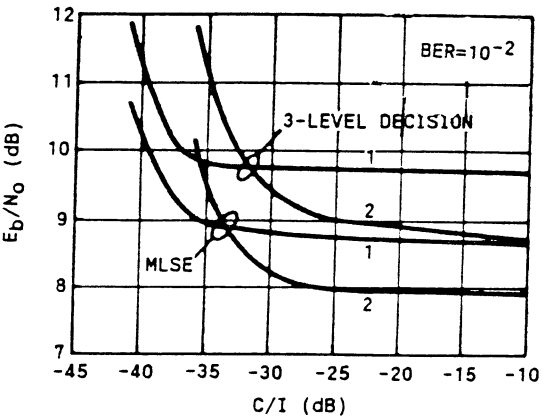

Fig 2.4.1 - Sensitivity to an adjacent channel interference; GMSK modulation and discriminator, AWGN channel.

1) BT = 0.25
2) BT = 0.315

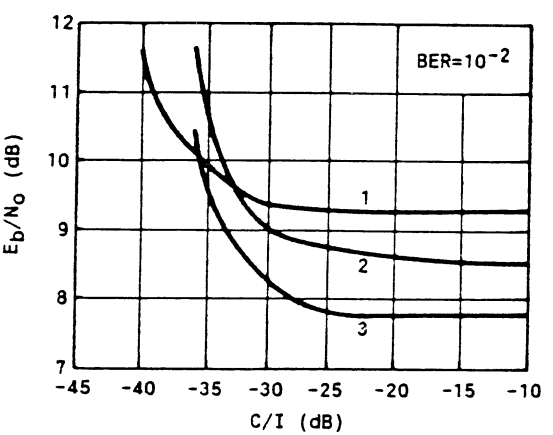

Fig 2.4.2 - Sensitivity to an adjacent channel interference; GTFM modulation and discriminator, AWGN channel.

1) $\phi = 55$ $\rho = 0.42$
2) $\phi = 60^{o}$ $\rho = 0.42$
3) As curve 2), but with MLSE decision.

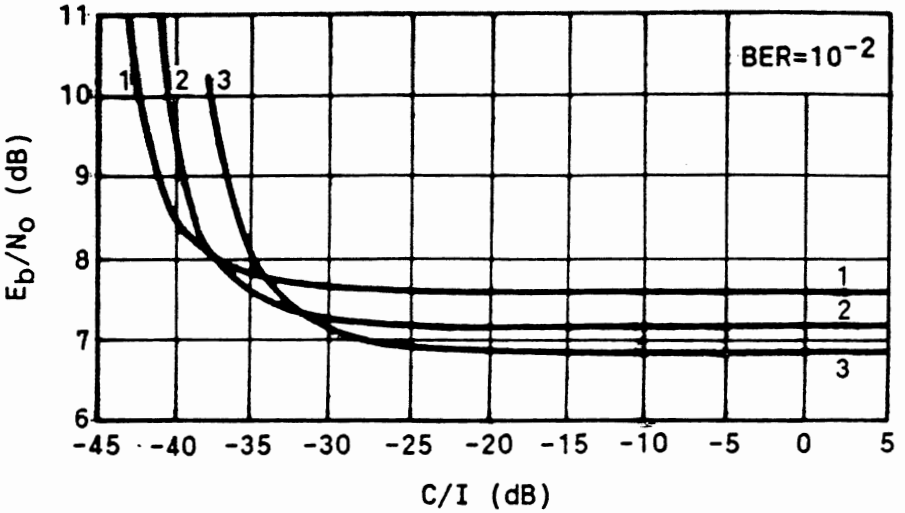

Fig 2.4.3 - Sensitivity to an adjacent channel interference; PAM/FM modulation and discriminator, AWGN channel.

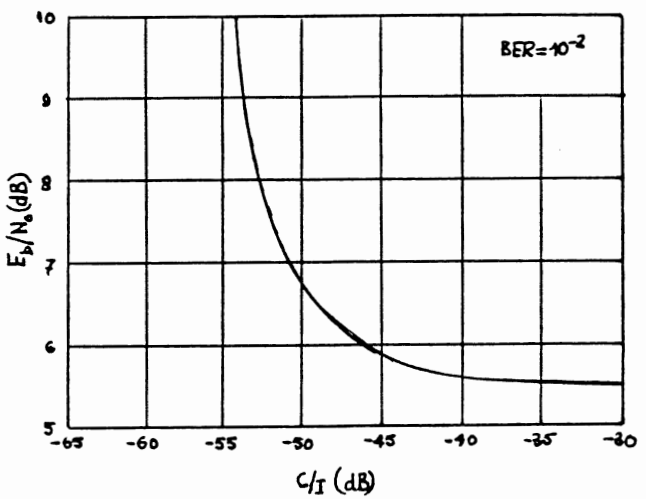

Fig 2.4.4 - Sensitivity to an adjacent channel interference; GTFM modulation and coherent detection, AWGN channel.

$\phi = 60^{o}$, $\rho = 0.42$

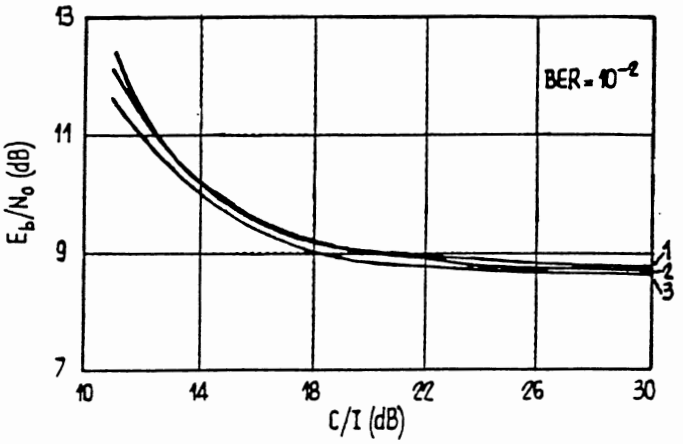

Fig 2.4.5 - Sensitivity to cochannel interference; discriminator detection and AWGN channel

Modulation 1) GTFM, $\emptyset = 60^{o}$, $\rho = 0.42$
2) GMSK, BT = 0.315
3) GMSK, BT = 0.25

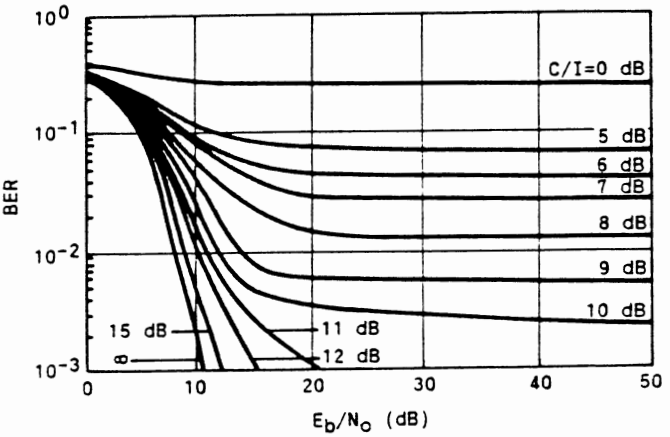

Fig 2.4.6 - BER performance in an AWGN channel with co-channel interference of gaussian pdf and discriminator detection

GTFM ($\emptyset = 60^{o}$, $\rho = 0.42$) and GMSK (BT = 0.315)

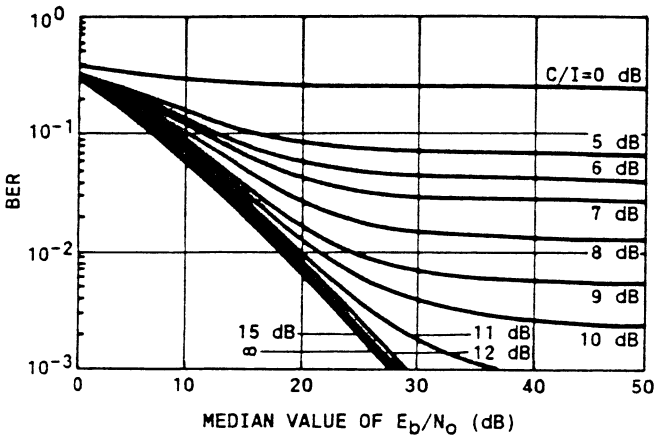

Fig 2.4.7 - As Fig 2.4.6 , but with multipath propagation (urban environment and a slowly moving terminal (v ≃ 0km/h). Parameter C/I is the ratio of the short-term median power of the useful signal to the short-term power of interference.

The BER curves are obtained by averaging the BER curves of the above figure over the Rayleigh statistics of the amplitude of the useful signal.

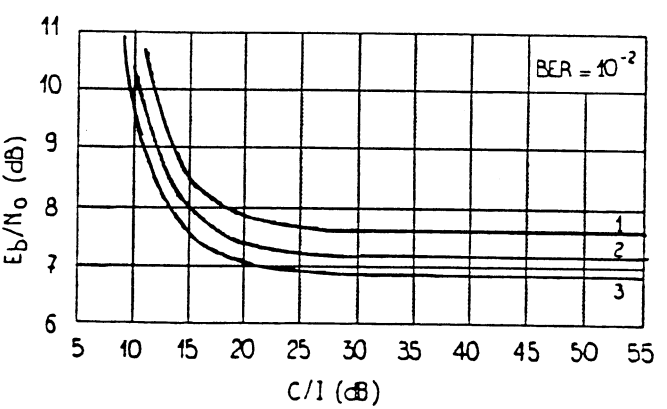

Fig 2.4.8 - Sensitivity to cochannel interference; Discriminator Detection and AWGN Channel.

Modulation PAM/FM 1) mf = 0.22
2) mf = 0.25
3) mf = 0.28

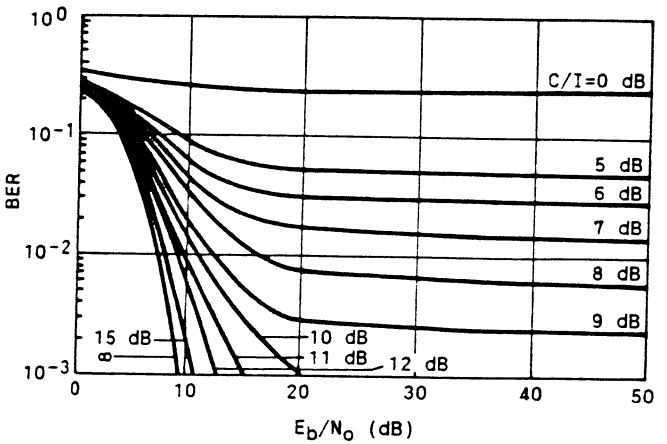

Fig 2.4.9 - BER performance in a AWGN channel with co-channel interference with gaussian pdf and discriminator detection.

PAM/FM with $M_f = 0.25$

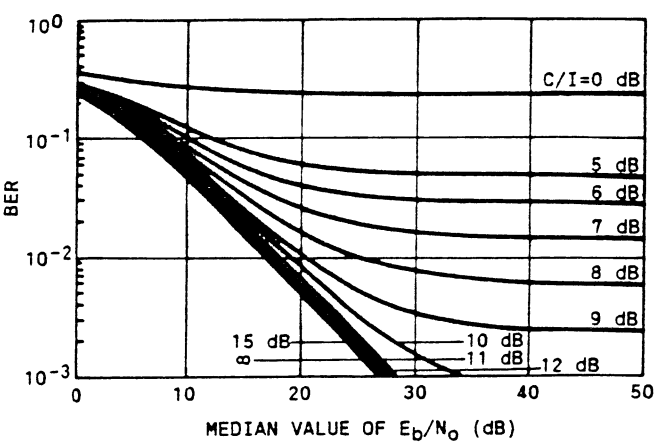

Fig 2.4.10 - As Fig 2.4.9 but with multipath propagation (urban environment), and a slowly moving terminal ($v \simeq 0$ km/h). Parameter C/I is the ratio of the short-term median power of the useful signal to the short-term median power of interference.

The BER curves are obtained by averaging the BER curves of over the Rayleigh statistics of the amplitude of the useful signal.

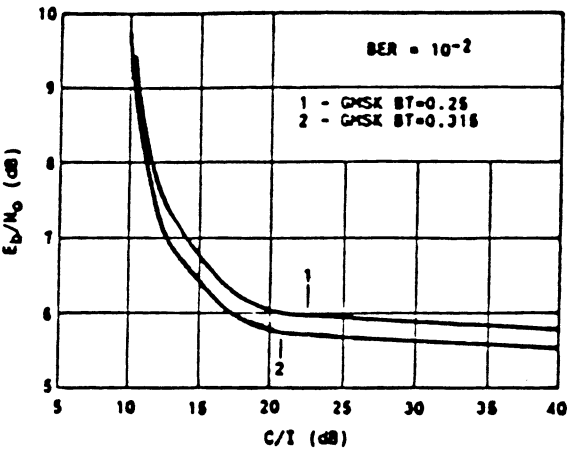

Fig 2.4.11 - Sensitivity to co-channel interference; coherent detection and AWGN channel.

1) GMSK, BT = 0.25
2) GMSK, BT = 0.315

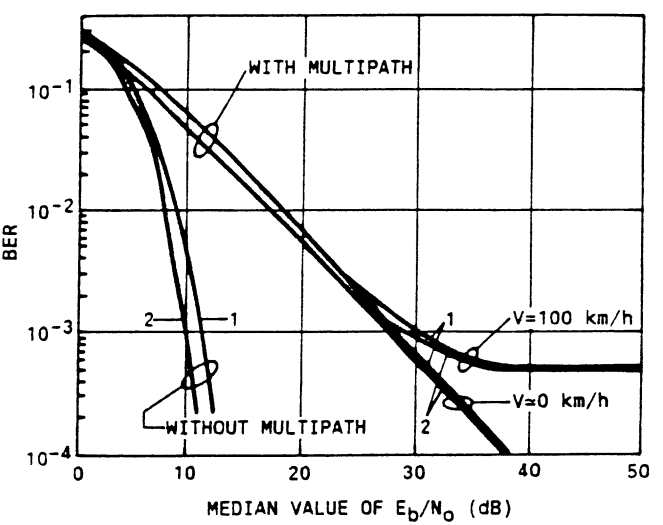

Fig 2.4.12 - Urban environment; GMSK, BT = 0.315 and discriminator detection

1 = bit-by-bit decision
2 = MLSE

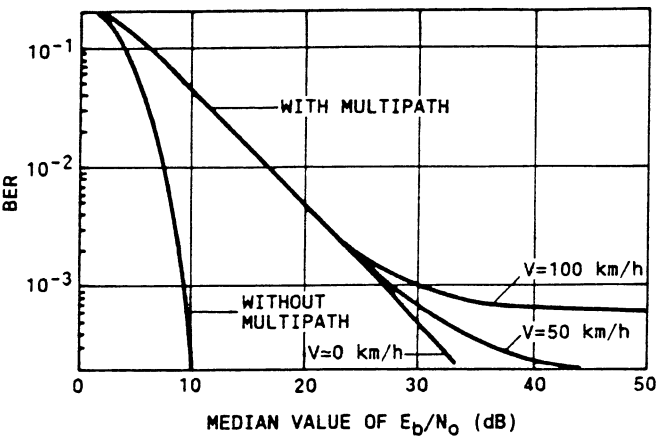

Fig 2.4.13 - Urban Environment; PAM/FM, m_f = 0.25 and discriminator detection

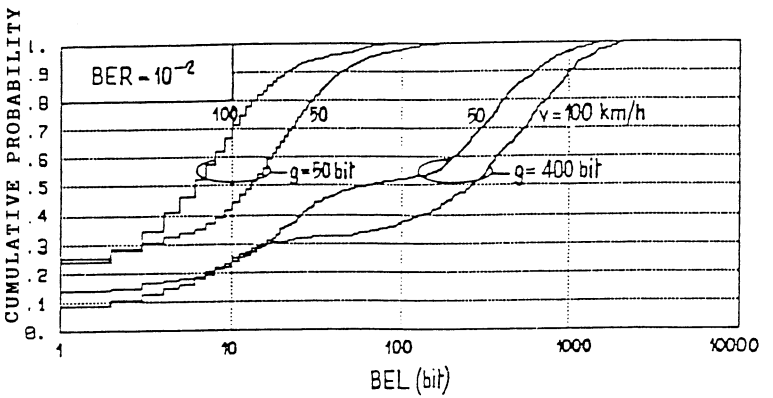

a) Cumulative distribution of BEL (Burst Error Length), computed for bit-by-bit decision

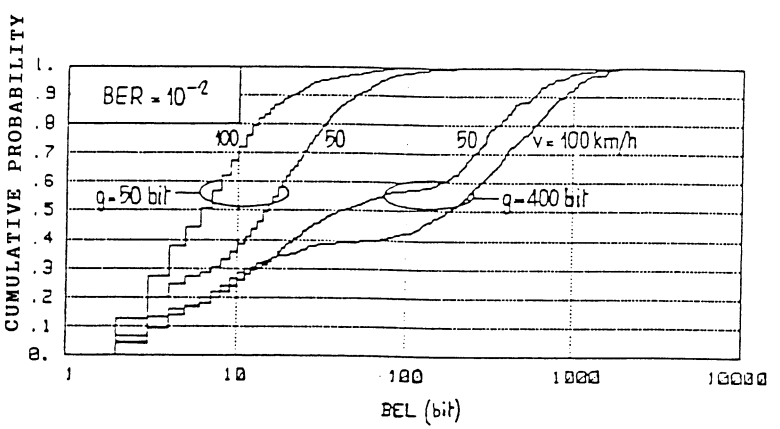

b) As above, but for MLSE decision

Fig 2.4.14 - Transmission-Error Statistics (Burst-Error Length)

Modulation : GTFM $\emptyset = 60^{o}, \rho = 0.42$
Discriminator detection

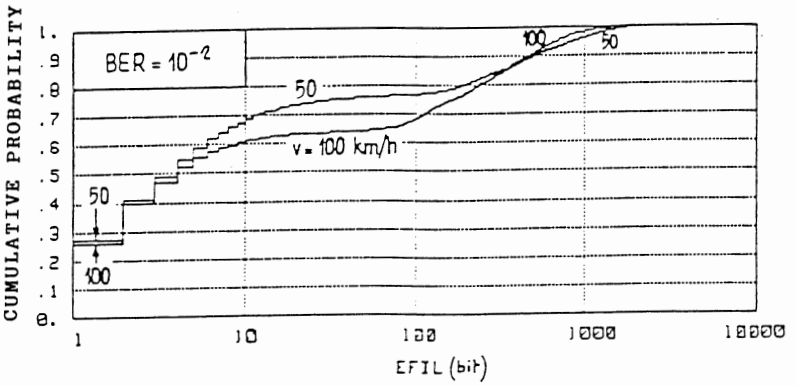

a) Cumulative distribution of EFIL (Error Free Interval Length), for bit-by-bit decision

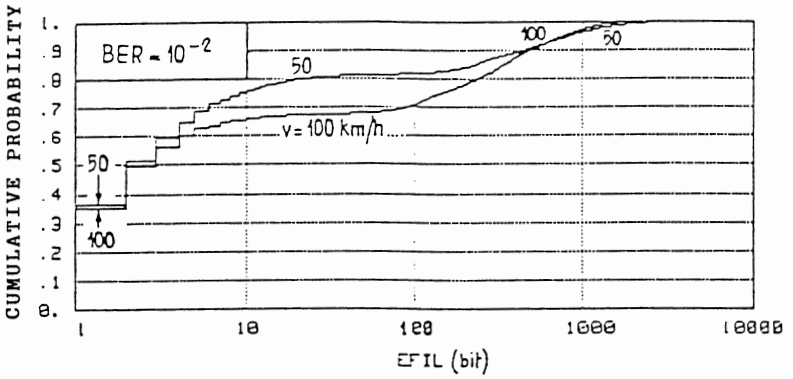

b) As above, but for MLSE decision

Fig 2.4.15 - Transmission-Error Statistics (Error-free Interval)

Modulation : GTFM $\emptyset = 60^{o}, \rho = 0.42$
Discriminator detection

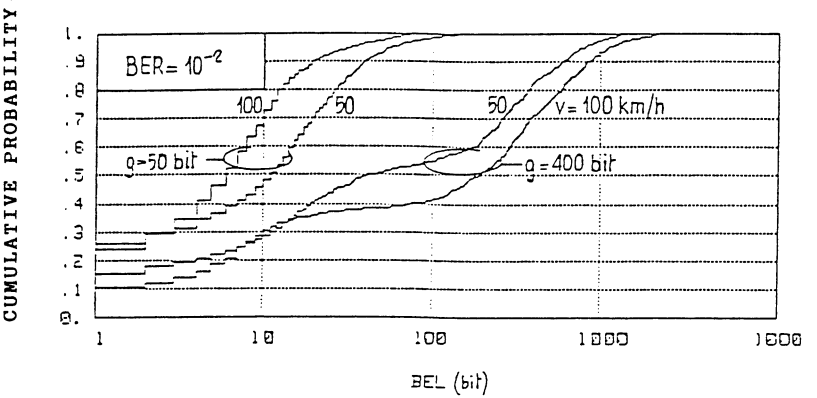

a) Cumulative distribution of BEL (Burst Error Length).

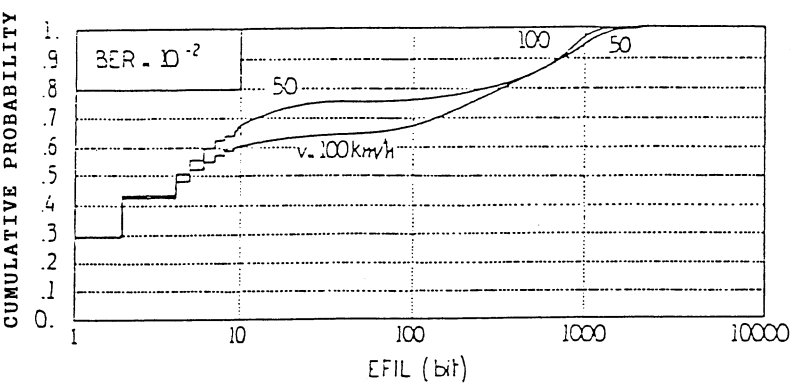

b) Cumulative distribution of EFIL (Error Free Interval Length).

Fig 2.4.16 - Transmission-Error Statistics

Modulation : PAM/FM, M_f = 0.25
Discriminator detection

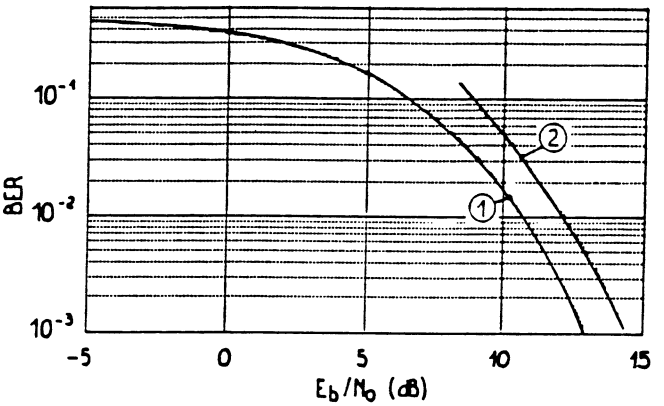

a) bit-by-bit decision

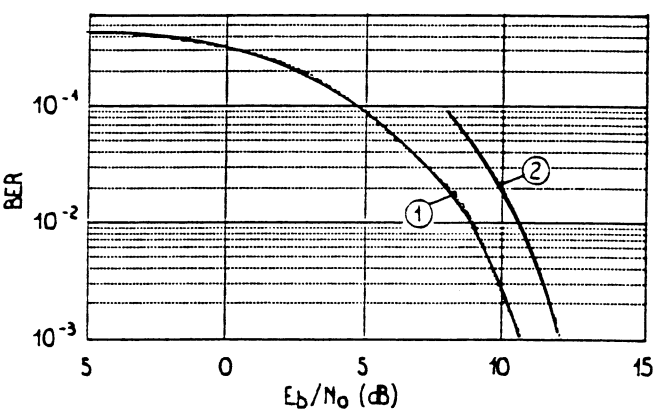

b) MLSE

Fig 2.4.17 - Simulated (1) and experimental modem (2) performance;
AWGN channel and discriminator detection.
Modulation: GTFM $\emptyset = 55.8^{\circ}$; $\rho = 0.36$

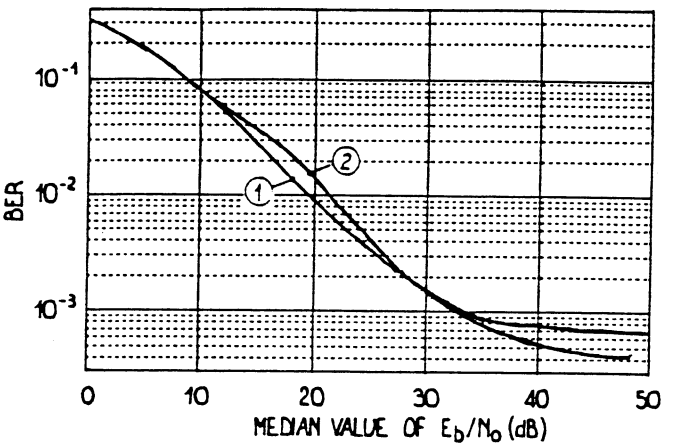

a) bit-by-bit decision

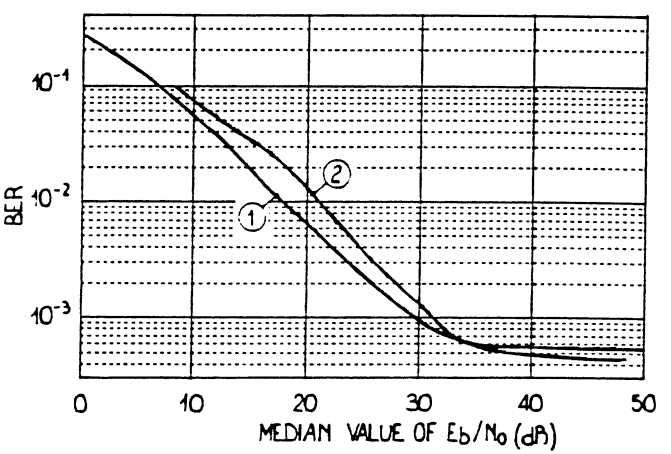

b) MLSE

Fig 2.4.18 - Simulated (1) and experimental modem (2) performance
urban environment
Modulation; GTFM, $\emptyset = 55.8^{o}$, $\rho = 0.36$
Discriminator detection

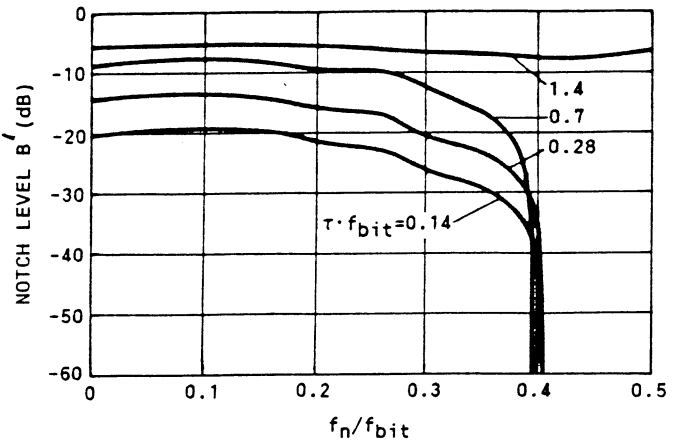

Fig 2.5.1 - Signature curves of 4-level PAM/FM channel
$M_f = 0.25$

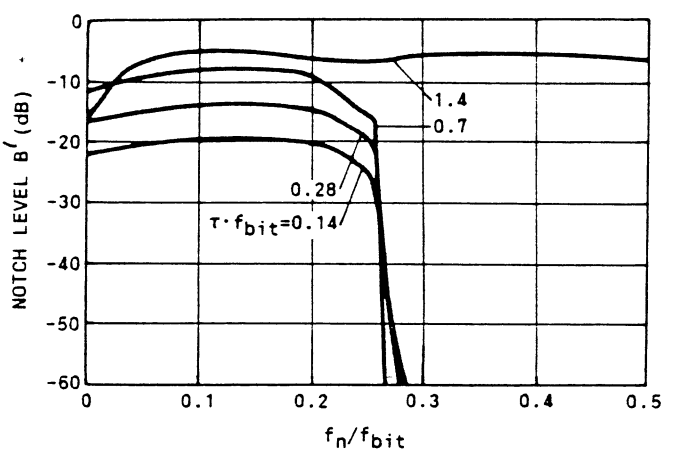

Fig 2.5.2 - Signature curves of GTFM channel ($\phi = 60^{\circ}$, $\rho = 0.42$) and GMSK (BT = 0.315)

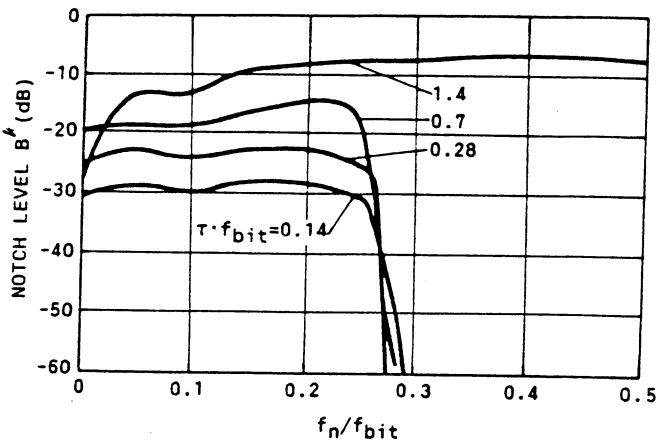

Fig 2.5.3 - As Fig 2.5.2, but with MLSE decision

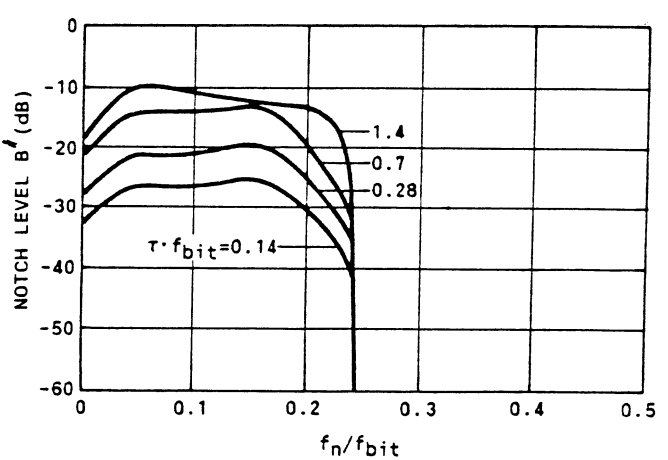

Fig 2.5.4 - Signature curves of GMSK channel (BT = 0.315) with coherent demodulation and bit-by-bit decision.

3. ADAPTIVE EQUALISERS

3.1. INTRODUCTION

It is well known that if the bit rate in a communications system is increased beyond the channel capacity, the resulting dispersion can cause signal distortion and severe intersymbol interference. Thus in typical urban conditions, the channel impulse response may have an effective width of several μs, whereas in a typical hilly terrain environment this can be up to 20μs or more, and therefore operation without an equaliser would restrict a mobile system to low data rates, and would make narrowband TDMA techniques unfeasible.

Another important feature of the mobile radio environment at about 900 MHz carrier frequency is the fact that channel characteristics may change very fast, either due to transmitter/receiver movements, or to the surrounding environment. Therefore, it is important for the receiver to track these channel variations to minimise the resulting impairments.

In the work reported here, two basic types of equalisers were considered: Decision Feedback Equalisers (DFE's) and Equalisers based on Maximum Likelihood Sequence Estimation (MLSE) using the Viterbi Algorithm (VA). The main difference between the two is that the DFE attempts to continuously track the channel distortion, whereas the MLSE in its usual form must re-estimate the channel response at a fast enough rate such that any variations in between are minimal and do not affect the receiver performance. Since in the GSM system frame structure a synchronisation sequence is transmitted at each TDMA slot, the two equalisers differ essentially in their behaviour within the TDMA slot. Having fixed the length of the slot, there will clearly be a limit to the rate of channel variation that the MLSE equaliser can withstand. Equally, a

DFE should be able to work with acceptable performance at a faster rate (or vehicle speed). This issue constitutes one of the main topics of this report.

Initially, a tutorial section on both types of equalisers is included, with a view to clarifying the design techniques employed. Then a descriptive list of all channel models used for equaliser testing is presented. This includes static and Rayleigh fading multipath channels. Section 3.4 presents relevant material on the GSM system specifications, and associated synchronisation and channel estimation techniques. Performance results obtained using computer simulation are presented and discussed for the DFE and the MLSE-based equaliser respectively in sections 3.5 and 3.6. Finally, section 3.7 lists some conclusions taken from the results obtained, and suggests some topics for future work.

3.2. THEORETICAL BACKGROUND

3.2.1. Adaptive linear transversal and decision feedback equalisers

In this section the baseband equalisers of the linear transversal type and of the nonlinear decision-feedback type are considered. In general, the decision-feedback equaliser (DFE), whose block diagram is shown in Fig.3.2.1, is an efficient way to combat intersymbol interference and has better error rate performance than the linear transversal equaliser (LTE), especially for those channels that have nulls in their spectrum.

Notice that the LTE is a special case of the DFE, with only the feedforward transversal filter (see Fig.3.2.1).

On the other hand, DFEs become much more complex than LTEs when the number of coefficients increases (the total number of coefficients should not be greater than 7-8); moreover, long DFEs may exhibit error propagation.

The most difficult problem encountered in equalisation of the mobile radio channel is the tracking of the time-varying channel characteristics. To solve this problem a number of adaptation algorithms are conceivable for the considered application, depending on the cost function. The final choice should be based on three main items, i.e. very fast initial converging properties (during the "training phase"), good tracking of the time-varying channel characteristics (during the "information" or "tracking phase"), and low computational complexity. With reference to the latter, we initially considered two main classes of methods, i.e., the Stochastic Gradient (SG) algorithms and the Recursive Least Squares (RLS) algorithms. In the first class we considered the Gradient Steepest-Descent (GSD) and the Gradient Lattice (GL) algorithms, and in the second class the Kalman, Fast-Kalman (FK), Square-Root Kalman (SRK), and the Least Squares Lattice (LSL) algorithms.

By computational complexity we mean the number of operations to perform in a symbol period. With the currently available devices, additions and multiplications need about the same computation time, while divisions cannot be performed with only one instruction, but need a dedicated macro-instruction. This implies that the number of divisions M_D is a fundamental feature, even if the number M_M of additions and multiplications is lower. Moreover, we are interested in computational complexities that allow real-time implementations, using DSP's or dedicated circuitry.

With reference to a DFE structure with L=M+N tap coefficients (M and N being the number of feedforward and feedback taps, respectively), Fig.3.2.2 compares the previously mentioned adaptation algorithms.

It turns out that the less complex algorithm is the gradient steepest-descent, but it it well known that its speed of convergence is too low (i.e., > 400 - 500 symbol periods) for our application. Apart form the GSD algorithm, for 4<L<7 (i.e., the range of interest), the best method from the M_M

standpoint is the SRK, but it requires L divisions. Similar considerations can be done for GL and the LSL algorithms. For large values of L the Kalman algorithm is the most complex, but it becomes feasible for low L. The Fast-Kalman algorithm is the least complex for large values of L and has a complexity similar to that of the Kalman algorithm for $4<L<7$.

In conclusion, from the complexity point of view the Fast-Kalman algorithm turns out to be a good solution if the performance required can only be achieved with a minimum of 5 taps.

The decision feedback equaliser of Fig.3.2.1. consists of two branches (because of the quadrature-type modulation), each with a feedforward and a feedback section. In this work we have assumed a tap spacing equal to 2T, but it is worth noting that a tap spacing smaller than 2T ("fractional tap spacing") can lead to better performance of the equaliser in the presence of carrier phase estimation errors.

A description of the basic principles and equations of the complex equaliser with the Fast-Kalman algorithm (called Complex Fast Kalman Algorithm, CFKA) can be found in [1,2]. Basically, having defined the mean square error $\epsilon = E\,[D(n)-I(n)]^2$, where D(n) is the ideal output at time n and I(n) is the equaliser complex output at time n, the CFKA algorithm minimises an exponentially weighted squared error, i.e.,

$$\epsilon = \sum_{h=1}^{n} \lambda^{n-h}\,[D(n) - \underline{Y}_L^*(n)\cdot\underline{C}_L(n)]^2 \qquad (3.2.1.)$$

where λ is a positive integer close to, but less than 1, $\underline{Y}_L(n)$ is the L-dimensional equaliser input complex sequence and $\underline{C}_L(n)$ is the L-dimensional vector of equaliser complex coefficients. The complement $1-\lambda$ is the memory of the algorithm. The sequence of sets of coefficients $\{\underline{C}_L(n)\}$ is generated recursively as

$$\underline{C}_L(n) = \underline{C}_L(n-1) + \underline{K}_L(n).e^*(n) \qquad (3.2.2)$$

where $\underline{K}_L(n)$ is the L-dimensional Kalman gain vector. Notice that the rapid convergence of the Kalman algorithm is due to the control applied to each tap coefficient through a corresponding element of $\underline{K}_L(n)$. In contrast, the gradient algorithm, expressed by

$$\underline{C}_L(n) = \underline{C}_L(n - 1) + \Delta \cdot \underline{Y}_L(n) \cdot e^*(n) \qquad (3.2.3)$$

has only one variable parameter, i.e., the step size Δ.

Figs.3.2.3 and 3.2.4. show the time-behaviour of the coefficients of the 5-coefficient LTE with the CFKA. From these plots we can see that the LTE with the CFKA has a rapid convergence rate, i.e., within 26 bits, and a very good steady state behaviour (this remains true until the observed sequence is about 2,000 bit long, then a reinitialisation can be easily accomplished in a TDMA system in each basic time slot).

3.2.1.1. The CFKA Algorithm

The procedure of the CFKA to time update the set of coefficients $\underline{C}_L(n)$ can be organised in the following steps, having previously introduced the following quantities :

- The overall equaliser input sequence at time n:

$$\underline{Y}_2^*(n) = [\underline{y}^*(n) \,|\, \underline{D}^*(n)]$$

$$= [y^I(n) - jy^Q(n) \,|\, D^I(n) - jD^Q(n)] \qquad (3.2.4)$$

$$(\text{or } \underline{Y}_2^*(n) = [\underline{y}^*(n) \,|\, \underline{I}^*(n)] = [y^I(n) - jy^Q(n) \,|\, I^I(n) - jI^Q(n)])$$

where $\underline{y}$ is the input to the feedforward filter.

- the overall equaliser output sequence at time n :

$$\underline{Y}_2^*(n-L) = [\underline{Y}^*(n-M)\,|\,\underline{D}^*(n-N)] \qquad (3.2.5.)$$

$$(\text{or } \underline{Y}_2^*(n-L) = [\underline{Y}^*(n-M)\,|\,\underline{I}^*(n-N)])$$

- the forward and backward predictors $\underline{F}_L(n)$ and $\underline{B}_L(n)$ that form the least squares predictions of $\underline{Y}_2(n)$ and of $\underline{Y}_2(n-L)$;

- the forward prediction error:

$$\underline{f}(h|K) = \underline{Y}_2(h) - \underline{Y}_L(h)\cdot\underline{F}_L(k);$$

- the backward prediction error:

$$\underline{b}(h|K) = \underline{Y}_2(h-L) - \underline{Y}_L(h+1)\cdot\underline{B}_L(k);$$

- the forward prediction residual power $r^f(n)$;

- the Kalman complex gain vector $\underline{K}_L(n)$;

- the channel matrix

$$\underline{P}_{LL}(n) = \left[\sum_{h=1}^{n} \lambda^{n-h}\ \underline{Y}_L^*(h)\cdot\underline{Y}_L(h) + \delta\ \lambda^n\ \underline{A}_{LL}\right]^{-1},$$

where δ is a small positive constant to ensure nonsingularity and which turns out to be an estimate of the final mean square error.

The forward and backward predictors $\underline{F}_L(n)$ and $\underline{B}_L(n)$ seek to minimise the square forward and backward errors ϵ_f and ϵ_b, respectively, i.e.,

$$\epsilon_f = \sum_{h=1}^{n} \underline{f}(h|n)\ \underline{f}^*(h|n), \qquad (3.2.6)$$

$$\epsilon_b = \sum_{h=1}^{n} \underline{b}(h|n)\ \underline{b}^*(h|n) \tag{3.2.7}$$

Step 1: for n = 0, initialise $\underline{P}_{LL}(0) = \delta^{-1}\ \underline{A}_{LL}$,

$$r^f(0) = \lambda,\ \underline{C}_L(0) = \underline{0},\ \underline{Y}_L(0) = \underline{0},\ \underline{K}_L(0) = \underline{0},\ \underline{F}_L(0) = \underline{0},\ \underline{B}_L(0) = \underline{0}$$

Step 2: for $n \geq 1$, $\underline{K}_L(1) = \underline{0}$,

$$\underline{f}(n|n-1) = \underline{Y}_2(n) - \underline{Y}_L(n)\cdot\underline{F}_L(n-1) \tag{3.2.8}$$

$$\underline{F}_L(n) = \underline{F}_L(n-1) + \underline{K}_L(n)\cdot\underline{f}(n|n-1) \tag{3.2.9}$$

$$\underline{f}(n|n) = \underline{Y}_2(n) - \underline{Y}_L(n)\cdot\underline{F}_L(n) \tag{3.2.10}$$

Step 3: for $n \geq 1$,

$$r^f(n) = r^f(n-1) + \underline{f}^*(n|n)\cdot\underline{f}(n|n-1) \tag{3.2.11}$$

Step 4: for $n \geq 1$,

$$\begin{bmatrix} \underline{g}_L(n) \\ \\ g(n) \end{bmatrix} = \begin{bmatrix} \underline{f}^*(n|n)/r^f(n) \\ \\ \underline{K}_L(n) - [\underline{F}_L(n)\cdot\underline{f}^*(n|n)/r^f(n)] \end{bmatrix} \tag{3.2.12}$$

Step 5: for $n \geq 1$,

$$\underline{b}(n|n-1) = \underline{Y}_L(n-L) - \underline{Y}_L(n+1)\cdot\underline{B}(n-1) \tag{3.2.13}$$

$$\underline{K}_L(n+1) = [\underline{g}_L(n) - \underline{g}(n)\cdot\underline{B}_L(n-1)]/[1 - \underline{g}(n)\cdot\underline{b}(n|n-1)] \tag{3.2.14}$$

$$\underline{B}_L(n) = \underline{B}_L(n-1) + \underline{K}_L(n-1)\cdot\underline{b}(n|n-1) \tag{3.2.15}$$

Finally, the sequence of sets of coefficients $\{\underline{C}_L(n)\}$ is generated recursively as

$$\underline{C}_L(n) = \underline{C}_L(n-1) + \underline{K}_L(n) \cdot e^*(n) \qquad (3.2.16)$$

3.2.2.

Equalisers based on Maximum Likelihood Sequence Estimation (MLSE)

The algorithms to be described in this section do not, in the strict sense, attempt to equalise the received waveform. Rather, they use the knowledge of the channel characteristics and of the received signal in order to find the most likely transmitted data sequence. The performance of such equalisers is therefore dependent on the available estimate of the channel impulse response as well as on the sample timing. However, these topics are left to later sections, and in what follows the channel is assumed to be static and well defined.

One specific algorithm [3] will first be derived and discussed in some depth, illustrating the MLSE technique as applied to equalisation. Other algorithms mentioned later are implemented using broadly similar approaches, and less detail will therefore be provided.

3.2.2.1. GMSK as an offset QAM modulation

All MLSE techniques to be discussed treat the GMSK signal as an offset QAM signal, so that conventional QAM approaches to equalisation can be employed [3,4,5]. Thus the modulation is assumed to be linear, that is, the modulated signal is modelled as resulting from a simple frequency translation or mixing of two suitably filtered baseband data streams with in-phase and quadrature carriers respectively. The transmitted signal can therefore be represented as:

$$f(t) = \mathrm{Re}\left[x(t)\ e^{j\omega_c t} \right] \qquad (3.2.17)$$

where ω_c is the carrier frequency and x(t) is:

$$x(t) = \sum_{k=0}^{N} a_k \, g(t-2kT) + j \sum_{k=0}^{N} b_k \, g(t-2kT-T) \quad (3.2.18)$$

where g(t) is the impulse response associated with the data shaping network, and a_k and b_k represent respectively the in-phase (I) channel data and the quadrature (Q) channel data, with possible values of ±1. The overall bit rate is 1/T and each channel transmits at half this rate.

For GMSK, exact formulation of the modulated signal according to eqn.(3.2.18) is not possible, due to the essentially non-linear nature of the modulation process. However, as shown by Laurent [6], a very close approximation can be achieved using a real function g(t) whose shape depends on the GMSK BT product. For the standard BT value of 0.3, it has been shown that the approximating function g(t) has a wide mainlobe yielding some intersymbol interference (ISI), as expected from the known received GMSK eye patterns [7]. The basic function of the maximum likelihood sequence estimator is then to remove the ISI caused by the combined effect of such pulse shaping, the channel characteristics and any receiver filtering. It therefore follows that the best performance obtainable is that of ideal matched filter reception of OQPSK in an all-pass additive white gaussian noise channel (AWGN), since the MLSE merely attempts to combat the channel dispersion.

3.2.2.2. Channel effects

The signal at the receiver will in general have passed through a frequency selective channel with a complex impulse response $g_c(t)$, and in addition it will probably be passed through a receiver filter with an impulse response $g_r(t)$ in order to reduce adjacent channel interference and noise. The received signal is then:

$$f(t) = \mathrm{Re}\left[s(t) \, e^{j\omega_c t} \right] \quad (3.2.19)$$

with s(t) given by

$$s(t) = \sum_{k=0}^{N} a_k \, h(t-2kT) + n_1(t)$$
$$+ j \sum_{k=0}^{N} b_k \, h(t-2kT-T) + j \, n_2(t) \qquad (3.2.20)$$

where $n_1(t)$ and $n_2(t)$ are both independent white Gaussian noise processes with two-sided spectral density $\eta_o/2$ and

$$h(t) = g(t) \otimes g_c(t) \otimes g_r(t) \qquad (3.2.21)$$

where $\otimes$ denotes convolution. The impulse response h(t) therefore accounts for the overall selectivity of channel and receiver as well as the pulse shaping associated with the modulation itself. This impulse response is generally complex and may therefore be assumed to account also for constant phase offsets between the received signal carrier and the receiver local oscillator.

3.2.2.3. <u>The Likelihood Function</u>

A metric is required in order to discriminate between the 2^{2N+2} possible transmitted sequences. This metric is based on the assumption that the function h(t) is known and hence the received signal in the absence of noise may be reconstructed for each possible sequence. Let the reconstructed complex baseband signal for the mth sequence be denoted $s_m(t)$. Then,

$$s_m(t) = \sum_{k=0}^{2N+1} \alpha_k^m \, h(t-kT) \qquad (3.2.22)$$

where for compactness the parameters α_k are alternately real and imaginary, i.e., $\alpha_0^m = a_0^m$, $\alpha_1^m = jb_1^m$, etc. Since the noise is Gaussian, the most likely sequence is that which maximises the likelihood function [4]:

$$\mathcal{L}_m = \exp\left[-\frac{2}{\eta_o} \int_{-\infty}^{+\infty} |s(t) - s_m(t)|^2 \, dt \right] \qquad (3.2.23)$$

This is equivalent to maximising the function

$$\Lambda_m = 2 \, \mathrm{Re}\left[\int_{-\infty}^{+\infty} s(t) \, s_m^*(t) \, dt \right] - \int_{-\infty}^{+\infty} |s_m(t)|^2 \, dt \qquad (3.2.24)$$

It can be shown following [3,4,5] that, after substituting for $s(t)$ and $s_m(t)$, this function may be re-expressed as:

$$\Lambda_m = 2 \, \mathrm{Re}\left[\sum_{k=0}^{2N+1} (\alpha_k^m)^* \, y_k \right] - \sum_{k=0}^{2N+1} \sum_{i=0}^{2N+1} (\alpha_k^m)^* \, \alpha_i^m \, x_{k-i} \qquad (3.2.25)$$

where y_k is a sample taken at time kT at the output of a filter matched to the overall impulse response $h(t)$ when its input is the received signal $s(t)$, and x_k is a sample of the same filter when its input is $h(t)$.

Computation of the likelihood function then requires passing $s(t)$ through a matched filter with impulse response $h^*(-t)$ followed by processing of the sampled outputs of the matched filter according to equation (3.2.25). It is apparent that the brute force approach of computing the value of the function for each of the 2^{2N+2} data sequences would be computationally very inefficient. Instead, the Viterbi algorithm is employed to reduce the computational load by discarding 'unlikely' sequences as described in the next section.

3.2.2.4. The Viterbi Algorithm and MLSE Detection

To reduce the complexity of the calculation of eqn.(3.2.25), we note first that it can be computed recursively. Thus, if Λ_{mn} is used to refer to the partial computation of the metric up to k=n for the mth sequence (where $n < 2N+1$), then

$$\Lambda_{mn} = 2 \text{ Re} \left[\sum_{k=0}^{n} (\alpha_k^m)^* \, y_k \right] - \sum_{k=0}^{n} \sum_{i=0}^{n} (\alpha_k^m)^* \, \alpha_i^m \, x_{k-i} \qquad (3.2.26)$$

It may easily be shown that Λ_{mn} may be computed recursively from the previous partial sum for the same sequence, $\Lambda_{m(n-1)}$ as follows:

$$\begin{aligned} \Lambda_{mn} = \Lambda_{m(n-1)} &+ 2 \text{ Re} \left[(\alpha_n^m)^* \, y_n \right] \\ &- 2 \text{ Re} \left[(\alpha_n^m)^* \sum_{k=0}^{n-1} \alpha_k^m \, x_{n-k} \right] \\ &- |\alpha_n^m|^2 \, x_0 \qquad (3.2.27) \end{aligned}$$

To derive the algorithm, it should now be noted that the complexity of the incremental metric depends critically on the summation in the second term, and thus on the coefficients x_k. These coefficients are samples of the autocorrelation function of the function h(t) taken at times kT. Now since any practical response h(t) will be time-limited to LT sec, then the coefficients x_k will be zero for $|k|>L$. Applying this to the above equation shows that the incremental metric depends only on $\alpha_n^m, \alpha_{n-1}^m, \ldots, \alpha_{n-L}^m$, that is, on the last L+1 bits of the sequence concerned. It is this fact that allows the application of the Viterbi algorithm to equaliser systems.

If we consider all sequences with identical data α_n, $\alpha_{n-1}, \ldots, \alpha_{n-L}$ but with different prefixes $\alpha_0, \alpha_1, \ldots, \alpha_{n-L-1}$, then from a knowledge of the matched filter output samples up to y_n we can identify the most likely sequence by computing the metrics up to k=n. Now if we consider all possible extensions of all these sequences with a postfix $\alpha_{n+1} = \pm 1$, then it is apparent that the most likely sequence up to k=n+1 must be an extension of the most likely sequence up to k=n, since the incremental metric does not depend on the prefix. This is of

course true for longer postfixes, so that in fact all but the most likely sequence of this set at k=n can be discarded. This sequence is known in the VA literature as a survivor. Each survivor is associated with a state which is characterised by the set of L values $\alpha_n, \ldots, \alpha_{n-L+1}$, since these are the only values required for computation of the next incremental metric for extensions of this sequence. Note that the total number of states (and therefore survivors) will be 2^L.

To summarise, at each instant kT all sequences going into the same state have their metrics compared and a survivor is chosen. The process is repeated for each of the 2^L states. Thus for binary signalling ($\alpha_k = \pm 1$), each survivor gives rise to two extended sequences, but these are then pruned back to their original number by metric comparison of the two incoming sequences to each state.

Finally some simplifications to the metric computation may still be made for GMSK. Referring to eqn.(3.2.27), it may be seen that, since $\alpha_k = \pm 1$ or $\pm j$, the last term will always yield the same value for a given channel characteristic and can be discarded, as can the factor of 2 for the other two terms. In addition, it may be seen that computation of the first term is equivalent to recalling either the real or the imaginary part of y_n, but not both. Hence, the matched filter implementation may be somewhat simplified. Finally, the second term can only have 2^{L+2} possible values, and hence these can be stored in a table prior to VA operation, to be recalled when required. The simplified metric computation is now:

$$\Lambda_{mn} = \Lambda_{m(n-1)} + \mathrm{Re}\left[(\alpha_n^m)^* \quad (y_n - T_s) \right] \qquad (3.2.28)$$

where T_s is a complex number read from a look-up table corresponding to the state s for which a survivor is being searched. Thus the VA operation will require computation of the matched filter outputs plus two additions per metric computation (i.e., a total of four additions per state [8]).

The scheme described so far was first proposed by Ungerboeck [3] and represents an exact solution to the problem of maximum likelihood estimation of a data sequence modulated onto a carrier. In the next sections, some alternative techniques are briefly described.

3.2.2.5. Equalisation based on a Whitened Matched Filter

This approach was proposed by Forney [9], and follows the standard Viterbi algorithm [10], which will now be described briefly. For operation of the VA, it is usually assumed that a set of sufficient statistics z_k is available. Each z_k can be expressed as:

$$z_k = \sum_{l=0}^{L} h_l \, \alpha_{k-l} + n_k \tag{3.2.29}$$

where h_l represent known coefficients (e.g., samples of the channel impulse response), α_k represents the kth bit of the original data sequence, and the n_k 's are independent Gaussian white noise samples. All these quantities may be assumed to be real for simplicity. In this case, the log-likelihood function will be [10]:

$$\Lambda_m = \sum_{k=0}^{N} \left[z_k - \sum_{l=0}^{L} h_l \, \alpha_{k-l}^{m} \right]^2 \tag{3.2.30}$$

for the mth sequence to be tested. Note that the values of the likelihood function can simply be added because the noise samples are independent of each other.

It is apparent that the likelihood function can be calculated recursively, as follows:

$$\Lambda_{mn} = \Lambda_{m(n-1)} + \left[z_n - \sum_{l=0}^{L} h_l \alpha_{n-l}^{m} \right]^2 \tag{3.2.31}$$

As with eqn.(3.2.27), it may be noted here that the incremental metric is only dependent on α_n^m, and the previous L symbols up to α_{n-L}^m. Thus the development of the VA algorithm as described then is also valid here, the main difference being the use of a different expression for the metric calculation.

The Whitened Matched Filter (WMF) equaliser [9] uses the above metric computation, although some pre-processing is required before samples are passed to the VA. Thus, the signal is initially passed through a matched filter. This maximises the signal to noise ratio but does not cancel the intersymbol interference. In addition, the noise samples n_k at the output of the matched filter will in general be correlated, and thus the VA as described above cannot be directly applied. Thus the output of the matched filter must first be passed through a so-called noise whitening filter. The combination of the two filters is called a whitened matched filter, and the sampled outputs of this filter represent a set of sufficient statistics for data estimation, with independent Gaussian noise samples. They can therefore be passed to a standard VA which will use the metrics of eqns.(3.2.30) and (3.2.31), and will perform maximum likelihood estimation of the incoming sequence.

3.2.2.6. Comparison between the two equaliser structures

Both equalisers described perform MLSE of a digital sequence. However, the Whitened Matched Filter (WMF) equaliser uses the standard VA, and requires squaring operations for metric computation. The Matched Filter (MF) equaliser described initially uses a modified VA, where only additions are required, and which operates on the sampled outputs of the matched filter (thus requiring no noise whitening).

It appears that the MF equaliser would be simpler to implement in general, although a complete assessment should take into account the total processing required not only for

metric calculation but also for preparation of look-up tables and filter implementation, as well as the memory requirements of each algorithm.

It should also be noted that the theoretical development of both algorithms assumes that sampling takes place after the filters and just before operation of the VA algorithm. In addition, timing is assumed to be ideal. In practice all filters will be digital and so oversampling may be required, depending on the characteristics of the pulse shaping and the channel.

3.2.2.7. Variations of Equaliser Structure

Various VA based equalisers have been proposed which include simplifications or enhancements designed to achieve specific goals. Qureshi [11] has considered the feasibility of substituting the whitened matched filter by a filter designed to partially cancel the ISI, effectively narrowing the width of the impulse response as seen by the VA, and reducing its complexity. With this approach, noise samples at the input to the VA will be correlated, but degradation appears to be small [11]. Another related possibility is that of using a fixed filter rather than a matched filter, with or without noise whitening. Such a filter would typically be a bandpass filter already existent in the receiver structure [12], so that essentially no processing would be required apart from signal sampling and operation of the standard VA. This type of receiver may be considered to be matched to the average channel, but degradation due to noise enhancement will be apparent if the channel response exhibits notches near the carrier frequency. However, this approach may also offer a useful complexity reduction.

One of the weaknesses of the VA based equaliser is that there is no obvious mechanism for tracking changes in the channel response (as with Decision Feedback Equalisers). However, it is possible to adapt the matched filter response and the look-up table coefficients used in the operation of the

VA, either by re-estimating the channel at regular intervals, or by continuously adapting the receiver parameters with the aid of a decision-directed technique. The latter approach was proposed by Ungerboeck for the implementation of the MF equaliser [3]. A steepest descent algorithm is used, and the adaptation of the various coefficients is proportional to the estimated noise component. A recent implementation of this adaptive algorithm has been reported in [8]. Other approaches are possible, particularly by attempting to combine DFE's and the VA into a single receiver structure with good performance and adaptivity [11,13,14].

3.3. PROPAGATION CHANNEL MODELS

In order to test and compare equaliser performance, a number of specific channel models have been defined. These include both static and dynamic (Rayleigh) channel models, and both single-path and multipath models. The most important models used are described below:

3.3.1. Channel Model 1 (static two-path)

The transfer function is defined as follows:

$$H(f) = 1 - b \exp[-j2\pi(f - f_o)\tau] \qquad (3.3.1,$$

where f_o is the frequency offset of the notch from the carrier frequency f_c, τ is the relative delay between the two paths, and b is the amplitude of the second path with respect to the main path.

The above transfer function can also be used in the characterisation of system behaviour using signature curves [15] which are a plot of the critical notch depth $B_c = 20 \log|1 - b|$ that causes outage against f_o, for a given value of the echo delay τ. The criterion defining outage may be closure of the eye diagram or a given bit error rate threshold. It has been verified that the two criteria yield similar results.

3.3.2. Channel Model 2 (Rayleigh two-path)

The transfer function is defined as follows:

$$H(f) = a - b\,\alpha\,\exp[-j2\pi(f - f_o)\tau] \qquad (3.3.2)$$

where parameters a and b are time-varying Rayleigh distributed random processes, and f_o is a time-varying uniformly distributed random process (for a given τ, the phase term $2\pi f_o\tau$ is uniformly distributed in $[0, 2\pi]$). The channel can therefore be specified by the values of α and τ.

When moving through the multipath fading environment, the channel parameters a, b and f_o will change, and their rate of variation will be a function of vehicle speed. The channel therefore requires a third parameter (v, the vehicle speed) for complete definition. The special case when the vehicle speed is slow enough such that the channel parameters can be regarded as constant over one TDMA burst will be referred to as $v \to 0$km/h. Note that in this case the channel parameters still follow their specific distributions when a sufficiently large number of bursts is observed.

Signature curves cannot be applied to this type of channel model, and hence system performance is assessed using bit error rate curves against Eb/No for specified values of α, τ, and v.

3.3.3. Channel Model 3 (flat Rayleigh fading)

This is an important special case of channel model 2, and corresponds to a single path Rayleigh fading channel (e.g., as for eqn.(3.3.2) with parameter a permanently set to 0). In this channel there is no frequency selective distortion, and the channel is fully identified by the vehicle speed v. System performance is again evaluated through the bit error rate against Eb/No characteristic.

3.3.4. Channel Model 4 (hilly terrain)

This has the following power delay profile [16]:

$$P(t) = \begin{cases} \exp(-3.5t) & 0<t<2 \\ 0.1\exp(15-t) & 15<t<20 \\ 0 & \text{elsewhere} \end{cases} \qquad (3.3.3)$$

where t is in μs. Software modelling is performed on two independent and parallel branches, to obtain $Re[H(t_o,\omega)]$ and $Im[H(t_o,\omega)]$ by starting from the power densities P(t) of delays. First, the modulus $|P_m^2|$ of the real part of the complex form of P(t) is constructed; a simulation of phases (assumed uniformly distributed in $[0,2\pi]$) leads to the complex form of P(t). Then, introducing the usual symmetry restrictions, i.e., considering the real part as an even function and the imaginary part as an odd one, the Fourier Transform of a real signal is obtained. An inverse Fourier Transform gives the frequency pattern of $Re[H(t_o,\omega)]$. The other branch yields the corresponding $Im[H(t_o,\omega)]$ in a similar way.

The simulation of the dynamic channel is obtained by forcing a frequency realisation $H(t_o,\omega)$ to assume at a particular frequency (for example at the mid-band frequency ω_c) the same value as provided by a time realisation $H(t,\omega_c)$ at $t=t_o$ (where t_o corresponds to the beginning of the simulation), and so on, in the following time intervals.

Alternatively, software modelling of the propagation channel can be obtained by using 6 or 12 paths, with delays and relative power as defined in [16].

System performance is evaluated through the BER against Eb/No characteristic, for a specific value of vehicle speed v.

3.3.5. Channel Model 5 (rural area)

This has the following power delay profile [16]:

$$P(t) = \begin{cases} \exp(-9.2t) & 0<t<0.7 \\ 0 & \text{elsewhere} \end{cases} \tag{3.3.4}$$

System performance is evaluated as for channel model 4.

3.3.6. Channel Model 6 (typical urban area)

This has the following power delay profile [16]:

$$P(t) = \begin{cases} \exp(-t) & 0<t<7 \\ 0 & \text{elsewhere} \end{cases} \tag{3.3.5}$$

System performance is evaluated as for channel model 4.

3.3.7. Channel Model 7 ('equaliser model')

This has the power delay profile defined by six tap settings [16]:

Tap Number	Relative time (μs)	Average relative power (dB)	Doppler spectrum
1	0.0	0.0	S(f)
2	3.2	0.0	S(f)
3	6.4	0.0	S(f)
4	9.6	0.0	S(f)
5	12.8	0.0	S(f)
6	16.0	0.0	S(f)

where [16]:

$$S(f) = A/\sqrt{[1-(f/f_d)^2]} \quad , \text{ for } -f_d < f < +f_d$$

3.3.8. Channel Model 8 (simplified hilly terrain model)

This model was proposed as a result of discussion within COST-207, and it is intended as an approximation to the characteristics of Channel Model 4 (hilly terrain model) but using a much smaller number of paths. The relative delays and mean powers of the four paths have been specified as follows:

Tap Number	Relative time (μs)	Average relative power (dB)
1	0.0	0.0
2	1.7	-2.0
3	12.0	-8.0
4	16.0	-7.0

3.4. GSM SYSTEM CHARACTERISTICS

3.4.1. Time slot structure and transceiver

This report is concerned with the so-called Normal Burst (NB) of the narrowband TDMA transmission scheme adopted by GSM [17,18] (see Fig.3.4.1), which is used to carry information on traffic and control channels. It contains 116 encrypted bits consisting of two parts of 57 bits (plus 1 header bit for each part). A 26 bit preamble is placed in between the two 58 bit blocks to allow symbol timing and carrier phase recovery, channel estimation (necessary to the Viterbi equaliser), and initial training for the LTE or DFE. In particular, eight different preamble sequences have been defined [17], with very good cross-correlation properties in order to avoid transmitters at the same frequency interfering with each other. Moreover, to provide an optimum initial training of

the adaptive equaliser for a fast convergence, they have been designed according to proper criteria, as outlined in [1]. One of the resulting sequences used in this work is 0010010111000010001001011 1; notice that only the central 16-bit sequence has been selected for suitable correlation properties, while the first and last 5 bits have been added to account for time-jitter of the received sequence.

At the two ends three tail bits complete the burst: they provide a defined modulated signal after ramp-up and before ramp-down, and allow the channel memory to be exploited for the last bits as well, as discussed in section 3.2.2 for the Viterbi equaliser.

Finally, a guard space of 8.25 bits is introduced between two consecutive bursts. Notice that the so-called active part of the burst, i.e., the part for which the on/off switching transients need to be settled, is 148 bits long. Very different transient shapings are possible within the burst time-mask defined in [17], from the instantaneous step-like ramp to the smooth ramp lasting 7 bits [19].

Since the preamble is placed in the middle of the time slot, the adaptive equalisers start their operation from the information bits close to the preamble, which should undergo similar channel distortions, and work rightward and leftward (the received time slot is completely stored before starting its processing).

The general block diagrams of the simulated systems are depicted in Figs.3.4.2 and 3.4.3 for the cases of the Viterbi equaliser and of the Kalman DFE respectively. The modulation format adopted by CEPT/GSM is the 12PM3 modulation corresponding to Gaussian Minimum Shift Keying [20] with coherent demodulation, which proves to have good performance features in the typical narrowband TDMA channels.

All the results presented throughout this work refer to BT=0.3 for the pre-modulation Gaussian filter; the modulating

signal bit rate is 270.8 kb/s.

The coherent demodulation receiver includes an IF RX filter (ideally equalised 7-pole Butterworth with 3 dB bandwidth equal to 1.56 f_{bit}), and a baseband RX filter (ideally equalised 5-pole Butterworth, with 3 dB bandwidth equal to 0.5 f_{bit}).

Before entering the GMSK modulator, each data value $d_i \in \{0,1\}$ is precoded as:

$$d_i = d_i \oplus d_{i-1} \tag{3.4.1}$$

where $\oplus$ denotes modulo 2 addition. In this way, at the decision point after the coherent demodulator the sampled data value on each branch is uncorrelated with respect to the preceding data values, and the demodulation process becomes practically equivalent to an Offset-QAM (OQAM), provided that the BT product of the pre-modulation filter is greater than 0.25, and a sign inversion is applied to every other sample.

3.4.2. Synchronisation techniques

Two strategies have been adopted in this work to compute the optimum decision instant t_o and the carrier phase Φ_o corresponding to the minimum peak distortion. An outline of the first method is as follows [19]:

Initially, the magnitude M(t) of the correlation function $R_{PS}(t)$ of the received 26-bit preamble sequence P with the central 16 bits S of the reference sequence stored in the receiver is computed, starting from the in-phase and quadrature components $R^I_{PS}(t)$ and $R^Q_{PS}(t)$:

$$M(t) = \sqrt{[R^I_{PS}(t)]^2 + [R^Q_{PS}(t)]^2} \tag{3.4.2}$$

and t_o is given by the peak instant of M(t). Note that the search for t_o may be performed using a sampling rate higher than the bit rate.

The received preamble sequence P is then synchronised according to the obtained value of t_o. The magnitude of the correlation function between the 25-bit long received and reference sequences p and s is computed and its peak instant t_{MAX} is searched for.

Finally, the carrier phase rotation Φ_o is given by

$$\Phi_o = - \text{arctg}[\ R^Q_{PS}(t_{MAX}) \ / \ R^I_{PS}(t_{MAX})\ ] \qquad (3.4.3)$$

Notice that the correlation $R_{ps}(t)$ is performed over 25 bits because of the offset quadrature modulation.

Examples of correlation function $R_{ps}(t)$ in the case of undistorted radio channel 1 with $f_o = 0$, $\tau/T_{bit} = 1.35$, B = -30 dB are shown in Fig.3.4.4.

An alternative simpler method computes the carrier phase as follows:

$$\Phi_o = - \text{arctg}[\ R^Q_{PS}(t_o) \ / \ R^I_{PS}(t_o)\ ] \qquad (3.4.4)$$

In this way the second correlation $R_{ps}(t)$ is not necessary.

Notice that as reference signal we can use either the actual GMSK modulated signal or a 2-level quantised version of it, with each level lasting two bits. Fig.3.4.5 shows an example of these two reference signals. We have verified that the performance is similar in the two cases, and adopted the second reference because it simplifies the receiver storage requirements.

The values of t_o and Φ_o are affected by an estimation error resulting from the non-optimum auto- and cross-correlation properties and from the additive noise. To check the range of effectiveness of the correlation-based synchronisation method and the accuracy of t_o and Φ_o, we compared its

performance against that of an optimum method based on a set of simultaneous time and phase shiftings of the received signal, to search for those values producing zero errors over the simulated sequence at the decision point.

A comparison is depicted in Fig.3.4.6 which shows the signature curves computed according to the optimum timing and phase synchronisation and to the correlation-based synchronisation technique. We noticed that the main part of the difference between the two results is due to the sub-optimality of the correlation-based synchronisation, which computes t_o and Φ_o separately.

3.4.3. Channel impulse response (CIR) estimation

The Viterbi algorithm needs the knowledge of the CIR, which is computed according to the following method [19]:

1) 26 reference signal samples $\{v_i\}$ are generated from the sequence $\{a_i\}$ as follows (see also Fig.3.4.4):

$$v(t) = \sum_{i=1}^{N/2} a_{2i-1}\, \delta[t-2(i-1)T] + j \sum_{i=1}^{N/2} a_{2i}\, \delta[t-(2i-1)T] \quad (3.4.5)$$

where N=26.

2) 16 received decoded signal samples $\{x_i\}$ are taken from the decoder as follows:

$$x(t) = \sum_{i=1}^{M/2} x^{I}_{2i-1}\, \delta[t-2(i-1)T] + j \sum_{i=1}^{M/2} x^{Q}_{2i}\, \delta[t-(2i-1)T] \quad (3.4.6)$$

where M=16.

3) The complex correlation $R_{xv}(t)$ is performed between v(t) and x(t), which results in

$$R_{xv}(t) = \int x(\tau+t)\, v^{*}(\tau)\, d\tau \quad (3.4.7)$$

$$= \int \sum_{i=1}^{M/2} \sum_{k=1}^{N/2} x_{2i-1}^{I} \, a_{2k-1} \, \delta(\tau-2(i-1)T+t) \, \delta(\tau-2(k-1)T) \, d\tau$$

$$+ \int \sum_{i=1}^{M/2} \sum_{k=1}^{N/2} x_{2i}^{Q} \, a_{2k} \, \delta(\tau-2(i-1)T+t) \, \delta(\tau-(2k-1)T) \, d\tau$$

$$- j \int \sum_{i=1}^{M/2} \sum_{k=1}^{N/2} x_{2i-1}^{I} \, a_{2k} \, \delta(\tau-2(i-1)T+t) \, \delta(\tau-(2k-1)T) \, d\tau$$

$$+ j \int \sum_{i=1}^{M/2} \sum_{k=1}^{N/2} x_{2i}^{Q} \, a_{2k-1} \, \delta(\tau-(2i-1)T+t) \, \delta(\tau-2(k-1)T) \, d\tau$$

It is worth noting that actually $R_{xv}(t)$ represents the convolution between the overall impulse response $h(t)$ (that we want to estimate) and the autocorrelation $R_{vv}(t)$ of the preamble sequence, i.e., $R_{xv}(t) = R_{vv}(t) \otimes h(t)$:

$$R_{xv}(t) = \int x(\tau+t) \, v^{*}(t) \, d\tau$$

$$= \int \int v(\tau+t-\alpha) \, h(\alpha) v^{*}(\tau) \, d\tau \, d\alpha$$

$$= \int R_{vv}(t-\alpha) \, h(\alpha) \, d\alpha = R_{vv}(t) \otimes h(t) \qquad (3.4.8)$$

Using the preamble sequence reported in section 3.4.1, $R_{vv}(t)$ turns out to be a delta function within the neighbourhood of ±5 bits around its central value.

Considering the transceiver characteristics of section 3.4.1, we obtain the CIR's reported in Fig.3.4.7 in the cases of undistorted channel and of channel 1 with $f_o = 0$, $\tau/T_{bit} = 1.35$ and $B = -30$ dB.

3.5.
PERFORMANCE RESULTS OF LTE AND DFE AS APPLIED TO CEPT/GSM SYSTEM

3.5.1. Signature curves

Assuming channel 1, Fig.3.5.1 shows the signature curves of the CEPT/GSM system without adaptive equalisation and with perfect time and phase recovery. As already discussed in section 3.4.2, Fig.3.4.6 compares the signatures for τ/T_{bit} = 2.71 and 4.33 against those obtained by using the correlation-based synchronisation. It is worth noting that the value τ/T_{bit} = 4.33 corresponds, with f_{bit} = 270.8 kbit/s, to the maximum echo delay that the system has to cope with according to the CEPT/GSM working assumptions [16,21].

Fig.3.5.2 shows the same signatures of Fig.3.5.1 but in the presence of a linear transversal equaliser with 5 complex coefficients and adapted according to the CFKA. In the same situation we have found that a DFE with 2 forward and 3 feedback coefficients (denoted as (2,3)DFE) is capable of keeping the signature curves below the -40 dB level, and for this reason they do not appear in Fig.3.5.2.

3.5.2. BER in a static frequency selective channel

The BER performance for channel 1 is summarised in Figs.3.5.3 and 3.5.4. The channel parameters are specified in the caption of Fig.3.5.3. In particular, Fig.3.5.3 shows the BER curves without equalisation, together with the reference performance in the presence of white Gaussian noise only, and Fig.3.5.4 shows the improvement given by the use of a (2,3)DFE. It is worth noting that in this case the BER curves are fairly independent of the echo delay value (at least up to τ/T_{bit} = 4.33). Also notice that the correlation-based synchronisation technique produces a degradation of the Eb/No ratio of about 1 dB at BER = 10^{-2}.

3.5.3. BER in a flat Rayleigh fading channel

Fig.3.5.5 shows the BER performance in a single path Rayleigh fading channel (model 3) with a vehicle speed of $v \to 0$km/h.

3.5.4. BER in a frequency selective fading channel

The BER performance for channel 2 is given in Figs.3.5.6 and 3.5.7 for a vehicle speed of 50 km/h. In particular, Fig.3.5.6 shows that when the two paths are subjected to uncorrelated Rayleigh fading with equal average power of the two rays, i.e., $\alpha = 1$, there is further degradation of performance with respect to channel 1, but the (2,3)DFE is still capable of removing the irreducible BER.

Fig.3.5.7 shows the BER vs the relative echo delay τ when the Eb/No ratio is 17 dB. It can be seen that the (2,3)DFE with the CFKA can keep the BER below 10^{-2} for the whole range of values of τ (i.e., 0-16 μs) currently specified by CEPT/GSM. This remains true also for much higher vehicle speeds.

Comparing the results of Figs.3.5.6 and 3.5.7 with those of 3.5.5 relevant to channel 3, we see that the equaliser works better when there is time dispersion in the channel (i.e., frequency selective distortion) compared to a flat Rayleigh channel. This means that the adaptive equaliser together with the two-path channel provides a form of diversity reception.

3.5.5. Discussion

Adaptive baseband equalisation by means of linear transversal and non-linear decision feedback equalisers is a feasible solution to cope with very fast varying frequency-selective distortions, provided that a Kalman-type algorithm is adopted to ensure a fast convergence (i.e., within the 26-bit long training sequence) of the equaliser coefficients to

the steady state values, and a rapid track of the channel variations. To reduce computational complexity the 'Complex Fast Kalman Algorithm' (CFKA) is used.

The length of 26 bits fixed by the CEPT/GSM for the training sequence is sufficient, provided that it is optimised according to the criterion mentioned in section 3.4.2.

Timing and carrier phase synchronisation must be recovered before performing the adaptation process. The correlation-based synchronisation technique exploiting the 26 bit training sequence has been compared to a perfect synchronisation technique by means of the signature and BER curves. The BER curves show a degradation of the Eb/No of about 2 dB at BER = 10^{-2} in the presence of the (2,3)DFE, when applied to a distorted two-path channel.

It has been found that a (2,3) complex decision feedback equaliser is capable of reducing the signature curves below the -40 dB level over the whole range of echo delay values specified by CEPT/GSM. Also the BER is kept below 10^{-2} at an Eb/No value of 17 dB, for the whole range of echo delay values (0-16 μs) and vehicle speeds (0-300 km/h) [19,21].

From the hardware implementation point of view, it is important to keep the number of bits used to represent the signal samples fed to the adaptive equaliser, the equaliser coefficients and the arithmetic of the adaptation processor as small as possible. For a narrowband TDMA system with channel bursts of about 150 bits, which has a 'built-in' re-starting procedure, a minimum of 10 bits seems to be required for the binary words [1]. In practice we have implemented the CFKA with a 16 bit DSP.

As regards the accuracy of the A/D converter at the equaliser input and of the coefficient values, we have tested the equaliser performance when 6-bit, 8-bit and infinite accuracy is assumed. It has been found [1] that the dominant cause of degradation is the equaliser coefficient accuracy,

while the A/D converter accuracy is not a critical item as long as it is ≥ 8 bits.

3.6. PERFORMANCE RESULTS OF VITERBI EQUALISERS AS APPLIED TO THE CEPT/GSM SYSTEM

3.6.1. Introduction

The results presented below have been obtained through the use of computer simulation. The receiver simulated includes a simple version of a VA equaliser, with 16 states but no matched filter (i.e., the VA operates directly on samples of the receiver I and Q channels). These results may therefore be improved upon, particularly at high Eb/No values, when the channel estimation becomes sufficiently reliable for the correct choice of the matched filter coefficients. It should also be noted that the performance using an equaliser structure similar to that proposed by Ungerboeck [3] was also studied during the course of the COST project [19], but such results are not included here for reasons of space.

The GSM frame structure has been assumed, which implies that the equaliser works rightwards and leftwards from the centre of the timeslot. Since the VA parameters are obtained through the use of the synchronisation sequence located at the centre, it follows that the equaliser must cope with variations in channel characteristics over a period of about half a timeslot (58 bits, or 214 μs). The effect of these variations during the timeslot at high vehicle speeds has been considered, as has the use of longer information bursts.

3.6.2. Signature curves

The signature curve tests are performed without noise. Under these conditions, the VA equaliser/receiver is able to correctly estimate the channel and to adequately cancel the intersymbol interference, and the data is estimated without any errors. It was in fact found that, for this reason,

signature curves cannot be drawn for delays less than approximately four bit periods. Above this delay, errors appear for small fade depths, irrespective of notch position.

3.6.3. BER in a static frequency-selective channel

The BER performance for channel 1 is summarised in Fig.3.6.1. It may be seen that correlation-based synchronisation degrades the ideal performance of GMSK by just over 1 dB at a BER of 10^{-2}. When a two-path channel is introduced, the performance is similar irrespective of echo delay for the values shown until the delay is greater than four bit periods. At this point, the equaliser operation starts to degrade, and eventually an irreducible BER is found.

3.6.4. BER in flat and frequency selective Rayleigh fading channels

The BER performance for channels 2 and 3 is depicted in Figs.3.6.2 to 3.6.6 for a range of vehicle speeds and relative delays between the two paths. The mean power of both paths in channel 2 is taken to be the same (i.e., $\alpha = 1$). It may be seen that in all cases there is a further degradation of performance as compared to channel 1, but the VA equaliser is able to remove the irreducible BER provided the relative delay is smaller than four bit periods, and the vehicle speed is not excessively high (leading to appreciable changes of the channel characteristics within the burst).

Fig.3.6.7 shows the BER vs relative echo delay τ when the Eb/No ratio is 17 dB. It may be seen that the BER tends to increase as the vehicle speed increases. Similarly, BER degradation becomes catastrophic when the relative delay reaches about 16 μs irrespective of vehicle speed. Note however that at this value of Eb/No, the error rate remains below 10^{-2} for speeds below 200 km/h, and for relative echo delays up to 15μs.

It is also apparent from these results that, as with the

DFE, the VA equaliser has a better performance in a Rayleigh channel when there is time dispersion, since such dispersion effectively provides a diversity function as long as the receiver is able to equalise it.

Fig.3.6.8 shows a plot of the irreducible BER against vehicle speed. It may be seen from this that outside the breakdown region, where the performance is equally bad for all speeds, the irreducible BER is always below 10^{-3} for vehicle speeds up to 100 km/h.

3.6.5.
BER in multipath Rayleigh fading channels (channels 4-8)

Fig.3.6.9 compares the performance of the VA equaliser using four of the channels recommended by CEPT/GSM [16], here deemed channel models 4-7. The channel is assumed to be burst stationary ($v \rightarrow 0$km/h).

In this case ($v \rightarrow 0$km/h), it may be seen that the worst performance corresponds to channel 4 (hilly terrain model). This channel is perceived by the equaliser essentially as a two-path characteristic where the second path delay is larger than 4 bit periods, and hence an irreducible BER results. Channel 5 (rural area) has a slightly better performance which is very similar to channel 3 (single-path Rayleigh fading). This is to be expected since all the energy in the channel impulse response is contained within a window which spans about 20% of the bit period. Channel 6 (typical urban area) gives an even better performance. In this case, the impulse response spans a longer time interval (about two bit periods), and the diversity function already discussed in the last section comes into play, giving an improvement of over 2 dB at a BER of 10^{-2} with respect to the 'rural area' model. Finally, channel 7 ('equaliser model') represents an interesting case where at low Eb/No, the BER performance is the best of the four channels considered. This is because the channel impulse response is very wide, giving a high diversity gain. However, a fraction of the impulse response is outside the equaliser

window, and hence the BER tends to an irreducible level (albeit low) at large Eb/No values. Note that if the vehicle speed is 50 km/h, the relative performances of the various models may be different [21].

Fig.3.6.10 compares the performance using channel 4 (hilly terrain) and channel 8 (simplified hilly terrain model) The latter was designed as an approximation to the hilly terrain characteristic, but it can be seen that the curves are somewhat different. However, it is interesting to study an optimisation of the channel parameters in order to achieve a better approximation of the hilly terrain model using a simplified four path model. This was done simply by altering the relative amplitude of the fourth path in channel 8, and the BER performance is also depicted in Fig.3.6.10. It may be seen from this that model 8C (for which the fourth path amplitude has been increased by about 4 dB relative to channel 8) yields an improved fit to the hilly terrain BER, and can be used if tests using more than four paths are not practical.

Finally, the limiting case for simplified approximations of a hilly terrain model is clearly that of a two path model where the second path is placed just outside the equaliser window. Thus we have considered a relative delay of 16μs between the two paths, and adjusted their relative amplitudes to achieve a good fit of the BER curves. One sample result is shown in Fig.3.6.11, and it may be seen that even in this case a good approximation can be obtained with this simple model. However, a two path model may not fully test the ability of the equaliser to 'equalise', and hence it may be more appropriate to use channel model 8C. For different vehicle speeds, different parameter adjustments would be required for both the two-path and the four-path models [21].

3.6.6. Error statistics for channel 2

A record of the number of errors at different positions in the information part of the channel timeslot was kept, and the number was averaged over one thousand simulations in order

to estimate the BER distribution across the burst.

Figs.3.6.12, 3.6.13 and 3.6.14 show sets of curves for five different vehicle speeds and for three different values of Eb/No (8, 11 and 14 dB). It may be seen that the BER rises appreciably at the higher speeds towards the end of the burst, although this effect is masked at the lower values of Eb/No.

Fig.3.6.15 shows a similar plot for a given value of Eb/No and a fixed speed (100 km/h). It may be seen from this graph that little difference is found between BER distributions as long as the two paths are sufficiently separated to be resolved by the equaliser.

3.6.7. Discussion

The results have shown that a simple VA based equaliser can be used for GMSK reception to achieve reasonable performances even in severe multipath Rayleigh fading channels. Since the receiver used did not include a filter matched to the channel characteristic, it is to be expected that some improvement may be obtained when the channel exhibits deep notches near the carrier frequency, and also that the receiver sensitivity to timing may be reduced. However, even in this case any improvement would be dependent on accurate setting of the matched filter coefficients, which will be corrupted by noise at the critical low values of Eb/No.

The synchronisation and estimation of the channel impulse response are performed using the GSM preambles, and it was found that this led to a small degradation (about 1 dB) in an undistorted channel, with over 2 dB in static frequency selective channels.

In a two-path Rayleigh fading environment, it was found that the error rates do increase as the vehicle speeds increase, due to the fact that the VA does not attempt to track channel fluctuations. As a result, it appears that the VA equaliser may not give an acceptable performance above

vehicle speeds of 100 km/h. Below this limit, however, the equaliser can compensate for second path delays of up to 15 μs. It is expected that this figure could be slightly increased simply by widening the rather narrow bandwidth used for the receiver filter.

The performance with complex multipath channels has also been considered, and it has been found that the error rates are reduced if the channel exhibits severe dispersion as long as this is within the limits of equaliser operation. This is due to a diversity-type effect, and as a result a 'typical urban' channel may give better performance than a 'rural' channel. However, the equaliser cannot cope with channel impulse response widths greater than about 15 μs, and such delayed echos function as co-channel interference to the receiver, as seen with the 'hilly terrain' channel.

3.7. CONCLUSIONS

3.7.1. Overview of results obtained

This work has shown that an adaptive equaliser (either a Kalman DFE or a Viterbi-based receiver) is indispensable for a narrowband TDMA system with the CEPT/GSM characteristics, working in a digital cellular mobile radio environment.

In particular, adaptive baseband equalisation by means of linear transversal and non-linear decision feedback equalisers is a feasible solution to cope with the very fast varying frequency selective distortions, provided that a low complexity Kalman-type adaptation algorithm is used to ensure a fast (i.e., within the 26-bit long training phase) convergence of the equaliser coefficients to the steady state values, and a rapid tracking of the channel variations. To reduce computational complexity, the 'Complex Fast Kalman Algorithm' (CFKA) has been proposed: its implementation complexity is competitive with that of a Viterbi equaliser if the required number of states of the latter is $\geq$ 32. For a narrowband TDMA system with channel bursts of about 150 bits, which has a 'built-in'

re-starting procedure, the DFE with the CFKA requires a minimum of 10 bits for the binary words and of 8 bits for the A/D converters.

The (2,3)DFE with the CFKA can meet the CEPT/GSM objectives over the whole specified range of echo delay values (i.e., 0-16 μs) and also at high vehicle speeds (i.e., up to 300 km/h) thanks to its ability to track the channel variations also during the information data transmission.

Timing and carrier phase synchronisation must be recovered before performing the adaptation process. The correlation-based synchronisation technique exploiting the 26-bit long training sequence has been compared to a perfect synchronisation technique by means of the signature and BER curves. The latter show a degradation of the Eb/No ratio of BER = 10^{-2} of about 1 dB in an undistorted channel In the case of distorted two-path static channel, the degradation is about 0.4 dB and 2 dB with and without the (2,3)DFE, respectively.

The results on the Viterbi equaliser have shown that this solution can also be used for GMSK reception to achieve reasonable performances even in severe multipath Rayleigh fading channels. In particular, the Viterbi equaliser, which is adapted only once for each channel burst using the 26-bit preamble sequence, can cope with the channel distortions produced by echo delays up to about 15 μs and for vehicle speeds up to about 200 km/h.

The synchronisation and estimation of the channel impulse response performed using the GSM preamble lead to a small degradation (about 1 dB in an undistorted channel, and over 2 dB in static frequency selective channels).

The performance with multipath channels has also been considered, and it has been found that the error rates are reduced if the channel exhibits severe dispersion as long as this is within the limits of equaliser operation. It may be seen that the worst performance corresponds to the hilly

terrain model.

A comparison between the performance with the hilly terrain model and with a simplified four-path model proposed during the activity of COST 207 has also been carried out. It has been found that a good approximation of the hilly terrain model using the simplified four-path model can be achieved (when the vehicle speed $v \rightarrow 0$km/h) simply by altering the relative amplitude of the fourth path.

3.7.2. Future developments

Several topics about adaptive equalisation would be worth studying in the framework of future COST activities. In particular the following points should be considered:

1. Adaptation of the Viterbi equaliser to cope with high vehicle speeds.

2. Optimisation of the Viterbi algorithm processing operations either to improve its distortion compensation capabilities through the use of a greater number of states, or to reduce the complexity of the 16 state equaliser.

For both the Viterbi and the DFE equalisers, the following issues are of interest:

3. Studies of error and synchronisation statistics for a joint optimisation of coding and adaptive equalisation techniques.

4. Optimisation of the receiver filter.

5. Study of the improvement on the performance provided by channel coding.

6. Study of different time slot structures (including different preamble sequences) for future systems.

7. Development of efficient and optimised implementations.

3.8. REFERENCES

[1] G.D'Aria, R.Piermarini and V.Zingarelli, 'Fast adaptive equalisers for narrowband TDMA mobile radio', submitted to IEEE Journal on Selected Areas in Communications, 1988.

[2] G.D'Aria and V.Zingarelli, 'Adaptive baseband equalisers for narrowband TDMA/FDMA mobile radio systems', Proc International Conference on Digital Land Mobile Radio Communications, pp.280-289, Venice, June 30-July 3rd 1987.

[3] G.Ungerboeck, 'Adaptive maximum likelihood receiver for carrier modulated data transmission systems', IEEE Transactions on Communications, vol.COM-22, pp.624-636, May 1974.

[4] A.S.Acampora, 'Analysis of maximum-likelihood sequence estimation performance for quadrature amplitude modulation', Bell System Technical Journal, vol.60, no.6, pp.865-885, July-Aug 1981.

[5] J.G.Proakis, 'Digital Communications', chapter 6, McGraw-Hill, 1983.

[6] P.A.Laurent, 'Exact and approximate construction of digital phase modulations by superpositions of amplitude modulated pulses', IEEE Transactions on Communications, vol.COM-34, pp.150-160, Feb 1986.

[7] K.Murota and K.Hirade, 'GMSK modulation for digital mobile radio telephony, IEEE Transactions on Communications, vol.COM-29, pp.1044-1056, July 1981.

[8] L.Moreno and R.d'Avella, 'Maximum likelihood adaptive techniques in the digital mobile radio environment', Proc. International on Digital Land Mobile Radio Communications, pp.227-236, Venice, June 30-July 3rd 1987.

[9] G.D.Forney, 'Maximum likelihood sequence estimation of digital sequences in the presence of intersymbol

interference', IEEE Transactions on Information Theory, vol.IT-18, pp.363-378, May 1972.

[10] G.D.Forney, 'The Viterbi algorithm', IEEE Proceedings, vol.61, no.3, pp.268-278, March 1973.

[11] S.U.H.Qureshi and E.E.Newhall, 'An adaptive receiver for data transmission over time-dispersive channels', IEEE Transactions on Information Theory, vol.IT-19, pp.448-457, July 1973.

[12] B.Rashidzadeh, L.B.Lopes and P.A.Matthews, 'Design and performance of a Viterbi equaliser for GMSK modulation', Proc. IEE Colloquium on 'Methods of combatting multipath effects in wideband digital cellular radio systems', digest no. 1987/91, pp.3.1-3.8, Oct 1987.

[13] F.R.Magee and J.G.Proakis, 'Adaptive maximum likelihood sequence estimation for digital signaling in the presence of intersymbol interference', IEEE Transactions on Information Theory, vol.IT-19, pp.120-124, Jan 1973.

[14] W.U.Lee and F.S.Hill, 'A maximum likelihood sequence estimator with decision feedback equalisation', IEEE Transactions on Communications, vol.COM-25, pp.971-979, Sep 1977.

[15] S.Benedetto, E.Biglieri and V.Castellani, 'Digital Transmission Theory', Englewood Cliffs, NJ, Prentice-Hall, 1987.

[16] CEPT/CCH/GSM Recommendation no.05.05: 'Transmission and reception'.

[17] CEPT/CCH/GSM Recommendation no.05.02: 'Multiplexing and multiple access on the radio path'

[18] CEPT/CCH/GSM Recommendation no.05.03: 'Channel coding'

[19] G.D'Aria and V.Zingarelli, 'Design and performance of synchronisation techniques and adaptive equalisers for narrowband TDMA mobile radio', Proc. Third Nordic Seminar on

Digital Land Mobile Radio Communication, Copenhagen, Sep 13-15, 1988.

[20] CEPT/CCH/GSM Recommendation no.05.04: 'Modulation'

[21] CEPT/CCH/GSM Recommendation no.03.30: 'Radio network planning aspects'

[22] G.D'Aria and V.Zingarelli, 'Results on Fast Kalman and Viterbi adaptive equalisers for mobile radio with CEPT/GSM system characteristics', Proc. IEEE Globecom'88, Hollywood, FL, Nov.28-Dec 1, 1988.

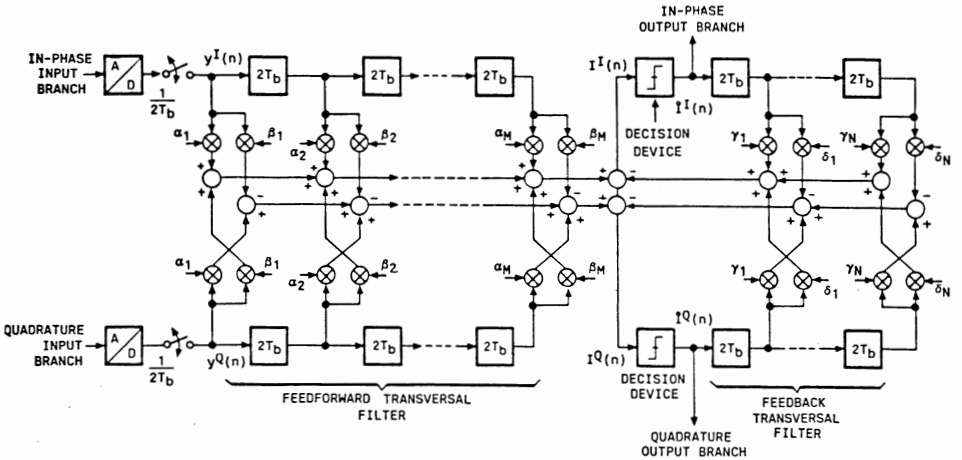

Fig.3.2.1 Block diagram of the decision-feedback equaliser

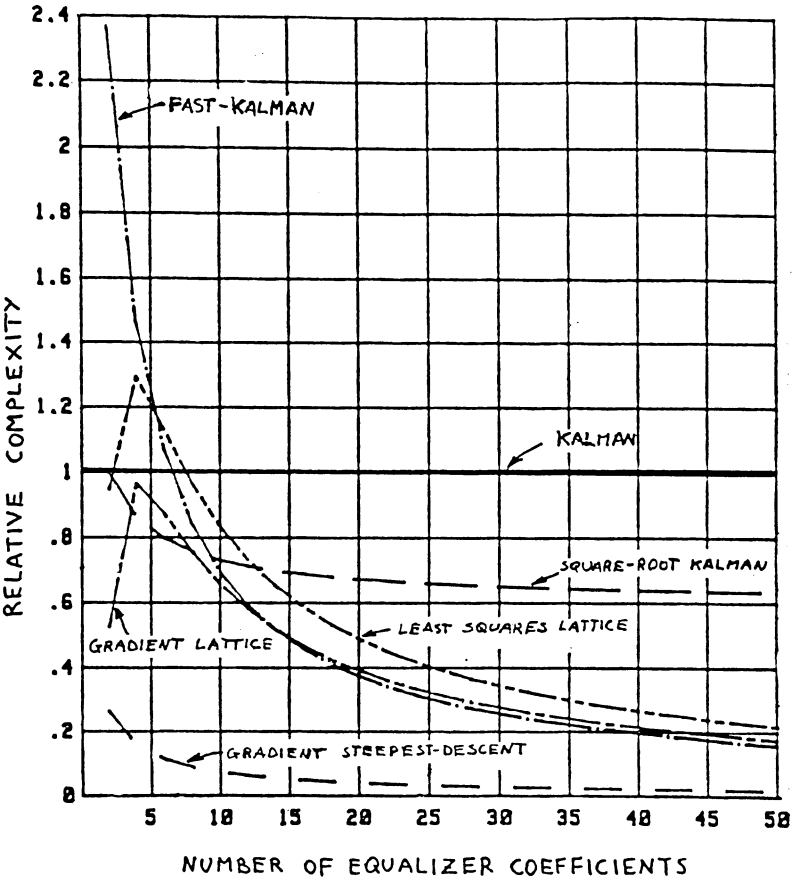

Fig.3.2.2 Computational complexities (number of additions and multiplications) of the Stochastic Gradient and Recursive Least Squares algorithms relative to that of the Kalman algorithm

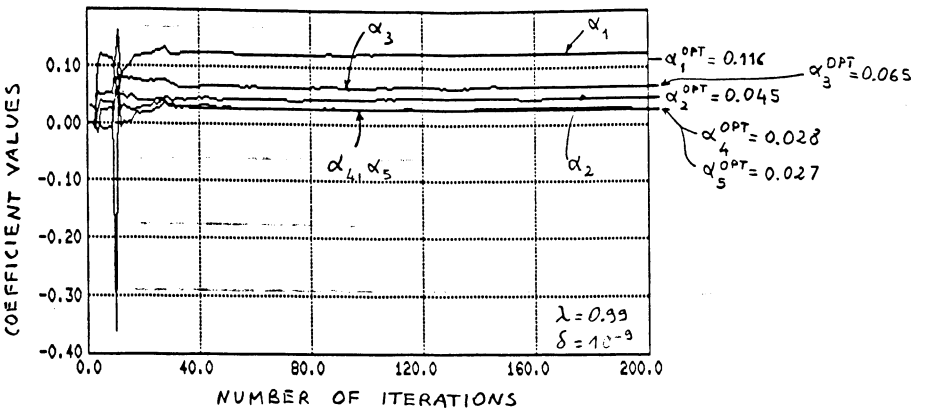

Fig.3.2.3 Real parts of the five coefficients of a linear transversal equaliser with the CFKA
Step transition from a flat channel to a two-path channel with B=-30 dB, $\tau f_{bit}=1.35, f_o=0$.
GMSK modulation (BT=0.3); coherent demodulation.

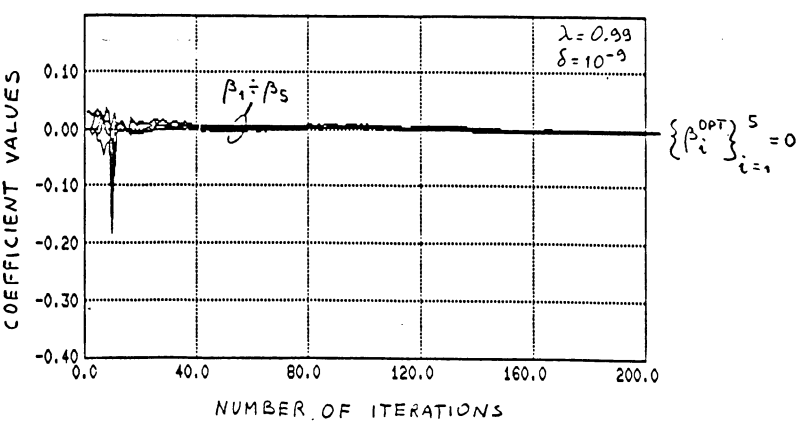

Fig.3.2.4 As Fig.3.2.3, but for the imaginary parts

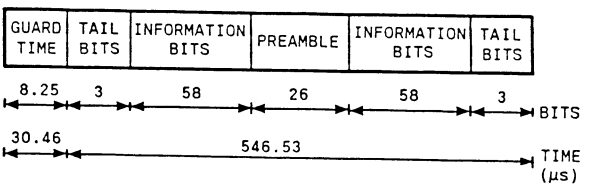

Fig.3.4.1 Basic time slot structure

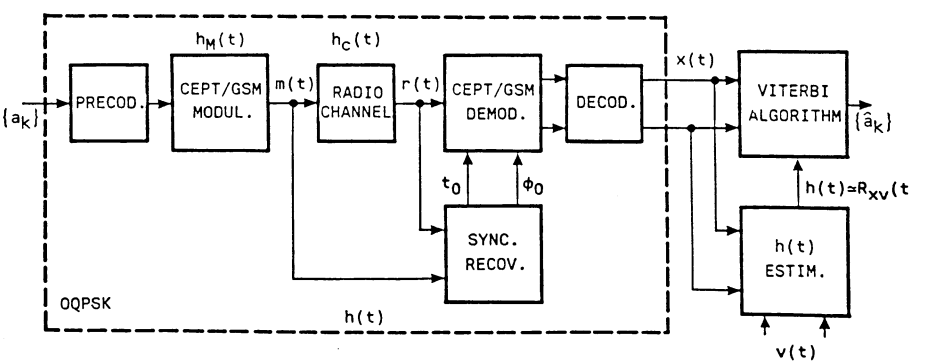

Fig.3.4.2 Block diagram of the simulated CEPT/GSM system in the case of a Viterbi equaliser

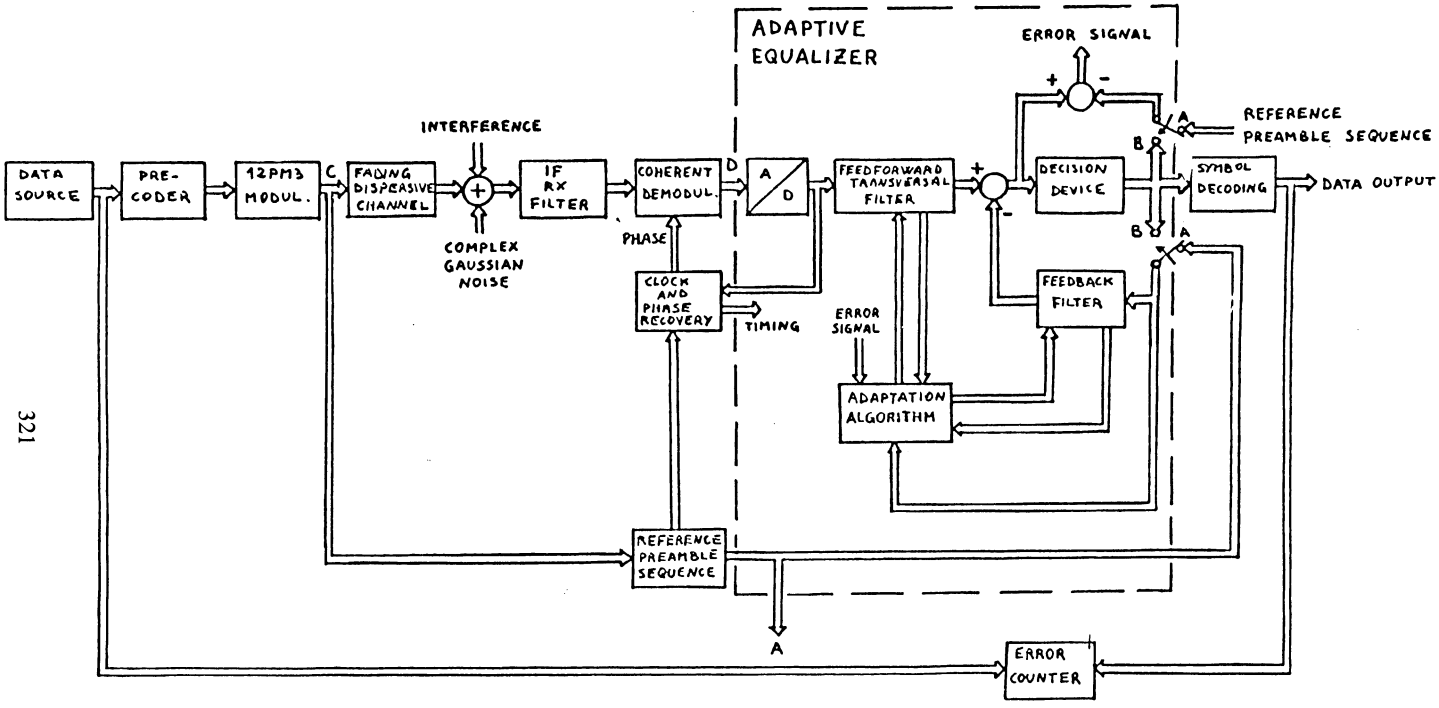

Fig.3.4.3 Block diagram of the simulated CEPT/GSM system in the case of Kalman decision feedback equaliser

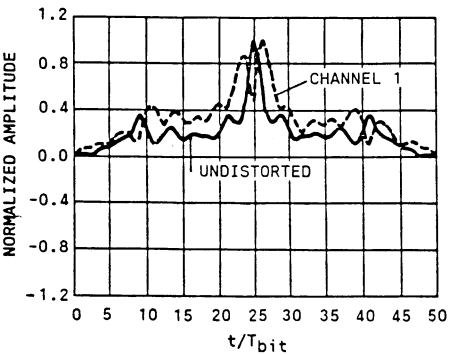

Fig.3.4.4 Amplitude of the correlation function of the preamble sequence in undistorted (solid line) and distorted (dotted line) radio channels

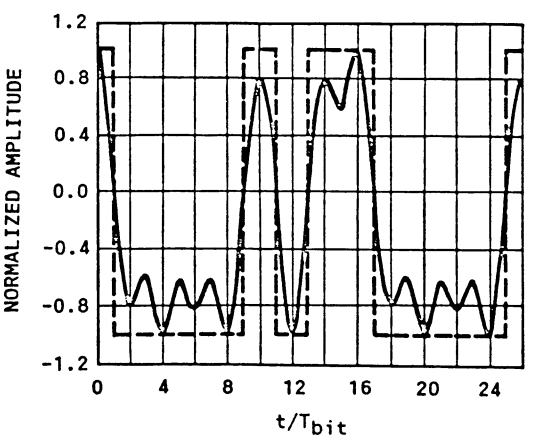

Fig.3.4.5 Reference in-phase waveforms used for sync recovery

——— unquantised GMSK modulated signal

- - - 2-level quantised signal

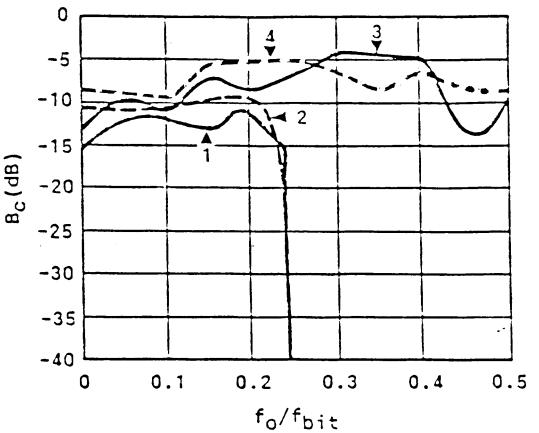

Fig.3.4.6 Signature curves for different values of normalised echo delays

----- optimum timing and phase synchronisation

- - - correlation-based synchronisation

Curves 1,2: τ/T_{bit} = 2.71; 3,4: τ/T_{bit} =4.33

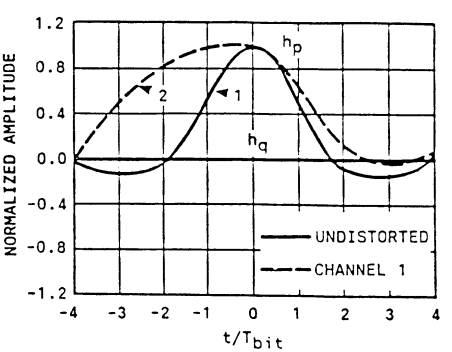

Fig.3.4.7 Estimated channel impulse responses

----- undistorted channel

- - - channel 1

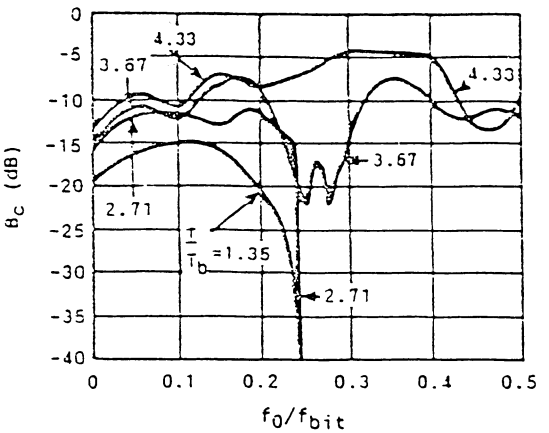

Fig.3.5.1 Signature curves of the system without adaptive equalisation, for several values of echo delay τf_{bit}. Case of perfect timing and synchronisation.

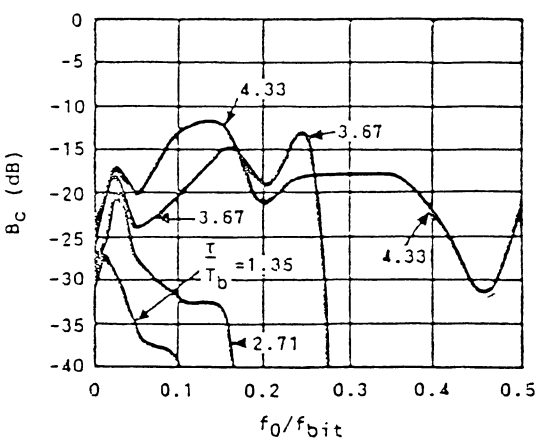

Fig.3.5.2 Signatures of the linear transversal equaliser with 5 complex coefficients, adapted according to the Complex Fast Kalman algorithm.
Case of perfect timing and phase recovery.
The corresponding signature curves of the (2,3)DFE are always below the -40 dB level.

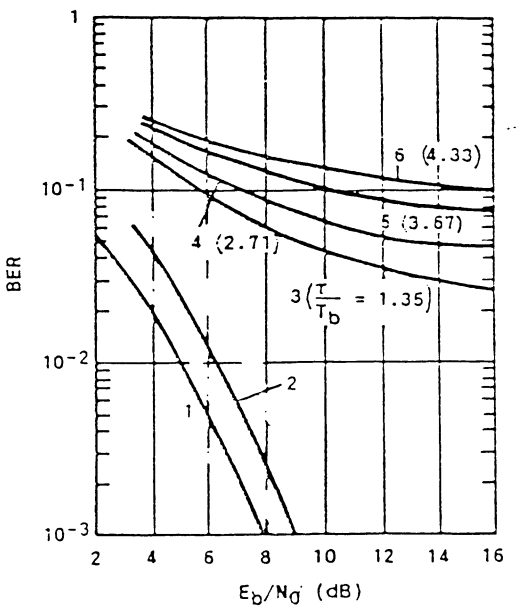

Fig.3.5.3 BER performance without adaptive equalisation

1) Undistorted channel, perfect synchronisation
2) Undistorted channel, correlation-based synchronisation
3) Channel 1 (B=-15 dB, τf_{bit}=1.35, f_o=0, correlation-based synchronisation
4) As 3), but for τf_{bit}=2.71
5) As 3), but for τf_{bit}=3.67
6) As 3), but for τf_{bit}=4.33

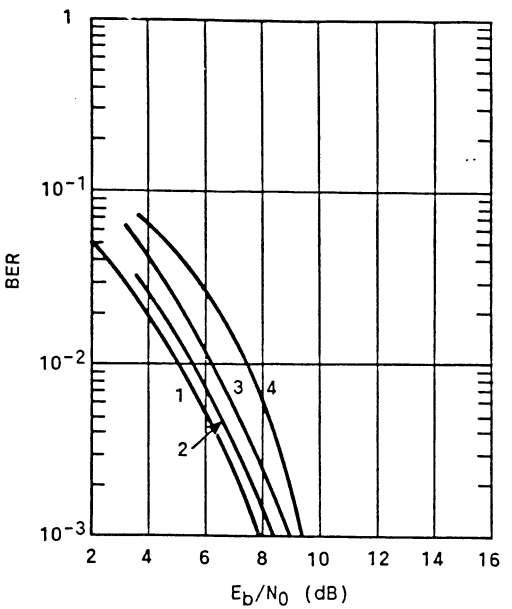

Fig.3.5.4 BER performance with and without the (2,3)DFE

1) Undistorted channel, perfect synchronisation
2) Channel 1 (B=-15 dB, f_o=0, any τf_{bit}), perfect synchronisation, with the (2,3)DFE
3) Undistorted channel, correlation-based synchronisation
4) Channel 1 (B=-15 dB, f_o=0, any τf_{bit}), correlation-based synchronisation, with the (2,3)DFE

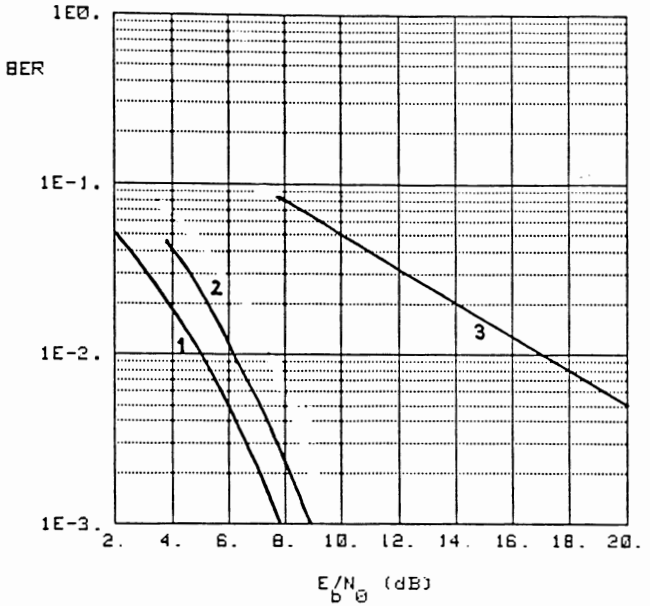

Fig.3.5.5 BER performance with and without the (2,3)DFE

1) Undistorted channel, perfect synchronisation
2) Undistorted channel, correlation-based synchronisation
3) Channel 3, v→0km/h, correlation-based synchronisation, with (2,3)DFE

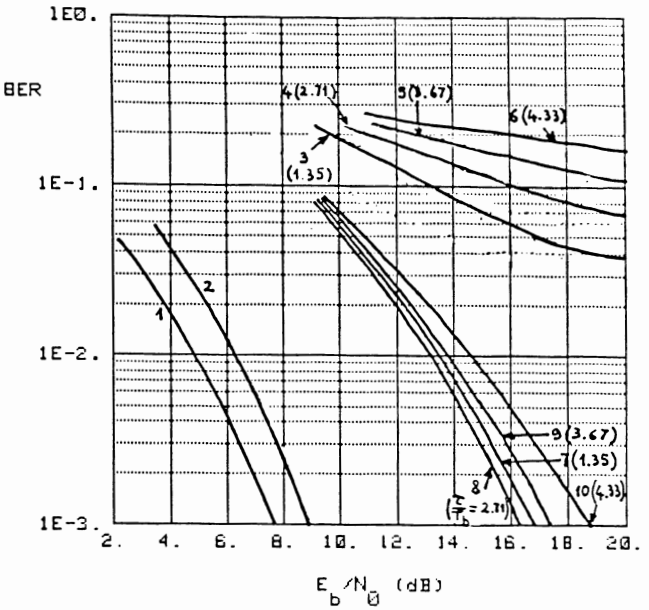

Fig.3.5.6 BER performance with and without the (2,3)DFE

1) Undistorted channel, perfect synchronisation
2) Undistorted channel, correlation-based synchronisation
3)-6) Channel 2, α=1, v=50 km/h, without equalisation, correlation-based synchronisation
7)-10) As for 3)-6), but with the (2,3)DFE

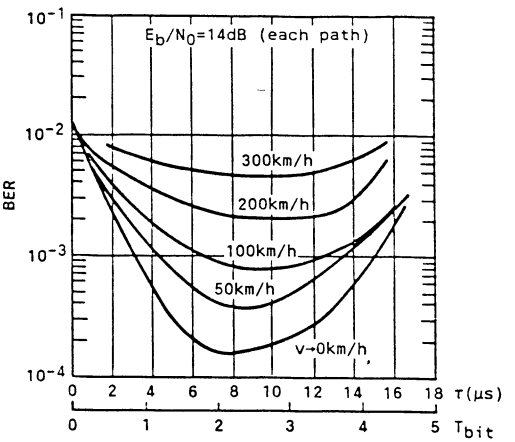

Fig.3.5.7 Variation of BER with the relative echo delay τ
in the case of channel 2
Eb/No=14 dB for each path
(2,3)DFE with correlation-based synchronisation

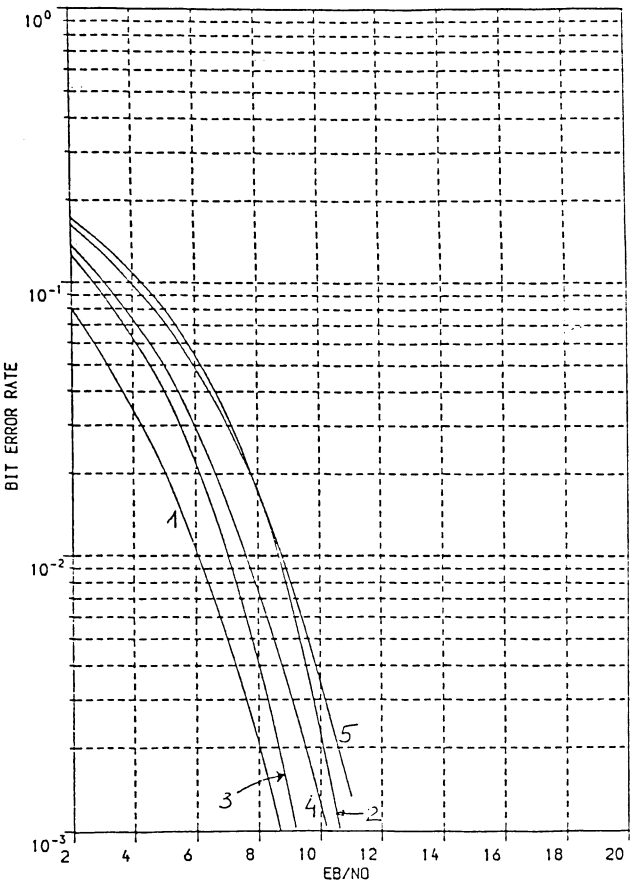

Fig.3.6.1 BER performance in a static channel with Viterbi equaliser

1) Undistorted channel
2) Channel 1 (B=-100 dB, f_o=0, τf_{bit}=1.35)
3) As for 2 with τf_{bit}=2.71
4) As for 2 with τf_{bit}=3.67
5) As for 2 with τf_{bit}=4.33

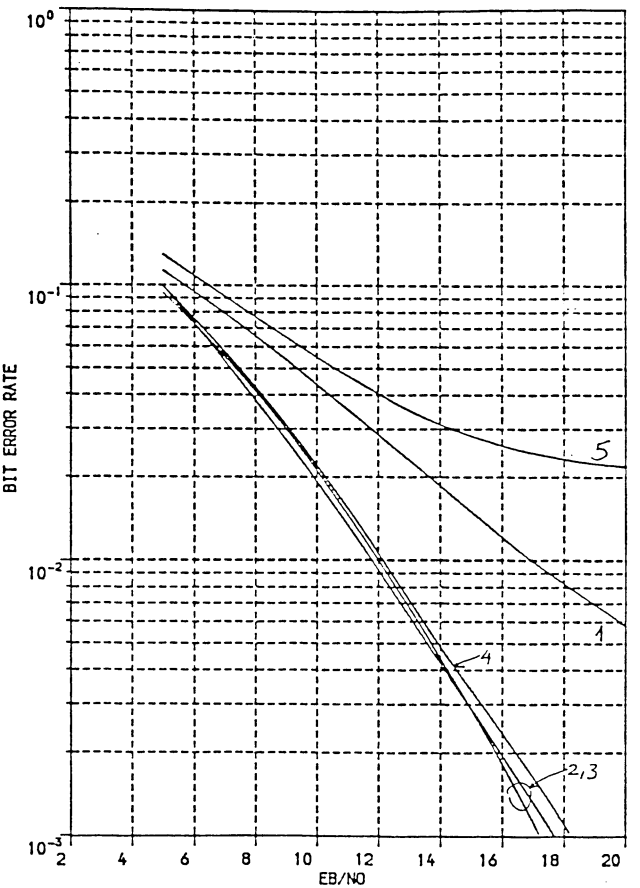

Fig.3.6.2 BER performance with Viterbi equaliser at v→0km/h

1) Channel 3
2) Channel 2 (α = 1, τf_{bit} = 1.35)
3) Channel 2 (α = 1, τf_{bit} = 2.71)
4) Channel 2 (α = 1, τf_{bit} = 3.67)
5) Channel 2 (α = 1, τf_{bit} = 4.33)

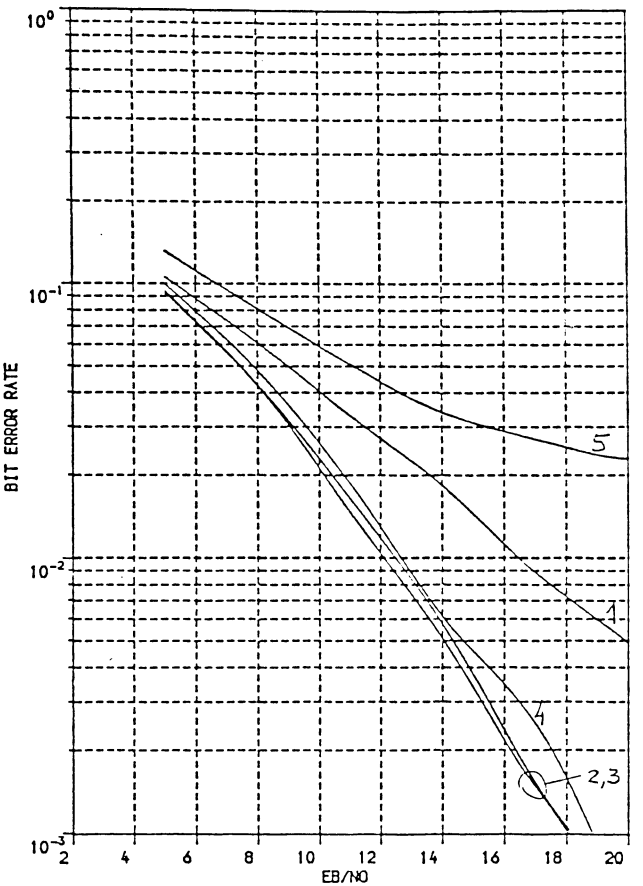

Fig.3.6.3 BER performance with Viterbi equaliser at v = 50 km/h

1) Channel 3
2) Channel 2 (α = 1, τf_{bit} = 1.35)
3) Channel 2 (α = 1, τf_{bit} = 2.71)
4) Channel 2 (α = 1, τf_{bit} = 3.67)
5) Channel 2 (α = 1, τf_{bit} = 4.33)

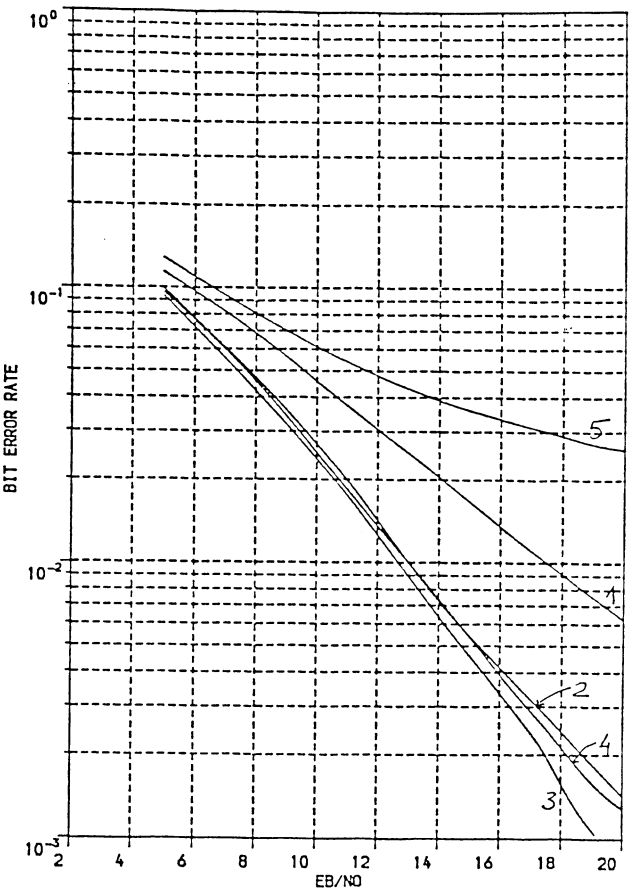

Fig.3.6.4 BER performance with Viterbi equaliser at v = 100 km/h

1) Channel 3
2) Channel 2 (α = 1, τf_{bit} = 1.35)
3) Channel 2 (α = 1, τf_{bit} = 2.71)
4) Channel 2 (α = 1, τf_{bit} = 3.67)
5) Channel 2 (α = 1, τf_{bit} = 4.33)

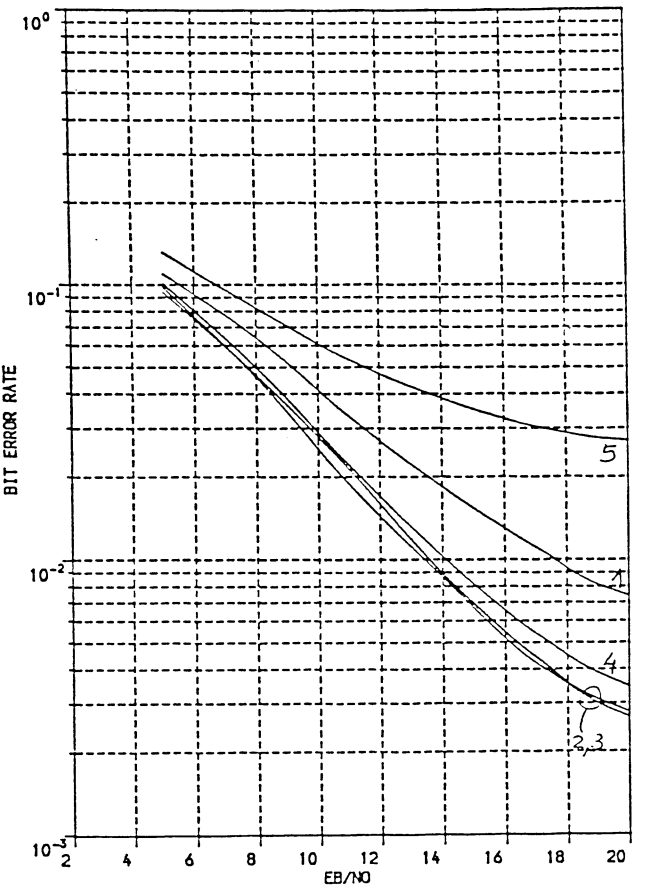

Fig.3.6.5 BER performance with Viterbi equaliser at v = 200 km/h

1) Channel 3
2) Channel 2 (α = 1, τf_{bit} = 1.35)
3) Channel 2 (α = 1, τf_{bit} = 2.71)
4) Channel 2 (α = 1, τf_{bit} = 3.67)
5) Channel 2 (α = 1, τf_{bit} = 4.33)

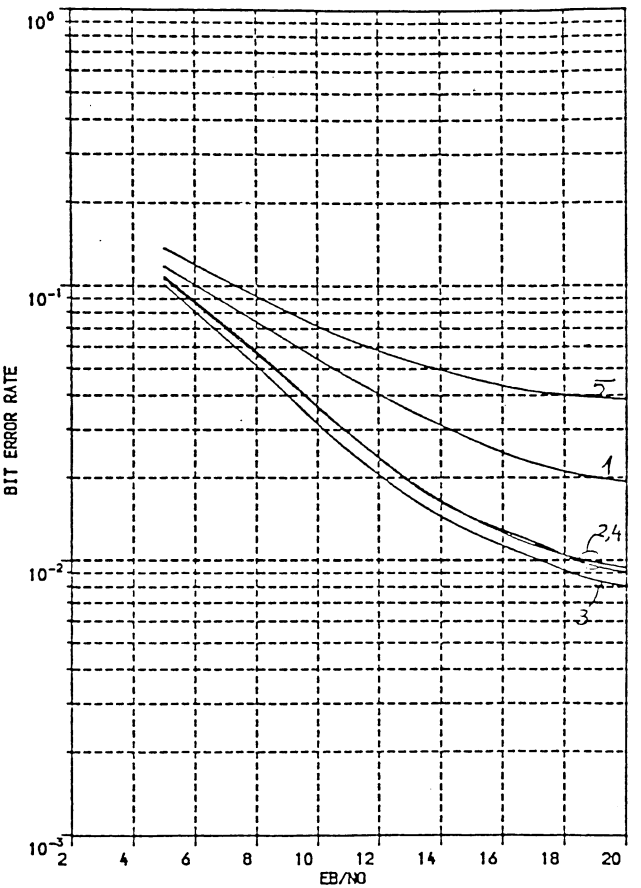

Fig.3.6.6 BER performance with Viterbi equaliser at v = 300 km/h

1) Channel 3
2) Channel 2 (α = 1, τf_{bit} = 1.35)
3) Channel 2 (α = 1, τf_{bit} = 2.71)
4) Channel 2 (α = 1, τf_{bit} = 3.67)
5) Channel 2 (α = 1, τf_{bit} = 4.33)

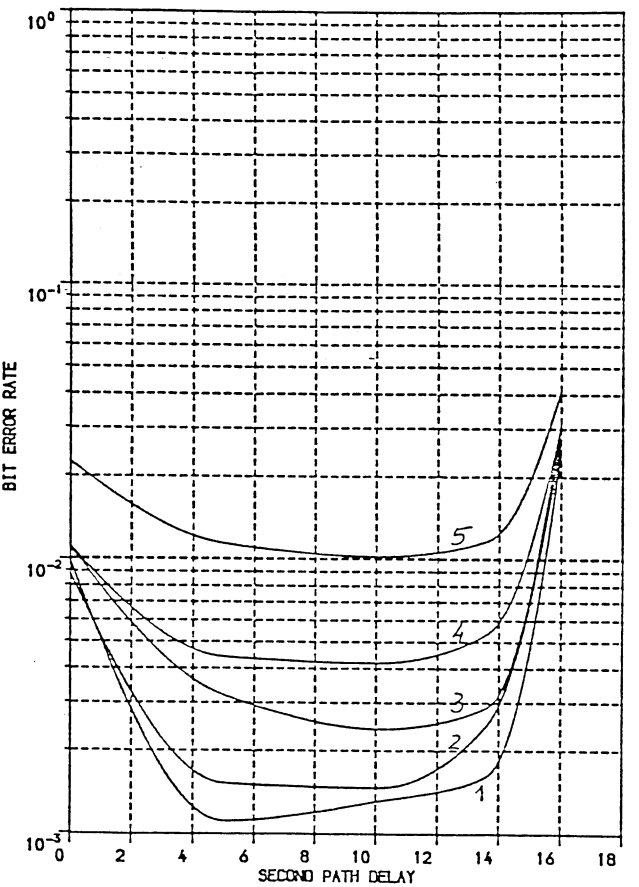

Fig.3.6.7 Variation of BER with second path delay (channel 2)
Eb/No = 17 dB

1) v→0km/h
2) v = 50 km/h
3) v = 100 km/h
4) v = 200 km/h
5) v = 300 km/h

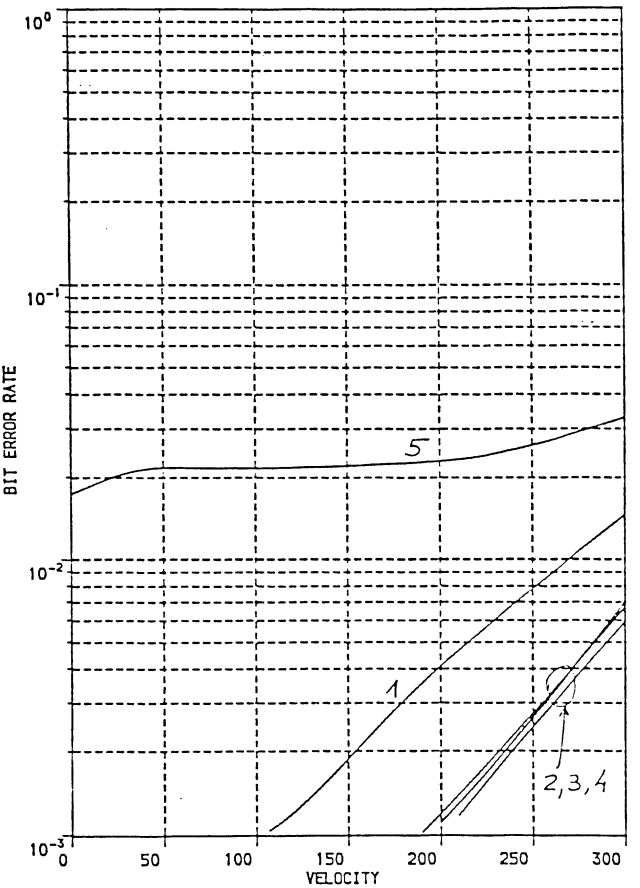

Fig.3.6.8 Irreducible error rate against vehicle speed

1) Channel 3
2) Channel 2 (α = 1, τf_{bit} = 1.35)
3) Channel 2 (α = 1, τf_{bit} = 2.71)
4) Channel 2 (α = 1, τf_{bit} = 3.67)
5) Channel 2 (α = 1, τf_{bit} = 4.33)

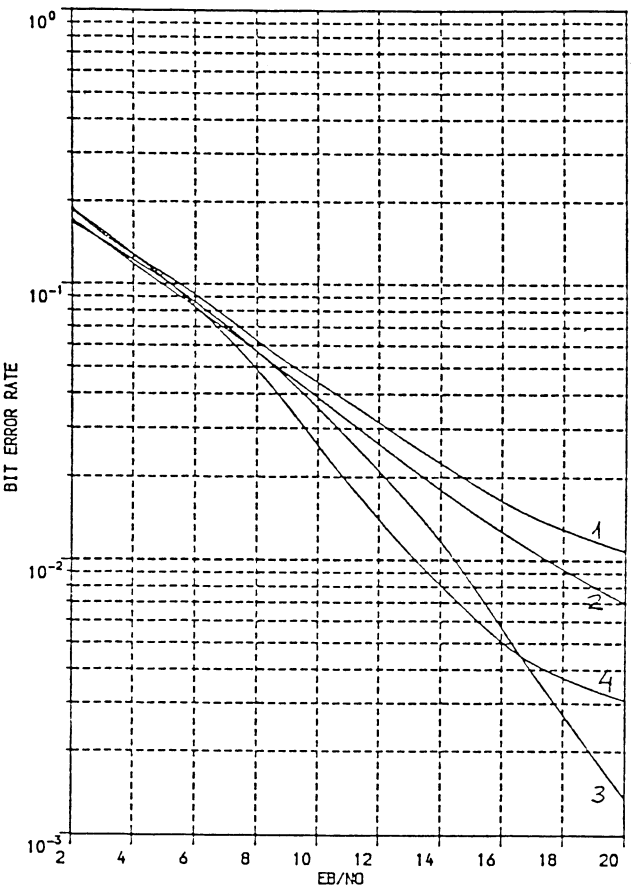

Fig.3.6.9 BER performance for different channel profiles

1) Hilly terrain channel model
2) Rural area channel model
3) Typical urban area channel model
4) Equaliser channel model

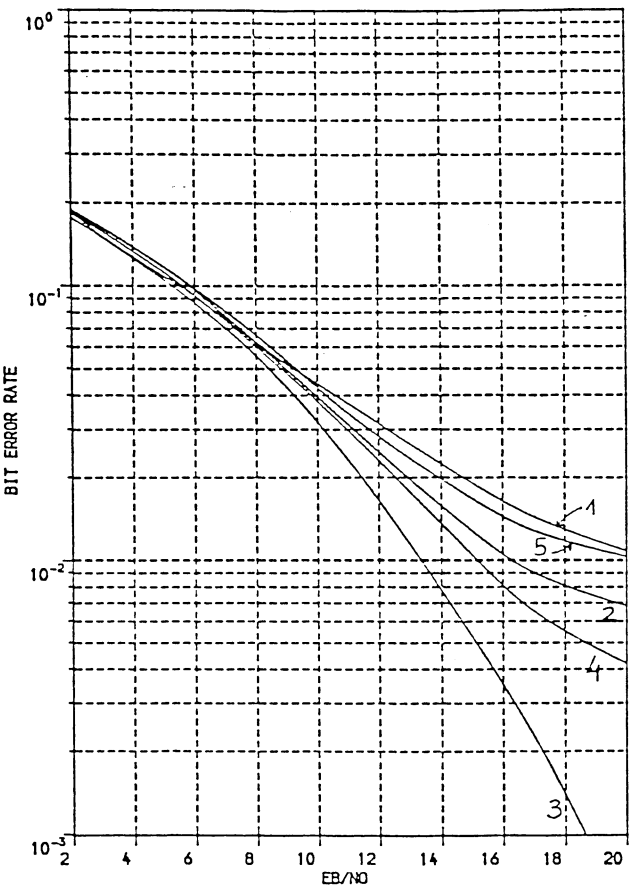

Fig.3.6.10 BER performance for the hilly terrain model and approximations based on a simplified four path model

1) Hilly terrain channel model
2) Simplified hilly terrain channel model (ch. 8)
3) Model 8A (identical to 8 with fourth path amplitude = 0.0)
4) Model 8B (identical to 8 with fourth path amplitude = 0.33)
5) Model 8C (identical to 8 with fourth path amplitude = 0.67)

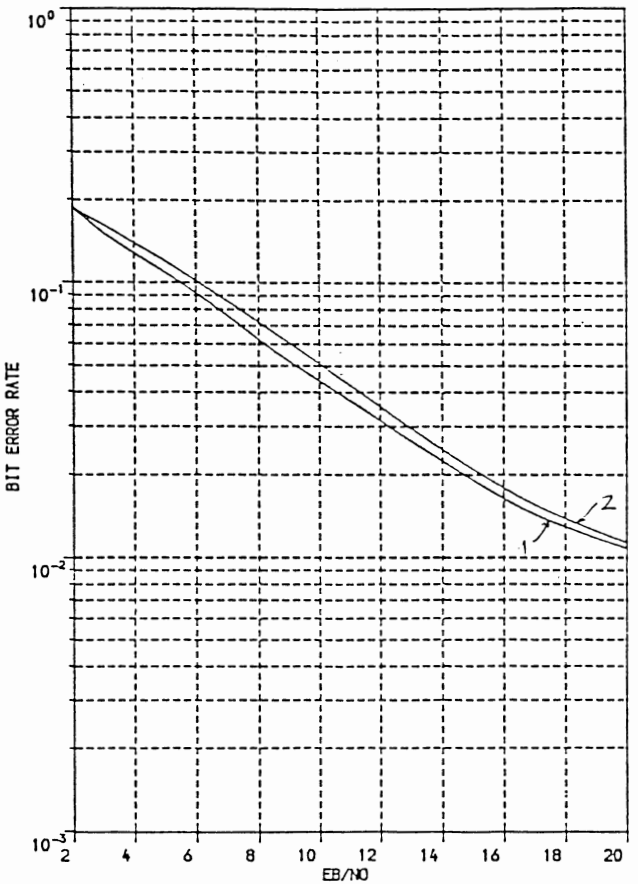

Fig.3.6.11 BER performance for the hilly terrain model and an approximation using a two-path model

1) Hilly terrain channel model
2) Channel model 2, with $\tau f_{bit} = 4.33$ and $\alpha = 0.325$

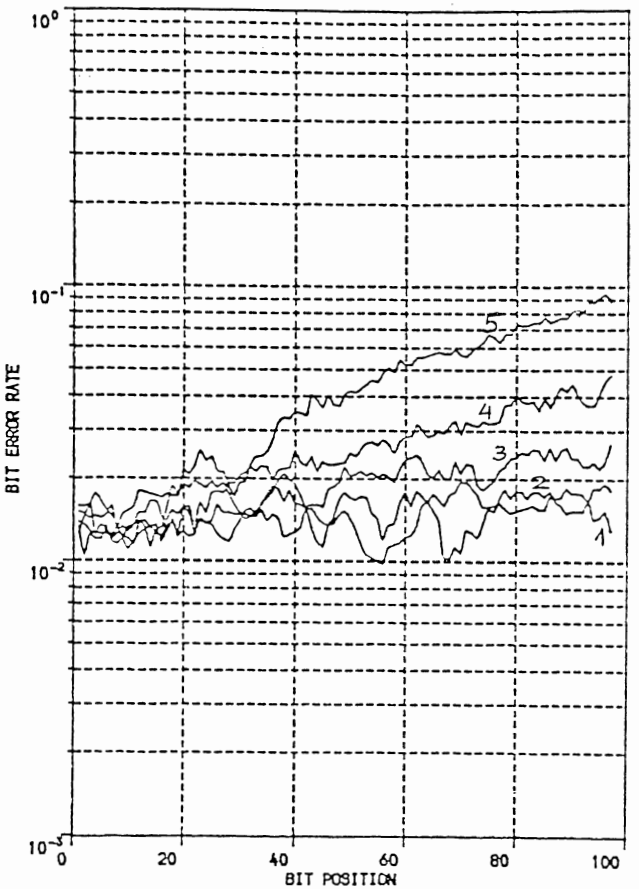

Fig.3.6.12 BER estimate against bit position in burst
Channel 2, τf_{bit} = 2.71
Eb/No = 11 dB

1) v→0km/h
2) v = 50 km/h
3) v = 100 km/h
4) v = 200 km/h
5) v = 300 km/h

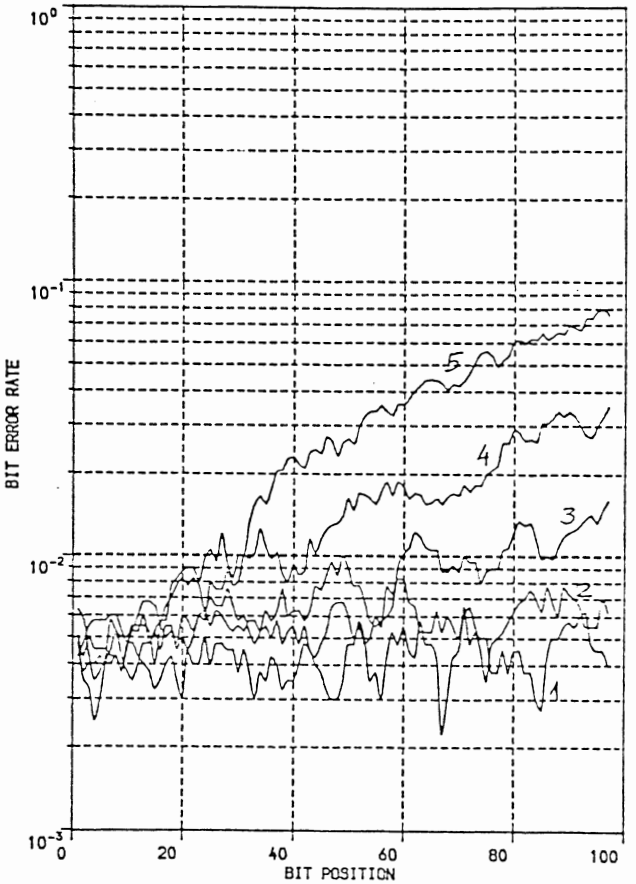

Fig.3.6.13 BER estimate against bit position in burst
Channel 2, τf_{bit} = 2.71
Eb/No = 14 dB

1) v→0km/h
2) v = 50 km/h
3) v = 100 km/h
4) v = 200 km/h
5) v = 300 km/h

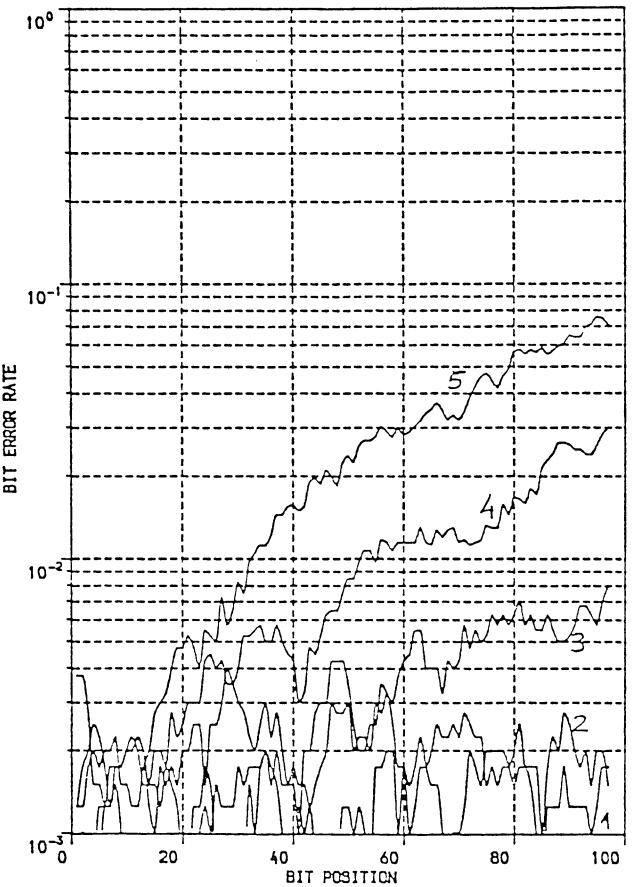

Fig.3.6.14 BER estimate against bit position in burst
Channel 2, τf_{bit} = 2.71
Eb/No = 17 dB

1) v→0km/h
2) v = 50 km/h
3) v = 100 km/h
4) v = 200 km/h
5) v = 300 km/h

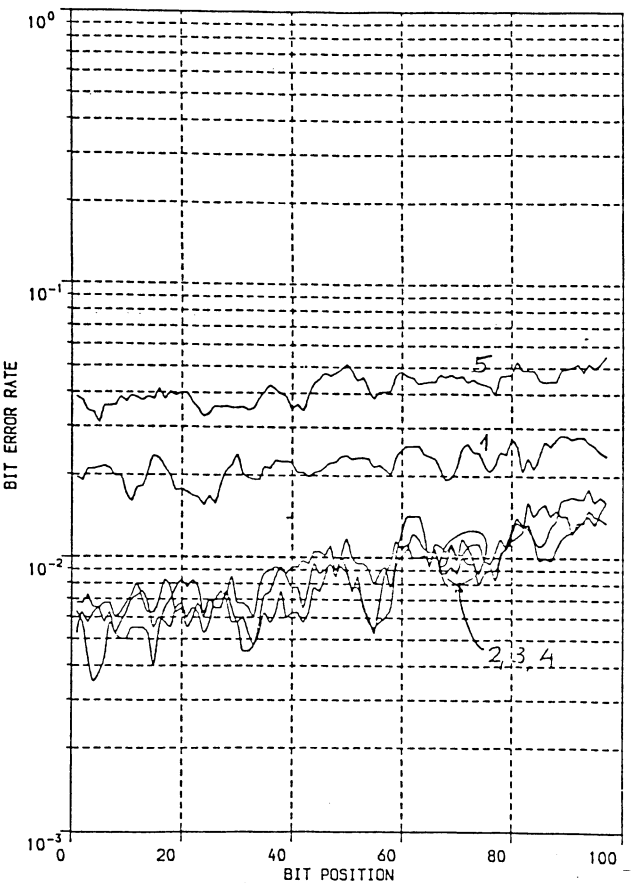

Fig.3.6.15 BER performance against bit position in burst

Eb/No = 14 dB, v = 100 km/h

1) Channel 3
2) Channel 2 (α = 1, τf_{bit} = 1.35)
3) Channel 2 (α = 1, τf_{bit} = 2.71)
4) Channel 2 (α = 1, τf_{bit} = 3.67)
5) Channel 2 (α = 1, τf_{bit} = 4.33)

4. REED-SOLOMON FORWARD ERROR CORRECTING CODES

4.1 Introduction

Narrowband digital mobile radio is impaired by several factors; multipath fading causing amplitude fluctuations and random FM noise, time-variant shadowing, man-made noise, co-channel and adjacent channel interference, and so on. The transmission errors caused by these disturbances tend to occur in bursts, and so they have annoying effects on the transmission quality. In order to improve the performance of digital land mobile radio systems it is necessary to design suitable FEC (Forward Error Correcting) coding techniques. Therefore it is necessary to collect information about the bit error structure to obtain several parameters for an optimized FEC code; e.g. statistics of bit error patterns and BER.

The codes considered in this report belong to the class of Reed-Solomon (R.S.) codes [1] with different degrees of interleaving. This class of codes has been chosen because of the following constraints; i) low redundancy to keep bandwidth occupancy and adjacent channel interference at acceptable levels, ii) low transmission delay, iii) consistency with a preassigned frame structure. The first aim in this application of coding techniques is to reduce the transmit power required to guarantee a specified BER threshold (e.g., 10^{-2}).

A further improvement to the BER performance (i.e. a higher coding gain) can be achieved by exploiting some information on the channel state given to the decoder [3].

The performance of a simple scheme that extracts information on the channel state for the error and erasure correction [4] related to an interleaved Reed-Solomon code is presented.

It is the purpose of this report to present a review of the main concepts of R.S. codes for error and erasure correction applied to mobile radio, together with their formal specifications, and to give some results, obtained by computer simulation, on these topics with reference to a 900 MHz land mobile radio system in urban environment, employing both a PAM/FM (Pulse Amplitude Modulation/Frequency Modulation) [5] and a modulation belonging to the 12PM3 class (12-state Phase Modulation with correlation over 3 consecutive bits) [2].

4.2 FEC coding specifications

A block code is a set of words (codewords) with some specified properties; every word consists of a constant number of symbols, composed of symbols from a specified alphabet.

In practical applications, the alphabet is a set of symbols taken from an algebraic entity called "finite field": each symbol is uniquely associated to a binary m-tuple that represents it.

A key concept in coding theory is the Hamming distance: the Hamming distance between two words is the number of places in which they differ. Everywhere, in what follows, distance will mean Hamming distance.

The minimum distance of a code is the smallest distance between all possible pairs of codewords.

It is useful to define the distance of a given word from a set (the code, as an example) as the smallest distance of the considered word from any other word in the set.

Furtherly, the distance between two sets of words is the smallest distance of each single word in the first set from the second one. The following symbolic notation will be used [1];

m : number of bits per symbol,
n : total number of symbols in a codeword,
k : number of information symbols in a codeword,
$q=2^m$: dimension of the finite field we are working on,
GF(q): finite field of order q (Galois field),
d : minimum distance (in symbols) of the code,
t : symbol-error correction capability, or packing radius of the code ($t=(d-1)/2$),
R : code rate ($R=k/n$).

Since R.S. codes are maximum distance separable (MDS), i.e. they satisfy with equality the Singleton bound [1], the error correcting capability is given by $t=(n-k)/2$.

4.2.1 Correcting capability

Because of transmission errors the received words at a channel output may differ from the transmitted codeword and one of the three following situations may occur;

(1) the distances of the received word from the transmitted one and from the code are both smaller than or equal to t,

(2) the distance of the received word from the transmitted one is greater than t, but the distance from the code is smaller than or equal to t,

(3) the distance of the received word from the code is greater than t.

Accordingly, the decoder action will be;

(1) the symbol-errors are corrected, i.e. the decoder outputs the unique codeword that has minimum distance from the received word (correct decoding),

(2) the decoder finds one codeword with distance less than or equal to t from the received word then it outputs that codeword though it is different from the transmitted one; in this case the number of symbol-errors at the decoder output can be substantially greater than that at the decoder input (decoding error),

(3) more than t symbol-errors are detected and the decoder does not try to correct them but it outputs the received word unchanged; in other words it fails to find a codeword with distance smaller than or equal to t (decoding failure).

As already said, in case 2 the decoder action impairs the channel performance but in practical cases, when the block length of the code is sufficiently large, the rate of decoding errors is so small that can be neglected.

It is possible to obtain a substantial improvement on the performance of the decoder by flagging the less reliable symbols in the received word as erasures; in this case the decoder considers the set of words that has all possible combinations of symbols in the erasure positions, from this set one word is selected that has minimum distance from the code. When this word is unique and its distance from the code is not greater than t (packing radius), then the decoder outputs that codeword; otherwise a decoding failure happens and the decoder puts out the received word unchanged without trying to correct any errors.

When perfect information on the erasures (all the errors are detected as erasures and no false detection of erasure occurs) is available the maximum BER reduction can be achieved.

Reed-Solomon codes are able to correct any single error burst in a received word of length up to $b=m(t-1)+1$ bit errors (or a burst of length up to $(2t-1)m+1$ bit erasures when an ideal information on them is available), since any burst of such length covers at most t symbols (or 2t, respectively).

An additional parameter to be taken into account is the interleaving degree i. Interleaving consists in a re-ordering of the transmitted symbols (from GF(q)) or bits stored column by column in an $i \cdot n$ matrix, and transmitted row by row on the communication channel. An example is shown in Fig. 4.2.1. This operation allows the error bursts to be spread out, but it generally reduces the Shannon capacity of the channel [6]. R.S. codes with symbol-by-symbol interleaving are able to correct any burst of length up to $b=(i \cdot t-1)m+1$ bit errors (or a burst of length up to $b=(i \cdot 2t-1)m+1$ bit erasures, when an ideal information on them is available) provided $g=i \cdot n \cdot m-b$ correct bits exist between adjacent bursts. We noted that with the same rate and total block length ($i \cdot n$ symbols, i.e. $i \cdot n \cdot m$ bits) as the interleaving degree i increases the correcting capability of the overall code decreases.

4.2.2 Specification of a Reed-Solomon code with interleaving

In order to specify a R.S. code with interleaving the following notation will be used:

a) R.S. $[(n,k,d) \cdot m] \cdot i$ for bit-by-bit interleaving
b) R.S. $[(n,k,d) \cdot i] \cdot m$ for symbol-by-symbol interleaving.

When no interleaving is performed, i.e. i=1, the parameter i can be omitted without ambiguity.

In all cases the round parentheses denote the code over a finite field, the square brackets denote its binary image, the notation "·i" means interleaving over the left-hand code entities (bits or symbols).

4.2.3 Performance results

Figs. 4.2.2-4.2.5 [3], [5], [7] show performance of typical narrowband land mobile radio channels obtained by applying R.S. codes. These results have been obtained by applying the coding techniques to the error patterns obtained by the simulation programs developed in CSELT.

Assuming a certain code it is not possible to say if, in general, performance is better with bit-by-bit or symbol-by-symbol interleaving since it depends on too many conditions that characterize the channel. Among them, the output BER; the error statistics, and the interleaving degree play an important role. Tab. 4.2.1 reports some results obtained by simulation, comparing bit-by-bit to symbol-by-symbol interleaving.

4.3 Error and erasure correction concept

A location within the received codeword is called an erasure when it is intended to give the decoder no information about the actual symbol present in it. Since all the symbols from the alphabet (generally a finite field [1]) are equally likely and the channel is assumed symmetric, the decoder tries to fill that position with the symbol which minimizes the distance between the received word and the coresponding codeword.

It is known from coding theory [1] that any code having minimum Hamming distance d is able to correct e errors and g erasures, provided that $2e+g \leq d-1$. This is equivalent to say that e errors can be corected if $2e \leq d-1-g$.

The assertion that some locations in the received codeword are erasures permits the decoder to give better error recovery if there is a high probability that those locations actually correspond to errors. In fact, suppose that $g=g'+g''$ erasures are given to the decoder, g' corresponding to symbol errors and g'' corresponding to correct symbols, then the actual number of correctable errors is at most $[(d-1-g'-g'')/2]+g'=[(d-1+g'-g'')/2]$. Consequently, the recovering ability increases if and only if $g'>g''+1$ (for odd d), i.e. the number of erasures on symbol errors is greater than the number of erasures on correct symbols.

For example, if no erasures are given to the decoder, i.e. $g=0$, at most $[(d-1)/2]$ errors can be recovered by the decoder. Now assume that two erasures in the received codeword are given to the decoder corresponding to symbol errors, then at most $[(d-3)/2]+2=[(d+1)/2]$ erros can be recovered thus increasing the correcting ability of the decoder for odd d. On the other hand, assume that one erasure is given to the decoder corresponding to a correct symbol then at most $[(d-2)/2]=[d/2]-1$ errors can be recovered, thus decreasing the recovering ability of the decoder.

It is plain that if a technique exists such to give very reliable erasure detection (in the sense that $g'>g''+1$ in most cases) the average correcting ability of the decoder increases, thus improving performance in terms of BER reduction.

In the sequel, the extreme condition when all the errors in the received codeword are detected as erasures, and no erasure is pointed out in a position corresponding to a

correct symbol (in other words e=0, g"=0 with the notations introduced above), will be referred to as the ideal erasure detection. It can be easily recognized that this condition allows the corecting capability of the code to be doubled.

Usually codes with odd minimum distance are adopted for error recovery, i.e., d=2t+1, being t the packing radius of the code [1], corresponding to the maximum number of err os that the decoder can correct without any erasure detection. From what stated, a natural limit exists to the number of erasures g that can be pointed out in order to mantain a non-negative correcting ability, and this limit is exactly d-1(=2t). It means that whenever a codeword contains more than 2t erasures the only possible strategy to deal with it, from the decoder standpoint, is to point out a decoding failure, so that the received word is left unchanged.

The performance of a FEC block coding scheme with an ideal erasure detection was analysed in [3], but no particular technique was presented to fully achieve such condition.

4.3.1 Erasure detection

The analysed erasure detection technique [4] is based upon the reliability information coming from the decision circuit.

Since the decision circuit for the PAM/FM compares the received sampled signal against fixed thresholds, suitable regions around the decision thresholds (unreliability regions, Fig. 4.3.1) are introduced so that a channel symbol is said to be unreliable whenever the corresponding received signal sample lies in such regions.

The study refers to a bit-interleaved RS code over GF(64), i.e. $[(63,45,19)\cdot 6]\cdot 2$.

Different strategies can be devised to point out a code symbol erasure; an erasure on a code symbol location occurs whenever at least 1, or at least 2, or at least 3 channel symbols are unreliable.

In what follows performance is evaluated assuming that an erasure happens whenever at least 1 of the channel symbols forming the code symbol is unreliable. Results not reported here for the sake of brevity show that such an assumption gives better performance than those obtained assuming at least 2 or at least 3 unreliable channel symbols.

4.3.2 Results and comparisons

The definition of the unreliability regions described before requires a parameter to be specified (see Fig. 4.3.1). This parameter is the normalized width ε of the unreliability regions and is in the range 0 to 1.

When $\varepsilon=0$ no unreliable channel symbol is detected so that error correction only is performed; when $\varepsilon=1$ all channel symbols are unreliable and no codeword can be corrected because all code symbols are erased. As a matter of fact, simulation results show that performance depends on the normalized width of the unreliability regions; an optimum value of ε exists that minimizes the BER after the decoder.

In particular, Fig. 4.3.2 shows that increasing ε from 0 to 0.25 the BER after decoding first decreases until ε is about 0.13 then it increases again, consequently 0.13 represents an optimum value for the parameter ε. This case refers to an $E_b/N_o=10$ dB, corresponding to a BER of about $4\cdot 10^{-2}$ without the decoder.

Furthermore, an upper limit L to the number of erasures per codeword to be considered has been imposed; when the number of detected erasures exceeds L, all the erasure flags are reset, and so the decoder performs error correction only. For a fixed value of ε, an optimum value for L can be found.

Numerical results show that the value of L lies around t. Fig. 4.3.3 shows that for ε=0.15 and E_b/N_o=10 dB, the optimum value of L is 12. The greater either ε, or L, the greater the overall number of erasures. In general, starting from ε=0 and L=0, the performance in terms of BER reduction improves until the number of detected erasures exceeds the correcting ability t of the code.

Fig. 4.3.4 compares different operating conditions of the channel. Curve 1 refers to uncoded transmission, curve 2 refers to BER after decoding with error correction only, curve 3 refers to error and erasure decoding according to the technique of erasure detection described in this work (ε=0.15, L=9), curve 4 refers to error and erasure decoding with ideal erasure detection. The diagram shows that passing from curve 2 to curve 3 the coding gain improves about 0.3 dB.

REFERENCES

[1] R.E. Blahut, Theory and Practice of Error Control Codes, Reading, MA: Addison Wesley Co., 1983.

[2] Annex 3, Section 2

[3] G. D'Aria, G. Taricco, and V. Zingarelli, "Performance and burst error characteristics of PAM/FM modulations in mobile radio channels", Proc. IEEE GLOBECOM '86, Houston, TX, pp. 31.4.1-31.4.5, Dec. 1-4, 1986.

[4] G. D'Aria, "Reed-Solomon error and erasure correction for PAM/FM mobile radio systems", Proc. IEEE Vehicular Technology Conference, Philadelphia, PA, pp. 485-488, June 15-17, 1988.

[5] G. D'Aria and V. Zingarelli, "Pulse Amplitude Modulation/Frequency Modulation (PAM/FM) techniques for digital mobile radio", Proc. IEEE GLOBECOM '86, Houston, TX, pp. 31.3.1-31.3.5, Dec. 1-4, 1986.

[6] R.G. Gallager, Information Theory and Reliable Communication, New York, NY: Wiley & Sons, 1968.

[7] G. D'Aria, G. Taricco, and V. Zingarelli, "Burst error characteristics of narrowband digital systems in land mobile radio", Proc. IEEE Vehicular Technology Conference, Dallas, TX, pp. 253-261, May 20-22, 1986.

DETECTION SCHEME	INPUT BER	R.S. (63, 45, 19) code over GF (2^6) with interleaving degree = 2			
		errors-only correction		erasures-only correction	
		bit-by-bit interleaving	symbol-by-symbol interleaving	bit-by-bit interleaving	symbol-by-symbol interleaving
bit-by-bit	$3.4\cdot10^{-2}$	$1.8\cdot10^{-2}$	$2.2\cdot10^{-2}$	$0.37\cdot10^{-2}$	$0.82\cdot10^{-2}$
	$2.1\cdot10^{-2}$	$0.76\cdot10^{-2}$	$1.1\cdot10^{-2}$	$0.13\cdot10^{-2}$	$0.37\cdot10^{-2}$
	$0.98\cdot10^{-2}$	$0.1\cdot10^{-2}$	$0.21\cdot10^{-2}$	$0.011\cdot10^{-2}$	$0.032\cdot10^{-2}$
MLSE	$3.3\cdot10^{-2}$	$1.7\cdot10^{-2}$	$2.0.10^{-2}$	$0.54\cdot10^{-2}$	$0.89\cdot10^{-2}$
	$2.4\cdot10^{-2}$	$0.98\cdot10^{-2}$	$1.3\cdot10^{-2}$	$0.14\cdot10^{-2}$	$0.42\cdot10^{-2}$
	10^{-2}	$0.15\cdot10^{-2}$	$0.27\cdot10^{-2}$	$0.016\cdot10^{-2}$	$0.085\cdot10^{-2}$

DETECTION SCHEME	INPUT BER	R.S. (14, 10, 5) code over GF (2^6) with interleaving degree = 9			
		errors-only correction		erasures-only correction	
		bit-by-bit interleaving	symbol-by-symbol interleaving	bit-by-bit interleaving	symbol-by-symbol interleaving
bit-by-bit	$3.4\cdot10^{-2}$	$2.1\cdot10^{-2}$	$1.8\cdot10^{-2}$	$0.59.10^{-2}$	$0.47\cdot10^{-2}$
	$2.1\cdot10^{-2}$	10^{-2}	$0.85\cdot10^{-2}$	$0.25\cdot10^{-2}$	$0.2\cdot10^{-2}$
	$0.98\cdot10^{-2}$	$0.2\cdot10^{-2}$	$0.18\cdot10^{-2}$	$0.02\cdot10^{-2}$	$0.016\cdot10^{-2}$
MLSE	$3.3\cdot10^{-2}$	$2.1\cdot10^{-2}$	$1.7.10^{-2}$	$0.79\cdot10^{-2}$	$0.59\cdot10^{-2}$
	$2.4\cdot10^{-2}$	$1.3\cdot10^{-2}$	10^{-2}	$0.33\cdot10^{-2}$	$0.21\cdot10^{-2}$
	10^{-2}	$0.28\cdot10^{-2}$	$0.25\cdot10^{-2}$	$0.033\cdot10^{-2}$	$0.029\cdot10^{-2}$

Tab. 4.2.1 - Comparison examples between bit-by-bit interleaving and symbol-by-symbol interleaving. Channel characteristics as in Fig. 4.2.2

INPUT STREAM:

```
... A1 A2 A3 A4 A5 A6 A7 A8 B1 B2 B3 B4
    B5 B6 B7 B8 C1 C2 C3 C4 C5 C6 C7 C8 ...
```

MATRIX FILLED BY COLUMNS:

A1	A4	A7	B2	B5	B8	C3	C6
A2	A5	A8	B3	B6	C1	C4	C7
A3	A6	B1	B4	B7	C2	C5	C8

OUTPUT STREAM OBTAINED BY READING THE MATRIX BY ROWS:

```
... A1 A4 A7 B2 B5 B8 C3 C6 A2 A5 A8 B3
    B6 C1 C4 C7 A3 A6 B1 B4 B7 C2 C5 C8 ...
```

Fig. 4.2.1 - Example of interleaving technique.
Number of bits or symbols per codeword: 8
Interleaving degree : 3
A1,A2,...,B1,B2,...,C1,C2,... have to be considered
Bits or symbols in the cases of bit-by-bit or
symbol-by-symbol interlaving, respectively

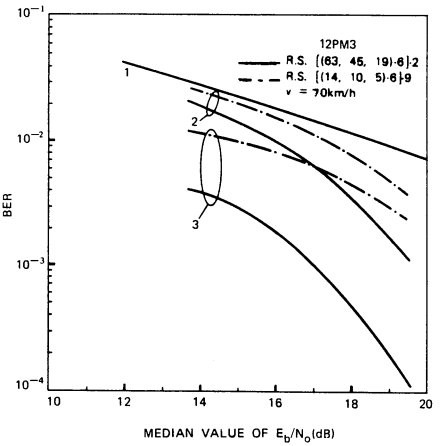

Fig. 4.2.2 - Computed BER with channel coding
Modulation : GTFM, ϕ=60°, ρ=0.42
Bit Rate : 16 kbit/s
Carrier frequency : 900 MHz
Receiver : described in [2], Section 2
Decision : 3-level decision
Curve 1) without channel coding
Curve 2) with FEC coding correcting errors without erasure detection
Curve 3) with FEC coding correcting errors with perfect erasure detection

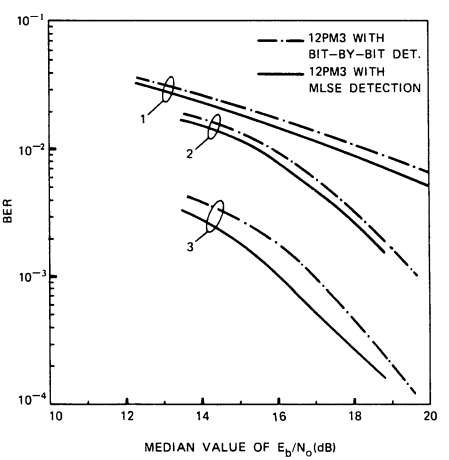

Fig. 4.2.3 - As Fig. 4.2.2, but comparing performance of 3-level decision with MLSE against bit-by-bit decision, using R.S. [(63,45,19)·6]·2 FEC coding

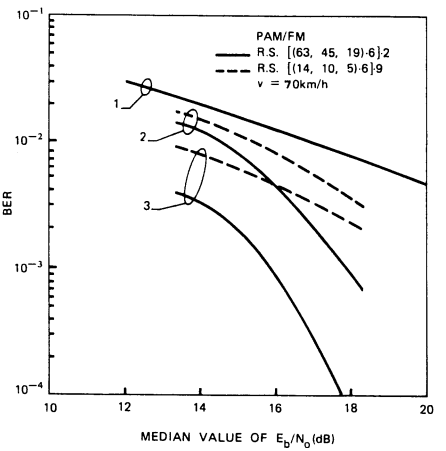

Fig. 4.2.4 - As Fig. 4.2.2, but for the 4-level PAM/FM modulation and receiver defined in [2]

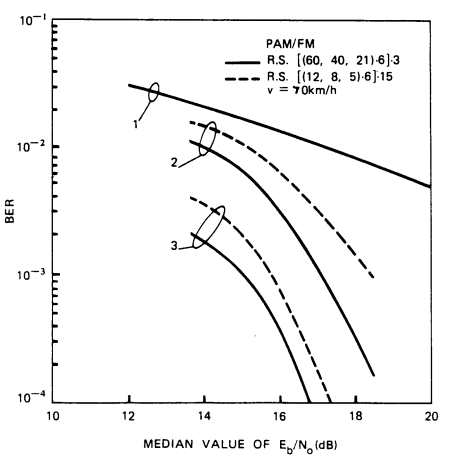

Fig. 4.2.5 - As Fig. 4.2.4 for the two FEC codings R.S. [60,40,21)·6]·3 and R.S. [(12,8,5)·6]·15

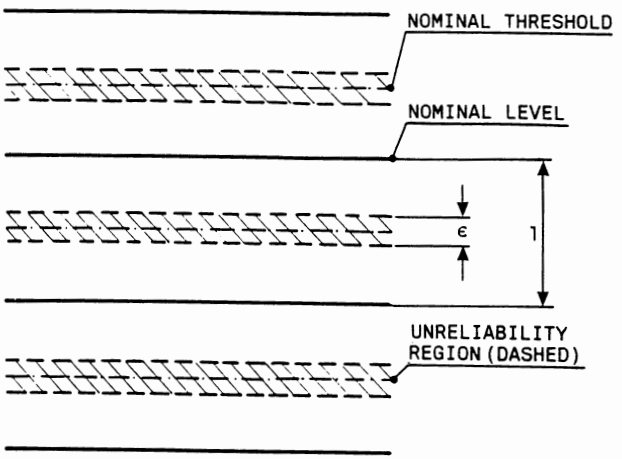

Fig. 4.3.1 - Unreliability regions for a 4-level PAM/FM decision circuit. ε =normalized width of the unreliability regions

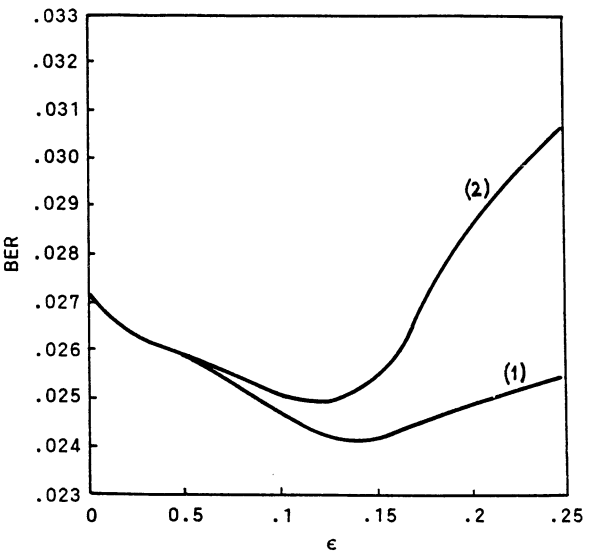

Fig. 4.3.2 - Performance of the error and erasure correction decoder vs the normalized width ε of the unreliability regions. R.S. [(63,45,19)·6]·2.
(1) upper limit to erasures per codeword L=9
(2) upper limit to erasures per codeword L=18
Transmission rate on the channel: 25.2 kbit/s
Speed of the mobile unit: 100 km/h

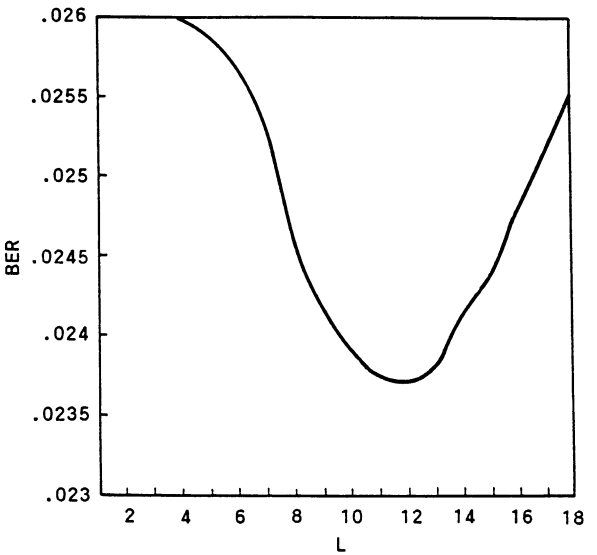

Fig. 4.3.3 - Performance of the error and erasure correction decoder vs the upper limit L to erasures per codeword with ε=0.15. R.S. [(63,45,19)·6]·2.

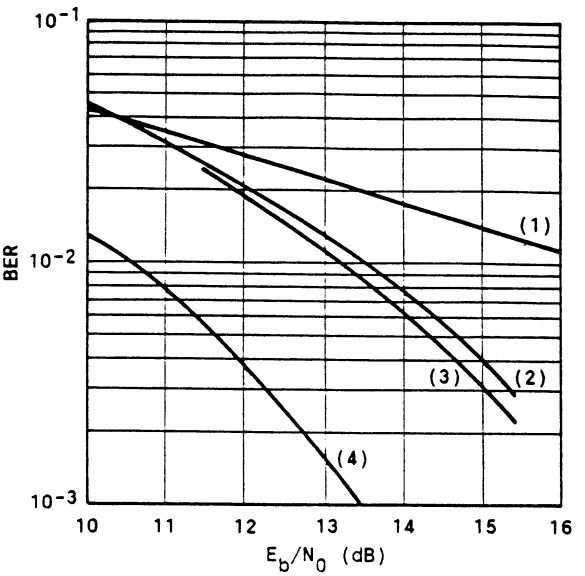

Fig. 4.3.4 - Performance of the error and erasure correction decoder vs the signal to noise ratio. R.S. [(63,45,19)·6]·2.

ANNEX 4

List of participants in the Management Committee

ANNEX 4

LIST OF PARTICIPANTS IN THE MANAGEMENT COMMITTEE

SWITZERLAND	J.P. de WECK Section VD 2 Direction Générale des PTT Berne
	P. KARTASCHOFF Section VD 2 Direction Générale des PTT Berne
	P. MERKI Section VD2 Direction Générale des PTT Berne
FEDERAL REPUBLIC OF GERMANY	H.J. BRAUN Forschungsinstitut der DBP beim FTZ FI 13 d
	Chr. GUTZEIT FI 23e
	R.W. LORENZ FI 32
	K. LOW FI 32a
	H.W. SCHUESSLER Lehrstuhl für Nachrintentechnik Univ. Erlangen/Nürnberg
DENMARK	J.E. ANDRESEN Telecom Denmark Post Telegrafvaesenet
	J. Bach ANDERSEN Institute of Electronic Systems, Aalborg Univ.

	P. EGGERS
	H. FREDSKILD Telelaboratoriet Telecom Denmark
	G. JUUL-NYHOLM
	J. KRISTIANSEN STORNO
	F. MENO
	H. NIELSEN Telecommunications Research Laboratory
ESA	G. BJORNSTROM
	W. KRIEDTE
EUR	E. BALLABIO CEE Brussels
FRANCE	D. BERTOUMIEUX CNET, PAB, ETR, SMC
	J. de BRITO CNET, PAA, RDS, RCM
	D. DUPONTEIL CNET, PAB
	C. HAVEL CNET, PAB, ETR
	Mr. A. SOUBIGOU CNET, LAA, TSS
ITALY	E. DAMOSSO CSELT
	R. FAILLI SIP-Direzione Generale
	G. FALCIASECCA Università di Bologna
	M. FRULLONE Fondazione U Bordoni
	R. MONTAGNA CSELT

	P. PORZIO GIUSTO CSELT
	G.B. VALENTINO Istituto Superiore P T
	V. ZINGARELLI CSELT
THE NETHERLANDS	W.A. KOTTERMAN Dr Neher Laboratories
	W. VAN ECK Dr Neher Laboratories
	H. van Noort
SWEDEN	G. FREMIN Swedish Telecom Adm.
	R. HULTHEN Swedish Telecom Radio Laboratory
	O. MAEKITALO
	M. NILSON
	O RUE
	J.E. STETJERNVALL Ericsson Radio Systems
	J. UDDENFELDT
FINLAND	T. KAJAMAA General Directorate of Post & Telecom, Radio Department
	A. KOIVUMAKI Technical Research Centre of Finland
	E. KUISMA Nokra-Mobira
	V.A. SANTOMAA Technical Research Centre of Finland
	S. TIAINEN General Directorate of Post and Telecom.

UNITED KINGDOM

M.R. BOWMAN
Rutherford Appleton Lab.

P.G. DAVIS

E. GURDENLI
British Telecom Lab.

M.R. HEATH
University of Leeds

P.W. HUISH
British Telecom Research

L.B. LOPES
University of Leeds

P.A. MATTHEWS
University of Leeds

R.S. SWAIN
British telecom Research

ANNEX 5

Proposal for a follow-on project on the "Evolution of land mobile radio (including personal) communication"

ANNEX 5

MEMORANDUM OF UNDERSTANDING
FOR THE IMPLEMENTATION OF A EUROPEAN RESEARCH PROJECT
ON THE EVOLUTION OF LAND MOBILE RADIO
(INCLUDING PERSONAL) COMMUNICATION

(COST PROJECT 231)

The Signatories to this Memorandum of Understanding, declaring their common intention to take part in a European research project on the evolution of land mobile radio (including personal) communication have reached the following understanding:

SECTION 1

1. The Signatories intend to co-operate in a project to promote research into the field of land mobile radio (including personal) communication (hereinafter referred to as the "Project").

2. The main objective of the Project is to co-ordinate and promote European research in specific areas of digital land mobile communications in order to support the CEPT GSM and to determine, and carry out, research activities appropriate to the anticipated European personal communication systems in the 1990's.

3. The Signatories hereby declare their intention of carrying out the Project jointly, in accordance with the general description given in Annex II, adhering as far as possible to a timetable to be decided by the Management Committee referred to in Annex I.

4. The Project will be carried out through concerted action, in accordance with the provisions of Annex I.

5. The value of the activities of the Signatories under the Project is estimated at approximately 400 000 ECU per Signatory at 1988 prices.

6. The Signatories will make every effort to ensure that the necessary funds are made available under their internal financing procedures.

SECTION 2

Signatories intend to take part in the Project in one or several of the following ways:

(a) by carrying out studies and research in their technical services or public research establishments (hereinafter referred to as "public research establishments");

(b) by concluding contracts for studies and research with organizations (hereinafter referred to as "research contractors");

(c) by contributing to the provision of a Secretariat and/or other co-ordinatory services or activities necessary for the aims of the Project to be achieved;

(d) by making information on existing relevant research, including all necessary basic data, available to other Signatories;

(e) by arranging for inter-laboratory visits and by co-operating in a small-scale exchange of staff in the later stages.

SECTION 3

1. This Memorandum of Understanding will take effect for four years on its signing by at least four Signatories.

2. This Memorandum of Understanding may be amended in writing at any time by arrangement between the Signatories.

3. A Signatory which intends, for any reason whatsoever, to terminate its particpation in the Project will notify the Secretary-General of the Council of the European Communities of its intention as soon as possible, preferably not later than three months beforehand.

4. If at any time the number of Signatories falls below four, the Management Committee referred to in Annex I will examine the situation which has arisen and will consider whether or not this Memorandum of Understanding should be terminated by decision of the Signatories.

SECTION 4

1. This Memorandum of Understanding will, for a period of six months from the date of the first signing, remain open for signing, by the Governments which took part in the Ministerial Conference held in Brussels on 22 and 23 November 1971 and also by the European Communities.

The Governments referred to in the first subparagraph, and the European Communities may take part in the project on a provisional basis during the abovementioned period, even though they may not have signed this Memorandum of Understanding.

2. After this period of six months has elapsed, applications to sign this Memorandum of Understanding from the Governments referred to in paragraph 1 or from the European Communities will be decided upon by the Management Committee referred to in Annex I, which may attach special conditions thereto.

3. Any Signatory may designate one or more competent public authorities or bodies to act on its behalf in respect of the implementation of the Project.

SECTION 5

This Memorandum of Understanding is of an exclusively recommendatory nature. It will not create any binding legal effect in public international law.

SECTION 6

1. The Secretary-General of the Council of the European Communities will inform all Signatories of the signing dates and date of entry into effect of this Memorandum of Understanding and will forward to them all notices which he has received under this Memorandum of Understanding.

2. This Memorandum of Understanding will be deposited with the General Secretariat of the Council of the European Communities. The Secretary-General will transmit a certified copy to each of the Signatories.

CO-ORDINATION OF THE PROJECT

CHAPTER I

1. A Management Committee (hereinafter referred to as "the Committee") will be set up, composed of not more than two representatives for each Signatory. Each representative may be accompanied by such experts or advisers as he or she may need.

The Governments which took part in the Ministerial Conference held in Brussels on 22 and 23 November 1971 and the European Communities may, in accordance with the second subparagraph of Section 4(1) of the Memorandum of Understanding, participate in the work of the Committee before becoming Signatories to the Memorandum without, however, having the right to vote.

When the European Communities are not a Signatory to the Memorandum of Understanding, a representative of the Commission of the European Communities may attend Committee meetings as an observer.

2. The Committee will be responsible for co-ordinating the Project and in particular, for making the necessary arrangements for:

(a) the choice of research topics on the basis of those provided for in Annex II, including any modifications submitted to Signatories by the competent public authorities or bodies; any proposed changes to the Project framework will be referred for an opinion to the Technical Committee "Telecommunications" (COST);

(b) advising on the direction which work should take;

(c) drawing up detailed plans and defining methods for the different phases of execution of the Project;

(d) co-ordinating the contributions referred to in subparagraph (c) of Section 2 of the Memorandum of Understanding;

(e) keeping abreast of the research being done in the territory of the Signatories and in other countries;

(f) liaising with appropriate international bodies;

(g) exchanging research results among the Signatories to the extent compatible with adequate safeguards for the interests of Signatories, their competent public authorities or bodies and research contractors in respect of industrial property rights and commercially confidential material;

(h) drawing up the annual interim reports and the final report to be submitted to the Signatories and circulated as appropriate; drawing up a non-confidential report to be submitted annually to the Technical Committee "Telecommunications" (COST);

(i) dealing with any problem which may arise out of the execution of the Project, including those relating to possible special conditions attached to accession to the Memorandum of Understanding in the case of applications submitted more than six months after the date of the first signing.

3. The Committee will establish its rules of procedure.

4. The Secretariat of the Committee will be provided at the invitation of the Signatories by either the Commission of the European Communities or one of the Signatory States.

CHAPTER II

1. Signatories will invite public research establishments or research contractors in their territories to submit proposals for research work to their respective competent public authorities or bodies. Proposals accepted under this procedure will be submitted to the Committee.

2. Signatories will request public research contractors, before the Committee takes any decision on a proposal, to submit to the public authorities or bodies referred to in paragraph 1 notification of previous commitments and industrial property rights which they consider might preclude or hinder the execution of the Projects of the Signatories.

CHAPTER III

1. Signatories will request their public research establishments or research contractors to submit periodical progress reports and a final report.

2. The progress reports will be distributed to the Signatories only, through their representatives on the Committee. The Signatories will treat these progress reports as confidential and will not use them for purposes other than research work. The final reports on the results obtained will have much wider circulation, covering at least the Signatories' public research establishments or research contractors concerned.

CHAPTER IV

1. In order to facilitate the exchange of results referred to in Chapter I, paragraph 2(g), and subject to national law, Signatories intend to ensure, through the inclusion of appropriate terms in research contracts, that the owners of industrial property rights and technical information resulting from work carried out in implementation of that part of the Project assigned to them under Annex II (hereinafter referred to as "the research results") will be under an obligation, if so requested by another Signatory (hereinafter referred to as "the applicant Signatory"), to supply the research results and to grant to the applicant Signatory or to a third party nominated by the applicant Signatory a licence to use the research results and such technical know-how incorporated therein as is necessary for such use if the applicant Signatory requires the granting of a licence for the execution of:

- work in respect of the Project;

- research and development work within the framework of the applicant Signatory's projects in the same field;

- research and development work within the framework of any associated European project undertaken subsequently and in which all or several of the Signatories may be prepared to take part.

Such licences will be granted on fair and reasonable terms, having regard to commercial usage.

2. Signatories will, by including appropriate clauses in contracts placed with research contractors, provide for the licence referred to in paragraph 1 to be extended on fair and reasonable terms, having regard to commercial usage, to previous industrial property rights and to prior technical know-how acquired by the research contractor insofar as the research results could not otherwise be used for the purpose referred to in paragraph 1.

Where a research contractor is unable or unwilling to agree to such extension, the Signatory will submit the case to the Committee, before the contract is concluded; hereafter, the Committee will state its position on the case, if possible after havng consulted the interested parties.

3. Signatories will take any steps necessary to ensure that the fulfilment of the conditions laid down in the present Chapter will not be affected by any subsequent transfer of rights to ownership of the research results. Any such transfer will be notified to the Committee.

4. If a Signatory terminates its participation in the Project, any rights of use which it has granted, or is obliged to grant, to, or has obtained from, other Signatories in application of the Memorandum of Understanding and concerning work carried out up to the date on which the said Signatory terminates its participation will continue thereafter.

5. The provisions of paragraphs 1 to 4 will continue to apply after the period of operation of the Memorandum of Understanding has expired and will apply to industrial property rights as long as these remain valid, and to unprotected inventions and technical know-how until such time as they pass into the public domain other than through disclosure by the licensee.

GENERAL DESCRIPTION OF THE PROJECT

1. INTRODUCTION

Following current mobile developments (e.g. CEPT GSM, CEPT Cordless Telephone) the demand for personal mobile communications will increase dramatically. It has been suggested that by the end of the century, one hundred million handsets may be in service in Europe.

This demand will require major advances in mobile communication techniques and the opening up of new frequency bands to ensure that all current mobile services and those yet to achieve operational status are efficiently combined into one optimized operational system to the advantage of both the network operators, the manufacturers and the customers. Such system and spectrum developments demand the early availability of research data to ensure effective planning.

In order to determine appropriate research activities in this field those major land mobile systems expected to be operational in Europe during the 1990's have been considered.

For each of these systems, research activities in the fields of propagation, baseband processing, modulation and system aspects, would seem to be appropriate. In choosing those activities for which a COST project is considered appropriate, the following criteria have been adopted:

- to avoid a COST involvement in areas where industries are already working in a competitive environment;

- to propose a COST project for those activities which could take advantage of the knowledge and expertise of those resources which are specific to COST projects; that is research institutes and universities whose resources are in danger of not being fully exploited in other programmes;

- to take into account the related work of other international bodies.

Four mobile communication systems have been considered of possible interest for COST projects:

(a) the GSM system as presently defined, which is expected to be put into operation in 1991;

(b) the evolution of the GMS system with the utilization of a half rate speech coder which should be put into operation at mid 1990's (say 1995);

(c) the "personal" or "universal" system, the characteristics of which have still to be defined, to be put into operation towards the end of the century;

(d) a satellite based system, carrying both voice and data, possibly integrated with a terrestrial system (b) or (c).

For system (c) reference should be made both to the RACE programme and to the CCIR interim Working Party 8/13 activity. For system (d) reference should be made to CCIR interim Working Party 8/14 and to the recently established Joint Group among CEPT, INMARSAT and EUTELSAT.

A COST Project (227: Integrated space/terrestrial mobile networks) is in the process of approval, so that satellite based systems will be covered by such a project.

Concerning the development of specifications for the half-rate coder, views have been expressed within CEPT that this task should be given to the expert group already working on speech coding (the Joint COST 207-CEPT TM3 group) with close liaison to appropriate CEPT bodies (GSM, TM3). This solution is also considered appropriate by the MC of the COST 207 Project.

The 231 Project should concentrate its research activities on the GSM system and personal communications development. With regard to the spectrum needs of the last subject, propagation data for frequencies between 1 and 3 GHz are urgently required so that spectrum regulators can perform their function effectively.

2. OBJECTIVES OF THE PROJECT

The main objectives of the Project are:

- to co-ordinate and promote European research in specific areas of digital mobile communications in order to support the CEPT-GSM in these areas;

- to determine and carry out research activities in support of personal communication systems for the 1990's considering the transmission system requirements of cellular, microcellular and in-building environments.

3. PROPOSED RESEARCH ACTIVITIES

3.1 The GSM system

For the GSM system the following activities relating to propagation and to system aspects will be covered:

3.1.1 Development of harmonized models for accurate and efficient field strength prediction based on geographic information systems

For the planning of small/medium scale cell systems (e.g. $\leq$ 2 km diameter), it is essential that an accurate and computationally efficient radiopath loss prediction model be developed. This model should be able to use various existing information systems and should be capable of predicting C/I values as well. This topic has been only partially investigated by COST 207 and the goal of defining a harmonized prediction method is still to be reached. The activities envisaged comprise:

- determination of the required field strength parameters and the subsequent harmonization of existing measured data, obtained at various test sites across Europe (representing different topographic conditions);

- judgement on suitability of available geographic information systems;

- testing of available propagation models and synthesis of a harmonized model for use in European conditions.

COST 231 Project will contribute to co-ordination, between participants, of the European research activities directed towards the work of CCIR Study Group 5 in this area, and particularly Interim Working Party 5/5.

3.1.2 Propagation characteristics in tunnels

3.1.3 Antenna characteristics and diversity techniques

3.1.4 Cellular coverage techniques

3.2 Universal or Personal Communication

The spectrum regulators are set firmly toward finding spectrum space between 1 and 3 GHz for personal communication systems in the 1990's. This activity clearly indicates a need for an early understanding of the propagation and system characteristics appropriate to this band. Such knowledge will enable effective system decisions to be made. In this context a variety of mobile radio systems and services are envisaged requiring for their study cellular, microcellular and in-building (pico-cellular) coverage and traffic data. For the longer-term, spectrum in the range 30-90 GHz will also need to be exploited for micro-cellular and in-building systems (pico-cellular). The following research activities have been identified:

3.2.1 The development and harmonization of field-strength and time-delay propagation models for cellular, micro-cellular and in-building systems at frequencies in the ranges 1-3 GHz and 30-90 GHz.

3.2.2 The application of propagation models to achieving reliable system coverage both inside and outside buildings.

3.2.3 The development of telecommunications traffic models and data bases (e.g. Erlangs/m^3) for cellular, micro-cellular and in-building systems in order to design effective systems and plan base-station dispositions.

3.2.4 The development of C/I prediction models.

3.2.5 The continued study of advanced modulation method, multiple access, channel equalisation, coding, duplex transmission techniques and diversity schemes appropriate to these systems.

4. FORM OF CO-OPERATION

The suggested form of co-operation is that Signatories are represented in the Management Committee by delegates who should be expected to:

- attend and contribute to meetings of the Management Committee; usually two to four meetings per year;

- be involved in an active programme fitting in with the objectives and time scale of the project;

- set up national working groups for specific items;

- seek at least annually the advice of the Technical Committee Telecommunications (TCT) to achieve a working liaison between the Project and other related COST telecommunication and teleinformatics projects;

- establish and maintain, in particular, close co-operation with COST project 227;

- be responsible for liaising between the Management Committee and national research groups in the participating countries.

When necessary, the Management Committee may arrange working sessions for participating researchers, where results can be presented and discussed, on either ad hoc or a regular basis.

5. ENVISAGED COSTS FOR THE ACTIVITY

The minimum overall costs per Signatory for a four-year period is estimated to be 400 000 ECU including manpower, co-ordination and travel expenses.

European Communities — Commission

EUR 12160 — COST 207 — Digital land mobile radio communications

Management Committee

Luxembourg: Office for Official Publications of the European Communities

1989 — VIII, 388 pp. — 16.2 × 22.9 cm

Information technologies and sciences series

EN

ISBN 92-825-9946-9

Catalogue number: CD-NA-12160-EN-C

Price (excluding VAT) in Luxembourg: ECU 32.50

This report summarizes the results of the activities of COST 207 'Digital land mobile radio communications'.

It is organized around the three research areas into which the project has been subdivided: propagation, baseband processing and modulation.

The main activities and results carried out within the project are as follows:

(i) The definition of frequency-selective fading simulator characteristics and the choice of parameter setting for GSM test measurements, taking into account the results of propagation measurements carried out in different countries participating in COST 207.

(ii) Measurements of man-made noise in the 900 MHz band and construction of a noise simulator.

(iii) Modulation methods originally seen as possible candidates for the GSM system; GTFM, PAM/FM and GMSK.

(iv) Adaptive baseband equalization techniques.

(v) Forward error-correction codes.

(vi) Specification of the 13 Kbit/s net bit-rate codec and corresponding test sequences.

(vii) Specifications relating to voice-activated transmission intended to conserve battery energy in hand-held terminals, and to reduce interferences.

Venta y suscripciones · Salg og abonnement · Verkauf und Abonnement · Πωλήσεις και συνδρομές
Sales and subscriptions · Vente et abonnements · Vendita e abbonamenti
Verkoop en abonnementen · Venda e assinaturas

BELGIQUE / BELGIË

Moniteur belge / Belgisch Staatsblad
42, Rue de Louvain / Leuvenseweg 42
1000 Bruxelles / 1000 Brussel
Tél. 512 00 26
Télécopieur: 511 01 84
CCP / Postrekening 000-2005502-27

Sous-dépôts / Agentschappen:

Librairie européenne / Europese Boekhandel
Avenue Albert Jonnart 50 / Albert Jonnartlaan 50
1200 Bruxelles / 1200 Brussel
Tél. 734 02 81
Télécopieur: 735 08 60

Jean De Lannoy
Avenue du Roi 202 /Koningslaan 202
1060 Bruxelles / 1060 Brussel
Tél. (02) 538 5169
Télex 63220 UNBOOK B

CREDOC
Rue de la Montagne 34 / Bergstraat 34
Bte 11 / Bus 11
1000 Bruxelles / 1000 Brussel

DANMARK

J. H. Schultz Information A/S
EF-Publikationer
Ottiliavej 18
2500 Valby
Tlf: 36 44 22 66
Telefax: 36 44 01 41
Girokonto 6 00 08 86

BR DEUTSCHLAND

Bundesanzeiger Verlag
Breite Straße
Postfach 10 80 06
5000 Köln 1
Tel. (02 21) 20 29-0
Fernschreiber:
ANZEIGER BONN 8 882 595
Telefax: 20 29 278

GREECE

G.C. Eleftheroudakis SA
International Bookstore
4 Nikis Street
105 63 Athens
Tel.: 3226-323
Telex: 219410 ELEF
Telefax: 3254 889

Sub-agent for Northern Greece:

Molho's Bookstore
The Business Bookshop
10 Tsimiski Street
Thessaloniki
Tel. 275 271
Telex 412885 LIMO

ESPAÑA

Boletín Oficial del Estado
Trafalgar 27
E-28010 Madrid
Tel. (91) 446 60 00

Mundi-Prensa Libros, S.A.
Castelló 37
E-28001 Madrid
Tel. (91) 431 33 99 (Libros)
431 32 22 (Suscripciones)
435 36 37 (Dirección)
Telex 49370-MPLI-E
Telefax: (91) 275 39 98

FRANCE

Journal officiel
Service des publications
des Communautés européennes
26, rue Desaix
75727 Paris Cedex 15
Tél. (1) 40 58 75 00
Télécopieur: (1) 4058 7574

IRELAND

Government Publications Sales Office
Sun Alliance House
Molesworth Street
Dublin 2
Tel. 71 03 09

or by post

Government Stationery Office
EEC Section
6th floor
Bishop Street
Dublin 8
Tel. 78 16 66

ITALIA

Licosa Spa
Via Benedetto Fortini, 120/10
Casella postale 552
50 125 Firenze
Tel. 64 54 15
Telefax: 64 12 57
Telex 570466 LICOSA I
CCP 343 509

Subagenti:

Libreria scientifica Lucio de Biasio - AEIOU
Via Meravigli, 16
20 123 Milano
Tel. 80 76 79

Herder Editrice e Libreria
Piazza Montecitorio, 117-120
00 186 Roma
Tel. 67 94 628/67 95 304

Libreria giuridica
Via 12 Ottobre, 172/R
16 121 Genova
Tel. 59 56 93

GRAND-DUCHÉ DE LUXEMBOURG

Abonnements seulement
Subscriptions only
Nur für Abonnements

Messageries Paul Kraus
11, rue Christophe Plantin
L-2339 Luxembourg
Tél. 48 21 31
Télex 2515
CCP 49242-63

NEDERLAND

SDU uitgeverij
Christoffel Plantijnstraat 2
Postbus 20014
2500 EA 's-Gravenhage
Tel. (070) 78 98 80 (bestellingen)
Telefax: (070) 476351

PORTUGAL

Imprensa Nacional
Casa da Moeda, E.P.
Rua D. Francisco Manuel de Melo, 5
1092 Lisboa Codex
Tel. 69 34 14

Distribuidora Livros Bertrand Lda.
Grupo Bertrand, SARL
Rua das Terras dos Vales, 4-A
Apart. 37
2700 Amadora Codex
Tel. 493 90 50 - 494 87 88
Telex 15798 BERDIS

UNITED KINGDOM

HMSO Books (PC 16)
HMSO Publications Centre
51 Nine Elms Lane
London SW8 5DR
Tel. (01) 873 9090
Fax: GP3 873 8463

Sub-agent:

Alan Armstrong Ltd
2 Arkwright Road
Reading, Berks RG2 OSQ
Tel. (0734) 75 17 71
Telex 849937 AAALTD G
Fax: (0734) 755164

SUISSE

OSEC
Stampfenbachstraße 85
CH-8035 Zürich
Tél. (01) 365 51 51
Fax: (01) 365 52 21

ÖSTERREICH

Manz'sche Verlagsbuchhandlung
Kohlmarkt 16
1014 Wien
Tel. (0222) 531 61-0
Telex 11 25 00 BOX A
Telefax: (0222) 531 61-81

TÜRKIYE

Dünya süper veb ofset A.Ş.
Narlibahçe Sokak No. 15
Cağaloğlu
Istanbul
Tel. 512 01 90
Telex: 23822 dsvo-tr.

UNITED STATES OF AMERICA

UNIPUB
4661-F Assembly Drive
Lanham, MD 20706-4391
toll free (800) 274-4888
Fax. (301) 459-0056
Télex 7108260418

CANADA

Renouf Publishing Co., Ltd
61 Sparks Street
Ottawa
Ontario K1P 5R1
Tel. Toll Free 1 (800) 267 4164
Ottawa Region (613) 238 8985-6
Telex 053-4936

JAPAN

Kinokuniya Company Ltd
17-7 Shinjuku 3-Chome
Shiniuku-ku
Tokyo 160-91
Tel. (03) 354 0131

Journal Department
PO Box 55 Chitose
Tokyo 156
Tel. (03) 439 0124

AUTRES PAYS
OTHER COUNTRIES
ANDERE LÄNDER

Office des publications officielles
des Communautés européennes
2, rue Mercier
L-2985 Luxembourg
Tél. 49 92 81
Télex PUBOF LU 1324 b
CC bancaire BIL 8-109/6003/700

07/89